Pathogen-induced cell wall remodeling and production of Danger Associated Molecular Patterns (DAMPs)

Dissertation

for the award of the degree

“Doctor rerum naturalium”

of the University of Goettingen

within the doctoral program

International Research Training Group 2172 - PRoTECT

of the Georg-August University School of Science (GAUSS)

submitted by

Sina Barghahn

from Oldenburg (Oldb), Germany

Göttingen 2020

Thesis Committee

Prof. Dr. Volker Lipka
Department of Plant Cell Biology, Albrecht-von-Haller Institute for Plant Science, University of Goettingen

PD Dr. Till Ischebeck
Department of Plant Biochemistry, Albrecht-von-Haller Institute for Plant Science, University of Goettingen

Prof. Dr. Harry Brumer
Department of Chemistry, Michael Smith Laboratories, University of British Columbia

Members of the Examination Board

Referee: **Prof. Dr. Volker Lipka**
Department of Plant Cell Biology, Albrecht-von-Haller Institute for Plant Science, University of Goettingen

2nd Referee: **PD Dr. Till Ischebeck**
Department of Plant Biochemistry, Albrecht-von-Haller Institute for Plant Science, University of Goettingen

Further members of the Examination Board

Prof. Dr. Harry Brumer
Department of Chemistry, Michael Smith Laboratories, University of British Columbia

Prof. Dr. Ivo Feußner
Department of Plant Biochemistry, Albrecht-von-Haller Institute for Plant Science, University of Goettingen

Prof. Dr. Gerhard Braus
Department of Molecular Microbiology and Genetics, Institute of Microbiology and Genetics, University of Goettingen

Dr. Marcel Wiermer
Department of Molecular Biology of Plant-Microbe Interactions, Albrecht-von-Haller Institute for Plant Science, University of Goettingen

Tag der mündlichen Prüfung: 26th March 2020

Promovierenden-Erklärung
der Georg-August-Universität Göttingen

Die Gelegenheit zum vorliegenden Promotionsvorhaben ist mir nicht kommerziell vermittelt worden. Insbesondere habe ich keine Organisation eingeschaltet, die gegen Entgelt Betreuerinnen und Betreuer für die Anfertigung von Dissertationen sucht oder die mir obliegenden Pflichten hinsichtlich der Prüfungsleistungen für mich ganz oder teilweise erledigt.

Hilfe Dritter wurde bis jetzt und wird auch künftig nur in wissenschaftlich vertretbarem und prüfungsrechtlich zulässigem Ausmaß in Anspruch genommen. Insbesondere werden alle Teile der Dissertation selbst angefertigt; unzulässige fremde Hilfe habe ich dazu weder unentgeltlich noch entgeltlich entgegengenommen und werde dies auch zukünftig so halten.

Die Ordnung zur Sicherung der guten wissenschaftlichen Praxis an der Universität Göttingen wird von mir beachtet.

Eine entsprechende Promotion wurde an keiner anderen Hochschule im In- oder Ausland beantragt; die eingereichte Dissertation oder Teile von ihr wurden/werden nicht für ein anderes Promotionsvorhaben verwendet.

Mir ist bekannt, dass unrichtige Angaben die Zulassung zur Promotion ausschließen bzw. später zum Verfahrensabbruch oder zur Rücknahme des erlangten Grades führen können.

Sina Barghahn Göttingen, den 30. Januar 2020

Abstract

For a plant pathogen, overcoming the plant cell wall is crucial for a successful infection. Thus, pathogens evolved different strategies to invade their host plants. These include entry through natural openings such as stomata and wounds or direct penetration of plant cell walls with specialised invasion structures that generate high pressure as well as cell wall degrading enzymes (CWDEs). CWDEs can be classified into different groups according to their potential function and include e.g. Glycoside Hydrolases (GHs), which are implicated in the hydrolysis of glycosidic linkages in complex carbohydrates such as the plant cell wall component cellulose. GHs have been shown to be involved in pathogenicity of hemibiotrophic and necrotophic plant-pathogenic fungi. However, the role of GHs in biotrophic plant-pathogenic fungi has not been elucidated so far.

The first part of the present study focused on the identification and functional characterization of GH17 family members of the powdery mildew *Blumeria graminis* f.sp. *hordei* (*Bgh*) that may contribute to pathogenicity due to a transcriptional induction during infection of immunocompromised Arabidopsis plants. Of these, *Bgh* GH17 protein BGH06777 was successfully expressed in the heterologous system *P. pastoris*, purified and functionally characterized. The glycosylated enzyme showed optimal activity at pH 5.5 in a temperature range from 25°C - 51°C and hydrolysed β-1,3-glucans with a minimum length of four glucose residues. The catalytic efficiencies for hydrolysis of the β-1,3-glucan hexamer and pentamer were 1.858 $mM^{-1}\,s^{-1}$ and 0.3836 $mM^{-1}\,s^{-1}$, respectively. ^{18}O labelling of the products revealed that the enzyme contains at least six substrate binding sites comprised of four negative and two positive subsites. In conclusion, the detailed biochemical characterization conducted in this study suggests that BGH06777 might degrade β-1,3-glucans present in plant papillae, however, the exact function and localization of this protein remains to be shown.

Plants are able to perceive potential pathogens through the recognition of conserved non-self microbial structures, so-called pathogen or microbe-associated molecular patterns (PAMPs/MAMPs), at the plant surface via pattern recognition receptors (PRRs). Furthermore, plants can detect self-molecules that are only abundant upon cell damage or wounding, which are called damage or danger-associated molecular patterns (DAMPs). Both, MAMP or DAMP recognition triggers a signaling cascade that leads to the induction of defence responses. It is conceivable to postulate that the activity of CWDEs results in the release of cell-wall derived oligosaccharides with DAMP capacity.

Thus, the second part of this study aimed at identifying novel cell-wall derived DAMPs and molecular components of the corresponding plant perception and signaling machinery. As a major result of this work, mixed linkage glucan (MLG) oligosaccharides were shown to trigger immune responses in the dicot model plant Arabidopsis and the monocot barley. The MLG-induced responses were similar to plant responses to the well-characterized MAMPs and DAMPs chitin, flg22 and OGs. In contrast to other MAMPs and DAMPs, MLG oligosaccharides did not elicit a detectable generation of reactive oxygen species or affect seedling growth in Arabidopsis. MLGs are abundant cell wall components of monocot grasses, e.g. barley, and the plant-pathogenic fungus *Rhynchosporium commune* (formerly *R. secalis*) but are absent in the dicot model plant Arabidopsis. Thus, MLG oligosaccharides might

function in a plant-species specific manner as MAMP or DAMP (or both). A reverse genetic screen conducted with a collection of known DAMP/MAMP receptor and co-receptor mutants revealed that MLG perception and downstream signaling is likely to involve so far unknown molecular components.

Zusammenfassung

Für ein Pflanzenpathogen ist das Überwinden der Zellwand entscheidend für eine erfolgreiche Infektion. Daher haben Pflanzenpathogene verschiedene Strategien entwickelt, um in Pflanzen einzudringen. Diese Strategien schließen das Eindringen über natürlich vorkommende Öffnungen wie Stomata oder Verwundungen, direkte Penetration mit spezialisierten Strukturen, die einen hohen Druck erzeugen, sowie Zellwand hydrolysierende Enzyme (CWDEs)[1] ein. Abhängig von ihrer potentiellen Funktion, können CWDEs in verschiedene Gruppen klassifiziert werden. Unter Anderem gibt es die Klasse der Glycosyl Hydrolasen (GHs), die glykosidische Bindungen in komplexen Karbohydraten spalten wie zum Beispiel Zellulose, einem Bestandteil der pflanzlichen Zellwand. Es wurde gezeigt, dass GHs wichtig für die Pathogenität von hemibiotrophen und necrotrophen Pflanzenpathogenen sind. Die Rolle von GHs in biotrophen Pflanzenpathogenen wurde hingegen noch nicht geklärt.

Der erste Teil dieser Arbeit konzentrierte sich auf die Identifizierung und Charakterisierung der Mitglieder der GH17 Familie des Mehltau Pilzes *Blumeria graminis* f.sp. *hordei* (*Bgh*). Diese Familie spielt möglicherweise eine Rolle in der Pathogenität, da die Transkription dieser Familie während der Infektion von immunsupprimierten Arabidopsis Pflanzen induziert ist. Das *Bgh* Protein BGH06777 konnte erfolgreich in dem heterologen Expressionssystem *P. pastoris* exprimiert und schließlich aufgereinigt und funktional charakterisiert werden. Das glykolisierte Protein zeigte die optimale Aktivität bei einem pH Wert von 5.5 in einem Temperaturbereich von 25°C bis 51°C und hydrolisierte β-1,3-glukane mit einer minimalen Länge von vier Glukosemolekülen. Die katalytischen Effizienzen für die Hydrolyse des β-1,3-glukan Hexamers und β-1,3-Glukan Pentamers lagen bei jeweils 1.858 $mM^{-1}\,s^{-1}$ und 0.3836 $mM^{-1}\,s^{-1}$. Die Markierung der Hydrolyseprodukte mit ^{18}O ergab, dass das Enzym mindestens sechs Bindestellen für das Substrat hat bestehend aus vier negativen und zwei positiven Bindestellen. Die detallierte biochemische Analysis deutet an, dass BGH06777 β-1,3-glukane, die in pflanzlichen Papillen zu finden sind, hydrolysieren könnte. Die exakte Funktion sowie die Lokalisierung dieses Enzyms müssen jedoch noch gezeigt werden.

Pflanzen können potentielle Pathogene durch das Erkennen von konservierten mikrobiellen Struktuen, sogenannten Pathogen- oder Mikroben-assoziierten molekularen Mustern (PAMPs/MAMPs), an der Oberfläche durch membranständige Rezeptoren wahrnehmen. Weiterhin können Pflanzen auch Moleküle wahrnehmen, die von der Pflanze selbst stammen, aber nur nach Verwundung oder Beschädigung der Zelle vorhanden sind. Diese Moleküle werden Schaden- oder Gefahr-assoziierte molekulare Muster (DAMPs) genannt. Sowohl MAMPs als auch DAMPs aktivieren eine Signalkaskade, die zur Induktion der Immunantwort führt. Es ist vorstellbar, dass Zellwandfragmente mit DAMP Kapazität durch die Aktivität von CWDEs entstehen.

Der zweite Teil der Arbeit fokussiert sich daher auf die Identifizierung von neuen DAMP Molekülen, die von der Zellwand stammen, sowie den jeweiligen molekularen Komponenten, die an der Perzeption und der Signaltransduktion beteiligt sind. Eines der wichtigsten Ergebnisse dieser Arbeit

[1] Im Folgenden werden für sämtliche Abkürzungen die englischen Abkürzungen verwendet (siehe auch: List of Abbreviations, V)

ist, dass β-1,3;1,4-glukan Oligosaccharide Immunantworten in der dikotylen Pflanze Arabidopsis und der monokotylen Nutzpflanze Gerste auslösen. Diese Immunantworten ähneln den pflanzlichen Abwehrantworten, die durch die gut charakterisierten MAMPs und DAMPs Chitin, Flagellin und Oligogalakturonide ausgelöst werden. Im Gegensatz zu anderen MAMPs und DAMPs aktivieren die Oligosaccharide jedoch nicht die Generierung von reaktiven Sauerstoffspezies und beeinflussen auch nicht das Wachstum von Arabidopsis Setzlingen. Das β-1,3;1,4-glukan Polymer ist ein Bestandteil der Zellwand von monokotylen Gräsern, wie zum Beispiel Gerste, und dem Pflanzenpathogen *Rhynchosporium commune* (ehemals bekannt als *R. secalis*), aber ist kein Zellwandkomponent der dikotylen Modellpflanze Arabidopsis. Dies legt den Schluss nahe, dass β-1,3;1,4-glucan Oligosaccharide in einer Pflanzenart-spezifischen Weise als MAMP oder DAMP (oder beidem) agieren. Ein revers genetischer Ansatz mit einer Kollektion von bekannten MAMP/DAMP Rezeptor- und Co-Rezeptor Mutanten zeigte, dass die Perzeption sowie die Signaltransdkution wahrscheinlich bisher unbekannte molekulare Komponenten involviert.

List of Abbreviations

α	alpha/anti
°C	degree Celsius
µg	microgramm
µl	microliter
µM	micromolar
A. fumigatus	*Aspergillus fumigatus*
AP	alkaline phosphatase
APS	ammonium persulfate
A. thaliana	*Arabidopsis thaliana*
BAK1	BRI-1 ASSOCIATED KINASE 1
B. cinerea	*Botrytis cinerea*
Bgh	*Blumeria graminis* f.sp. *hordei*
BIK1	BOTRYTIS INDUCED KINASE1
BMGY	Buffered Glycerol-complex medium
BMMY	Buffered Methanol-complex medium
BRI-1	brassinosteroid sensitive 1
BSA	bovine serum albumin
B. subtilis	*Bacillus subtilis*
Ca^{2+}	Calcium
CBB	Coomassie Brilliant Blue
CBM	carbohydrate binding domain
cDNA	complementary DNA
CE	carbohydrate esterases
CEBiP	CHITIN ELICTOR BINDING PROTEIN
CERK1	CHITIN ELICITOR RECEPTOR KINASE 1
Col-0	Columbia-0
CSL	cellulose synthase like
CWDE	cell wall degrading enzyme
DAMP	danger/damage-associated molecular pattern
ddH_2O	double-distilled water
DNA	deoxyribonucleic acid
DNase	deoxyribonuclease
dNTP	desoxyribonucleotidetriphosphate
DTT	Dithiothreitol

E. coli	*Escherichia coli*
e.g.	exempli gratia
EDTA	Ethylenediaminetetraacetic acid
EFR	elongation factor thermo unstable receptor
EF-Tu	elongation factor thermo unstable
et al.	*Et alii*; and others
ETI	effector triggered immunity
EtOH	ethanol
ETS	effector triggered susceptibility
flg22	flagellin (22 amino acid peptide)
FLS2	FLAGELLIN SENSING 2
f.sp.	*forma specialis*
g	gramm
GH	Glycoside Hydrolase
GT	Glycosyltransferase
h	hour(s)
HCl	hydrochloric acid
HIGS	Host-induced gene silencing
HPAEC-PAD	High-performance-anion-exchange chromatography with pulsed amperometric detection
HR	hypersensitive response
HRP	Horseradish peroxidase
Hv	*Hordeum vulgare*
kDa	kilo Dalton
l	liter
LYK	LysM-receptor like kinase
LYM	LysM containing receptor-like proteins
LysM	lysine motif
M	Molar (mol/l)
mA	milli Ampere
MD	Minimal Dextrose Medium
MM	Minimal Methanol Medium
MAGIC	Multiparent Advanced Generation Inter-Cross
MALDI-TOF	matrix-assisted laser desorption ionization with time-of-flight detection

MAMP	microbe associated molecular pattern
MAPK	mitogen activated protein kinase
min	minute(s)
ml	milliliter
MLG	mixed linkage glucan
mM	millimolar
M. oryzae	*Magnaporthe oryzae*
MS	Murashige-Skoog
MTI	MAMP triggered immunity
OD_{600}	Optical Density at a wavelength of 600 nm
OGs	oligogalacturonides
O. sativa	*Oryza sativa*
Os	*Oryza sativa*
PCR	Polymerase Chain Reaction
PEPR	Pep receptor
Pep	plant elicitor peptides
pH	negative decimal logarithm of the H^+ concentration
PIC	Protease Inhibitor Cocktail
PL	polysaccharide lyase
P. pastoris	*Pichia pastoris*
PRR	Pattern recognition receptor
PTI	PAMP-triggered immunity
PVDF	polyveniylidene fluoride
R. commune	*Rhynchosporium commune*
RLCK	Receptor like cytoplasmic kinase
RLK	receptor-like kinase
RLP	receptor-like protein
RNA	ribonucleic acid
ROS	reactive oxygen species
rpm	rounds per minute
RPM	reads per million
RT	room temperature
s	second(s)
SCFE1	SCLEROTINIA CULTURE FILTRATE ELICITOR1
SDS	Sodium dodecyl sulfate
SDS-PAGE	Sodium dodecyl sulfate polyacrylamide gel electrophoresis

SOBIR	SUPPRESSOR OF BIR1-1
Taq	*Thermus aquaticus*
TAE	Tris-acetic acid EDTA
TBS-T	Tris buffered saline – Tween-20
T-DNA	Transfer-DNA
TEMED	Tetramethylethylenediamine
TLC	Thin Layer Chromatography
U	Unit
V	Volt
WAK1	Wall-Associated kinase1
Ws	Wassilewskija
YNB	Yeast Nitrogen Base
YPD	Yeast Extract-Peptone-Dextrose

Table of contents

1 Introduction

1.1 The plant immune system

Plants are constantly exposed to a variety of different microbial pathogens. Microbial pathogens can be bacteria, fungi or oomycetes that exhibit different lifestyles and infection strategies (Jones and Dangl, 2006). In order to protect and defend themselves, plants rely on an innate immune system that includes a variety of defensive barriers and inducible responses (Dodds and Rathjen, 2010).

The first physical barriers that are encountered by microbial pathogens are the cuticle and the plant cell wall (Houston *et al.*, 2016). Pathogens have evolved strategies to overcome the cuticle and the plant cell wall by entering the plant through natural openings such as stomata or wounds, formation of appressoria and/or the secretion of cell wall degrading enzymes (CWDEs) (Chisholm *et al.*, 2006). Once the pathogen has overcome the plant cell wall, it faces the plasma membrane and the two-layered plant immune system. The first layer of plant immunity is referred to as microbe/pathogen associated molecular pattern (MAMP/PAMP)-triggered immunity (MTI/PTI) (Jones and Dangl, 2006; Chisholm *et al.*, 2006). MTI/PTI is based on the recognition of non-self MAMPs, e.g. fungal chitin (Jones and Dangl, 2006). MAMPs are defined as essential and highly conserved molecular structures that cannot easily be modified and are present in a whole class of microbes but absent from host plants (Postel and Kemmerling, 2009). Besides the perception of MAMPs, plants can perceive host-derived molecules, e.g. cell wall derived oligogalacturonides (OGs), that are only abundant upon cell damage or pathogen attack. These host-derived molecules are referred to as damage/danger-associated molecular patterns (DAMPs) (Boller and Felix, 2009). MAMPs and DAMPs are perceived by pattern recognition receptors (PRRs) that reside in the plasma membrane (Figure 1) (Jones and Dangl, 2006; Boller and Felix, 2009). Upon perception of MAMPs or DAMPs, MTI is activated leading to a variety of cellular responses (Boller and Felix, 2009). The defence responses induced upon either MAMP or DAMP recognition are very similar and only differ in their threshold, timing and amplitude (Yu *et al.*, 2017). The induced immune responses can be classified as early and late responses. Early responses are induced within minutes up to half an hour and include the influx of Ca^{2+} ions into the cytosol, the generation of reactive oxygen species (ROS) by plasma membrane localized NADPH oxidases, phosphorylation of proteins such as mitogen-activated protein kinases (MAPKs) or calcium dependent protein kinases (CDPKs) and transcriptional reprogramming (Boller and Felix, 2009). The activation of late responses occurs within hours and days and includes the inhibition of seedling growth and deposition of callose at the cell wall (Boller and Felix, 2009). PTI is effective against a broad spectrum of pathogens. However, pathogens have evolved strategies to overcome PTI by secreting effector molecules leading to effector triggered susceptibility (ETS) (Figure 1) (Jones and Dangl, 2006). Effectors are molecules that have the ability to change cell structures as well as cell functions and facilitate infection (Selin *et al.*, 2016). They can be active in different cellular compartments and can either act in the apoplast (apoplastic effectors) or in the cytosol (cytoplasmic effectors) (Kamoun, 2006). To secrete effectors, fungal pathogens use haustoria or internal hyphae, while bacterial effectors are delivered directly into the host cell via the type III secretion system (Chatterjee *et al*., 2013; Selin *et al*., 2016). Upon secretion, effector molecules can interfere with PTI

in various ways. Effectors are able to inhibit the kinase activity of certain PRRs (Xiang *et al.*, 2008), dephosphorylate MAPK to inhibit further downstream signaling (Zhang *et al.*, 2007), disturb vesicle trafficking (Block *et al*., 2008) or prevent the accumulation of the phytohormone salicylic acid, that is involved in defence against biotrophic pathogens (Block *et al*., 2008). In turn, plants evolved intracellular R-proteins to recognize effectors directly or indirectly by monitoring the status of host targets (Jones and Dangl, 2006) (Figure 1). R-proteins typically contain a nucleotide-binding (NB) domain and a leucine rich repeat (LRR) domain but differ in their N-terminal domain. The N-terminal domain of R-proteins can either contain a Toll, interleukin1-receptor (TIR) or a coiled-coiled (CC) domain (Dodds and Rathjen, 2010). The detection of effectors or the activity of effectors leads to a strong and rapid activation of defence responses which is referred to as effector triggered immunity (ETI) (Figure 1). Defence responses induced upon effector recognition strongly overlap with MAMP/DAMP induced responses but are typically stronger and include a hypersensitive response (HR). HR is programmed cell death and stops the growth of biotrophic pathogens (Jones and Dangl, 2006).

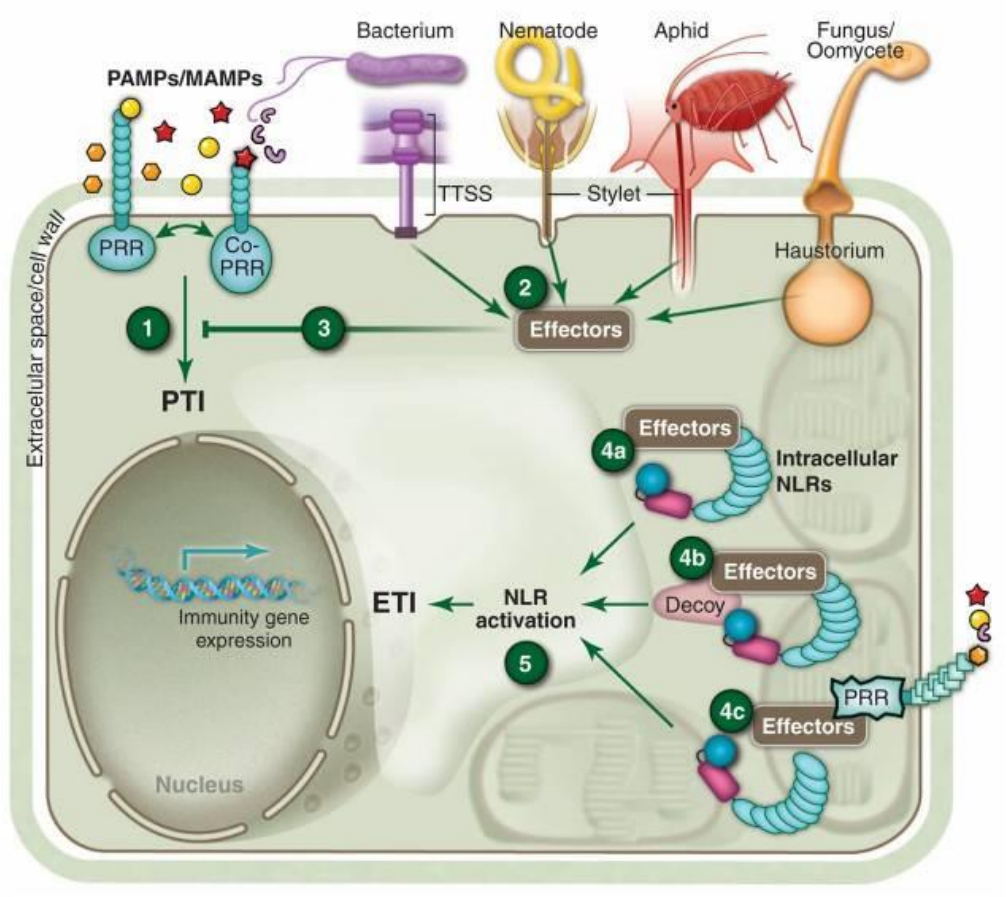

Figure 1. Schematic overview of the two-layered plant immune system. Plasma membrane located pattern recognition receptors (PRRs) perceive pathogen- or microbe associated molecular patterns (PAMPs/MAMPs) which results in the activation of PAMP-triggered immunity (PTI) (1). Pathogens evolved effector molecules that are secreted into the plant cell (2) to suppress PTI (3). The successful suppression of PTI results in effector triggered susceptibility (ETS). Plants, in turn, evolved R-proteins containing a nucleotide-binding domain and a leucine rich repeat domain (NLRs) to detect effectors either directly (4a) or indirectly (4b and 4c). Upon NLR activation (5), effector triggered immunity (ETI) is activated. The figure was adapted from Dangl *et al.*, 2013.

1.2 The plant cell wall

1.2.1 The structure of the cell wall

Plant cells are surrounded by a cell wall which is found between the plasma membrane and the middle lamella (Figure 2). The plant cell wall does not only provide shape to the cell but also retains flexibility for cell division. It is involved in intercellular adhesion and communication as the cell wall of young cells is porous and thus allows diffusion of water, hormones and low-molecular weight nutrients (Burton *et al.*, 2010). Furthermore, the plant cell wall forms a structural barrier against various biotic as well as abiotic stresses (Malinovsky *et al.*, 2014).

Typically, two different types of the plant cell wall can be distinguished: the primary and the secondary cell wall. Young growing cells are enclosed by primary cell walls, while secondary cell walls surround cells that have stopped to grow and to divide (Keegstra, 2010; Burton *et al.*, 2010). Both, the primary and the secondary cell wall are composed of a complex matrix of diverse polysaccharides and a comparatively small amount of secreted, cell wall-specific proteins (Lagaert *et al.*, 2009; Zhong and Ye, 2015). The three main classes of polysaccharides found in plant cell walls are cellulose, hemicelluloses and pectic polysaccharides. In brief, cellulose is cross linked to hemicelluloses and embedded in a matrix of pectin (Figure 1) (Lagaert *et al.*, 2009). Notably, although cell walls are composed of these three polysaccharides, the fine structure as well as the three dimensional structure of the plant cell wall differs considerably between different species and different tissues (Burton *et al.*, 2010; Malinovsky *et al.*, 2014).

Cellulose is the most abundant component in primary and secondary cell walls of monocots and dicots and is a homopolymer consisting of β-1,4-linked glucose monomers. The glucan chains are synthesized individually at the plasma membrane by the cellulose synthase complex that consists of cellulose proteins and other protein complex partners (Keegstra, 2010; McFarlane *et al.*, 2014). Upon synthesis, the glucan chains are able to crystallize into cellulose microfibrils by van der Waals forces or by forming hydrogen bonds (McFarlane *et al.*, 2014). The crystallinity, length and the angle of the cellulose microfibrils in the cell wall mainly determine the physical properties of the cell wall as cellulose is the main polysaccharide (McFarlane *et al.*, 2014).

Hemicelluloses are connected to cellulose microfibrils via hydrogen bonds and are thought to further interconnect and strengthen the cellulose network (Figure 1) (McFarlane *et al.*, 2014). Hemicelluloses represent a diverse group of polysaccharides including xyloglucan, heteroxylans, heteromannans and mixed linkage glucans (MLGs). Disregarding MLGs, hemicelluloses are typically composed of a backbone of β-1,4-linked hexosyl residues that can be further substituted with various side chains (Pauly *et al.*, 2013). The major hemicellulose present in the primary cell wall of dicots is xyloglucan (Scheller and Ulvskov, 2010). Xyloglucan consists of a backbone of β-1,4-linked glucose monomers that are decorated with xylosyl residues. In several species, three glycosyl residues are substituted with xylose followed by one unsubstituted glycosyl residue (Park and Cosgrove, 2015). The xylosyl residue can be further substituted with e.g. fucose, galactose, xylose or galacturonic acid (Schultink *et al.*, 2014). Another group of hemicelluloses are heteroxylans. Heteroxylans are the most abundant hemicelluloses in monocot cell walls and secondary cell walls of dicots. Generally, heteroxylans are

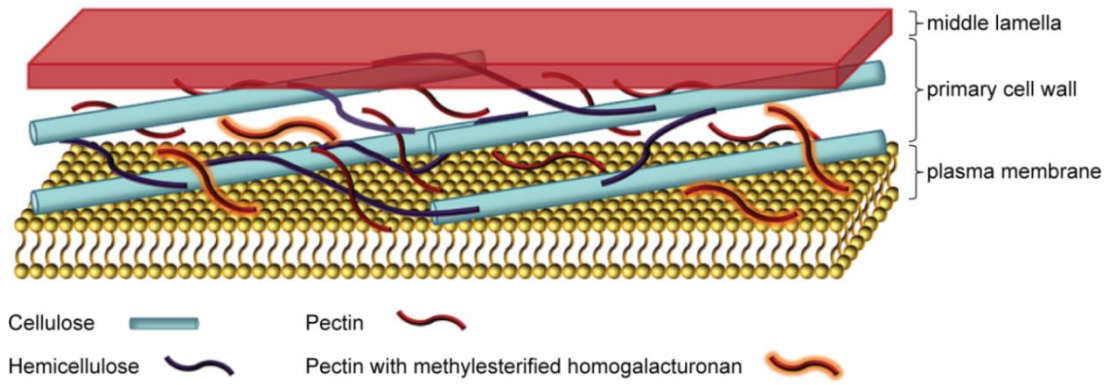

Figure 2. The structure of the primary cell wall. The primary cell wall is composed of cellulose microfibrils, hemicelluloses and pectic polysaccharides. The figure legend and the figure were modified from Malinovsky *et al.*, 2014.

composed of a linear backbone of xylose. The xylose chains can be substituted with various residues e.g. glucuronosyl or arabinose depending on the species and the tissue (Scheller and Ulvskov, 2010). For example, glucuronoxylan has a xylose backbone substituted with glucuronosyl and methyl glucuronosyl residues and is mainly found in dicots, whereas glucuronoarabinoxylan contains arabinofuranosyl as well as methyl-glucuronosyl residues and is mainly found in monocots (Scheller and Ulvskov, 2010; Pauly *et al.*, 2013). The hemicelluloses classified as heteromannans can be further divided into four classes, namely mannan, glucomannan, galactomannan and galactoglucomannan (Pauly *et al.*, 2013). The backbone of mannan and galactomannan is composed of β-1,4-linked mannose, while glucomannan and galactoglucomannan are composed of glucose and mannose residues. Furthermore, galactosyl residues can be found as side chains in galactomannan as well as galactoglucomannan (Scheller and Ulvskov, 2010). The synthesis of hemicelluloses occurs in the Golgi apparatus and involves several glycosyl transferases (GTs) for the synthesis of mannans and heteroxylans as well as cellulose synthase like family C (CSLC) genes for the synthesis of xyloglucans (Scheller and Ulvskov, 2010; Pauly *et al.*, 2013). MLGs represent an untypical class of hemicelluloses since they are composed of unsubstituted glucose monomers that are connected through both β-1,3- and β-1-4-linkages resulting in a β-1,3;1,4-polymer. Usually, cellotriosyl or cellotetrasyl units are connected through β-1,3-linkages (Burton and Fincher, 2014). In higher plants, MLGs are only present in the cell wall of grasses (Pauly *et al.*, 2013). The grass-specific CSL gene families *CSLF* of rice and *CSLH* in barley were shown to be involved in MLG synthesis (Burton *et al.*, 2006; Doblin *et al.*, 2009).

Pectic polysaccharides represent the most complex cell wall polysaccharide and can be subdivided into three groups, namely homogalacturonan, rhamnogalacturonan I and rhamnogalacturonan II (Atmodjo *et al.*, 2013). Homogalacturonan and rhamnogalacturonan II are composed of an α-1,4-linked galacturonic acid backbone. In contrast to homogalacturonan which is only partially methylesterified or acetylated, rhamnogalacturonan II can be substituted with four different side chains consisting of 12 different glycosyl residues e.g. methyl xylose (Caffall and Mohnen, 2009; Patova *et al.*, 2014). Rhamnogalacturonan I consists of a backbone of alternating rhamnose and

galacturonic acid in which galacturonic acid residues can be acetylated. Rhamnogalacturonan I can further be substituted with e.g. arabinan or galactan depending on the cell type and developmental stage (Atmodjo *et al.*, 2013; Patova *et al.*, 2014). Synthesis of pectic polysaccharides takes place in the Golgi and involves several GTs, methyltransferases and acetyltransferases (Atmodjo *et al.*, 2013). Pectic polysaccharides are less prominent in secondary cell walls compared to primary cell walls (Caffall and Mohnen, 2009; Malinovsky *et al.*, 2014). However, secondary cell walls are further reinforced with lignin to enhance the mechanical support (Zhong and Ye, 2015).

1.2.2 The role of the plant cell wall in plant immunity

The plant cell wall is not only a passive physical barrier but is also actively modified and reinforced upon pathogen attack (Underwood, 2012). The phenolic polymer lignin is deposited in the cell wall upon pathogen attack and is thought to be involved in cell wall reinforcement (Bellincampi *et al.*, 2014). Also, callose-enriched appositions, called papillae, are formed in close proximity to fungal penetration sites between the cell wall and the plasma membrane (Bacete *et al.*, 2018). Besides the β-1,3-glucan callose, papillae are composed of pectic polysaccharides, xyloglucan, cell wall structural proteins, peroxidases, ROS and phenolic compounds including lignin (Underwood, 2012). Papillae are thought to reinforce the plant cell wall and thus, slow down invasion of a pathogen. However, the impact of papillae formation and especially callose deposition on plant immunity is not clear (Voigt, 2014; Bacete *et al.*, 2018). Nevertheless, it was shown that the effectiveness of papillae depends on the composition. Papillae that hinder penetration of the obligate powdery mildew *Blumeria graminis* f.sp. *hordei* (*Bgh*) in barley contain a higher amount of cellulose, callose and arabinoxylan compared to papillae that could not stop penetration of the powdery mildew (Chowdhury *et al.*, 2014). Additionally, β-1,3-glucan oligosaccharides were shown to induce immune responses including the influx of Ca^{2+} ions and the activation of MAPK in *A. thaliana* (Mélida *et al.*, 2018). In *Nicotiana tabacum* as well as in *Vitis vinifera*, the β-1,3-glucan polymer laminarin was shown to induce e.g. generation of ROS and expression of defence genes (Klarzynski *et al.*, 2000; Aziz *et al.*, 2003). Although elicitor active β-1,3-glucans might derive from fungal cell walls as it is an abundant fungal cell wall component, it might be possible that callose in papillae represent a source for DAMPs (Mélida *et al.*, 2018).

Besides modifying the plant cell wall, the status of the plant cell wall is monitored. Defence responses are activated upon changes in expression or activity of proteins that play in role in cell wall remodeling and/or synthesis. These alterations can occur upon cell wall damage induced by pathogens (Bacete *et al.*, 2018). Furthermore, the plant cell wall represents a source for DAMPs that may be generated upon action of CWDEs (Bacete *et al.*, 2018). The probably best-studied DAMPs are OGs. OGs are likely derived upon degradation of the pectic polysaccharide homogalacturonan by polygalacturonases (Ferrari *et al.*, 2013). During the early stages of infection, pectin degrading enzymes are secreted and start hydrolyzing pectic polysaccharides. However, plants have polygalacturonase inhibiting proteins (PGIPs) that inhibit the activity of pectin degrading enzymes and

thereby favor the generation of PTI inducing OGs (De Lorenzo and Ferrari, 2002; Ferrari *et al.*, 2013; Bellincampi *et al.*, 2014). OGs with a length of 10 - 15 were shown to be elicitors of defence responses in plants (Ferrari *et al.*, 2007; Denoux *et al.*, 2008), although shorter fragments with less than 10 residues also exhibit elicitor activity (Davidsson *et al.*, 2017). Upon perception of OGs, the generation of ROS, the phosphorylation of MAPK6 and MAPK3 as well as the transcriptional reprogramming is induced (Galletti *et al.*, 2008; Galletti *et al.*, 2011; Davidsson *et al.*, 2017). Furthermore, *A. thaliana* plants pre-treated with OGs show an increase in resistance against *Botrytis cinerea* and *Pectobacterium carotovorum* (Ferrari *et al.*, 2007; Davidsson *et al.*, 2017). Besides OGs, cellulose-derived oligomers were shown to induce immune responses in *A. thaliana*. Upon treatment of *A. thaliana* with cellobiose several immune responses are activated including influx of Ca^{2+}, activation of MAPK and transcriptional reprogramming. Pretreatment with cellobiose also increased resistance against the bacterial pathogen *Pseudomonas syringae* pv *tomato* DC3000 (de Azevedo Souza *et al.*, 2017). Furthermore, the hemicellulose xyloglucan was recently identified as DAMP in *A. thaliana* and *V. vinifera*. Xyloglucan triggers the activation of MAPK and the expression of defence-related genes but not the generation of ROS in *A. thaliana* and *V. vinifera* (Claverie *et al.*, 2018). In *Nicotiana benthaminana* and *Oryza sativa*, mannan oligosaccharides with a length of 2-6 residues trigger the influx of Ca^{2+} ions, the generation of ROS, the activation of MAPK and lead to an increase in resistance against pathogens. These results indicate that mannan oligosaccharides act as DAMP (Zang *et al.*, 2019). The fact that *A. thaliana* and other plant species can recognize break down products of the plant cell wall and in turn activate immune responses indicate that plants monitor the status of the cell wall and that changes in the cell wall lead to activation of immune responses (de Azevedo Souza *et al.*, 2017; Bacete *et al.*, 2018).

1.3 Cell wall degrading enzymes

In order to successfully infect a plant, pathogens have to overcome the plant cell wall (Chisholm *et al.*, 2006; Malinovsky *et al.*, 2014). One of the strategies to overcome the cell wall is the secretion of CWDEs. CWDEs are enzymes that can act on and degrade specific components of the cell wall. Thereby, the cell wall structure is loosened which allows the pathogen to enter (Kubicek *et al.*, 2014). CWDEs can be classified into different enzyme classes based on their function, namely carbohydrate esterases (CEs), polysaccharide lyases (PLs), glycoside hydrolases (GHs) and carbohydrate-binding modules (CBMs) (Carbohydrate Active Enzymes database, http://www.cazy.org/, Lombard *et al.*, 2014). The different enzyme classes can be further divided into families based on sequence similarities which originated from the classification of GHs (Henrissat, 1991). The annotation of enzymes to families according to sequence similarities is based on the concept that the three dimensional structure of a protein depends on the amino acid sequence and that the structure of a protein determines its function (Davies and Henrissat, 1995). Currently, CEs comprise 17 families, while 40 families for PLs and more than 160 families for GHs are described (Carbohydrate Active Enzymes database, http://www.cazy.org/, Lombard *et al.*, 2014).

CEs are involved in the release of ester-linked acyl groups of substituted carbohydrates, e.g. in pectin methyl esters or acetylated xylan. Furthermore, cutinases that act on cutin are classified as CEs (Nakamura *et al.*, 2017). CEs may use different reaction mechanisms but the most common one is the deacetylation mediated by a serine-histidine-aspartic acid catalytic triad, which is similar to the mechanism employed by lipases (Nakamura *et al.*, 2017). The release of the acylated residues is believed to allow degradation of these polysaccharides since it may facilitate the access of GHs to the polysaccharide (Christov and Prior, 1993).

PLs cleave polysaccharides containing uronic acid, e.g. pectic polysaccharides and hydrolyse β-1,4-linkages via a β-elimination mechanism, which is a three stage reaction (Garron and Cygler, 2014). Briefly, as a first step, the carboxyl group of the substrate is neutralized and subsequently, a proton of the fifth carbon atom of the uronic acid is subtracted and an intermediate is formed. As a last step, electrons are removed from the carboxylic group of the substrate which results in the formation of a double bond between the fourth and fifth carbon atom of the substrate and consequently in the cleavage of the glycosidic bond (Michaud *et al.*, 2003).

The hydrolysis of glycosidic linkages in glycosides, e.g. cellulose or xylose, is catalyzed by proteins classified as GH (Vuong and Wilson, 2010). Typically, two reaction mechanisms are found in GHs, which classify them as either retaining GH or inverting GH. With few exceptions, either retaining or inverting GHs are found in one family (Koshland, 1953; Vuong and Wilson, 2010; Ardèvol and Rovira, 2015). Inverting GHs, use a one-step catalysis in which the nucleophilicity of a water molecule is enhanced by the enzymatic residue acting as base. The water molecule attacks the anomeric center and facilitates cleavage of the glycosidic bond (Figure 3 A) (Vuong and Wilson, 2010). Retaining GHs, however, use a two-step mechanism to catalyze the hydrolysis (Figure 3 B). First, a proton is donated from the enzymatic acid residue to the oxygen atom of the substrate and the nucleophile of the enzyme attacks the anomeric center of the substrate. As a consequence, the intermediate is covalently bound to the enzyme and a glycosyl enzyme intermediate is formed. Next, the deprotonated carboxylate behaves as a base and facilitates together with an activated water molecule the hydrolysis of the glycosyl enzyme intermediate resulting in the release of the product (Vuong and Wilson, 2010).

CBMs do not possess catalytic activity themselves, however, are involved in binding of carbohydrates. They can be found at the C- or N-terminus of a CWDE or a carbohydrate active enzyme involved in the synthesis of carbohydrates. CBMs can increase the hydrolytic activity of an enzyme by directing the enzyme to its substrate (Shoseyov *et al.*, 2006).

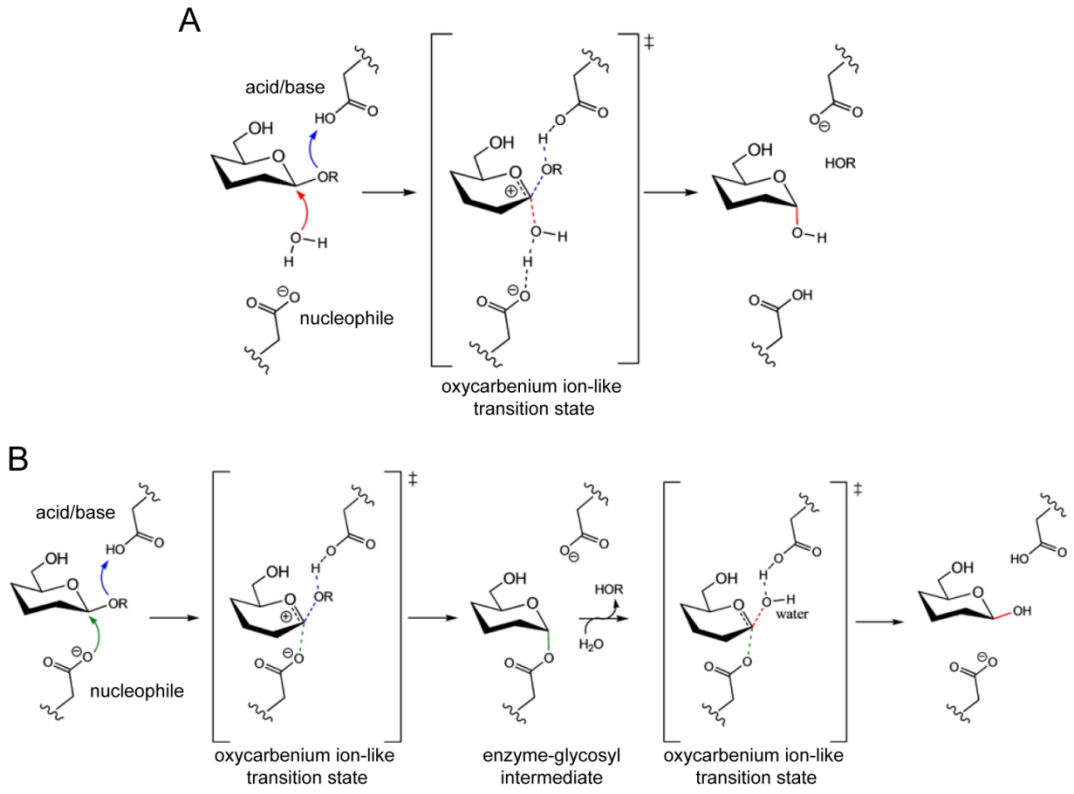

Figure 3. Mechanism of glycoside hydrolysis by GH. (A) Hydrolysis mechanism of inverting GH. (B) Hydrolysis mechanism of retaining GH. Figure and figure legend were modified from Ardèvol and Rovira, 2015.

1.4 The role of CWDEs in fungal pathogenicity

Fungal genomes harbour several genes encoding for CWDEs including CEs, GHs that can deconstruct cellulose, hemicelluloses and pectic polysaccharides as well as PLs that act on uronic acid-containing polysaccharide, e.g. on rhamnogalacturonan (Kubicek *et al.*, 2014). However, genome analyses revealed that the arsenal of CWDEs differs between fungal species and that this difference might reflect the lifestyle as well as host specificity of the fungus (King *et al.*, 2011; Zhao *et al.*, 2014). Fungi that infect dicot species are characterized by a higher number of enzymes degrading pectic polysaccharides than fungi infecting monocot plants (Zhao *et al.*, 2014). This observation reflects the fact that cell walls of dicot species contain more pectin than cell walls of monocot species (Kubicek *et al.*, 2014). Furthermore, the number of genes encoding for CWDEs is higher in necrotrophic and hemibiotrophic fungi that eventually kill their host compared to the number of CWDE genes identified in biotrophic fungi, which rely on the living host and typically employ a stealth strategy for infection (Zhao *et al.*, 2014). The obligate biotrophic fungus *Bgh* is the causal agent of powdery mildew on barley. A genome study conducted in 2010 showed that the genome of *Bgh* is characterized by a dramatically reduced number of genes encoding for enzymes involved in cell wall degradation. In this study, *Bgh* was shown to be equipped with only two lignocellulose-degrading enzymes, four hemicellulose degrading enzymes and one pectin β-1,3-glucan hydrolyzing enzyme but does not possess cellulose-, xylan- or pectin-degrading enzymes (Spanu *et al.*, 2010).

1.5 Perception of MAMPs and DAMPs by PRRs

So far, all known plant PRRs that perceive MAMPs or DAMPs are located at the plasma membrane and are either receptor-like kinases (RLKs) or receptor-like proteins (RLPs) (Macho and Zipfel, 2014; Mélida *et al.*, 2018). RLKs contain an intracellular kinase domain, a single-pass transmembrane domain as well as an ectodomain that is involved in ligand perception. RLPs resemble RLKs structurally, however, they lack an intracellular kinase domain and the attachment to the plasma membrane of RLPs can be facilitated by a transmembrane domain or a GPI-anchor (Monaghan and Zipfel, 2012; Macho and Zipfel, 2014). RLKs and RLPs can be grouped into different categories depending on the domains present in the ectodomain. They can contain leucine-rich repeat domains (LRRs), lysin motifs (LysMs), epidermal growth factor (EGF) domains or lectin motifs. While LRR domain containing RLKs and RLPs were shown to perceive proteinaceous MAMPs, e.g. bacterial flagellin (flg), RLKs or RLPs that contain LysM, EGF-like domains or lectin motifs recognize carbohydrate MAMPs, e.g. fungal chitin (Macho and Zipfel, 2015; Tang *et al.*, 2017). As RLPs lack an intracellular kinase domain, they likely associate with co-receptor RLKs to induce signal transduction. Additionally, the formation of homo- and heterocomplexes of RLK- and RLP-PRRs at the plasma membrane has been shown to be important for ligand perception and signal transduction (Macho and Zipfel, 2014). To transduce the signal from the plasma membrane to downstream signaling components, PRRs and their complex partners need cytoplasmic partners. Receptor-like cytoplasmic kinases (RLCK), that lack an extracellular domain, were shown to be direct targets of PRR complexes and involved in signal transduction (Liang and Zhou, 2018).

1.5.1 Peptide MAMP perception by LRR-RLKs

One example for a well-studied LRR-RLK is FLAGELLIN SENSING 2 (FLS2). The LRR-RLK FLS2 perceives the bacterial MAMP flg, the major component of bacterial flagella. FLS2 mediates flg perception in several plant species including Arabidopsis, rice, tomato and tobacco (Gómez-Gómez and Boller, 2000; Robatzek *et al.*, 2007; Hann and Rathjen, 2007; Takai *et al.*, 2008). An N-terminal epitope of flg consisting of 22 amino acids (flg22) is sufficient for perception via FLS2 and the subsequent induction of immune responses (Gómez-Gómez and Boller, 2000; Chinchilla *et al.*, 2006). The influx of Ca^{2+} ions, the generation of ROS, the activation of MAPK and transcriptional reprogramming represent typical immune responses initiated upon flg22 perception (Monaghan and Zipfel, 2012). Plants that do not have a functional FLS2 were shown to be more susceptible towards bacterial pathogens (Zipfel *et al.*, 2004).

The LRR-RLK ELONGATION FACTOR THERMO UNSTABLE RECEPTOR (EFR) is another well-characterized PRR. EFR perceives the bacterial elongation factor TU (EF-TU), which is highly conserved in bacteria (Zipfel *et al.*, 2006). Epitopes of either 26 or 18 amino acids present at the acetylated N-terminus of EF-TU (elf26 or elf18) are sufficient to trigger MAMP-induced responses (Kunze *et al.*, 2004). The responses induced upon elf18 perception are very similar to responses

induced by flg22. Furthermore, loss of EFR in *A. thaliana* results in an enhanced susceptibility towards *Agrobacterium tumefaciens* (Zipfel *et al.*, 2006).

In the last years, it became apparent that PRRs do not act alone but are present in multi-protein complexes at the plasma membrane (Monaghan and Zipfel, 2012; Macho and Zipfel, 2014). The BRI1-ASSOCIATED KINASE1/SOMATIC EMBRYOGENESIS RECEPTOR KINASE 3 (BAK1/SERK3) was initially shown to be involved in brassinosteroid (BR) signaling as a positive regulator of the BR receptor BR INSENSITIVE 1 (BRI1) (Nam and Li, 2002; Li *et al.*, 2002). Furthermore, BAK1 plays a role in immune signaling as an essential component of PRR LRR-RLK complexes (Liebrand *et al.*, 2014). Thus, a defect in BAK1 results in compromised responses towards BR and MAMPs (Li *et al.*, 2002; Chinchilla *et al.*, 2007; Roux *et al.*, 2011). BAK1 is a kinase active LRR-RLK with a short cytoplasmic domain (Liebrand *et al.*, 2014). It directly interacts with the flg22 receptor FLS2 and the elf18 receptor EFR in a ligand dependent manner (Chinchilla *et al.*, 2007; Roux *et al.*, 2011). Upon ligand perception, a heterodimer between BAK1 and either EFR or FLS2 is formed and transphosphorylation events at the intracellular domains occur (Chinchilla *et al.*, 2007; Roux *et al.*, 2011; Heese *et al.*, 2007; Schulze *et al.*, 2010). The transphosphorylation events between BAK1 and the respective PRR LRR-RLK also involve the RLCK BOTRYTIS-INDUCED KINASE 1 (BIK1). BIK1 directly interacts with FLS2, EFR and BAK1. Upon flg22 perception, BIK1 is phosphorylated by BAK1 and subsequently, phosphorylates FLS2 and BAK1. After the transphosphorylation events, BIK1 is released from the complex and activates downstream signaling (Lu *et al.*, 2010; Zhang *et al.*, 2010).

Several LRR-RLPs have been identified as immune receptors in the last years (Jehle *et al.*, 2013a; Jehle *et al.*, 2013b; Zhang *et al.*, 2013; Zhang *et al.*, 2014; Albert *et al*., 2015). As RLPs lack an intracellular kinase domain, they require a signaling partner to transduce the signal upon ligand perception. The LRR-RLK SUPPRESSOR OF BIR1-1/EVERSHED (SOBIR1/EVR) was shown to interact constitutively with several LRR-RLP in tomato and *A. thaliana* and to be required for their function in plant immunity (Liebrand *et al.*, 2013; Jehle *et al.*, 2013a; Zhang *et al.*, 2013; Zhang *et al.*, 2014). RLPs that form a complex with RLKs are supposed to be bimolecular equivalents to RLKs (Gust and Felix, 2014). In Arabidopsis, the LRR-RLPs RLP1/ReMAx, RLP30, RLP23 as well as RLP42/RBPG1 have been shown to contribute to immunity in a SOBIR1-dependent manner. RLP1/ReMAX perceives the *Xanthomonas campestris* peptide MAMP eMAX. A *sobir* mutant lacks the ability to respond to eMAX demonstrating that SOBIR1 is involved in eMAX perception (Jehle *et al.*, 2013a; Jehle, *et al.*, 2013b). NECROSIS- AND ETHYLENE INDUCING PEPTIDE 1 (NEP1)-LIKE PROTEINs (NLPs) are peptidic MAMPs that trigger leaf necrosis. A conserved peptide of 20 amino acids from NLPs (nlp20) is sufficient to induce immune responses and is perceived by RLP23. RLP23 is constitutively found in a complex with SOBIR1 that mediates signal transduction (Bi *et al.*, 2014; Albert *et al*., 2015). The SCLEROTINIA CULTURE FILTRATE ELICITOR1 (SCFE1) is a proteinaceous elicitor from *Sclerotinia sclerotiorum* that triggers typical MAMP responses in Arabidopsis and is perceived by RLP30. The activation of typical MAMP responses was shown to be dependent on SOBIR1 as *sobir* mutants show compromised immune responses upon SCFE1 treatment (Zhang *et al.*, 2013). Furthermore, fungal endopolygalacturonases act as MAMP and are perceived by RLP42/RBPG1. In agreement with the model, RLP42/RBPG1 was shown to

constitutively interact with SOBIR1 independent from ligand perception and is essential for RBPG1-mediated responses (Zhang *et al.*, 2014). Interestingly, BAK1 is also required for the perception of nlp20, SCFE1 and fungal polygalacturonases (Zhang *et al.*, 2013; Zhang *et al.*, 2014; Albert *et al*., 2015).

1.5.2 Perception of carbohydrate MAMPs by LysM domain containing RLKs

The LysM domain represents a CBM that is important for binding *N*-acetylglucosamine. In plants, LysM domain containing RLKs have been demonstrated to be involved in symbiosis or plant defence (Antolín-Llovera *et al.*, 2014).

The fungal cell wall component chitin is composed of β-1,4-linked *N*-acetylglucosamine (Muzzarelli, 1977). Polymeric as well as oligomeric chitin can act as MAMP and induce defence responses in plants (Boller and Felix, 2009).

In *O. sativa*, chitin perception and subsequent signal transduction is facilitated by CHITIN ELICTOR BINDING PROTEIN (*Os*CEBiP) and CHITIN ELICITOR RECEPTOR-LIKE KINASE1 (*Os*CERK1). The plasma membrane residing LysM RLP *Os*CEBiP is the main chitin receptor and directly binds chitin via its second LysM domain (Kaku *et al.*, 2006; Shimizu *et al.*, 2010; Hayafune *et al.*, 2014). One chitin molecule can bind to two *Os*CEBiP molecules which leads to the formation of a homodimer. The homodimer might then associate with two molecules of the LysM-RLK *Os*CERK1 for signal transduction (Hayafune *et al.*, 2014; Shinya *et al.*, 2015). Silencing of *Os*CEBiP and *Os*CERK1 leads to a reduction in chitin-induced defence responses and an increase in susceptibility towards fungal pathogens (Kaku *et al.*, 2006; Kishimoto *et al.*, 2010; Shimizu *et al.*, 2010; Kouzai *et al.*, 2014a; Kouzai *et al.*, 2014b). Besides *Os*CERK1 and *Os*CEBiP, the *Os*RLCK185 can be found in the receptor complex. *Os*RLCK185 is phosphorylated upon chitin perception and triggers subsequent signaling events (Yamaguchi *et al.*, 2013; Wang *et al.*, 2017).

In *A. thaliana*, the LysM-RLK CHITIN ELICITOR RECEPTOR LIKE KINASE1 (CERK1) is crucial for chitin perception and confers resistance to fungal pathogens. Arabidopsis mutants lacking functional CERK1 are dramatically compromised in chitin induced immune responses e.g. the generation of ROS and show enhanced susceptibility towards fungal pathogens (Miya *et al.*, 2007; Wan, *et al.*, 2008b). The ectodomain of CERK1 harbours three LysM domains of which the second LysM domain was shown to directly bind chitin (Miya *et al.*, 2007; Liu *et al.*, 2012b). Binding of polymeric chitin or chitin octamers facilitates homodimerization of CERK1 and consequent phosphorylation of the intracellular domain (Petutschnig *et al.*, 2010; Liu *et al.*, 2012b). As shorter chitooligomers can bind to CERK1 but do not induce CERK1 phosphorylation and consequent immune responses, phosphorylation of CERK1 seems to be indispensable for signal transduction and activation of immune responses (Petutschnig *et al.*, 2010; Liu *et al.*, 2012b). Three *Os*CEBiP-related proteins are present in Arabidopsis, namely LYM1, LYM2 and LYM3 (LysM-containing receptor-like proteins 1-3) (Antolín-Llovera *et al.*, 2014). LYM1 and LYM3 were demonstrated to be involved in bacterial peptidoglycan signaling (Willmann *et al.*, 2011). The closest homolog of *Os*CEBiP, LYM2, binds chitin,

however, is not required for the activation of chitin-triggered immune responses but regulates plasmodesmata flux in response to chitin (Shinya *et al.*, 2012; Faulkner *et al.*, 2013). In a proteomics approach, the LysM-RLKs LYK4 and LYK5 were shown to have chitin binding activity and represent possible receptor complex partners of CERK1 (Petutschnig *et al.*, 2010). Although both, LYK4 and LYK5, have an intracellular kinase domain, they lack kinase activity (Wan *et al.*, 2012; Cao *et al.*, 2014). The knock-out mutant *lyk4*-1 shows a reduction in chitin induced responses, e.g. induction of chitin responsive genes, demonstrating the involvement of LYK4 in chitin signaling (Wan *et al.*, 2012). The role of LYK5 in chitin signaling, however, is ambiguous. A T-DNA mutant in the Landsberg (Ler) background (*lyk5*-1) does not show a reduced induction of *WRKY53* or *MAPK3* upon chitin treatment (Wan *et al.*, 2008b; Wan *et al.*, 2012), but a minor reduction in CERK1 phosphorylation and MAPK activation (Cao *et al.*, 2014). In contrast, a second T-DNA mutant in the Columbia-0 (Col-0) background (*lyk5*-2) shows reduction of chitin induced responses, e.g. Ca^{2+} influx (Cao *et al.*, 2014). The single mutants of *lyk4*-1 and *lyk5*-2 do not resemble the *cerk1*-2 mutant regarding the reduction of the chitin-triggered immune responses, however, the *lyk5*-2 *lyk4*-1 double mutant showed the same reduction in chitin triggered ROS generation and MAPK activation as *cerk1*-2 (Cao *et al.*, 2014). This demonstrates a role of LYK4 and LYK5 in chitin perception as well as functional redundancy of LYK4 and LYK5 (Cao *et al.*, 2014). Furthermore, LYK5 was shown to form homodimers in the plasma membrane in a ligand-independent manner and to associate with CERK1 upon chitin perception (Cao *et al.*, 2014). Based on these results, Cao et al (2014) proposed a new model for chitin perception: LYK5 is present at the plasma membrane as a homodimer without a stimulus. Upon chitin perception, LYK5 binds to CERK1 to form a heterotetramer consisting of two LYK5 and two CERK1 molecules. Consequently, CERK1 will be phosphorylated which is required for signal transduction (Cao *et al.*, 2014).

Another carbohydrate MAMP is peptidoglycan. It is an abundant cell wall component of Gram-positive and Gram-negative bacteria and is composed of alternating β-1,4-linked *N*-acetylglucosamine and *N*-acetylmuramic acid moieties (Lovering *et al.*, 2012). In tobacco, rice and Arabidopsis peptidoglycan act as a MAMP, however, receptors for peptidoglycan have only been identified in rice and Arabidopsis (Gust, 2015). In rice, the two LysM-RLPs *Os*LYP4 and *Os*LYP6, which are homologs of *Os*CEBiP, as well as *Os*CERK1 are required for peptidoglycan perception (Liu *et al.*, 2012a; Ao *et al.*, 2014). Silencing of either *Os*LYP4 or *Os*LYP6 results in a reduction of peptidoglycan induced responses and higher susceptibility towards bacterial pathogens (Liu *et al.*, 2012a). In the absence of a stimulus, *Os*LYP4 and *Os*LYP6 form a complex at the plasma membrane. Upon peptidoglycan perception, *Os*LYP4 and *Os*LYP6 dissociate and recruit *Os*CERK1 for signal transduction (Ao *et al.*, 2014). In Arabidopsis, LYM1 and LYM3 as well as CERK1 were shown to be critical components of peptidoglycan perception. LYM1 and LYM3 reside in the plasma membrane and might build a peptidoglycan binding module. Upon peptidoglycan binding, CERK1 is recruited and might be required to transduce the signal from the extracellular to the intracellular space (Willmann *et al.*, 2011).

Since CERK1 is involved in the perception of several carbohydrate MAMPs, it was proposed that CERK1 acts as a co-receptor in plasma membrane complexes analogously to BAK1 (Gimenez-Ibanez *et al.*, 2009; Postel and Kemmerling, 2009).

1.5.3 Perception of DAMPs

Besides MAMPs, plants can perceive host derived DAMP molecules which lead to the activation of immune responses. In 2006, a family of plant peptides in Arabidopsis was identified that induce the activation of immune responses, namely Peps (plant elicitor peptides) (Huffaker *et al.*, 2006). Active Peps might be derived from the precursor peptides PROPEPs which are small proteins of about 100 amino acids. However, whether PROPEPs need to be cleaved for activation is still under debate (Bartels and Boller, 2015). In Arabidopsis, the family of PROPEPs comprises eight members. All eight Peps were shown to be able to induce immune responses which were dependent on the plasma membrane residing LRR-RLKs PEP receptor 1 (PEPR1) and PEPR2. Consequently, a double mutant lacking PEPR1 and PEPR2 was shown to be insensitive to all Peps (Huffaker *et al.*, 2006; Yamaguchi *et al.*, 2006; Bartels *et al.*, 2013). Similar to FLS2 and EFR, PEPRs associate with the co-receptor BAK1 upon binding of the elicitor to the LRR domain and both, BAK1 and PEPRs, are subsequently phosphorylated similar to FLS2 and EFR (Tang *et al.*, 2015). Furthermore, the RLCK BIK1 is present in the receptor complex and gets phosphorylated upon ligand binding. Subsequently, BIK1 might dissociate from the complex and mediate downstream signaling (Liu *et al.*, 2013). PROPEPs have also been identified in several angiosperms including crop plants (Bartels and Boller, 2015).

Short fragments composed of α-1,4-linked galacturonic acid, called OGs, represent probably the best characterized plant DAMP and were already shown to induce immune responses in the 1980s (Ferrari *et al.*, 2013). OGs might be released upon degradation of the cell wall component homogalacturonan by microbial polygalacturonases (Ferrari *et al.*, 2013). The RLK wall-associated kinase 1 (WAK1) was shown to bind OGs via its N-terminal pectin binding domain (Decreux and Messiaen, 2005). The binding of OGs to WAK1 was stronger when dimers in a calcium-mediated egg-box confirmation were present (Cabrera *et al.*, 2008). Furthermore, a domain swap approach suggests that WAK1 is involved in the perception of OGs. In a chimera consisting of the WAK1 ectodomain and the EFR kinase domain, the kinase domain was stimulated upon OG elicitation. Furthermore, the WAK1 kinase domain was activated upon elf18 treatment in a chimera consisting of the WAK1 kinase domain and the EFR ectodomain (Brutus *et al.*, 2010).

Recently, β-1,3-glucan oligosaccharides were shown to induce immune responses in Arabidopsis (Mélida *et al.*, 2018). β-1,3-glucans are present in the plant in form of callose but are also abundant in the fungal cell wall, therefore might act as MAMP or DAMP. The mutant *cerk1*-2, lacking the CERK1 receptor, did not show activation of immune responses upon β-1,3-glucan elicitation indicating that CERK1 is involved in β-1,3-glucan oligosaccharides perception (Mélida *et al.*, 2018).

1.6 Thesis Aims

The plant cell wall is built of a complex network of cellulose, various hemicelluloses, pectic polysaccharides and glycoproteins and represents a physical barrier to invasive pathogens. In order to infect a plant, pathogens need to overcome the plant cell wall. To accomplish this, pathogens use penetration structures (appressoria) and/or secrete CWDEs (Chisholm *et al.*, 2006). However, information about the role of CWDEs in the pathogenicity of biotrophic fungi is still missing. Therefore, the first aim of this work was to identify and functionally characterize CWDEs of the obligate biotrophic barley powdery mildew *Bgh* that may be required for pathogenicity. To this end, genomic as well as public available transcriptomic data should be analysed regarding potentially secreted and highly expressed GH families. Selected candidate genes should be expressed heterologously in *Pichia pastoris* and the respective substrates should be identified. Furthermore, the pH optimum and temperature optimum, Michaelis-Menten kinetics as well as the hydrolysis mode of the recombinant proteins should be determined.

The action of CWDEs during the infection process is believed to result in the generation of cell-wall derived oligosaccharides (Bacete *et al.*, 2018). It is conceivable to postulate that plants evolved the capacity to perceive these cell-wall derived oligosaccharides resulting in the activation of immune responses. Thus, the second aim of this project was to identify new cell-wall derived DAMPs. Therefore, a collection of cell-wall derived oligo- and polysaccharides was purchased and analysed with regard to their ability to induce a Ca^{2+} influx in the Arabidopsis ecotype Col-0. As Arabidopsis ecotypes differ in their receptor repertoire, the generation of ROS as well as the activation of MAPK should be analysed upon oligo- or polysaccharide treatment in the three ecotypes Col-0, Wassilewskija-0 (Ws-0) and Ws-4. Furthermore, the DAMP activity of monocot specific poly- and oligosaccharides was analysed in barley by testing the generation of ROS and the activation of MAPK. Upon validation of candidate DAMPs, forward and reverse-genetic approaches should be used to identify molecular components involved in the perception of newly identified DAMP molecules.

2 Material and Methods

2.1 Material

2.1.1 Plants

2.1.1.1 *Arabidopsis thaliana*

T-DNA mutants and transgenic lines that were used in this work are listed in Table 1 and Table 2, respectively. *Arabidopsis thaliana* accessions that were used in this study are listed in Table 3.

Table 1. List of T-DNA insertion and transgenic lines used in this work.

Allele	AGI locus	Accession	T-DNA	Reference/Source
cerk1-2	At3g21630	Col-0	GABI_096F09	Miya *et al.*, 2007
fls2c	AT5G46330	Col-0	SAIL_691_C4	Cyril Zipfel
efr1	At5g20480	Col-0	SALK_044334	Zipfel *et al.*, 2006
bak1-4	AT4G33430.2	Col-0	SALK_116202	Chinchilla *et al.*, 2007
bak1-5	AT4G33430.2	Col-0	-	Schwessinger *et al.*, 2011
sobir1-12	AT2G31880.1	Col-0	SALK_050715	-
sobir1-14	AT2G31880.1	Col-0	GABI-Kat_643F07	-
lyk5-2 lyk4-2	At2g33580 At2g23770	Col-0	SALK_131911C GABI_897A10	PhD Thesis, Jan Erwig
lyk2-1	AT3G01840	Col-0	SALK_152226	-
lym2-1	At2g12170	Col-0	SAIL 343B03	Shinya *et al.*, 2012
lym2-4	At2g12170	Col-0	GABI-Kat 165 H02	-
lyt1-1	At5g62150	Col-0	SALK_144729	-

Table 2. List of transgenic Arabidopsis lines used in this work.

Background	Construct	Reference/Source
Col-0	35S::mcherry-AEQ	R. Panstruga[2]

[2] Ralph Panstruga, Institute for Biology I, Unit of Molecular Cell Biology, RWTH Aachen

Table 3. List of *Arabidopsis thaliana* accessions used in this work.

Accession	Abbreviation	Source	GWAS-ID
Aua/Rhon	Aa-0	Till Ischebeck[3]	700
Argentat	Ag-0	N901	-
Achkarren	Ak-1	Till Ischebeck[3]	6987
Ameland-Firehouse	Amel-1	Till Ischebeck[3]	6990
Antwerpen	An-1	Till Ischebeck[3]	6898
Angleur	Ang-0	Till Ischebeck[3]	6992
Annecy	Ann-1	Till Ischebeck[3]	6994
Blackmount	Ba-1	Till Ischebeck[3]	7014
Baarlo	Baa-1	Till Ischebeck[3]	7002
Blanes	Bla-1	Till Ischebeck[3]	7015
Boot	Boot-1	Till Ischebeck[3]	7026
Borky-1	Bor-1	Till Ischebeck[3]	5837
Borky-4	Bor-4	Till Ischebeck[3]	6903
Brunn	Br-0	Till Ischebeck[3]	6904
Basel	Bs-1	Till Ischebeck[3]	8270
Buchschlag	Bsch-0	Till Ischebeck[3]	7031
Burghaun	Bu-0	Till Ischebeck[3]	8271
Burren	Bur-0	N1028	-
Canary Island	Can-0	N1064	-
Chateaudun	Chat-1	Till Ischebeck[3]	7071
Ascot-17	CIBC-17	Till Ischebeck[3]	6907
Ascot-5	CIBC-5	Till Ischebeck[3]	6730
-	Co	Till Ischebeck[3]	7081
Columbia-0	Col-0	J. Dangl, University of North Carolina, USA.	-
Compiegne	Com-1	Till Ischebeck[3]	7092
Catania	Ct-1	N1094	-
Cape Verdi Islands	Cvi-0	Till Ischebeck[3]	6911

[3] Till Ischebeck, Department of Plant Biochemistry, Albrecht-von-Haller institute for plant sciences, Göttingen, Germany

Darmstadt	Da-0	Till Ischebeck[3]	7094
Dem	Dem-4	Till Ischebeck[3]	8233
Drall	DraII-1	Till Ischebeck[3]	8284
DraIII	DraIII-1	Till Ischebeck[3]	8285
Duk	Duk	Till Ischebeck[3]	6008
Edinburgh	Edi-0	N1122	-
Eifel	Ei-2	Till Ischebeck[3]	6915
East Malling	Ema-1	Till Ischebeck[3]	5736
St. Maria d. Feiria	Fei-0	Till Ischebeck[3]	8215
Gudow	Gd-1	Till Ischebeck[3]	8296
Geleen	Gel-1	Till Ischebeck[3]	7143
Gieben	Gie-0	Till Ischebeck[3]	7147
Goettingen	Got-22	Till Ischebeck[3]	6920
Glueckingen	Gu-0	Till Ischebeck[3]	6922
La Miniere	Gy-0	Till Ischebeck[3]	8214
Heythuysen	Hey-1	Till Ischebeck[3]	7166
Chisdra	Hi-0	Till Ischebeck[3]	8304
Hannover/Stroehen	Hs-0	Till Ischebeck[3]	8310
Horni Smrcne	HSm	Till Ischebeck[3]	8236
Innsbruck	In-0	Till Ischebeck[3]	8311
Isenburg	Is-0	Till Ischebeck[3]	8312
Jena	Je-0	Till Ischebeck[3]	7181
Vranov u Brna	Jl-3	Till Ischebeck[3]	7424
Jamolice	Jm-0	Till Ischebeck[3]	8313
Kelsterbach	Kelsterbach4	Till Ischebeck[3]	8420
Killean	Kil-0	Till Ischebeck[3]	7192
Kindalville	Kin-0	Till Ischebeck[3]	6926
Köln	Kl-5	Till Ischebeck[3]	7199
Kaunas	Kn-0	N1286	-
Khurmatov	Kondara	Till Ischebeck[3]	6929
Karagandy	Kz-9	Till Ischebeck[3]	6931

Loch Ness	Lc-0	Till Ischebeck[3]	8323
Landsberg	Ler-1	Till Ischebeck[3]	6932
Limburg	Li-7	Till Ischebeck[3]	7231
Lipowiec	Lip-0	N1136	-
Lisse	Lisse	Till Ischebeck[3]	8430
Llagostera	LL-0	Till Ischebeck[3]	6933
Le Mans	Lm-2	Till Ischebeck[3]	8329
Lipovec	Lp2-2	Till Ischebeck[3]	7520
Lund	Lu-1	Till Ischebeck[3]	8334
Mühlen	Mh-0	N1368	-
Miramare	Mir-0	Till Ischebeck[3]	8337
Mainz	Mnz-0	Till Ischebeck[3]	7244
Martuba	Mt-0	N1380	-
Merzhausen	Mz-0	Till Ischebeck[3]	6940
Ascot-10	NFA-10	Till Ischebeck[3]	6943
Ascot-8	NFA-8	Till Ischebeck[3]	6944
Nossen	No-0	N77128	-
Nieps	Np-0	Till Ischebeck[3]	7268
Neuweilnau	Nw-0	Till Ischebeck[3]	8348
Oberursel	Ob-0	N1418	-
Oldenburg	Old-1	Till Ischebeck[3]	7280
Bou Roubianne	Or-0	Till Ischebeck[3]	7282
Ovelgoenne	Ove-0	Till Ischebeck[3]	7287
Oystese	Oy-0	N1436	-
Perm	Per-1	Till Ischebeck[3]	8354
Corscalla	PHW-2	Till Ischebeck[3]	8243
Pitztal	Pi-0	N1454	-
Playa de Aro	Pla-0	Till Ischebeck[3]	7300
Poppelsdorf	Po-0	N1470	-
Point Grey	Pog-0	Till Ischebeck[3]	7306
Prudka2-23	Pu2-23	Till Ischebeck[3]	6951

Prudka2-7	Pu2-7	Till Ischebeck[3]	6956
Randan	Ra-0	Till Ischebeck[3]	6958
Rodenbach	Rd-0	Till Ischebeck[3]	8366
St. Josephs	Rmx-180	Till Ischebeck[3]	7525
Rouen	Rou-0	Till Ischebeck[3]	7320
Rschew	Rsch-4	N1494	-
San Eleno	Se-0	Till Ischebeck[3]	6961
Seatlle	Seatlle-0	Till Ischebeck[3]	8245
San Feliu	Sf-2	N1516	-
St. Georgen	Sg-1	Till Ischebeck[3]	7344
Pamiro-Alay	Sha	Till Ischebeck[3]	6962
Siegen	Si-0	Till Ischebeck[3]	7337
Sorbo	Sorbo	N931	-
Ascot-1	Sq-1	Till Ischebeck[3]	6966
Ascot-8	Sq-8	Till Ischebeck[3]	6967
Stockholm	St-0	Till Ischebeck[3]	8387
Tabor	Ta-0	-	-
Tammisari	Tamm-27	Till Ischebeck[3]	6969
Tossa de Mar	Ts-1	Till Ischebeck[3]	6970
Tsu	Tsu-0	N1564	-
Umkirch	Uk-1	Till Ischebeck[3]	7378
Ullstorp	Ull2-3	Till Ischebeck[3]	6973
Ottenhof	Uod-1	Till Ischebeck[3]	6975
Utrecht	Utrecht	Till Ischebeck[3]	7382
University of British Columbia	Van-0	Till Ischebeck[3]	6977
Warschau	Wa-1	Till Ischebeck[3]	6978
Lincoln Woods State Park	WAR	Till Ischebeck[3]	7477
Westercelle	Wc-1	Till Ischebeck[3]	7404
Weningen	Wei-0	Till Ischebeck[3]	6979
Wilna-1	Wil-1	Till Ischebeck[3]	0
Wilna-2	Wil-2	N1596	-

Wassilewskija-0	Ws-0		-
Wassilewskija-4	Ws-4		-
Wietze	Wt-5	N1612	-
Wurzburg	Wu-0	N6195	-
Zdarec	Zdr-1	Till Ischebeck[3]	6984
Zurich	Zu-0	N1626	-

2.1.1.2 *Hordeum vulgare*

For experiments with *H. vulgare*, the cultivar *H. vulgare* cv. Golden Promise was used.

2.1.2 Bacterial and Yeast Strains

2.1.2.1 *Escherichia coli*

For cloning purposes chemically competent *E. coli* TOP10 F' cells (Invitrogen, Carlsbad, USA) [*pro*AB, *lac*Iq, *lac*ZΔM15, Tn*10* (TetR)} *mcr*A, Δ(*mrrhsd*RMS-*mcr*BC), φ80*lac*ZΔM15, Δ*lac*X74, *deo*R, *rec*A1, λ–*ara*D139, Δ(*ara-leu*)7697, *gal*U, *gal*K, *rps*L(StrR), *end*A1, *nup*G] were used.

2.1.2.2 *Pichia pastoris*

For protein expression the *Pichia pastoris* wild-type strain X-33 (Invitrogen, Carlsbad, USA) [Mut+] was used.

2.1.3 Vectors

A list of vectors used or generated in this work is depicted in Table 4.

Table 4. List of vectors used/generated in this work.

Name	Description	Selection marker	Reference/Source
pPICZαA	Vector for expression of proteins in *Pichia pastoris*	Zeocin™	Invitrogen (Carlsbad, USA)
pPICZαA-*Bgh00219*	Vector for expression of *Bgh00219* cDNA with a C-terminal myc epitope and polyhistidine-tag under control of the *AOX1* promoter	Zeocin™	This work
pPICZαA-*Bgh00220*	Vector for expression of *Bgh00220* cDNA with a C-terminal myc epitope and polyhistidine-tag under control of the *AOX1* promoter	Zeocin™	This work
pPICZαA-*Bgh00734*	Vector for expression of *Bgh00734* cDNA with a C-terminal myc epitope and polyhistidine-tag under control of the *AOX1* promoter	Zeocin™	This work

pPICZαA-*Bgh00736*	Vector for expression of *Bgh00736* cDNA with a C-terminal myc epitope and polyhistidine-tag under control of the *AOX1* promoter	Zeocin™	This work
pPICZαA-*Bgh06777*	Vector for expression of *Bgh06777* cDNA with a C-terminal myc epitope and polyhistidine-tag under control of the *AOX1* promoter	Zeocin™	This work

2.1.4 Oligonucleotides

The oligonucleotides in this study were ordered from either Invitrogen (Darnstadt, Germany) or Integrated DNA Technologies (Iowa, USA). The lypohilized primers were diluted with ultrapure water to a stock concentration of 100 µM. Aliquots with a concentration of 10 µM were prepared with ultrapure water for standard usage. Oligonucleotides were stored at -20°C. All oligonucleotides used in this study are listed in Table 5.

Table 5. List of oligonucleotides used in this work.

Primer	Sequence	Purpose
Oligonucleotides used for cloning		
pPICZαA-forward	AGCTTCAGCCTCTCTTTTCTC	Amplification of pPICZαA for Gibson Assembly
pPICZαA - reverse	GAACAAAAACTCATCTCAGAAGAGGATC	Amplification of pPICZαA for Gibson Assembly
Bgh00220-Gibson-forward	AGA AAA GAG AGG CTG AAG CTC GTT TGA ATG GCT TCA ATG	Amplification of *Bgh00220* for cloning into pPICZαA via Gibson Assembly
Bgh00220-Gibson-reverse	TCT GAG ATG AGT TTT TGT TCG CAA GAA AGG TAG TAC AG	Amplification of *Bgh00220* for cloning into pPICZαA via Gibson Assembly
Bgh06777-Gibson-forward	AGAAAAGAGAGGCTGAAGCTTATTGGAAAGGATTTAACGC	Amplification of *Bgh06777* for cloning into pPICZαA via Gibson Assembly
Bgh06777-Gibson-reverse	TCTGAGATGAGTTTTTGTTCACAGGAGAGATCGTATTG	Amplification of *Bgh06777* for cloning into pPICZαA via Gibson Assembly
Oligonucleotides for Expression Analysis		
ActinF	TGCGACAATGGAACTGGAATG	Semi-quantitative RT-PCR of *ACTIN1*
ActinR	GGATAGCATGTGGAAGTGCATAC	Semi-quantitative RT-PCR of *ACTIN1*
JE75	GATTCCCCTGCTTTTGTCTCCTCC	Semi-quantitative PCR of *WRKY33*

JE76	CAGCTTGATTGTTTGGACGAGTC	Semi-quantitative PCR of *WRKY33*
JE30	GAAGAGTTTGCCGATGGAGG	Semi-quantitative PCR of *WRKY53*
JE31	CGAGGCTAATGGTGGTGTTC	Semi-quantitative PCR of *WRKY53*
DS64	GACGCTTCATCTCGTCC	qRT PCR of *UBIQUITIN5*
DS65	GTAAACGTAGGTGAGTCCA	qRT PCR of *UBIQUITIN5*
JE73	GGTCACAACAATCCGGAAGA	qRT PCR of *WRKY33*
JE74	GGAGAGACAAGAGAAGGAGAGA	qRT PCR of *WRKY33*
JE79	TCACCGAGCGTACAACTTATTCC	qRT PCR of *WRKY53*
JE80	CGTTTATCGATGCCGGAGATT	qRT PCR of *WRKY53*

2.1.5 Enzymes

2.1.5.1 Restriction endonucleases

Restriction endonucleases used in this work were obtained from Thermo Fisher Scientific (Waltham, USA) or New England Biolabs (Frankfurt (Main), Germany). The enzymes were used according to the manufacturer's instructions with the supplied 10x reaction buffers.

2.1.5.2 Polymerases

For standard polymerase chain reactions, homemade *Taq* polymerase was used. PCR products for cloning were amplified with Q5 High-Fidelity DNA Polymerase according to the manufacturer's instructions (New England Biolabs, Frankfurt/Main, Germany). cDNA was synthesized from total RNA with the RevertAid TM H Minus Reverse Transcriptase according to manufacturer's instructions (Thermo Fisher Scientific, Waltham, USA).

2.1.6 Chemicals

All chemicals used in this work were purchased from the following manufacturer: BioRad (Munich, Germany), Carbosynth (Compton, United Kingdom), Duchefa (Haarlem, The Netherlands), Invitrogen (Karlsruhe, Germany), WAKO Chemicals (Neuss, Germany), Megazyme (Bray, Ireland), Roth (Karlsruhe, Germany), Sigma-Aldrich (Munich, Germany), Thermo Fisher Scientific (Waltham, USA), PJK Biotech (Kleinblittersdorf, Germany) or VWR (Darmstadt, Germany).

2.1.7 Antibiotics

Media for bacteria and yeast were supplemented with antibiotics to prevent contamination and select for transgenic organisms. The antibiotics used in this study are listed in Table 6.

Table 6. List of antibiotics used in this study.

Antibiotic	Stock solution	Final concentration
Zeocin	100 mg/ml (provided by supplier)	25 µg/ml (*E.coli*) 100 / 500 µg/ml (*P. pastoris*)

2.1.8 Carbohydrates

All cell-wall derived carbohydrates were orderd from Megazyme (Bray, Ireland) or Carbosynth (Compton, United Kingdom) and are listed in Table 7. All carbohydrates were dissolved in ultrapure water at a concentration of 10 mg/ml or 5 mg/ml according to the manufacturer's instructions. Oligosaccharides were stored at -20°C. Polysaccharides were stored at 4°C. All information about the used carbohydrates are listed in Table 7 and were obtained from Megazyme (Bray, Ireland) or Carbosynth (Compton, United Kingdom).

Table 7. List of all carbohydrates used in this work.

Name	Company	Source	Purification Method (Purity)	Stock concentration
Polysaccharides				
β-1,3-glucans/mixed linkage glucans				
β-glucan	Megazyme	Barley	GLC + Size Exclusion Chromatography (~95%)	5 mg/ml
Curdlan	Megazyme	produced by *Alcaligenes faecalis* var. myxogenes 10C3K	-	5 mg/ml
Laminarin	Santa Cruz Biotechnology	*Laminaria digitata*	- (≥96 %)	10 mg/ml
Pachyman	Megazyme	sclerotia of *Poria cocos*	-	5 mg/ml
Hemicelluloses				
Arabinoxylan	Megazyme	Wheat Flour	GLC + Size Exclusion Chromatography (Purity ~95%)	10 mg/ml
Galactomannan	Megazyme	Carob	GLC + Size Exclusion Chromatography (Purity >94%)	10 mg/ml

Glucomannan	Megazyme	Konjac	- (Purity >98%)	10 mg/ml
Mannan	Megazyme	-	- (High Purity)	10 mg/ml
Xyloglucan	Megazyme	Tamarind	- (Purity ~95%)	10 mg/ml
Pectic Components				
Arabinan	Megazyme	Sugar Beet Pulp	GLC (Purity >95%)	10 mg/ml
Arabinogalactan	Megazyme	Larch Wood	GLC + size exclusion chromatography (Purity >95%)	10 mg/ml
Rhamnogalacturonan I	Megazyme	pectic galactan from potato fiber	exhaustive hydrolysis of potato pectic galactan and GLC (High Purity)	10 mg/ml
Rhamnogalacturonan	Megazyme	soy bean pectin	Exhaustive hydrolysis and GLC (High Purity, >97%)	10 mg/ml
Oligosaccharides				
β-1,3-glucans/mixed linkage glucans				
1,3:1,4-b-Glucotetraose (C)	Carbosynth	-	-	10 mg/ml
1,3:1,4-b-Glucotriose (A)	Carbosynth	-	-	10 mg/ml
1,3:1,4-b-Glucotriose (B)	Carbosynth	-	-	10 mg/ml

β-D-Cellotriosyl-glucose	Megazyme	Barley β-glucan	HPLC (>95%)	10 mg/ml
D-Cellobiosyl-cellobiose + β-D-Glucosyl-cellotriose	Megazyme	Barley β-glucan	HPLC (>95%)	10 mg/ml
Glucosyl-cellobiose	Megazyme	Barley β-glucan	HPLC (>95%)	10 mg/ml
Cellobiosyl-glucose	Megazyme	Barley β-glucan	HPLC (>95%)	10 mg/ml
Laminarihexaose	Megazyme	Curdlan	HPLC (>95%)	10 mg/ml
Laminaripentaose	Megazyme	Curdlan	HPLC (>90 %)	10 mg/ml
Laminaritetraose	Megazyme	Curdlan	HPLC (>95%)	10 mg/ml
Laminaritriose	Megazyme	Curdlan	HPLC (>95%)	10 mg/ml
Laminaribiose	Megazyme	Curdlan	HPLC (>95%)	10 mg/ml
Cellulose Derivatives				
Cellohexaose	Megazyme	-	HPLC + HPAEC-PAD (>95%)	10 mg/ml
Isomaltotriose	Megazyme	-	HPLC + HPAEC-PAD (>98%)	10 mg/ml
Maltotetraose	Megazyme	-	HPLC (>95%)	10 mg/ml
Hemicelluloses				
Arabinofuranosyl-xylotetraose	Megazyme	Arabinoxylan	HPLC (>95%)	10 mg/ml

Arabinofuranosyl-xylotetraose (XA3XX/XA2XX) mixture	Megazyme	Arabinoxylan	HPLC (>95%)	10 mg/ml
Mannohexaose	Megazyme	Mannan	HPLC (>90%)	10 mg/ml
α-D-Galactosyl-mannopentaose	Megazyme	Galactomannan	HPLC (>95%)	10 mg/ml
1,4-β-D-Glucosyl-D-Mannose + 1,4-β-D-Mannobiose	Megazyme	Glucomannan	HPLC (~96%)	10 mg/ml
1,4-β-D-Glucosyl-D-Mannobiose + 1,4-β-D-Cellobiosyl-D-Mannose	Megazyme	Glucomannan	HPLC (>90%)	10 mg/ml
Heptasaccharide (X3Glc4 – borohydride reduced)	Megazyme	Xyloglucan	HPLC (>90 %)	10 mg/ml
Heptasaccharide (X3Glc4)	Megazyme	Xyloglucan	HPLC (>90 %)	10 mg/ml
Higher Degree of Polymerisation Xyloglucan Oligosaccharides	Megazyme	Xyloglucan	(~95 %)	10 mg/ml
Xyloglucan (hepta+octa+nona saccharides)	Megazyme	Xyloglucan	HPLC (~95 %)	10 mg/ml
Xylohexaose	Megazyme	Xyloglucan	HPLC (>95%)	5 mg/ml
Pectic Component				
Arabino-octaose	Megazyme	Sugar beet	HPLC (>95%)	10 mg/ml
Others				
Kestopentaose	Megazyme	Fructan	HPLC (>95%)	10 mg/ml
Verbascose	Megazyme	Bean extract	HPLC (>95%)	10 mg/ml

2.1.9 Media

All media listed in Table 8 were prepared with ultrapure water and autoclaved for 20 min at 121°C. Antibiotics were added to the respective media after cooling down to 60°C. Liquid and solid media were stored at room temperature.

Table 8. Media used in this study.

Media for growing *A. thaliana* seedlings in-vitro		
½ MS + sucrose	Murashige and Skoog medium including Gamborg B5 vitamins	2.2 g/l
	Surcose	10 g/l
	Adjust to pH=5.7 with KOH For aqueous agar plates, 2 g/l plant agar were included	
Media for growing *Escherichia coli*		
Low Salt Luria-Bertani (LB) medium	Tryptone	10 g/l
	Yeast Extract	5 g/l
	NaCl	5 g/l
	pH = 7.5 For solid media, 15 g/l agar (bacterial grade) was added	
SOB medium	Tryptone	20 g/l
	Yeast Extract	5 g/l
	NaCl	0.5 g/l
	KCl	0.186 g/l
SOC medium	Tryptone	20 g/l
	Yeast Extract	5g/l
	NaCl	0.5 g/l
	KCl	0.186 g/l
	$MgSO_4$	2.408 g/l
	Glucose	3.6 g/l
Media for growing *Pichia pastoris*		
Buffered Glycerol-complex medium (BMGY)	Yeast Extract	10 g/l
	Peptone	20 g/l
	Autoclave 20 min at 121°C, then add:	
	Potassium phosphate buffer (1 M)	100 ml/l
	YNB (10x)	100 ml/l
	Biotin (500x)	2 ml/l
	Glycerol (10x)	100 ml/l
Buffered Methanol-complex medium (BMMY)		
	Yeast Extract	10 g/l
	Peptone	20 g/l
	Autoclave 20 min at 121°C	
	Potassium phosphate buffer (1 M)	100 ml/l
	YNB (10x)	100 ml/l
	Biotin (500x)	2 ml/l
	Methanol (30x)	100 ml/l

Minimal Dextrose medium (MD)	Autoclave 800 ml water for 20 min at 121°C. Let it cool down to 60°C and add:	
	YNB (10x)	100 ml/l
	Biotin (500 x)	2 ml/l
	Glucose (10x)	100 ml/l
	For MD plates, 15 g/l agar were added to the water.	
Minimal Methanol Medium (MM)	Autoclave 800 ml water for 20 min at 121°C. Let it cool down to 60°C and add:	
	YNB (10x)	100 ml/l
	Biotin (500 x)	2 ml/l
	Methanol (10x)	100 ml/l
	For MM plates, 15 g/l agar were included.	
Yeast Extract-Peptone-Dextrose (YPD) Broth	Yeast Extract	10 g/l
	Peptone	20 g/l
	Glucose / Dextrose	20 g/l
	For YPD plates, 20 g/l agar were included.	

Preparation of media for growth of *Pichia pastoris*

Biotin (500x)	Biotin	20 mg
	Dissolve in 100 ml water and filter sterilize	
Glucose (10x)	Glucose	200 g
	Dissolve in 1000 ml water and filter sterilize	
Glycerol (10x)	Glycerol	100 ml
	Mix with 900 ml water and sterilize by autoclaving	
Methanol (10x)	Methanol	2.5 ml
	Mix with 47.5 ml ddH_2O and filter sterilize	
Methanol (30x)	Methanol	7.5 ml
	Mix with 42.5 ml ddH_2O and filter sterilize	
Potassium Phosphate buffer (pH = 6)	K_2HPO_4 (1 M)	132 ml
	KH_2PO_4 (1 M)	868 ml
	Confirm the pH and sterilize by autoclaving	
YNB (10 x)	Yeast Nitrogen Base (without amino acids and ammonium sulfate)	3.4 g
	Ammonium sulfate	10 g
	Add 100 ml ddH_2O, stir until everything is dissolved and filter sterilize (pore size 0.22 µM)	

2.1.10 Buffers and Solutions

All buffers and solutions were prepared with ultrapure water and autoclaved for 20 min at 121°C. Buffers and solutions which were not autoclaved were sterilized by filtration with filters having a pore size of 0.2 µM. Solutions for the preparation of *Pichia pastoris* growth media were stored at 4°C. Table 9 lists all buffers and solutions used in this work.

Table 9. List of buffers and solutions used in this work.

Agarose Gel electrophoresis and PCR		
Agarose solution	Agarose TAE Buffer	1-3 % 1x
6x DNA Loading Dye	Orange G Xylencyanol FF Glyercol	0.25 % (w/v) 0.25 % /w/v) 30 % (v/v)
10x PCR reaction buffer for *Taq* polymerase	Tris base KCl $MgCl_2$ Triton X-100 pH = 9 (with KOH)	100 mM 500 mM 15 mM 1% (w/v)
50x TAE buffer	Tris base Glacial acetic acid EDTA (0.5 M, pH = 8)	2 M 57.1 ml/l 100 ml/l
Genomic DNA Extraction from Plants		
DNA Extraction Buffer	Tris-HCl (pH = 7.5) NaCl EDTA SDS	0.2 M 1.25 M 0.025 M 0.5% (w/v)
Protein Extraction from Plants		
Barley extraction buffer	Tris-HCl (pH =7.5) NaCl EGTA β-glycerophosphat $MgCl_2$ NaF Na_3VO_4 Na_2MoO_4 DTT Tween-20 Protease Inhibitor	50 mM 100 mM 20 mM 30 mM 20 mM 4 mM 4 mM 4 mM 10 mM 0.2 % 1:1000
CERK1 extraction buffer	Sucrose HEPES-KOH (pH = 7.5) Glycerol Na_2MoO_4 $Na_4P_2O_7$ NaF EDTA DTT Triton X-100 Protease Inhibitor Cocktail	250 mM 100 mM 5% (v/v) 1 mM 50 mM 25 mM 10 mM 1 mM 0.5% (w/v) 1:100

Protease Inhibitor Cocktail	4-(2-aminoethyl) benzenesulfonyl fluoride hydrochloride (EABSF)	1 g
	Bestatin hypochloride	5 mg
	Pepstatin A	10 mg
	Leupeptin hemisulfate	100 mg
	E-64 (trans-epoxysuccinyl-L-leucylamido-(4-guanidino)butane)	10 mg
	Phenantroline (1, 10-phenantroline monohydrate)	10 g
	All components were dissolved separately in a small amount of DMSO and then combined and filled up to 200 ml with DMSO. The mixture was aliquoted in 2 ml and stored at -20°C.	

Buffers used for SDS PAGE and Immunoblot analysis

4x SDS Loading Buffer	Tris-HCl (pH = 6.8)	200 mM
	DTT	400 mM
	SDS	8% (w/v)
	Glycerol	40% (v/v)
	Bromphenol Blue	0.1% (w/v)
	Store at -20°C	
10x SDS Running Buffer	Glycine	2 M
	Tris	250 mM
	SDS	1% (w/v)
20x Transfer buffer	Tris	1 M
	Boric Acid	1 M
	pH = 8.3	
Alkaline Phosphatase (AP) buffer	Tris-HCl, pH = 9.5	100 mM
	NaCl	100 mM
	$MgCl_2$	50 mM
Coomassie Staining Solution for PVDF membrane	Ethanol	300 ml
	Acetic Acid	100 ml
	ddH_20	300 ml
	Coomassie R250	0.05%
Destaining Solution for PVDF membrane	Ethanol	300 ml
	Acetic Acid	100 ml
	ddH_20	300 ml
20 x TBS-T	NaCl	3 M
	Tris-HCl (pH = 8)	200 mM
	Tween-20	1%
TBS-T + milk powder	TBS-T	
	Skimmed Milk Powder	40 g/l

Preparation of chemically competent *E.coli* cells

CCMB80	KOAc	10 mM
	$CaCl_2$ x 2 H_2O	80 mM
	$MnCL_2$ x 4 H_2O	20 mM
	$MgCL_2$ x 6 H_2O	10 mM
	Glycerol	10%
	Adjust pH to 6.4	

Solutions for purification of His-tagged proteins expressed in *P. pastoris*		
Buffer A	NaH_2PO_4 (500 mM) Na_2HPO_4 (500 mM) Add H_2O to 500 ml, adjust pH to 7.5, then add: NaCl Imidazole Filter sterile	8 ml 21 ml 8.73 g 0.34 g
Buffer C	NaH_2PO_4 (500 mM) Na_2HPO_4 (500 mM) Add H_2O to 500 ml, adjust pH to 7.5, then add: NaCl Imidazole Filter sterile	8 ml 21 ml 8.73 g 17.11 g
SEC Buffer	MOPS EDTA pH = 7.5	20 mM 1 mM
Thin Layer Chromatography (TLC)		
TLC running buffer	Isopropanol Ethylacetate Fill up to 500 ml with ddH_2O	200 ml 200 ml
TLC staining solution	Sulfuric acid In methanol	10%
ROS Burst Assay		
L-012	Horseradish Peroxidase L-012 In ddH_2O	10 µg/ml 100 µM
Calcium Assay		
Coelenterazine working solution	Coelenterazine In methanol	40 µM
Discharge Solution	$CaCl_2$ EtOH In ddH_2O	2 M 20 %

2.1.11 Antibodies

Primary and secondary antibodies that were used in this work are listed in Table 10. The primary antibody α-pMAPK Phospho p44/42 was stored at -20°C, whereas all other antibodies were aliquoted and stored at -80°C for long term storage. Aliquots of antibodies in use were kept at 4°C or -20°C.

Table 10. List of antibodies used in this study.

Primary Antibody	Produced in (organism)	Company
α-pMAPK Phospho p44/42 (Erk1/2) (Thr202/Tyr204) (used: 1:5000)	Rabbit, polyclonal	Cell Signaling Technology, Danvers, MA, USA
Secondary Antibody	**Produced in (organism)**	**Company**
Anti-rabbit IgG AP conjugate (used: 1:5000)	Goat, polyclonal	Sigma-Aldrich, Munich, Germany

2.1.12 Devices

Table 11. Devices used in this study.

Device	Model	Manufacturer
Blot Imaging System	ChemiDoc Touch	Bio-Rad (Hercules, CA, USA)
Bunsenburner	Phoenix eco	Schuett biotect (Göttingen, Germany)
Centrifuges	Pico 21	Thermo Fisher Scientific (Langenselbold, Germany)
Clean Bench	Hera safe	Thermo Fisher Scientific (Langenselbold, Germany)
Computer	OptiPlex5040	Dell (Halle (Saale), Germany)
Dewer	-	Nalgene (Rochester, NY, USA)
Freezer (-20°C)	Mediline	Liebherr (Kirchdorf an der Iller, Germany)
Freezer (-80°C)	Hera freeze	Thermo Fisher Scientific (Langenselbold, Germany)
Gel documentation system	GenoPlex	VWR (Hannover, Germany)
Gel electrophoresis equipment	-	BioRad (Hercules, CA, USA)
Gel running chamber	Sub Cell ® GT	BioRad (Hercules, CA, USA)
Growth Chamber	-	Johnson Controls (Milwaukee, WI, USA)
Heating Plate	OTS40	Medite (Burgdorf, Germany)

HPAEC-PAD	Dionex ICS-5000 with an AS-AP auto-sampler and a temperature-controlled sample tray run	Thermo Fisher Scientific
Analytical Column for HPAEC-PAD	3 * 250 mm Dionex CarboPac PA200	Thermo Fisher Scientific
Guard Column for HPAEC-PAD	3 x 50 mm guard column	Thermo Fisher Scientific
Ice Machine	-	Ziegra (Isernhagen, Germany)
Magnetic stirrer	RH basic 2 IKAMAG	IKA (Staufen, Germany)
Mass Spectrometry	Waters® Xevo® QTOF with a nanoACQUITY UPLC system	Waters (Milford, Massachusetts, USA)
MALDI-TOF	Autoflex MALDI-TOF equipped with Smartbeam-II 355 nm laser system	Bruker (Billerica, Massachusetts, USA)
PCR Cycler	MyCycler	BioRad (Hercules, CA, USA)
pH Meter	Inolab ®	WTW (Weilheim, Germany)
Photometer	Infinite M200	Tecan (Wiesbaden, Germany)
Photometer II	WPA Biowave II	Biochrom (Cambridge, UK)
Pipet	Pipetman	Gilson (Limburg-Offheim, Germany)
qRT-PCR Cycler	C199 Touch with CFX96 system	BioRad (Hercules, CA, USA)
Refrigerator	Mediline	Liebherr (Kirchdorf an der Iller, Germany)
Steam sterilizer	Varioklav 75S / 135S	Thermo Fisher Scientific (Langenselbold, Germany)
Thermomixer	Compact / Comfort	Eppendorf (Hamburg, Germany)
Vortexter	VF2	IKA (Staufen, Germany)
Water filter system	Arium ® 611 DI	Sartorius (Göttingen, Germany)

2.1.13 Software

Table 12. Software that was used in this study.

Software	Source
Acrobat Reader	http://get.adobe.com/uk/reader/ (Adobe Systems Inc., San José, CA; USA)
Adobe Illustrator CS5 v 15.0.0	(Adobe Systems Inc., San José, CA; USA)
Adobe Photoshop CS5 v 12.0	(Adobe Systems Inc., San José, CA; USA)
Bio-Rad CFX Manager 3.0	(Bio-Rad Laboratories, Hercules, CA, USA)
Chromeleon 7	ThermoFisher Scientific

Clone Manager Professional Suite v 8	http://www.scied.com/pr_cmpro.htm (Sci-Ed Software, Denver, CO, USA)
dBCan	http://bcb.unl.edu/dbCAN2 (Yin et al., 2012)
Geneious	http://www.geneious.com/ (Biomatters Ltd., Auckland, New Zealand)
NetNGlyc	http://www.cbs.dtu.dk/services/NetNGlyc/
NetPhos	http://www.cbs.dtu.dk/services/NetPhos
Office 2010	(Microsoft, redmont, WA, USA)
Origin Pro graphing software	OriginLab (Washington, USA)
SecretomeP 2.0	http://www.cbs.dtu.dk/services/SecretomeP/; (Bendtsen et al., 2004a)
SignalP 3.0	http://www.cbs.dtu.dk/services/SignalP/; (Bendtsen et al., 2004b)

2.2 Methods

2.2.1 Methods for working with plants

2.2.1.1 *Arabidopsis thaliana*

2.2.1.1.1 Sterilization

For growth of *A. thaliana* on soil, the seeds were frozen to kill off potential pathogens. To this end, seeds were put doubly into plastic backs and incubated for 48 h at -20°C. Before sowing, the seeds were warmed up again at room temperature.

For growth of *A. thaliana in-vitro*, seeds were sterilized with ethanol. Therefore, seeds were transferred into 1.5 ml tubes and washed three times for 2 min with 70% EtOH and 0.05% Tween-20. To ensure equal washing of the seeds, the tubes were incubated on a stirring wheel. Next, the seeds were washed twice with 100% EtOH for 1 min. A sterile filter paper was put into the lid of a petri dish. For drying, the seeds together with the EtOH were poured onto the paper. The seeds were used further when the EtOH was evaporated.
The procedure was performed under a sterile bench.

2.2.1.1.2 Plant growth conditions for growth on soil

The sterilized seeds were sown on damp soil (Frühstorfer Erde, Type T, Archut) that was steamed 30 min at 90°C. To enhance humidity and promote germination, a transparent lid was used to cover the pots. The pots were then brought to growth chambers (Johnson Controls, Milwaukee, WI, USA) with short day conditions (8h light, 22°C, 140 mol m^{-2} sec^{-1}, 65% relative humidity. The lids were removed when the seeds germinated. To induce flowering and setting of seeds, plants were transferred to long day conditions (16h light, 26°C, 200 m^{-2} sec^{-1}, 65% relative humidity).

2.2.1.1.3 Plant growth conditions for *in-vitro* culture

Arabidopsis seedlings used for calcium assays were grown *in-vitro* in petri dishes. For this purpose, seeds sterilized with ethanol were sown on ½ MS + sucrose semi-solid agar and grown for 7-9d in a growth cabinet (CLF Plant Climatics, Wertingen, Germany) with short day conditions (12h light, 12h darkness). The 7-9-day old seedlings were then transferred into 96-well plates. For the measurement, the seedlings were covered with 75 µl water and 25 µl coelenterazine and incubated overnight at room temperature in the dark.
Arabidopsis seedlings used for Immunoblot or gene expression analysis were grown *in-vitro* in 24-well plates. Therefore, seeds sterilized with ethanol were sown on ½ MS + sucrose aqueous agar. The seeds were allowed to germinate and grow for 7d in a growth cabinet (CLF Plant Climatics, Wertingen, Germany) with short day conditions (12h light, 12h darkness). The 7d old seedlings were then transferred to 24-well plates containing 500 µL ½ MS + sucrose medium and allowed to grow in a growth cabinet (CLF Plant Climatics, Wertingen, Germany) with short day conditions (12h light, 12h darkness). Two seedlings were transferred into one well. After 13d the medium was replaced with 500 µL new ½ MS + sucrose medium to ensure equal amounts of medium in each well. The next day (day 14), the seedlings were treated with chitin (10 µg ml^{-1}), flg22 (50 nM), oligogalacturonides (1, 5,

10 µg ml^{-1}) and medium as control as well as with different cell-wall derived oligo- and polysaccharides (10 µg ml^{-1}).

2.2.1.2 *Hordeum vulgare*

2.2.1.2.1 Sterilization

For growth of *Hordeum vulgare* on soil, the seeds were frozen to kill of potential pathogens. Therefore, seeds were transferred into a plastic bag and incubated overnight at -20°C. Before sowing, the seeds were allowed to warm up at room temperature.

2.2.1.2.2 Plant growth conditions for growth on soil

The surface sterilized seeds were sown and lightly covered with soil (Frühstorfer Erde, Type T, Archut) that was steamed beforehand for 30 min at 90°C. To promote germination, the pots were covered with a transparent lid and the pots were brought to a growth chamber (Johnson Controls, Milwaukee, WI, USA) with long day conditions (16h light, 26°C, 200 m^{-2} sec^{-1}, 65% relative humidity). Upon germination, the lid was removed.

2.2.1.2.3 Treatment of *H. vulgare* for immunoblot analysis

For analyzing the activation of MAPK in *H. vulgare* upon MAMP or carbohydrate treatment, 12-14 leaf discs of 4 mm diameter were harvested from second leaves of 14 d old *H. vulgare* plants. The harvested leaf discs were incubated for 16h in 24-well plates in 2 ml ddH_2O. Upon incubation, the leaf discs were transferred to a new 24-well plate with each well containing 500 µl ddH_2O. Then, the leaf discs were treated with either 500 µl ddH_2O as control, chitin (end concentration: 100 µg/ml), flg (end concentration: 50 nM) or carbohydrates (end concentration: 100 µg/ml). *H. vulgare* was only treated with carbohydrates belonging to the group of mixed linkage glucans (see Table 7).

2.2.2 Methods for working with *Escherichia coli*

2.2.2.1 Growth conditions for *E.coli*

E.coli cells were cultivated on solid LB plates or in liquid LB medium with the respective antibiotics as selective markers. Single colonies from LB plates were used to inoculate liquid medium.

LB plates with *E.coli* cells were incubated at 37°C overnight. Liquid cultures were grown at 37°C at 220 rpm.

2.2.2.2 Preparation of competent *E. coli* cells

One single colony of *E. coli* TOP10 F' cells was inoculated in 5 ml low salt LB medium and incubated at 37°C overnight while shaking. The next day, the 5 ml culture was transferred into 500 ml SOB medium and incubated at 37°C while shaking to an OD_{600} of 0.4. The culture was incubated for 30 min on ice and then centrifuged at 3000 rpm at 4°C for 10 min. The supernatant was discarded and the pellet was dissolved in 80 ml ice-cold CCMB80. After incubation of the solution for 20 min on ice, the solution was centrifuged at 4°C for 10 min at 3000 rpm. The supernatant was again discarded and the pellet resuspended in 10 ml ice-cold CCMB80. Next, the OD_{600} of a mixture of 200 µl SOC and 50 µl

of the resuspended cells was tested and the OD_{600} was adjusted to 1.0-1.5 with ice-cold CCMB80. Finally, aliquots of 100µl cells were prepared and frozen in liquid nitrogen. The cells were then stored at -80°C.

2.2.2.3 Transformation of *E. coli*

An aliquot of competent *E. coli* cells was thawed on ice. 2 µL of the Gibson Assembly mix were added to the cells and mixed. The cells were incubated on ice for 30 min, followed by a heatshock at 42°C for 45 sec. After the heatshock, the cells were incubated for 2 min on ice and then, 900 µL SOC or low salt LB medium were added to the cells. Upon incubation for 60 min at 37°C while shaking, the cells were plates on low salt LB medium containing the respective antibiotics.

2.2.3 Methods for working with *Pichia pastoris*

2.2.3.1 Growth conditions for *P. pastoris*

P. pastoris cells were cultivated on solid YPD plates in or liquid YPD medium with the respective antibiotic as selective marker. For determining the Mut phenotype, *P. pastoris* cells were grown on solid MD and MM plates. For expression studies, *P. pastoris* cells were grown in liquid BMGY and BMMY medium. Single colonies from YPD plates were used to inoculate liquid YPD or BMGY medium.

YPD plates with *P. pastoris* cells were incubated at 28°C-30°C for 2-3 d. Liquid cultures were grown at 30°C at 160 rpm. For expression studies, cultures were grown at either 16°C or 25°C at 160 rpm.

2.2.3.2 Preparation of competent *P. pastoris* cells

In the morning, a single colony of *P. pastoris* X-33 was inoculated two times in 2.5 ml YPD in a sterile 50 ml tube. The cultures were grown over the day at 30°C at 160 rpm. In the afternoon, 500 µL of the pre-culture were inoculated in 250 ml YPD and incubated overnight at 30°C at 160 rpm to an OD_{600} of 1.2-1.5. Next, the culture was centrifuged at 4°C at 2.000 g for 5 min. The supernatant was discarded and the pellet was gently resuspended in 100 ml YPD with 20 ml HEPES (pH = 8). 2.5 ml freshly prepared DTT (1 M) were gently mixed to the solution and the solution was incubated for 15 min at 30°C without shaking. The volume of the solution was adjusted to 400 ml with ice-cold sterile water. Again, the solution was centrifuged for 5 min at 2000 g at 4°C. The supernatant was discarded and the pellet was resuspended in 250 ml ice-cold sterile water. After centrifugation of the solution for 5 min at 2000 g at 4°C, the supernatant was discarded and the pellet was resuspended in 20 ml ice-cold sorbitol (1 M). The solution was transferred into a 50 ml tube and centrifuged for 5 min at 4°C for 5 min at 2000 g. Again the supernatant was discarded and the pellet was resuspended in 500 µl cold Sorbitol (1 M). Finally, aliquots of 80 µl cells were prepared. The cells could either be used directly or can be stored for 1-2 weeks at -80°C.

2.2.3.3 Transformation of competent *P. pastoris* cells

Prior to transformation of *P. pastoris* cells, the respective plasmids had to be linearized (see 2.2.4.8). 10 µL of the linearized plasmid were mixed with 80 µl competent *P. pastoris* cells and transferred into

an ice-cold 0.2 cm electroporation cuvette. Upon incubation of the cuvette for 5 min on ice, the cells were pulsed with a Micropulser (BioRad, Munich, Germany) according to the manufacturer's instructions. 1 ml ice-cold sorbitol (1 M) was added to the cells directly after the electro pulse. Then, the cells were transferred into a sterile 15 ml tube and incubated at 30°C for 1-2 h without shaking. After incubation, 80 µl, 100 µl and 150 µl cells were plated on separate YPD plates containing either 100 µg/ml or 500 µg/ml Zeocin.

2.2.3.4 Determination of the Mut phenotype

P. pastoris X-33 has a Mut^+ phenotype. However, during transformation of *P. pastoris* X-33, the recombination could occur at the 3'AOX1 region thereby disrupting the wild-type *AOX1* gene. Thus, transformants having a Mut^S phenotype can be generated. To test the Mut phenotype, growth of *P. pastoris* transformants was tested on MM and MD plates. To this end, 10 – 20 transformants were picked and streaked out on MM first and then onto MM plates and incubated for 2d at 30°C.
Upon confirming the Mut phenotype, the *P. pastoris* transformants were for tested for the expression of the gene of interest via small scale expression.

2.2.4 Molecular biology methods

2.2.4.1 Isolation of genomic DNA of *A. thaliana*

300 µl DNA extraction buffer were added to a small Arabidopsis leaf in a 1.5 ml tube. The leaf was grounded with a plastic pistil and incubated for 5 min at RT at 800 rpm on a shaker. Afterwards, the samples were centrifuged for 5 min at maximum 13.000 rpm at RT. 240 µl of the supernatant were transferred to a new tube and 300 µl isopropanol were added. Upon incubating the samples on a shaker for 5 min at RT, the samples were centrifuged for 10 min at RT at 13.000 rpm and the supernatant was discarded. To remove the remaining supernatant, the samples were again centrifuged for 1 min at RT at 13.000 rpm. Afterwards, the DNA pellet was air-dried and finally resuspended in 50 µl ddH_2O by incubating it at 40°C for 5 min on a shaker. The DNA was stored at -20°C or directly used for PCR.

2.2.4.2 Isolation of plasmid DNA from *E. coli*

2.2.4.2.1 Small Scale plasmid isolation

For small scale plasmid isolation, 5 ml overnight culture was spun down and used for plasmid isolation with the Presto™ Mini Plasmid Kit (Geneaid Biotech Ltd, Taipei, Taiwan) according to the manufacturer's instructions.

2.2.4.2.2 Medium Scale plasmid isolation

To purify a higher amount of plasmid, 100 ml culture was centrifuged and used for plasmid isolation using the Plasmid Mini, Midi, and Maxi Kit (QIAgen, Hilden, Germany) according to the manufacturer's instructions.

2.2.4.3 Polymerase Chain Reaction (PCR) for cloning

For generating DNA used for cloning, the Q5 High-Fidelity DNA polymerase (New England Biolabs, Frankfurt/Main, Germany) was used.

PCR Mix for one reaction	
5x Q5 reaction buffer	10 µl
dNTPs (10 mM)	1 µl
Primer 1 (10 µM)	2.5 µl
Primer 2 (10 µM)	2.4 µl
Q5 Polymerase	0.5 µl
cDNA/DNA template	1 µl

Table 13. General temperature profile for PCR with Q5 High Fidelity Polymerase.

Step	Temperature [°C]	Time [min]	Repeats
Initial denaturation	98	00:30	1x
Denaturation	98	00:15	30x
Annealing	55	00:15	
Elongation	72	00:30 / kb	
Final Extension	72	2:00	1x
Final Hold	4	5:00	1x

2.2.4.4 Agarose gel electrophoresis

To separate and visualize DNA fragments or to determine the RNA quality, an agarose gel electrophoresis was performed. Therefore, samples were mixed with 6x loading dye and loaded onto a 1% - 3% agarose gel by gel electrophoresis. To prepare the gel, the respective amount of agarose was mixed with 1x TAE buffer and heated in the microwave until the agarose was dissolved completely. The mix was then allowed to cool down to ~50°C and 5 µl HD Green (Intas Science Imaging Instruments GmbH, Göttingen, Germany) were added to 100 ml agarose. The solid gel was put into Sub-Cell GT tank (BioRad, Munich, Germany) and the tank was filled with 1x TAE buffer. GeneRuler™ 1 kB or 100 bp DNA ladder (Thermo Fisher Scientific, Waltham, USA) as well as the samples were loaded into the wells. The gels ran at 90-120V for about 30 min. After the run, the gel was analysed with a G:Box Genoplex Transilluminator gel documentation and analysis system (VWR, Lutterworth, UK).

2.2.4.5 Purification of DNA fragments

PCR fragments used for cloning were cleaned-up directly. For PCR product purification, the GeneJET GelExtraction and DNA CleanUp Micro Kit (Thermo Fisher Scientific, Waltham, USA) was used.

2.2.4.6 Gibson Assembly

Gibson assembly to generate pPICZαA-bgh06777 and pPICZαA-bgh00220 based on the protocol by Gibson *et al.*, 2009. A molar ratio of insert to vector from 2:1 was used.

The cloning was carried out as follows: The generation of pPICZαA-bgh06777 and pPICZαA-bgh00220 required two fragments. The first fragment (1) represents the plasmid backbone and was amplified from pPICZαA (Thermo Fisher Scientific, Waltham, USA). *Bgh06777* without the native signal peptide (nucleotides encoding amino acid 19-293) that additionally carried a 3' and 5' overhang matching pPICZαA or Bgh00220 without the native signal peptide (nucleotides encoding amino acid 19-293) that additionally carried a 3' and 5' overhang matching pPICZαA represented the second fragment (2). The second fragment was amplified from cDNA generated from *H. vulgare* plants infected with *Blumeria graminis* f.sp. *hordei*. The primers for amplification of the two fragments were designed using the Nebuilder web tool (New England Biolabs, Frankfurt/Main, Germany) and are listed in table Table 5. Upon incubation of the respective two fragments with the Gibson Master Mix for 1h at 50°C and 1 min at 95°C, 2 µl of the Gibson assembly mix were directly transformed into *E. coli* TOP 10 F' cells.

2.2.4.7 Sequencing of DNA

Generated plasmids were sequenced by genewiz (Vancouver, Canada) or Seqlab (Götingen, Germany). Sequencing reactions were prepared according to Genewiz or Seqlab sample requirements, respectively. The results were analysed with either ApE-A plasmid editor software v2.0.53c (California, USA) or the bioinformatics software Geneious version 7.1.5.

2.2.4.8 Restriction enzyme digest of DNA

The restriction enzymes used in this study were standard enzymes of Thermo Fisher Scientific (Waltham, USA). The enzymes were used according to the manufacturer's instructions.

For restriction digestions to linearize plasmids used for *P. pastoris* transformation, 10 µl 10x buffer were mixed with 50 U *Pme*I and 10 µg plasmid DNA. This mix was filled up with water to 100 µl and incubated for 2h at 37°C while shaking. Digestion products were analysed via agarose gel electrophoresis.

2.2.4.9 Isolation of RNA from plant material

Total RNA of *A. thaliana* seedlings and *H. vulgare* leaves infected with *Blumeria graminis* f.sp. *hordei* was isolated using the TRIZOL extraction method (Chomczynski, 1993).

Upon treatment, four 14 d old *A. thaliana* seedlings were transferred into 2 ml tubes containing stainless steel balls and frozen in liquid nitrogen. The seedlings were stored at -80°C until use. For RNA extraction from *H. vulgare*, leaves of 10 d old plants infected with *Bgh* were harvested and

frozen in liquid nitrogen. The plant material was ground to a fine powder using a TissueLyser LT (Qiagen, Hilden, Germany) and stored at -80°C until use.

1 ml Qiazol (company) were added to the powder and incubated for 10 min at RT on a shaker. Thereafter, 200 µl chloroform were added and again the samples were incubated for 10 min at RT on a shaker. The samples were then centrifuged for 60 min at 4°C at 13.000 rpm. 600 µl of the supernatant were transferred to a new tube and mixed with 440 µl isopropanol. The tubes were inverted several times and incubated for 10 min at 4°C. For precipitation of RNA, the samples were centrifuged for 15 min at 4°C at 13.000. After centrifugation, the supernatant was discarded and the RNA pellet was washed with 500 µl 70% EtOH. The supernatant was discarded and the RNA pellet was air-dried for 15 min and finally resuspended in 50 µl RNase-free water. To solve the RNA, the tubes were incubated for 10 min at 65°C in a thermomixer. The RNA concentration was measured using NanoDrop and used for cDNA synthesis.

2.2.4.10 DNase I digestion of RNA

Before the RNA was used for cDNA synthesis, RNA samples were digested with DNase I (Thermo Fisher Scientific; Waltham, MA, USA) according to the manufacturer's instructions.

17 µl RNA were mixed with 1 µL 10 x DNase I buffer with $MgCl_2$, 1 µl DNase I (1 U/ µl) and 0.5 µl RiboLock RNase Inhibitor (Thermo Fisher Scientific; Waltham, MA, USA). This mixture was incubated at 37°C for 30 min and next, 1 µl EDTA (50 mM) was added. The samples were further incubated at 65°C for 10 min at finally at 4°C for 2 min. The DNase I digested samples were then used for cDNA synthesis.

2.2.4.11 cDNA synthesis

DNase I digested RNA samples were used for cDNA synthesis according to the manufacturer's instructions (Thermo Fisher Scientific; Waltham, MA, USA).

First, DNase I digested RNA was adjusted to 250 ng/µl and 1 µg RNA was used for cDNA synthesis. The adjusted RNA was combined with 2 µl oligodT primer [100 µg/µl] and incubated for 10 min at 70°C. Upon cooling down to 4°C, 4 µl 5 x M-MulVRT buffer, 2 µl dNTPs [10 mM], 1 µl reverse transcriptase (RevertAid™ H Minus M-MulVRT 200 U/µl) were added to the samples. The samples were then incubated for 70 min at 42°C, followed by an incubation for 10 min at 70°C and finally, for 2 min at 4°C. For quantitative RT-PCR, samples were diluted 1:500 and stored at -20°C.

2.2.4.12 Quantitative reverse transcription PCR (qRT-PCR)

For qRT-PCR, the amplification and simultaneous quantification was carried out with the CFX96 Touch TM Real-Time PCR Detection System with the CFX Manager TM Software and the respective qRT-PCR-96-well plates (BioRad, Hercules, CA, USA). Reactions were set up as described below in Table 14 with Sso Fast EvaGreen supermix (BioRad, Munich, Germany).

Table 14. qRT-PCR reaction mix.

Component	Volume per 10 µl reaction [µl]
SsoFast EvaGreen supermix	5
Forward Primer (2 µM)	1
Reverse Primer (2 µM)	1
cDNA	3

The reactions were pipetted into clear 96 well plates (BioRad, Munich, Germany) with three technical replicates per sample. The following protocol was used (Table 15) for amplification and simultaneous quantifications.

Table 15. qRT-PCR program.

Step	Temperature	Time	Repeats
Denaturation	95°C	30 sec	
Annealing	95°C	5 sec	45x
Extension	55°C	10 sec	
Melting curve	60 – 95°C	5 sec	-

2.2.4.13 Calcium Assays

For analysing the influx of calcium ions upon MAMP or carbohydrate treatment, aequorin luminescence measurements were performed using Col-0 seedlings expressing the calcium-sensing protein aequorin. The assay was performed as described in Ranf *et al*., 2012 with little changes. The measurements were carried out using 96-wellplates and a TECAN infinite® M200 plate reader (Tecan Group Ltd, Männedorf, Switzerland).

Each well was filled with 75 µl ddH_2O. 7-9d old seedlings grown in-vitro were transferred one by one into the wells of a 96-well plate. One seedling was transferred into one well and should be covered fully with water. The coelenterazine working solution was prepared and 25 µl of the working solution were directly transferred into each well, resulting in an end concentration of 10 µM coelenterazine. The plate was covered and incubated overnight in the dark at room temperature.

The next day, MAMP and carbohydrate working solutions were prepared. Therefore, the respective MAMPs or carbohydrates were diluted in a 3-fold concentration in ddH_2O. Usually the MAMPs and carbohydrates were used at the following end concentrations: chitin [100 µg/ml], flg22 [50 nM] and carbohydrates [10, 50 or 100 µg/ml]. The carbohydrates used are listed in Table 7.

Next, the resting levels were measured. Therefore, the first wells were scanned every 6 sec for 1 min with 150 ms integration time. In the next step, 50 µl of the 3-fold concentrated MAMP or carbohydrate solutions were added to the first row. The luminescence (L) upon treatment is recorded in 6 sec

intervals for 20 min with 150 ms integration time. Finally, to measure the total remaining luminescence wells were discharged by adding 150 µl discharge solution and subsequent scanning of the wells for 3 min in a 6 sec interval. After completion of the measurements of the first row, the remaining rows were measured accordingly. As negative control, seedlings of one of the rows were treated with 50 µl ddH_2O instead of a 3-fold concentrated MAMP or carbohydrate solution.

The Ca^{2+} concentrations were calculated and normalized according to Rentel and Knight, 2004 and are depicted as L/L_{max} with L representing the luminescence at any time point upon carbohydrate or MAMP treatment and L_{max} representing the total remaining aequorin. To calculate L_{max}, the luminescence obtained upon treatment with the discharge solution was integrated.

2.2.4.14 ROS Burst Assays

For analysing the production of reactive oxygen species (ROS) upon MAMP or carbohydrate treatment in *A. thaliana* and barley, a chemiluminescence-based assay was performed using 96-well plates. For the standard set-up of this work, several treatments were carried out on one plate.

Each well was filled with 100 µl tap water. For analysing the ROS production in *A. thaliana*, 3-4 leaves per 5-7 week-old plant were harvested. Per leaf, 3-4 leaf discs with a diameter of 4 mm were harvested and transferred into the wells. Leaf discs of one plant were transferred into one row of the 96-well plate. Thus, eight plants were needed for one plate.

For analysing the ROS production in *H. vulgare*, 12 leaf discs of a diameter of 4 mm were harvested from second leaves of 10-14 day old *H. vulgare* plants and transferred into the wells. Leaf discs of one plant were transferred into one row of the 96 well plate. The plate was wrapped into a plastic bag und incubated overnight at room temperature.

The next day, the L-012 solution was prepared. The water in the wells was removed carefully and replaced with either 100 µl L-012 solution, L-012 solution with chitin (100 µg/ml), L-012 solution with flg22 (100 nM) or L-012 solution with carbohydrate (100 µg/ml) per well. The carbohydrates used are listed in table Table 7. The L-012 solution was added to the leaf discs directly before starting the measurement. The chemiluminescence was measured every minute over a period of 1 h using a TECAN infinite® M200 plate reader (Tecan Group Ltd, Männedorf, Switzerland). The obtained data were analysed with Excel.

2.2.4.15 Hydrolysis of β-1,3;1,4-polymer

To generate MLG oligosaccharide of varying length that were tested for their ability to act as elicitor, the respective β-1,3;1,4-polymer was hydrolysed. Therefore, 10 mg/ml barley β-1,3;1,4-polymer (Megazyme, Ireland) was dissolved in 100 mM Sodium Phosphate buffer (pH = 6.5) by heating and stirring. The solution was allowed to cool down and then either 0.025 U ml^{-1} or 0.05 U ml^{-1} *B. subtilis* lichenase (Megazyme, Ireland) were added to the solution. The hydrolysate was incubated for 0, 5, 15, 30, 45, 60, 120 and 240 min at 40°C at 160 rpm. To inactivate the enzyme, the solution was incubated for 15 min in boiling water. The hydrolysates were stored at RT or at 4°C.

To generate MLG oligosaccharides of varying lengths for the forward and reverse genetic screen, 10 mg/ml barley β-1,3;1,4-polymer (Megazyme, Ireland) was dissolved in 100 mM Sodium

Phosphate buffer (pH = 6.5) by heating and stirring. The solution was allowed to cool down and 1 U ml^{-1} *B. subtilis* lichenase was added to the solution. The solution was incubated at 40°C at 160 rpm for 1h and the reaction was inactivated by incubating the hydrolysate in boiling water for 15 min. The hydrolysate was stored at RT or at 4°C.

2.2.5 Biochemical methods

2.2.5.1 Protein extraction of *A. thaliana*

Protein extracts were prepared from 14-day old *A. thaliana* seedlings grown in an in-vitro culture. Upon treatment, 4 seedlings were transferred into one 1.5 ml tube and frozen in liquid nitrogen and stored at -80°C until usage. The frozen seedlings were ground with 200 µl CERK1 extraction buffer and half of a spatula of quartz sand using the IKA® RW digital drill (IKA-Werke, Staufen, Germany). The pistil was cleaned with another 200 µl of CERK1 extraction buffer and the sample was filled up with CERK1 extraction buffer to a volume of 600 µl. The samples were centrifuged for 10 min at 13.000 rpm at 4°C. The supernatant was transferred into a new tube and the protein concentration was determined via Bradford Assay (see 2.2.5.3). The concentrations were equalized to 1 - 1.5 µg/ml. 25 µl of the adjusted protein extract were then mixed with 75 µl 4x SDS buffer and stored at -20°C until usage.

2.2.5.2 Protein extraction of *H. vulgare*

Protein extracts were prepared from *H. vulgare* leaf discs that were treated with different MAMPs and mixed linkage glucans. Upon treatment, the leaf discs were carefully transferred into a 1.5 ml tube and frozen in liquid nitrogen and stored at -80°C until use.

The frozen leaf discs were ground with 200 µl barley extraction buffer and half of a spatula of quartz sand using the IKA® RW digital drill (IKA-Werke, Staufen, Germany). Upon grinding, the pistil was rinsed with another 200 µl barley extraction buffer and the sample was filled up to a volume of 600 µl with barley extraction buffer. The samples were centrifuged for 10 min at 13.000 rpm at 4°C. The supernatant was transferred into a new tube. The protein concentration was calculated using the Bradford assay (see 2.2.5.3). The concentrations were equalized and 25 µl of the samples were mixed with 4x SDS buffer and stored at -20°C until use.

2.2.5.3 Protein quantification via Bradford Assay

The protein concentration of the prepared protein extracts were quantified according to Bradford (Bradford, 1976). The Bradford reagent (Roti-Quant, Roth, Karlsruhe, Germany) was diluted 1:5 in ddH_2O. Next, 2 µl of each sample were mixed with 1 ml Bradford reagent. Additionally, a dilution series of 0, 3, 5, 7, 10 and 15 µg/ml bovine serum albumin was prepared. The samples were incubated for 10 min at RT and the absorbance at 595 nm was measured with a WPA Biowave II photometer (Biochrom AG, Berlin, Germany). A standard curve was generated by plotting A_{595} against the respective concentration. The generated standard curve was then used to calculate the protein concentration of the samples. To equalize protein concentrations, the samples were adjusted to 1 – 1.5 µg/ml with CERK1 or barley extraction buffer.

2.2.5.4 SDS-polyacrylamide gel electrophoresis (SDS-PAGE)

To separate protein according to their molecular mass, a SDS-PAGE was performed.

First, the resolving gel was mixed (see Table 16) and poured between two glass plates with a spacing of 1.5 mm in the respective gel stand and overlaid with isopropanol. Upon polymerization at RT, the isopropanol was removed and the stacking gel (see Table 16) was poured onto the resolving gel. Directly after pouring, a comb was inserted. The concentration of the resolving gel depends on the expected protein size and the purpose of the experiment. For immunoblot analysis, only 10% SDS gels with 1.5 mm spacing were used. For expression studies, Mini Protean TGX (4-20%) 15/10 well gels (BioRad, Munich, Germany) were used.

SDS-PAGE was performed in the Mini-PROTEAN® 3 System (BioRad, Munich, Germany). The gels were placed into the gel apparatus and the tank was filled up with 1x SDS running buffer. Before loading the samples to the gel, they were incubated for 3-5 min at 95°C and up to 20 µl were loaded depending on the comb size. As a size marker, PageRuler™ Prestained Plus protein Ladder (Thermo Fisher Scientific, Waltham, USA) was used. For immunoblot analysis, 1.5 mm gels ran at 30 mA per gel until the bromphenolblue front reached the end of the gel. For expression studies, the gel ran at 150 V until the bromphenolblue front reached the end of the gel. The apparatus was then disassembled and the gels were either used for immunoblot analysis or directly stained with Coomassie blue.

Table 16. Composition of SDS PAGE Gel buffers and mixes used in this study.

SDS PAGE Gel Buffer (250 ml)		
10 % resolving gel buffer	1 M Tris – HCl (pH = 8.8) SDS (10 %) ddH_2O	143.6 ml 3.79 ml 102.53 ml
Stacking gel buffer	1 M Tris – HCl (pH = 6.8) SDS (10 %) ddH_2O	38.85 ml 3.06 ml 208.24 ml
SDS-PAGE gel mixes (10 ml)		
10 % resolving gel	10 % resolving gel buffer 30% acrylamide APS (10%) TEMED	6.6 ml 3.3 ml 0.1 ml 0.004 ml
Stacking gel	Stacking gel buffer 30% acrylamide APS (10%) TEMED	8.16 ml 1.66 ml 0.05 ml 0.005 ml

2.2.5.5 Immunoblot analysis (Western Blot)

Extracted proteins were separated via SDS-PAGE before immunoblot analysis. Proteins were transferred via electroblotting using the TRANS-BLOT® CELL (BioRad, Munich, Germany) onto a PVDF membrane with a pore size of 0.45 µm (Roth, Karlsruhe, Germany). To this end, the PVDF membrane was activated by briefly dipping it into methanol before applying it to the gel. The blotting apparatus was assembled as follows:

cathode
---
black grid of the clamp
sponge
Whatman paper
gel (facing the cathode)
PVDF membrane
Whatman paper
sponge
transparent/red grid of the clamp
---
anode

The blotting was performed in 1x transfer buffer at 4°C for 2h at 80 V.
Upon blotting, the PVDF membrane was blocked for at least 1h with 10 ml TBST + 4% MP at RT on a rotary shaker. After blocking, the PVDF membrane was incubated with the primary antibody overnight at 4°C on a rotary shaker. Upon incubation with the primary antibody, the primary antibody was removed and the PVDF membrane was washed 5 times with TBS-T + 4% MP for 12 min. Next, the PVDF membrane was incubated for 2h with the secondary antibody at RT on a rotary shaker. The used antibodies are listed in Table 10. Upon incubation with the second antibody, the PVDF membrane was washed 5 times with TBS-T for 12 min. Next, the PVDF membrane was equilibrated for 5 min in AP buffer. 500 µL Immun-Star TM AP substrate (BioRad, Munich, Germany) was added to each membrane. The membranes were wrapped in plastic foil and incubated for 5-10 min in the dark. Upon incubated, the membranes were transferred to a new plastic bag and the chemiluminescence was detected using a detection device (ChemiDoc Touch; BioRad, Munich, Germany).

2.2.5.6 Coomassie Staining of PVDF membranes and SDS gels

2.2.5.6.1 PVDF membranes

To visualize protein bands, PVDF membranes were stained with Coomassie brilliant blue. To this end, PVDF membranes were covered with Coomassie staining solution and incubated for 5 min while shaking at RT. After incubation, the PVDF membrane was rinsed in water and the background was

then removed by incubating the membrane in destaining solution at RT while shaking. Finally, the membrane was rinsed in water again and dried.

2.2.5.6.2 SDS gels

To visualize protein bands on SDS gel, the gel was stained with Coomassie Blue. Therefore, the gel was incubated in Coomassie Staining solution for 5 min at room temperature while shaking. To remove background staining, the Coomassie staining solution was removed and the gel was covered with water and incubated in the microwave for 1 min. Then, the gel was incubated in water at room temperature while shaking. Depending on the staining intensity, the water had to be removed and the gel had to be put into the microwave several times.

2.2.5.7 Thin Layer Chromatography (TLC)

First, a TLC chamber was filled with TLC running buffer. In a next step, 5 µl of the analytes were dropped onto the TLC Silica gel plate (Merck, Darmstadt, Germany) and were allowed to dry at RT. Upon drying, the TLC plate was put into the chamber and the running buffer was allowed to run up the plate until it almost reached the top. The plate was again allowed to dry at room temperature under the fume hood. To stain the TLC, the TLC plate was wetted with TLC staining solution and then incubated on a heating plate at 99°C for 30 - 45 min.

2.2.5.8 Expression of His-tagged protein in *P. pastoris*

2.2.5.8.1 Small Scale Expression of secreted proteins in *P. pastoris*

To test expression of the gene of interest in the obtained *P. pastoris* transformants, a small scale expression was performed. Therefore, the transformants were grown under four different conditions for 7 days: The transformants were either grown at 16°C or at 25°C and fed with either 1% or 3% methanol (end concentration in the medium).

In the morning, yeast transformants were inoculated in a 50 ml tube containing 3 ml YPD and either 100 or 500 µg/ml Zeocin. The cultures were incubated over the day at 30°C at 225 rpm. In the afternoon, 600 µL of the pre-culture were inoculated in 10 ml BMGY in a 50 ml tube and incubated overnight at 30°C at 225 rpm. The cells were incubated in BMGY to ensure an optimal induction of expression in presence of methanol. Per transformant, four new tubes were inoculated. In the afternoon of the next day, all grown cultures were centrifuged for 15 min at 4.000 g at RT. The supernatant was discarded and the pellets were resuspended in 4 ml BMMY (containing 3% methanol). The cultures were further grown at either 16°C or 25°C at 160 rpm. The transfer of the cultured from BMGY to BMMY medium represents day 1 of the small scale expression. From the third day on, the cultures were fed every day with either 1% methanol (50 µl of 100% methanol) or 3% (150 µl of 100% methanol) methanol. Furthermore, samples were taken for testing the expression at day 3 and day 5. Therefore, 90 µl of the cultures were transferred into a 1.5 ml tube, centrifuged for 3 min at 10.000 g and frozen in liquid nitrogen. The samples were stored at -20°C until use. On day 7, the yeast cultures were centrifuged for 15 min at 3000 g at 4°C. The supernatant was filtered with a filter having a pore size of 0.22 µm into a 15 ml tube. The supernatant can be stored at 4°C until use.

To test for the presence of the protein in any of the supernatants, 40 µl of the supernatant obtained at day 7 were mixed with 10 µl SDS loading dye and used for SDS-PAGE.
According to the results of the small scale expression, a *P. pastoris* transformant was chosen that had the highest protein abundance at a particular growth condition for large scale expression.

2.2.5.8.2 Large Scale Expression of secreted proteins in *P. pastoris*

For expression of *Bgh06777*, a transformant was chosen that had the highest abundance of the protein while growing at 16°C with 1% methanol. For purification of the protein, the supernatant was collected at day 5 of the large scale expression.
In the morning, the respective yeast transformant was inoculated four times in 5 ml YPD containing 500 µg/ml Zeocin in 50 ml tubes. The cultures were grown over the day at 30°C at 160 rpm. In the afternoon, 10 ml of the pre-cultures were used to inoculate 500 ml BMGY in a 2l baffled flask. The cultures were grown overnight at 30°C at 220 rpm to an OD_{600} of 5-6. The next day, the cultures were centrifuged at 3700 rpm at RT. The supernatant was discarded and the cells resuspended in 400 ml BMMY (containing 3% methanol). The cultures were transferred to a 2l baffled flask and incubated at 16°C at 250 rpm (day 1). The culture was fed every 24h beginning of day 3 with 100% methanol to maintain a concentration of 1% methanol in the medium. On day 5, the culture was centrifuged for 10 min at 3700 rpm at RT and the supernatant was transferred to a beaker. After filtration of the supernatant, the pH of the supernatant was adjusted to 7.7 with NaOH and stored at 4°C until use for extraction and purification of the protein.

2.2.5.9 Extraction and purification of His-tagged protein in *P. pastoris*

To extract and purify BGH06777 from *P. pastoris*, the supernatant obtained from the large scale expression was first reduced in volume using Vivaflow 200 (Sartorius, Göttingen, Germany). The supernatant was then loaded onto a 1 ml HisTrap IMAC FF nickel-nitrilotriacetic acid column (GE Healthcare, Chicago, USA) using the Minipulse 3 Peristaltic Pump (Gilson, France). After loading of the supernatant, the column was washed with 5 ml buffer A. Next, the protein was eluted from the column with the FPLC Biologic Duoflow system (BioRad, Munich, Germany) using a linear gradient of 0 – 100 % buffer C. The fractions were monitored with A_{280} and collected with the Fraction Collector (Biofraction, BioRad, Munich, Germany). The fractions with the eluted protein were pooled and exchanged with SEC buffer using a 3 kDa Vivaspin centrifugal filter (GE Healthcare, Chicago, USA). The protein concentration was determined with the Epoch Microplate Spectrophometer (BioTek, Winooski, USA) and the molar extinction coefficient (BGH06777 = 2.3 M^{-1} cm^{-1}). The molar extinction coefficient was calculated using the ProtParam tool of the ExPASy Bioinformatics Resource Portal (Gasteiger *et al*., 2015). Upon concentrating the protein to 1 mg/ml, aliquots were frozen in liquid nitrogen and stored at -80°C. The protein purity was determined by SDS-PAGE.

2.2.5.10 Functional characterization of enzymes

2.2.5.10.1 Product Analysis using HPAEC-PAD

Carbohydrate Analysis was carried out using High-performance-anion-exchange chromatography with pulsed amperometric detection (HPAEC-PAD). HPAEC-PAD was performed using a Dionex ICS-5000 HPLC system equipped with an AS-AP autosampler in a sequential infection configuration using the Chromelion software version 7. 10 µl of the samples were injected on a 3 x 250 mm Dionex Carbopac PA200 column (Thermo Scientific, Waltham, USA). This equipment was used for all separations. The gradient was used as follows: 0-5 min, 10% B, 0% C (initial conditions); 5-12 min 10% B, linear gradient from 0 – 30% C; 12.0-12.1 min, 50% B, 50% C; 12.1 – 13.0 min, exponential gradient of B and C, back to initial conditions, 13-17 min initial conditions. Solvent A was ultrapure water, solvent B was 1 M sodium hydroxide and solvent C was 1 M sodium acetate.

2.2.5.10.2 Confirmation of protein mass by mass-spectrometry

The intact protein mass was determined using a Waters Q-Tof with a nanoACQUITY UPLC system according to Sundqvist *et al*., 2007

2.2.5.10.3 Identification of substrates

To identify the substrate of BGH06777, 1 µg/ml BGH06777 in 50 mM MES buffer (pH = 5) was incubated with either 0.05 mM laminarihexaose, 0.05 mM laminaripentaose, 0.05 mM laminaritetraose or 0.05 mM laminaritriose. Upon 1h (partial digest) and 12h (full digest) incubation at RT, the samples were subjected to product analysis using HPAEC-PAD. As standards, glucose, laminaribiose, laminaritriose, laminaritetraose, laminaripentaose and laminarihexaose were included.

2.2.5.10.4 Identification of the temperature optimum

The temperature optimum was identified in 50 mM citrate buffer (pH = 5) using 1 mM laminarihexaose and 2 µg/ml BGH06777. The reaction was prepared at 4°C in a total volume of 1000 µl. The reaction was mixed well and 50 µl of the digest were transferred into different PCR tubes. The 50 µl digests were incubated for 1 h at the following temperatures [°C]: 30, 32, 35.2, 39.3, 44.9, 49, 51.9, 54, 55, 57.1, 60.2, 64, 69.3, 73.5, 76.3 and 78. Afterwards, the reactions were stopped by incubating the digests for 5 min at 95°C and 1 min at 4°C. The different reactions were then transferred to HPAEC vials containing 450 µl ddH_2O and the area of the product peak (laminaribiose) was quantified using HPAEC-PAD. As standard, different concentrations of laminaribiose ranging from 0.00000156 mM to 1 mM were run on the HPAEC and the change in the peak area of laminaribiose was calculated using the excel linest function. The enzymatic rate was then calculated with the product peak obtained from the hydrolysis of laminarihexaose by BGH06777, the molar concentration of BGH06777 and the change of the peak area of laminaribiose (standard).

2.2.5.10.5 Identification of the pH optimum

To identify the pH optimum of BGH06777, 1µg/ml BGH06777 was incubated with 1 mM laminarihexaose in 50 mM buffer in a total volume of 50 µl. The reaction was incubated in

different buffers with different pH values that are listed in Table 17. The digests were incubated for 1 h at 25°C and the reactions were terminated by incubating them for 5 min at 95°C. The 50 µl reactions were transferred into HPAEC vials containing 450 µl ddH_2O, analysed via HPAEC-PAD and the area of the product peak (laminaribiose) was quantified. Different concentrations of laminaribiose (ranging from 0.00000156 mM to 1 mM) were analysed via HPAEC-PAD as a standard and the change in the product peak was calculated using the linest function of Excel. Next, the enzymatic rate of BGH06777 was calculated using the molar concentration of BGH06777, the change of the peak area of laminaribiose (standard) and the laminaribiose peak areas obtained upon laminarihexaose hydrolysis with BGH067777.

Table 17. Buffers used to identify the pH optimum of BGH06777.

Buffer (Substance)	pH
Citrate	3
Citrate	3.5
Citrate	4
Citrate	4.5
Citrate	5
Citrate	5.5
Citrate	6
Citrate	6.5
Citrate	7
Glycin-Glycin	8
Glycin-Glycin	9
Glycin	10

2.2.5.10.6 Michaelis-Menten Kinetics

Michaelis-Menten kinetics were determined using HPAEC-PAD. Therefore, an enzyme stock (5 or 50 µg/ml BGH06777 in 200 mM citrate buffer pH = 5.5) was mixed with a substrate stock (0.0078 to 1 mM final substrate concentration) preheated to 37°C. As substrates, laminarihexaose and laminaripentaose were used. For example, 50 µl of 5 µg/ml BGH06777 in 200 mM citrate buffer (pH = 5.5) was added to 450 µl of 1 mM laminarihexaose in ddH_2O preheated to 37°C. The sample (each 10 µl) was injected 5 times every 20 min onto the column. The change in the peak area of the resulting product laminaribiose was quantified with the linest function of excel for all used concentrations of the respective substrates. As standard, the change in the peak area of different concentrations (0.00000156 to 1 mM) of laminaribiose was calculated using the linest function of excel. The

enzymatic activity was then calculated with the change of the peak area of laminaribiose generated during the hydrolysis by BGH06777, the molar concentration of BGH06777 and the change of the peak area of laminaribiose (standard). The obtained enzymatic rates were fit to the Michaelis-Menten model (Michaelis and Menten, 1913; Johnson and Goody, 2011) using OriginPro graphing software.

2.2.5.10.7 Determination of the regiospecificity

The regiospecificity of laminarihexaose hydrolysis was determined by monitoring the ^{18}O incorporation from ^{18}O -water by mass spectrometry (Schagerlöf *et al.*, 2009). 1 µL BGH06777 (0.05 mg/ml bgh06777 in 1 M citrate buffer pH = 5.5) and 1 µl 10 mM laminarihexaose were mixed with 18 µL 97% ^{18}O water (Cambridge Isotope Laboratories) and mixed well by reciprocal pipetting. The reaction was transferred to a 50 µl gas-tight Hamilton syringe 80 (Hamilton, model 1705) and infected into a Waters Xevo QTof at 2 µl/min using a pump (Harvard Apparatus 11 Plus). The level of isotopic labelling was quantified using the ratio: $[M+Na]^+(^{16}O\text{-}1)$ to $[M+Na]^+(^{18}O\text{-}1)$ (McGregor *et al.*, 2016).

2.2.5.11 Carbohydrate Analysis

2.2.5.11.1 HPAEC-PAD

HPAEC-PAD was performed using a Dionex ICS-5000 HPLC system equipped with an AS-AP autosampler in a sequential infection configuration using the Chromelion software version 7. 10 µl of the samples were injected on a 3 x 250 mm Dionex Carbopac PA200 column (Thermo Scientific, Waltham, USA). 56 µM of the MLG tetramer or 45 µM of the MLG trimer were loaded onto the column. The following gradient was used: The gradient was used as follows: 0-5 min, 10% B, 3.5 % C (initial conditions); 5-12 min 10% B, linear gradient from 0 – 30% C; 12.0-12.1 min, 50% B, 50% C; 12.1 – 13.0 min, exponential gradient of B and C, back to initial conditions, 13-17 min initial conditions. Solvent A was ultrapure water, solvent B was 1 M sodium hydroxide and solvent C was 1 M sodium acetate.

2.2.5.11.2 MALDI-TOF

MALDI-TOF analysis of mixed-linkage glucans was performed with a Bruker Autoflex system (Bruker Daltonics) operated in reflectron mode. 10 mg/ml of the oligosaccharide were mixed 1:5 with a 2,5-dihiydroxybenzoic acid in 1:1 H_2O:MeOH on a Bruker MTP 384 grounded steel MALDI plate. The samples were allowed to dry and subsequently, analysed.

3 Results

3.1 Identification and functional characterization of *Bgh* CWDEs

3.1.1 Identification of potential candidate GHs of *Bgh*

The plant cell wall represents an effective structural barrier to microbial invasion. To breach the plant cell wall and to gain access to plant's nutrient resources, fungi secrete CWDEs that are often required for full pathogenicity (Kubicek *et al.*, 2014). One aim of this study was to identify and functionally characterize CWDEs of the powdery mildew *Bgh* that are required for pathogenicity. To this end, genomic and transcriptomic data were analysed for *in planta* expressed and potentially secreted GHs.
A genome analysis of *Bgh* conducted in 2010 revealed a reduced number of CWDEs in the genome of *Bgh* compared to other plant pathogenic fungi (Spanu *et al.*, 2010). In total only two lignocellulose-degrading enzymes (Auxiliary Activity Family 9, formerly known as GH61), four hemicellulose-degrading enzymes (GH16) and one pectin/β-1,3-glucan hydrolyzing enzyme (GH81) were identified in this study. Auxiliary activity proteins are lytic polysaccharide monooxygenases that act on cellulose or have other substrate specificities (Carbohydrate Active Enzymes database, http://www.cazy.org/, Lombard *et al.*, 2014). However, an independent genomic analysis by our collaborators at the IPK Gatersleben (research group of the late Dr. Patrick Schweizer) identified a total of 75 CWDEs including 62 GHs belonging to 18 different GH families, four CBMs of three different families and nine CEs designated to five different families in the genome of *Bgh*. Moreover, 26 putative CWDEs were identified that could not be assigned to a family (unpublished data; Dr. Patrick Schweizer, personal communication). To verify the 62 GHs identified by our collaborators, protein sequences of all identified GHs were searched for carbohydrate active enzyme domain signatures using the publicly available sources dbCAN (http://bcb.unl.edu/dbCAN2, Yin *et al.*, 2012) and Motif Scan (https://myhits.isb-sib.ch/cgi-bin/motif_scan). Of the 62 annotated GHs, only the protein BGH05207 designated to GH family 17 and the protein BGH02531 belonging to GH family 18 could not be verified and thus, were excluded from further analysis (Table S1).
In a next step, *in planta* gene expression of the 18 GH families of *Bgh* was analysed. The expression of a gene can be evaluated by calculating the reads per million (RPM) of the total amount of reads obtained from an RNAseq experiment. RPMs were calculated for all members of the 18 GH families identified in *Bgh* at different time points upon infection using publicly available *in planta* RNAseq data (Hacquard *et al.*, 2013). In particular, members of the GH families 5, 16, 17, 47 and 76 were highly expressed during the compatible interaction of *Bgh* and the immunocompromised Arabidopsis triple mutant *pen2 pad4 sag101* expressing *MLA1* either at a specific time point of infection or throughout the whole infection indicating a potential role in pathogenicity (

Table S2). This indicates that they might play a role in pathogenicity and thus represent interesting candidate GH families for further analysis.

3.1.2 The family GH17 was chosen for further analysis

The different GH families exhibit different substrate specificities (Carbohydrate Active Enzymes database, http://www.cazy.org/, Lombard *et al.*, 2014). To reduce the number of potential candidate families, GH families 5, 16, 17, 47 and 76 were analysed regarding their substrate specificities. Proteins designated to GH family 47 or 76 are known to hydrolyse mannans (Herscovics, 2001; Cuskin *et al.*, 2015), while proteins belonging to GH5 have been shown to act e.g. on cellulose, mannans, β-1,3-glucans, β-1,6-glucans and hemicelluloses (Aspeborg *et al.*, 2012). The GH family 16 is known to include enzymes that have activity on e.g. β-1,3;1,4-glucans, hemicelluloses, β-1,3-glucans as well as chitin (Viborg *et al.*, 2019) while family GH17 includes enzymes which mainly hydrolyse β-1,3-glucans and fungal β-1,3;1,6-glucans with a region of unbranched β-1,3-linkages (Hrmova and Fincher, 1993; Carbohydrate Active Enzymes database, http://www.cazy.org/, Lombard *et al.*, 2014). β-1,3-glucans are present in plants as callose, which is a major component of defence-associated papillae (Jacobs *et al.*, 2003; Underwood, 2012). In order to infect a plant, pathogens do not only need to breach the cell wall but also papillae. It was shown that papillae that only contain a low amount of callose were not effective in preventing fungal penetration and haustoria formation (Chowdhury *et al.*, 2014). This suggests that *Bgh* may overcome papillae with a combination of pressure and CWDEs. Since proteins designated to family GH17 hydrolyse β-1,3-linkages mainly in β-1,3-glucans and thus might be involved in penetration of papillae, this family was chosen for further bioinformatic analysis.

3.1.3 Bioinformatic analysis of *Bgh* GH17 proteins

To interact with the plant cell wall, fungal CWDEs have to be secreted and therefore, contain either a canonical signal peptide or an unconventional secretion signal. Thus, the seven members of *Bgh* GH family 17 were analysed using the publicly available server SignalP (http://www.cbs.dtu.dk/services/SignalP/) and SecretomeP (http://www.cbs.dtu.dk/services/SecretomeP/) for identifying conventional or unconventional secretion signals, respectively. Except for BGH00736, which harbours an unconventional secretion signal, all GH17 family members contain a canonical N-terminal signal peptide indicating that all GH family 17 members in *Bgh* are likely to be secreted by the fungus in order to act on the plant cell wall (Table 18). Additionally, N-glycosylation sites as well as phosphorylation sites were predicted with the public available tools NetNGlyc (http://www.cbs.dtu.dk/services/NetNGlyc/) and NetPhos

(http://www.cbs.dtu.dk/services/NetPhos/), respectively. All proteins belonging to GH17 harbour at least one predicted N-glycosylation site as well as several predicted phosphorylation sites (Table 18).

Table 18. Properties of *Bgh* GH 17 proteins.

BluGen Protein Number*	Protein Size [kDa]	Predicted Motif	Predicted N-Glycosylation Sites (Position)	Predicted Phosphorylation Sites	Secretion
BGH00219***	31.9	GH17 motif	2 (185; 204)	30	Signal Peptide
BGH00220***	32	GH17 motif	1 (274)	23	Signal peptide
BGH00734**	58.5	GH17 motif Threonine-rich region	2 (85; 530)	63	Signal peptide
BGH00736**	85.5	GH17 motif	4 (191; 460; 512; 678)	91	Unconventional secretion
BGH05070***	31.6	GH17 motif	4 (45; 185; 204; 253)	30	Signal peptide
BGH06298***	32.7	GH17 motif	1 (185)	25	Signal peptide
BGH06777***	31.9	GH17 motif	1 (191)	28	Signal peptide

* Protein identification numbers were retrieved from www.blugen.org.
** Nucleotide and amino acid sequence obtained from Dr. Patrick Schweizer
*** Nucleotide and amino acid sequence obtained from https://www.ebi.ac.uk/ena

3.1.4 Analysis of the potential role of *Bgh* GH17 genes in pathogenicity

Host-induced gene silencing (HIGS) represents a “tool to address gene function in obligate biotrophic fungi” and is based on RNA interference (RNAi) (Nowara *et al.*, 2010). RNAi molecules that target *Bgh* transcripts are expressed *in planta* and may be exchanged between the host and the established *Bgh* haustorium. The uptake of the RNAi construct by *Bgh* leads to silencing of the fungal target gene and allows to analyse the gene function (Nowara *et al.*, 2010). In order to analyse the contribution of specific genes to invasiveness, a first HIGS experiment was performed by our collaborators at the IPK Gatersleben (unpublished data; Dr. Patrick Schweizer, personal communication). These preliminary analyses suggested that silencing of *Bgh06298* and *Bgh05070* resulted in an enhanced penetration

rate indicating that these genes have a negative impact on pathogenicity and might either be directly recognized by the plant or involved in the generation of DAMPs. Although the penetration rate was not significantly increased, these candidates were excluded from further analysis. On the contrary, silencing of *Bgh06777* or *Bgh00734* might lead to a reduced penetration rate leading to the suggestion that these genes are involved in pathogenicity (unpublished data; Dr. Patrick Schweizer, personal communication). Thus, the GH17 family members BGH06777, BGH00219, BGH00220, BGH00734 and BGH00736 were chosen for further functional characterization.

3.1.5 Recombinant production of *Bgh* GH17 proteins in *Pichia pastoris*

Several heterologous expression systems are available that can be used to produce recombinant proteins, e.g. *Escherichia coli*, *Pichia pastoris* or *Saccharomyces cerevisiae*. In contrast to *E. coli*, *P. pastoris* and *S. cerevisiae* offer the advantage of eukaryotic protein processing, protein folding as well as posttranslational modifications. As *P. pastoris* in contrast to *S. cerevisiae* does not hyperglycosylate proteins (Daly and Hearn, 2005; Gomes *et al.*, 2016), *P. pastoris* was selected as heterologous expression system for the selected *Bgh* genes *Bgh00219*, *Bgh00220*, *Bgh06777*, *Bgh00734* and *Bgh00736*. The genes *Bgh00220* and *Bgh06777* without the signal peptide were amplified from cDNA and cloned into the pPICZα expression vector with a C-terminal His and Myc tag. pPICZα expression vectors for *Bgh00219*, *Bgh00734* and *Bgh00736* were synthesized by BioBasic (Markham, Ontario, Canada). The sequence for the expression vector for *Bgh00219* is based on the cDNA sequence of *Bgh00219* without the signal peptide, while the sequence for the expression vector of *Bgh00734* is based on the cDNA sequence with the signal peptide. For the synthesis of the *Bgh00736* expression vector, cDNA with the signal peptide was used as a template. The expression vectors for all genes were successfully transformed into *P. pastoris* X-33 cells. Three to four clones were tested for the presence of either BGH00219, BGH00220, BGH00734, BGH00736 or BGH06777 in a small scale expression test using four different conditions. The clones were either grown at 16°C or 25°C and either 1% or 3% methanol were added every 24h. For both BGH00219 and BGH00220 a distinct band at 34 kDa (with Myc and His-tag) was expected. However, no signal for either BGH00219 or BGH00220 was detected at the expected size. Instead, all clones transformed with the plasmid encoding for *Bgh00219* exhibited several signals at various sizes while clones expressing *Bgh00220* showed either several signals or no signal at all (Figure S1 A and B). For BGH00734 a signal migrating at 66 kDa (with Myc and His-tag) should be detected, while a signal at 87 kDa should be visible for BGH00736 (with Myc and His-tag). As for BGH00219 and BGH00220, no distinct signals at the expected sizes could be detected for either BGH00734 or BGH00736 (Figure S1 C and D). This indicates that none of the tested clones can be used to purify these four proteins. The detected signals might correspond to the respective proteins that were proteolytically cleaved, posttranslationally modified or might represent contaminations. For BGH06777 a signal at about 33 kDa (with Myc- and His tag) was expected. Fortunately, all tested clones expressed *Bgh06777* with clone #17 showing the highest expression while growing at 16°C and addition of 1% methanol

(Figure S1 E). Consequently, this clone was chosen for the scale-up expression to produce more of the respective protein. The recombinant protein was purified via FPLC, following size exclusion and the purification yield was 12 mg/L. According to SDS PAGE, purified BGH06777 migrated at a size of 35 kDa (calculated: 35 kDa corresponding to BGH06777 with N-linked oligosaccharides containing 14 mannose residues and N-terminal Myc and His-tag). To verify the glycosylation, recombinant BGH06777 was incubated with PNGase F which is an amidase that cleaves N-linked oligosaccharides from glycosylated proteins (Plummer *et al.*, 1984). Upon PNGase F treatment, BGH06777 migrated at 33 kDa (calculated: 32.967 kDa corresponding to BGH06777 with N-terminal Myc- and His-tag) indicating that *P. pastoris* glycosylated BGH06777 (Figure S2). In order to further verify the protein mass of recombinant BGH06777, mass spectrometry was performed. Several masses between 35169 Da and 36873 Da were identified during the analysis of glycosylated BGH06777 (Figure 4 A). The identified masses correspond to recombinant BGH06777 with N-linked oligosaccharides of varying length (11 - 20 mannose residues) and BGH06777 with phosphorylated N-linked oligosaccharides of varying length (13 - 18 mannose residues). Upon treatment with PNGase F, the major mass identified was 32977 Da which corresponds to the deglycosylated form of recombinant BGH06777 (Figure 4 B). In the following biochemical characterization, the glycosylated form of recombinant BGH06777 was used.

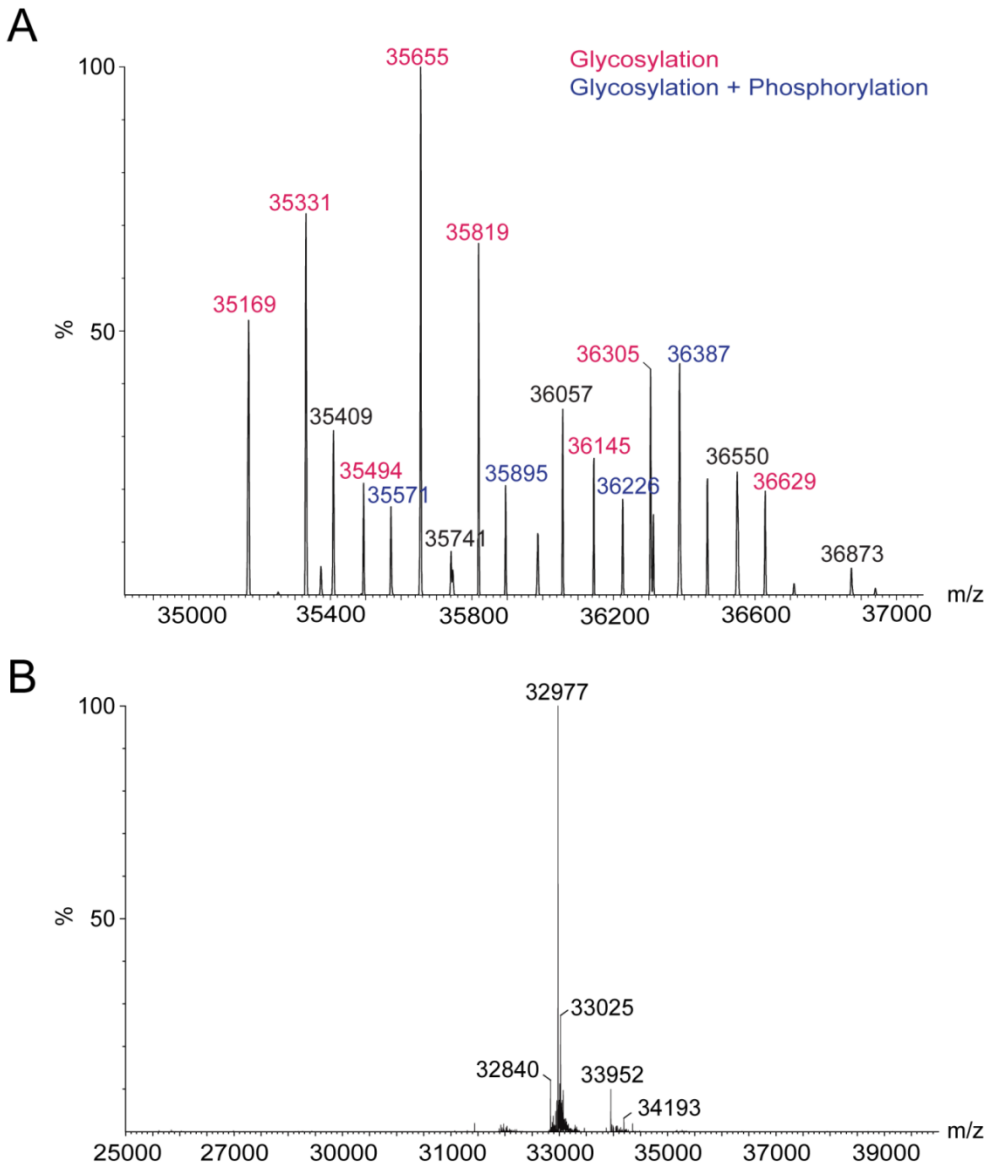

Figure 4. Mass spectra of recombinant BGH06777. (A) Mass spectra of glycosylated and phosphorylated BGH06777. Protein mass of purified BGH06777 was verified by analyzing the mass via mass spectrometry. Pink lettering indicates masses of N-glycosylated BGH06777 with varying length of mannose residues (11 - 20). Blue lettering indicates masses of N-glycosylated BGH06777 with varying length of mannose residues (13 - 18) and phosphorylation. (B) Mass spectra of deglycosylated BGH06777. To verify glycosylation of purified BGH06777, BGH06777 was treated with PNGase F overnight. Subsequently, the protein mass by determined via mass spectrometry.

3.1.6 β-1,3-glucan oligosaccharides are substrates of BGH06777

GH family 17 includes enzymes that hydrolyse β-1,3-glycosidic linkages in β-1,3-glucans (E.C.3.2.1.39, E.C.3.2.1.58) or β-1,3-glycosidic linkages in fungal β-1,3;1,6-glucans if a region of unbranched β-1,3-glucan residues is available. Furthermore, a β-1,3;1,4-glucan endo-hydrolase belonging to GH17 was shown to hydrolyse β-1,4-glycosidic linkages in plant β-1,3;1,4-glucans (E.C.3.2.1.73) if the β-1,4-glycosidic linkage is located at the reducing end (Woodward and Fincher, 1982; Hrmova and Fincher, 1993; Carbohydrate Active Enzymes database, http://www.cazy.org/, Lombard *et al.*, 2014). Based on the substrate specificities known for GH17 family members, recombinant BGH06777 was tested for activity on β-1,3-glucan oligosaccharides. Therefore, recombinant BGH06777 was incubated with β-1,3-glucan oligosaccharides of varying length (6-3) at room temperature in MES buffer (pH = 5) and the hydrolysis products were analysed by high-performance anion exchange chromatography with pulsed amperometric detection (HPAEC-PAD). HPAEC-PAD represents a highly sensitive method for oligosaccharide separation. The hydroxyl groups are ionized under strongly basic conditions and retain at the anion exchange column. The ionized oligosaccharides can be released at a certain retention time depending on e.g. the molecular size, the number of hydroxyl groups and the structure of the oligosaccharide. The mobile phase is composed of the oligosaccharide dissolved in water. To elute the oligosaccharides from the column a constant concentration of sodium hydroxide is used with an increasing concentration of sodium acetate over time. Sodium acetate is a stronger eluent compared to sodium hydroxide and is used to elute longer oligosaccharides or acidic sugars. To detect the carbohydrate, an electronic current that is generated upon oxidation of the oligosaccharide on a gold-electrode is measured (Corradini *et al.*, 2012).

Hydrolysis of laminarihexaose (G3G3G3G3G3G) yielded in the formation of laminaritetraose (G3G3G3G) and laminaribiose (G3G) (Figure 5). Upon 12h incubation of laminarihexaose (G3G3G3G3G3G) with BGH06777, laminarihexaose (G3G3G3G3G3G) was completely degraded (Figure 5, blue line). The resulting oligosaccharides from laminaripentaose (G3G3G3G3G) degradation were laminaritriose (G3G3G) and laminaribiose (G3G). As observed for laminarihexaose, laminaripentaose was completely degraded upon 12h incubation with BGH06777 (Figure 5, blue line). The degradation of laminaritetraose (G3G3G3G) resulted in the formation of laminaribiose (G3G), however, laminaritetraose was not completely degraded upon 12h incubation with the enzyme (Figure 5, blue line). The β-1,3-oligosaccharide laminaritriose was not degraded by BGH06777 (Figure 5). These results indicate that recombinant BGH06777 uses β-1,3-glucan oligosaccharides of a minimum length of four glucose monomers as substrates.

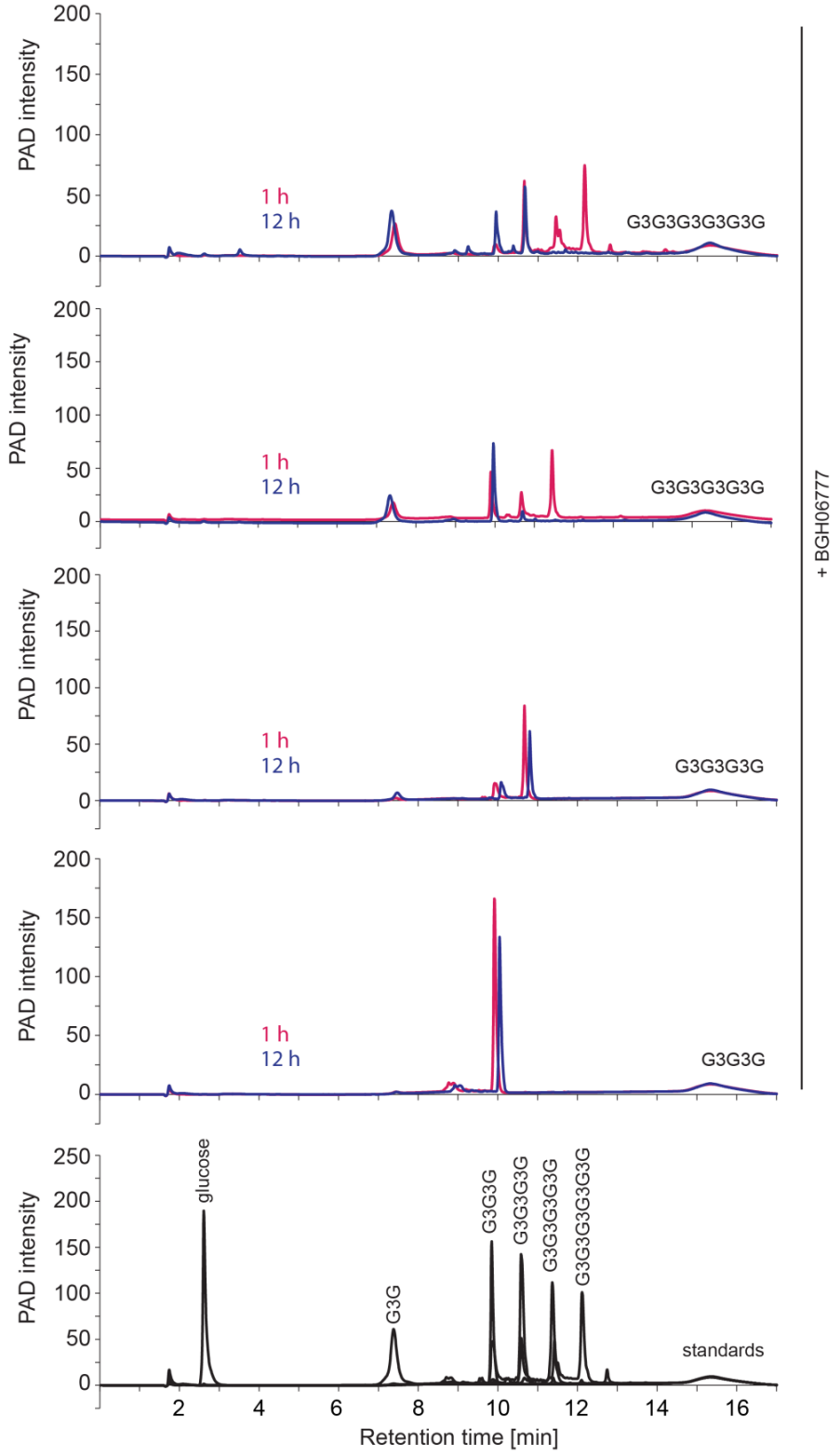

Figure 5. HPAEC-PAD chromatograms of β-1,3-glucan oligosaccharide hydrolysis by BGH06777. 1 µg ml^{-1} BGH06777 was incubated with 0.05 mM laminarihexaose (G3G3G3G3G3G), laminaripentaose (G3G3G3G3G), laminaritetraose (G3G3G3G) and laminaritriose (G3G3G) in 50 mM MES buffer (pH = 5) at room temperature. Upon 1h (pink line) or 12h (blue line) incubation, the hydrolysis products were analysed by HPAEC-PAD. As standards, the respective β-1,3-glucan oligosaccharides and glucose were included.

3.1.7 Optimal temperature and pH conditions for BGH06777

The activity of enzymes can be affected by changing environmental conditions, e.g. pH or temperature. Each enzyme has a pH and temperature optimum at which its activity rate is the highest (Robinson, 2015). To determine the optimal temperature of BGH06777, recombinant BGH06777 was incubated with laminarihexaose at different temperatures (5°C - 78°C) in 50 mM Citrate buffer (pH = 5) and the amount of the generated product laminaribiose was measured to determine the activity rate using HPAEC-PAD. Recombinant BGH06777 was active within a temperature range of 15°C to 57°C with the highest activity rate observed in a range from 25°C to 51°C (Figure 6 A).
In order to determine the optimal pH, recombinant BGH06777 was incubated with its substrate laminarihexaose in different buffers ranging from pH 3-10 at 30°C. The activity rate was measured as the amount of generated laminaribiose via HPAEC-PAD. Recombinant BGH06777 was active in a pH range from 4.5 to 8. The optimal pH for recombinant BGH06777 was shown to be at 5.5 (Figure 6 B).

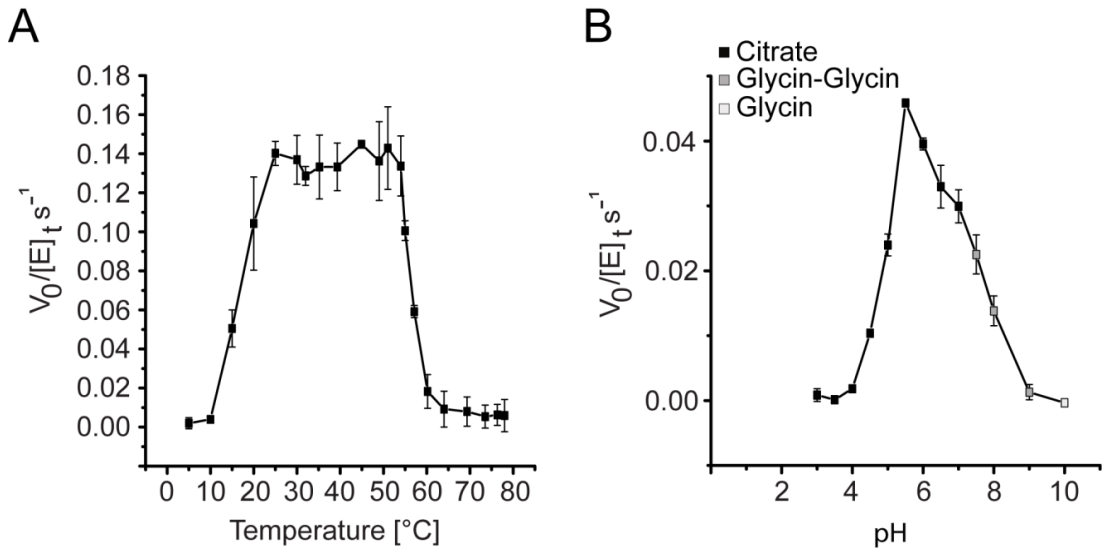

Figure 6. Temperature and pH profile of recombinant BGH06777. (A) Temperature optimum of BGH06777. For the temperature profile, 2 µg ml^{-1} BGH06777 were incubated in 50 mM Citrate buffer (pH = 5) with 1 mM laminarihexaose. The reaction was incubated for 15 min or 1h at the respective temperature. Upon deactivation of BGH06777, the enzymatic rate was measured as increase in product peak via HPAEC-PAD. Error bars represent standard deviation. (B) pH optimum for BGH06777. To determine the pH profile, 2 µg ml^{-1} BGH067777 were incubated with 10 mM laminarihexaose in 50 mM buffer with different pH ranging from 3-10. The following buffers were used: Citrate buffer from pH 3-7, Glycin-Glycin buffer from pH 7.5 to 9 and Glycin buffer for pH 10. The enzymatic rate was measured as increase in product peak over time. Error bars represent standard error.

3.1.8 Michaelis-Menten parameters of BGH06777

To characterize enzymes regarding activity rates and the influence of changing conditions on enzymatic activity, kinetic models are used. The most commonly used model is the Michaelis-Menten model. This model is based on the assumption that an enzyme (E) forms an unstable enzyme-substrate complex (ES) with its substrate (S) followed by decay to enzyme and product (P) (Michaelis and Menten, 1913) (Figure 7 A). Under three further assumption, that 1) the substrate concentration is much higher than the enzyme concentration, 2) only initial velocities are taken into account and thus, product formation does not influence the reaction and 3) the speed of the formation of enzyme-substrate complex is equal to the decay of enzyme-substrate complex, the enzymatic rate can be described in a mathematical equation as relation of the product formation rate and substrate concentration (Figure 7 B), where v is the initial velocity, k_{cat} (the turnover number) describes the number of substrate molecules that is converted to product per enzyme site per time, $[E]_0$ is the initial enzyme concentration, while the Michaelis-Menten constant (K_M) represents the substrate concentration that yield in half-maximal velocity (Michaelis and Menten, 1913). This equation can be used to calculate enzyme kinetics from enzyme reactions with varying substrate concentrations. Furthermore, the ratio of k_{cat} to K_M can be used to measure catalytic efficiency (Eisenthal *et al.*, 2007).

A

$$E + S \rightleftharpoons ES \xrightarrow{k_{cat}} E + P$$

B

$$v = k_{cat}\,[E]_0 \frac{[S]}{K_M + [S]}$$

Figure 7. Michaelis-Menten model for an enzymatic reaction and the resulting equation. (A) Model for an enzymatic reaction. Enzyme (E) forms a complex (ES) with its substrate (S) followed by the release of a product (P) and a free enzyme (E). The double arrow indicates that the formation of the enzyme-substrate complex (ES) is reversible. (B) Michaelis-Menten-Equation with v – initial velocity, k_{cat} – number of substrates converted to product per time, $(E)_0$ - enzyme concentration, [S] - substrate concentration, K_M – substrate concentration with which half-maximal velocity is achieved.

To identify Michaelis-Menten kinetics for recombinant BGH06777 for the two substrates laminarihexaose (G3G3G3G3G3G) and laminaripentaose (G3G3G3G3G), the enzyme was incubated with the respective substrates in eight different concentrations and the initial velocities were measured over time as increase in product peak (laminaribiose) via HPAEC-PAD. The obtained initial velocities were plotted against the substrate concentration and Michaelis-Menten parameters (k_{cat} and K_M) were determined by non-linear fit using the Michaelis-Menten model in the software OriginPro (Figure 8, Table 19).

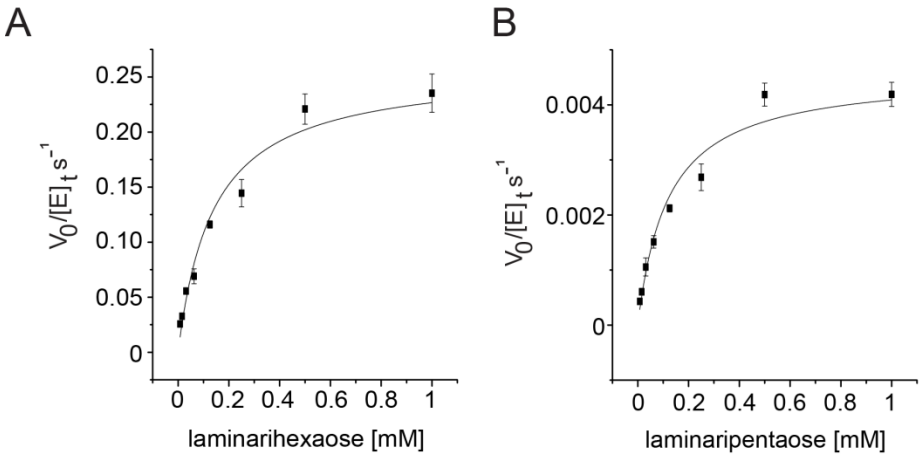

Figure 8. Michaelis Menten plots of BGH06777 acting on β-1,3-oligosaccharides. 0.5 µg ml^{-1} or 5 µg ml^{-1} BGH06777 were incubated with laminarihexaose (A) or laminaripentaose (B) in 200 mM Citrate Buffer (pH = 5.5) at 30°C. Initial velocities rates were measured for eight different substrate concentrations as increase in product peak over time via HPAEC-PAD. The initial velocities were plotted against substrate concentrations and Michaelis-Menten parameters were determined via non-linear fit using the Michaelis-Menten model in Origin Pro. Error bars represents standard errors.

Recombinant BGH06777 hydrolysed laminarihexaose with the highest k_{cat} values of the two tested substrates at a pH of 5.5 and 30°C (Table 19). Under these conditions, laminaripentaose was hydrolysed less efficiently with a 5.6 fold lower k_{cat} value as observed for laminarihexaose (Table 19). The K_M value of BGH06777 for laminarihexaose was higher compared to the K_M value obtained for laminaripentaose (Table 19). This indicates that a higher laminarihexaose concentration is required to result in the maximum reaction velocity in comparison to degradation of laminaripentaose. However, laminarihexaose was hydrolysed more efficiently than laminaripentaose as the k_{cat}/K_M value obtained for laminarihexaose hydrolysis was 4.8-times higher than for laminaripentaose hydrolysis (Table 19).

Table 19. Michaelis-Menten parameters for BGH06777 on β-1,3-oligosaccharides. Laminarihexaose (G3G3G3G3G3G) and laminaripentaose (G3G3G3G3G). Errors indicate errors in fitting the data to the Michaelis-Menten equation.

Substrate	k_{cat} [s^{-1}]	K_M [mM]	k_{cat} / K_M [mM^{-1} s^{-1}]
G3G3G3G3G3G	0.25809 ± 0.02611	0.13887 ± 0.03236	1.858
G3G3G3G3G	0.04577 ± 0.0039	0.11929 ± 0.02416	0.3836

3.1.9 BGH06777 has a -4/+2 binding/hydrolysis mode

The active site of an enzyme is the site where the substrate binds to the enzyme and gets hydrolysed. Active sites of GH can be designated to negative subsites (-n) towards the non-reducing end of the sugar and positive subsites (+n) towards the reducing end of the sugar with n being the number of either positive or negative subsites. The hydrolysis of oligosaccharides occurs between the -1 and +1 subsite (Davies *et al.*, 1997). During the hydrolysis, a new reducing end is generated due to the incorporation of a hydroxyl group to a carbon of the glycosyl intermediate in the -1 subsite. The incorporated hydroxyl group is derived from surrounding water (Varrot *et al*., 2001). In the presence of ^{18}O labelled water, ^{18}OH is incorporated to the newly formed reducing end which results in an increase of mass by two units (M+2) of the product bound to the negative subsites. The increase in mass can be monitored using mass spectrometry. Thus, the cleavage point of an oligosaccharide and therefore, the number of positive and negative subsites of an enzyme, can be determined by analysing the obtained hydrolysis products in the presence of ^{18}O labelled water via mass spectrometry (Schagerlöf *et al.*, 2009).

To determine the number of negative and positive subsites of BGH06777, BGH06777 in citrate buffer (pH = 5.5) was incubated with laminarihexaose in $H_2{}^{18}O$ and the ^{18}O incorporation was subsequently analysed using mass spectrometry. Hydrolysis products of laminarihexaose by BGH06777 are laminaritetraose (G3G3G3G) and laminaribiose (G3G). The M+2 peak of laminaribiose (G3G) did not increase compared to normal abundance of laminaribiose (G3G), while the M+2 peak of laminaritetraose (G3G3G3G) increased. This is further indicated by ^{18}O labelling of 91% of laminaritetraose (G3G3G3G) (Figure 9, A and B, Table 20). The exclusive labelling of laminaritetraose (G3G3G3G) reveals the presence of four negative and two positive subsites and a -4/+2 hydrolysis mode.

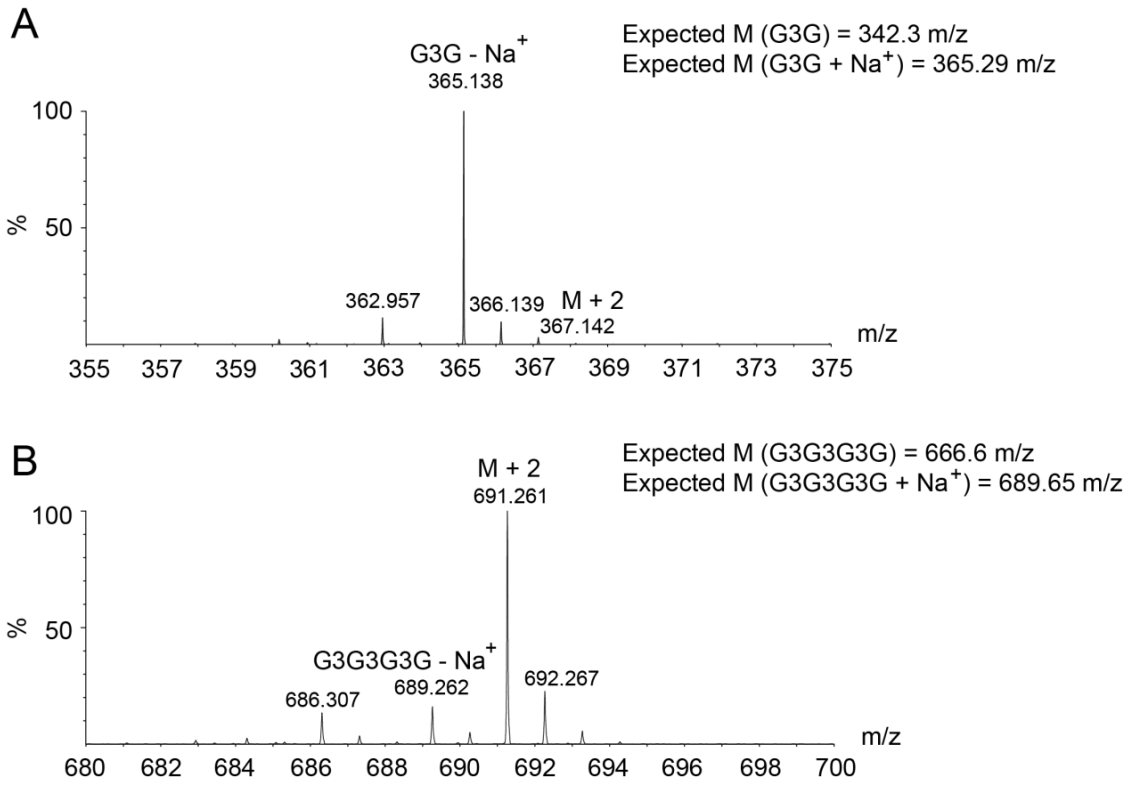

Figure 9. Mass spectrometric analysis of the hydrolysis of laminarihexaose in presence of $H_2{}^{18}O$ by BGH06777. (A) Mass spectra of laminaribiose (G3G) and (B) mass spectra of laminaritetraose (G3G3G3G). BGH067777 was incubated with laminarihexaose (G3G3G3G3G3G) in presence of $H_2{}^{18}O$. Upon incubation, the masses of the products laminaribiose (G3G) and laminaritetraose (G3G3G3G) were analysed via mass spectrometry. For each spectrum, the expected masses of the products are given. An increase in M+2 indicates ^{18}O incorporation.

Table 20. Degree of ^{18}O labelled laminaripentaose (G3G3G3G) and laminaribiose (G3G) derived from hydrolysis of laminarihexaose (G3G3G3G3G3G) by BGH06777. The percentage of labelling was calculated from peak integrations and corrected for $H_2{}^{16}O$ derived from substrate and enzyme solution.

Substrate	
Product	**%^{18}O labelled**
G3G3G3G3G3G	
G3G3G3G	91.16 ± 3.9
G3G	2.33 ± 3.9

To summarize, the *Bgh* GH17 protein BGH06777 employs a -4/+2 binding/hydrolysis mode and is able to hydrolyse β-1,3-glucan oligosaccharides with a minimum length of four glucose monomers. Furthermore, the optimal conditions at which the protein shows the highest activities were identified.

3.2 Identification and analysis of novel cell-wall derived DAMPs

3.2.1 Screen to identify cell-wall derived DAMPs in Arabidopsis

The plant cell wall composed of proteins, cellulose, hemicelluloses and pectic polysaccharides provides not only structure to the plant cell but is also a physical barrier to microbial invasion. Furthermore, it represents a potential source for DAMPs. In order to overcome the plant cell wall, pathogens secrete several CWDEs that are able to hydrolyse specific cell wall components (Malinovsky *et al.*, 2014). A variety of cell-wall derived oligosaccharides is likely to be generated by fungal CWDEs which might be perceived by the plant and consequently, lead to the activation of plant immune responses. These immune responses include the influx of Ca^{2+} ions into the cytosol, the generation of ROS and the activation of MAPK (Bigeard *et al.*, 2015).

A second aim of this study was to identify new cell wall derived DAMPs in the dicot model plant Arabidopsis. To this end, 37 cell-wall derived poly- and oligosaccharides that are present in the cell wall of the dicot model plant Arabidopsis were purchased from Megazyme (Bray, Ireland). These substances included a cellulose derivative, namely cellohexaose, hemicelluloses e.g. arabinofuranosyl-xylotetraose, pectic substances e.g. rhamnogalacturonan I, β-1,3-glucans e.g. laminarihexaose. All 37 substances (Table 7) were analysed regarding their ability to induce immune responses with three different methods. First, the influx of Ca^{2+} ions was analysed by using Arabidopsis Col-0 seedlings that express the calcium sensor protein aequorin. Different Arabidopsis ecotypes were shown to have a distinct receptor repertoire and might therefore be either sensitive or insensitive towards a specific MAMP. MAMP-sensitive and MAMP-insensitive accessions can be used to identify the respective receptor with a map-based cloning strategy (Jehle *et al.*, 2013b; Zhang *et al.*, 2014). To possibly identify DAMP-sensitive and DAMP-insensitive accessions, ROS burst generation as well as MAPK activation upon treatment with all substances was tested in Col-0, Ws-0 and Ws-4. 33 of the ordered substances did not induce PTI responses (Figure S3, Figure S4, Figure S5, Figure S6, Figure S7, Figure S8, Figure S9), while four carbohydrates could be identified that at least slightly induced the immune response.

The cellulose derivative cellohexaose was not able to induce the generation of ROS, however, did induce a slight influx of Ca^{2+} in Col-0 and activation of MAPK in Col-0, Ws-0 as well as Ws-4 (Figure S10, Figure S11) indicating a potential role as DAMP. In 2017, the group of Shauna Somerville released a publication showing that cellobiose acts as DAMP (de Azevedo Souza *et al.*, 2017), thus, confirming our results but excluding further analysis of cellohexaose as a DAMP.

Furthermore, the hemicellulose derivative xylohexaose could neither induce the generation of ROS in Col-0, Ws-0 and Ws-4 nor the influx of Ca^{2+} in Col-0 (Figure S12, Figure S13 A). However, xylohexaose treatment induced MAPK activation in Col-0, Ws-0 and Ws-4 (Figure S13 B). However, the obtained results for xylohexaose were not robust and thus, this oligosaccharide was also excluded from further analysis.

The β-1,3-glucan oligosaccharides laminarihexaose, laminaripentaose, laminaritetraose, laminaritriose and laminaribiose were not able to induce either the influx of Ca^{2+} in Col-0 or the ROS burst in Col-0, Ws-0 and Ws-4 (Figure S14, Figure S15 A). The activation of MAPK could only slightly

be induced by laminarihexaose and laminaripentaose in all three tested ecotypes (Figure S15 B). Since the tested β-1,3-glucans did only slightly induce the response in one of three assays, these substances were excluded from further analysis. In 2018, however, the research group of Antonio Molina could show that laminarihexaose acts as a robust elicitor of immune responses in Arabidopsis (Mélida *et al.*, 2018). The discrepancies in the results might be explained with the different concentrations used in the assays. Whilst 250 µM of the oligosaccharides were used by the research group of Antonia Molina, only 10 µM to 100 µM were used in this study.
In conclusion, none of the so far tested poly- and oligosaccharides will be used for further analysis as they were either not robustly inducing immune responses or were identified as DAMPs by other research groups during the course of this project.

3.2.2 Analysis of the DAMP capacity of MLGs in barley

In the collection of cell-wall derived poly- and oligosaccharides purchased from Megazyme, one MLG tetramer, namely cellotriosyl-glucose, one MLG tetramer mixture, called cellobiosyl-cellobiose plus glucosyl-cellotriose, and two MLG trimers, namely cellobiosyl-glucose and glucosyl-cellobiose were included. MLGs are composed of glucose monomers that are connected via both β-1,3- and β-1,4-linkages (Burton and Fincher, 2009). The MLG tetramer, the MLG tetramer mixture and the two trimers of our collection differ in the position of the β-1,3-linkage. For ease of understanding, the MLG oligomers will be abbreviated and the positions of β-1,3-linkage highlighted by color from now on, so that that the tetramer cellotriosyl-glucose is represented by G4G4G3G, cellobiosyl-cellobiose plus glucosyl-cellotriose as G4G3G4G + G3G4G4G and the two trimers cellobiosyl-glucose as G4G3G and glucosyl-cellobiose as G3G4G, with G standing for glucose and 3 and 4 representing the β-1,3- and β-1,4-linkages, respectively.
MLGs are abundant cell wall components in monocots e.g. in the crop plant barley but not in dicots. In first leaves of six-day old barley plants e.g. MLGs can be found in the cell walls of epidermal as well as in palisade and spongy mesophyll cells (Trethewey and Harris, 2002). Since MLGs are not present in the cell wall of Arabidopsis and thus, cannot act as DAMP, their DAMP activity was tested in barley. Therefore, the generation of ROS upon treatment with MLG oligomers in barley leaves was analysed with a luminol-based assay. Upon treatment with the MLG tetramer G4G4G3G, the tetramer mixture G4G3G4G + G3G4G4G and the two trimers G3G4G and G4G3G, the generation of ROS was induced in barley. The ROS burst induced by the tetramer G4G4G3G, however, was less pronounced in comparison to the ROS burst induced by the G4G3G4G + G3G4G4G mixture (Figure 10 A). Besides the generation of ROS, the activation of MAPK is a typical response towards MAMPs and was shown to be triggered in barley upon chitin and flg22 elicitation (Scheler *et al.*, 2016). To further verify the ability of MLGs to trigger immune responses in barley, the activation of MAPK upon MLG treatment was analysed via Western Blot using the p44/42 antibody which specifically detects phosphorylated MAPKs. As observed before for chitin and flg22, one signal could predominantly be detected in immunoblot analysis (Scheler *et al.*, 2016) (Figure 10 B). The MLG tetramer mixture

G4G3G4G + G3G4G4G as well as the trimer G4G3G induced MAPK phosphorylation, while G4G4G3G only slightly induced the activation of MAPK (Figure 10 B). The findings that MLG treatment induces the generation of ROS as well as the activation of MAPK in barley indicate that barley is able to perceive MLGs and consequently, immune responses are activated.

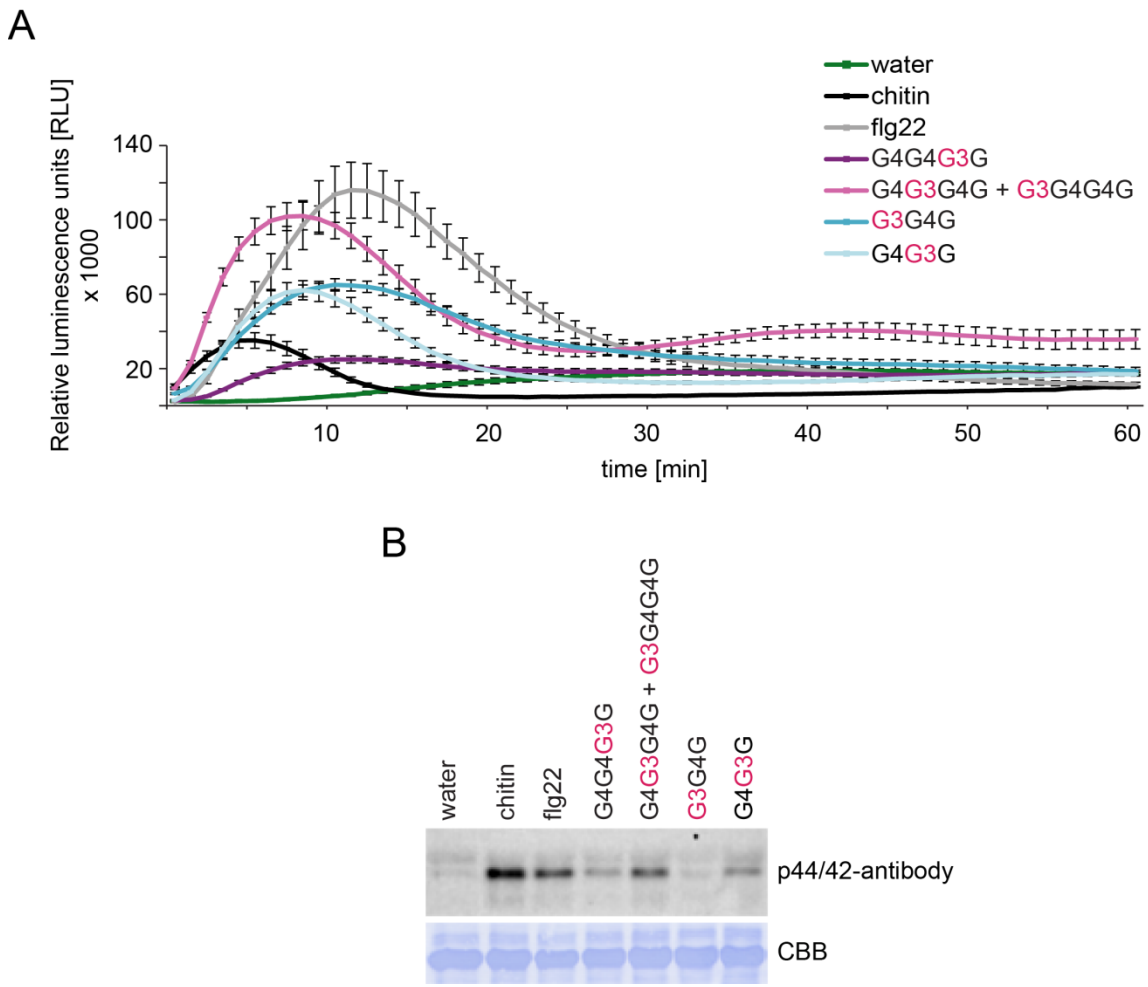

Figure 10. Activation of immune responses upon treatment with MLG oligomers in barley. (A) Generation of ROS in barley upon treatment with MLG oligomers. Leaf discs of second leaves of 10-day old barley plants were treated with water, 100 µg ml^{-1} chitin, 100 nM flg22 or 100 µg ml^{-1} MLG oligomers. Data show mean of eight leaf discs and error bars represent SEM. The experiment was performed three times with similar results. (B) MAPK activation upon MLG treatment. Leaf discs of second leaves of barley plants were treated for 12 min with water, 10 µg ml^{-1} chitin, 50 nM flg22 or 10 µg ml^{-1} MLG oligomers. Activation of MAPK was analysed via Western Blot using the p44/42-antibody. Lower panel shows Coomassie Brilliant Blue (CBB) staining as loading control.

3.2.3 MLGs induce immune responses in Arabidopsis

In the last years, MLGs were not only shown to be present in the cell wall of monocots, but also in bacteria and fungi. MLGs are present as exopolysaccharides in the endosymbiont *Sinorhizobium meliloti* (Pérez-Mendoza *et al.*, 2015). Furthermore, MLGs were shown to be abundant cell wall

components in the two ascomycete fungi *Aspergillus fumigatus* and *Rhynchosporium commune* (formerly known as *R. secalis*) (Pettolino *et al.*, 2009; Samar *et al.*, 2015). *R. commune* is a plant pathogenic fungus causing leaf blotch on barley and the inner hyphal cell walls of *R. commune* were shown to contain MLGs (Pettolino *et al.*, 2009). Due to the presence of MLGs in bacteria and fungi, MLGs might act as a MAMP in plant species that do not contain MLGs, e.g. Arabidopsis.

To test whether MLGs might be able to induce immune responses in Arabidopsis, the four MLGs were analysed regarding their ability to induce the influx of Ca^{2+} using Arabidopsis seedlings that express the Ca^{2+} sensor protein aequorin. Also, a luminol-based assay was used to analyse the generation of ROS and an immunoblot analysis was performed to test the phosphorylation of MAPK in Arabidopsis upon MLG treatment. Interestingly, all four MLG oligomers could elicit a rapid influx of Ca^{2+} in Col-0 with the Ca^{2+} influx being more intense upon treatment with MLG tetramers compared to treatment with MLG trimers (

Figure 11 A). Also, the Ca^{2+} influx seems to reach its peak faster upon MLG oligomer treatment than upon chitin or flg22 treatment (

Figure 11 A). The generation of ROS could only slightly be induced by the tetramer mixture G4G3G4G + G3G4G4G in Col-0, Ws-0 and Ws-4. In Ws-0, the ROS burst was also slight induced by the MLG tetramer G4G4G3G and the MLG trimer G3G4G (

Figure 11 B, Figure S16 A and B). Furthermore, all four MLG oligomers triggered the activation of MAPKs in Col-0, Ws-0 and Ws-4, in particular of MAPK6 and MAPK3. Notably, MAPK activation was more pronounced upon treatment with MLG tetramers than with MLGs trimers (

Figure 11 C, Figure S16 C), suggesting a higher binding affinity of the tetramers to the respective receptor compared to the binding affinity of the trimer to the receptor. Additionally, the level of MAPK activation induced by MLG tetramer treatment was higher compared to the MAPK activation upon treatment with the known carbohydrate DAMP OGs but less pronounced than upon elicitation with chitin or flg22. Although the calcium response, generation of ROS as well as activation of MAPK were stronger upon treatment with chitin or flg22, these results indicate that MLGs have the ability to induce immune responses in Arabidopsis.

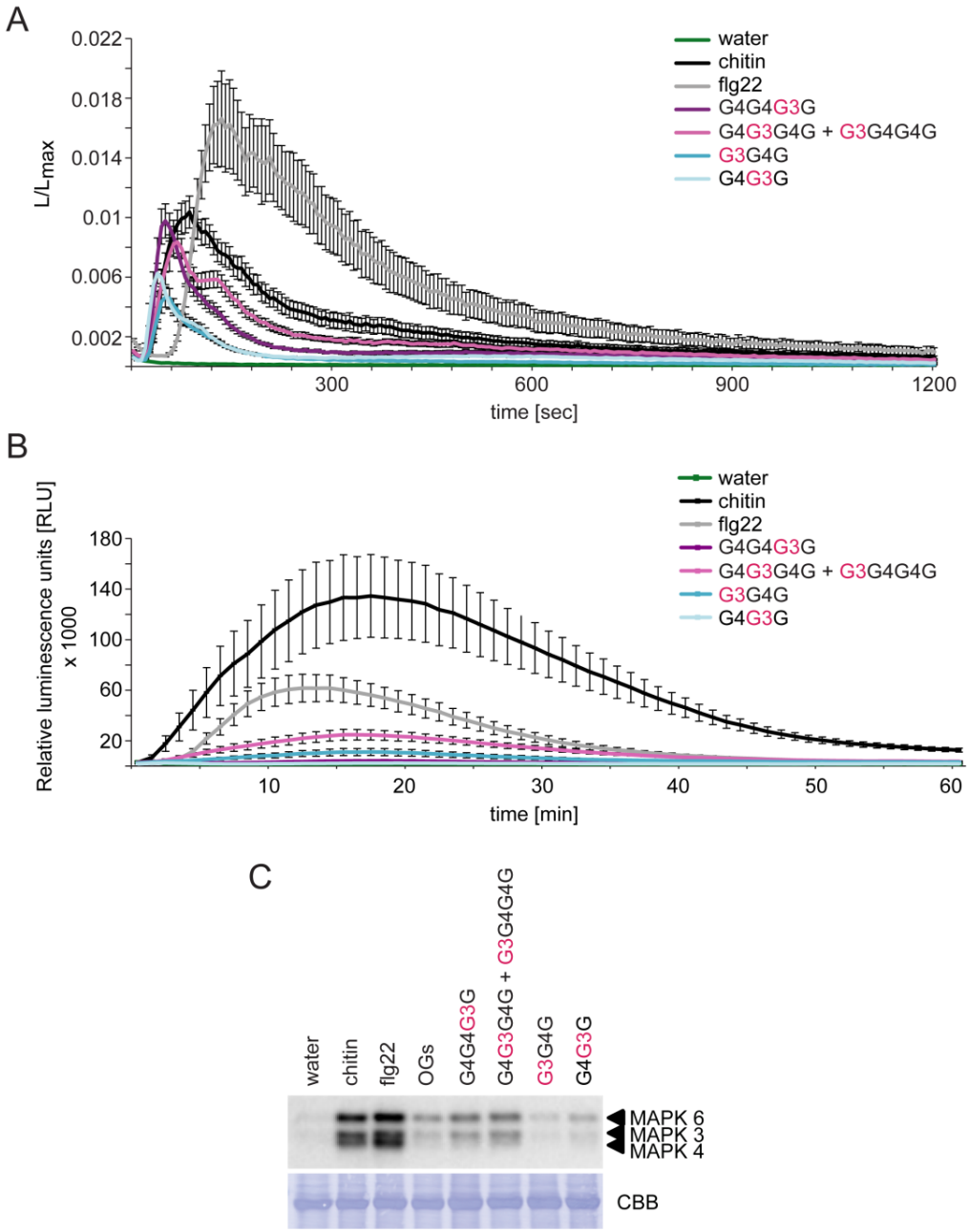

Figure 11. Activation of immune responses in Arabidopsis Col-0 by MLG oligomers from Megazyme. (A) Ca^{2+} influx upon MLG treatment. 8-10 day old Arabidopsis Col-0 seedlings expressing the Ca^{2+} sensor protein aequorin were treated with water, 100 µg ml^{-1} chitin, 100 nM flg22 or 100 µg ml^{-1} MLG oligomers and the Ca^{2+} elevation was measured for 1200 sec in 6 sec intervals. To obtain the total remaining luminescence (L_{max}), the remaining aequorin was discharged by adding $CaCl_2$ to each well and luminescence was recorded for 3 min in 6 sec intervals. For normalization, the elicitor induced luminescence per 6 sec (L) was divided by L_{max}. The data shown represent the mean of 12 seedlings and error bars represent SEM. The experiment was repeated three times with similar results. (B) Generation of ROS upon MLG treatment. Leaf discs of 5-7-week old Col-0 plants were treated with water, 100 µg ml^{-1} chitin, 100 nM flg22 or different 100 µg ml^{-1} MLG oligomers. Relative Light Units (RLU) were recorded directly upon the respective treatment for 60 min in 1 min intervals. The shown data represent the mean of 8 leaf discs per treatment and error bars represent SEM. The experiment was repeated four times with similar results. (C) MAPK activation upon MLG treatment. 14-day old *in-vitro* grown Arabidopsis Col-0 seedlings were treated with water, 10 µg ml^{-1} chitin, 50 nM flg22, 10 µg ml^{-1} oligogalacturonides (OGs) or 10 µg ml^{-1} MLG oligomers for 12 min. Activation of MAPK6, 3 and 4 was analysed by Western Blot using the p44/42 antibody. Lower panel shows Coomassie Brilliant Blue (CBB) staining of the membrane as loading control. The experiment was repeated four times with similar results.

Besides the influx of Ca^{2+}, generation of ROS and activation of MAPK, activation of PTI also leads to transcriptional reprogramming (Boller and Felix, 2009). To further verify the ability of MLGs to trigger immune responses, the expression of the defence genes *WRKY33* and *WRKY53* was analysed via qRT-PCR. Upon treatment with the MLG tetramers G4G4G3G and G4G3G4G + G3G4G4G or the MLG trimer G4G3G, the expression of *WRKY33* and *WRKY53* was induced significantly compared to the water control. The MLG trimer G3G4G did induce the expression of *WRKY53* significantly (Figure 12). As observed for the influx of Ca^{2+} and activation of MAPK, the induction of the expression of *WRKY33* and *WRKY53* was more pronounced upon treatment with MLG tetramers than with MLG trimers (Figure 12). The ability of MLGs to induce defence gene expression further indicates their potential role as elicitor of immune responses.

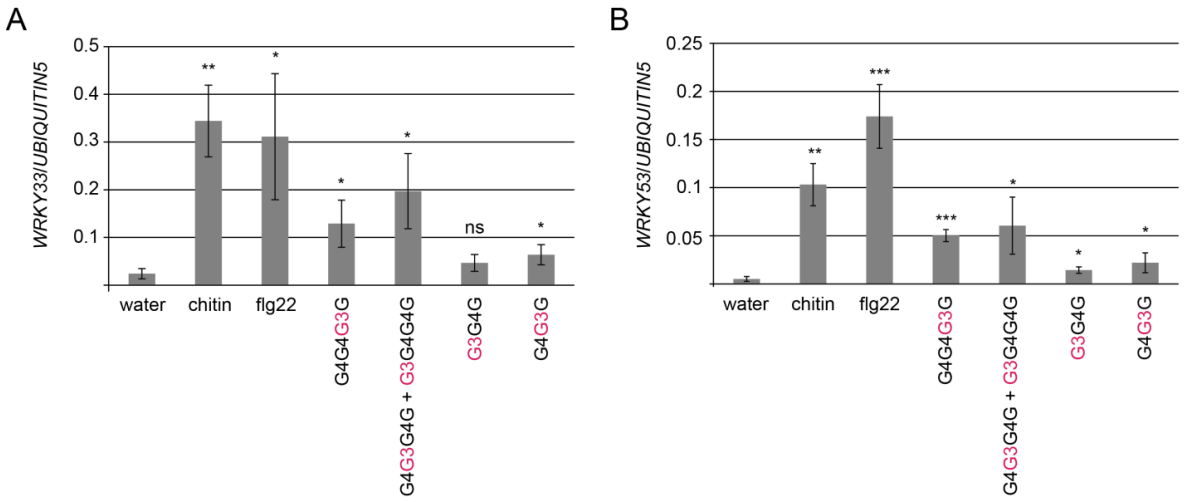

Figure 12. Defence gene expression upon Megazyme MLG oligomer treatment in Arabidopsis Col-0 seedlings. 14-day old *in-vitro* grown Arabidopsis Col-0 seedlings were treated with water, 10 µg ml^{-1} chitin, 50 nM flg22 or 10 µg ml^{-1} MLG oligomers for 30 min. Expression of *WRKY33* (A) and *WRKY53* (B) were analysed using qRT-PCR. *UBIQUITIN5* served as reference gene. The bars show the mean of three biological replicates with three technical replicates each. Error bars show standard deviation. Asterisks indicate statistical significance of the elicitor treatments compared to water treatment with not significant (ns) = $p > 0.5$, * = $p \leq 0.5$, ** = $p \leq 0.001$ and *** = $p \leq 0.001$. The unpaired student's t-teat was used to calculate p-values.

3.2.4 MLG oligosaccharides from a second company can induce immune responses in barley and Arabidopsis

To verify the ability of MLGs to induce immune responses in barley and Arabidopsis, one MLG tetramer (G4G3G4G) as well as two MLG trimers (G3G4G and G4G3G) were purchased from a second supplier for carbohydrates, Carbosynth (Compton, UK) and tested for their ability to induce immune responses. The two MLG trimers as well as the tetramer G4G4G3G are structurally the same as the MLGs obtained from Megazyme. However, Carbosynth offered the MLG tetramer G4G3G4G

as a single substance while it was only available as a mixture (G4G3G4G + G3G4G4G) at Megazyme.

Again, the generation of ROS as well as the activation of MAPK upon MLG treatment were analysed in barley. The MLG tetramer G3G4G4G but not the MLG trimers G3G4G and G4G3G did induce the generation of ROS (Figure 13 A). Furthermore, the activation of MAPK was clearly induced upon treatment with the tetramer G4G3G4G and comparable to the intensity of MAPK phosphorylation upon flg22. Also, the MLG trimers G3G4G and G4G3G did induce the MAPK activation in barley, however, the level of MAPK activation was lower in comparison to the induction upon MLG tetramer treatment (Figure 13 B).

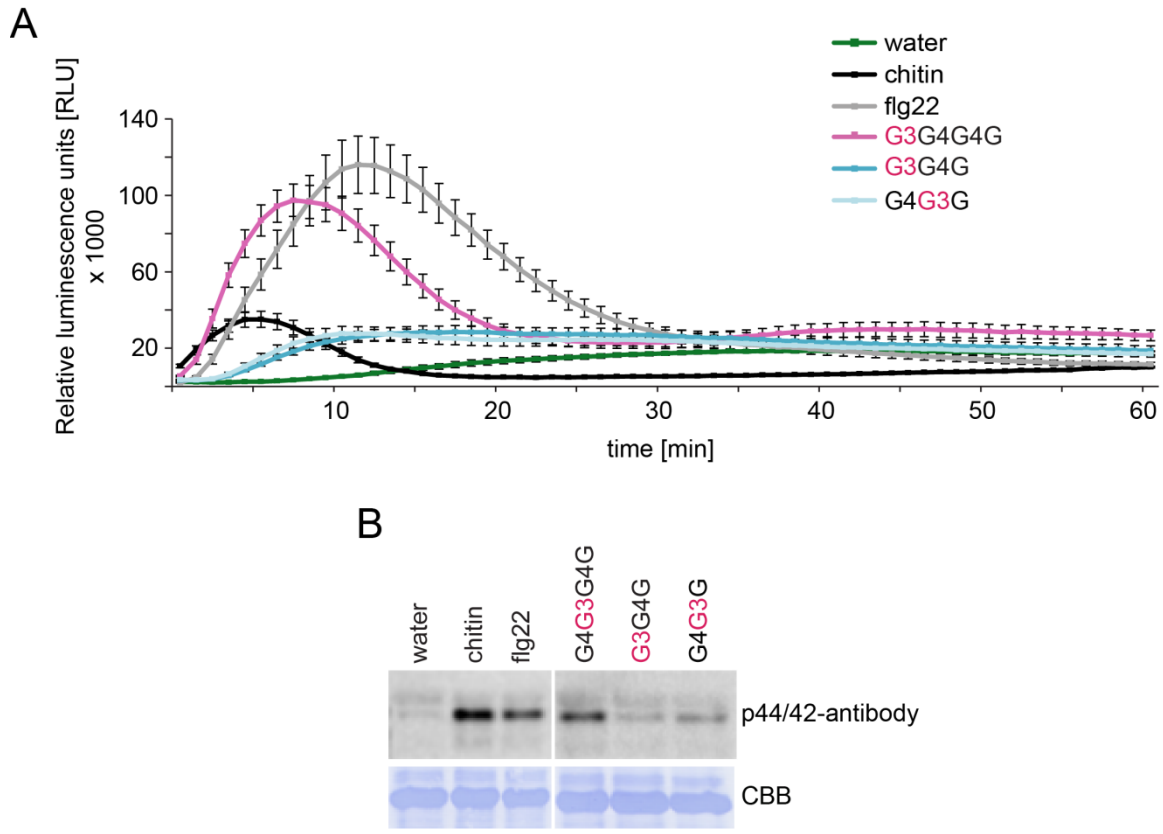

Figure 13. ROS burst generation and activation of MAPK in barley by MLG oligomers from Carbosynth. (A) Generation of ROS in barley upon treatment with a MLG tetramer and two MLG trimers. Leaf discs of second leaves of 10-day old barley plants were treated with water, 100 µg ml^{-1} chitin, 100 nM flg22 or 100 µg ml^{-1} MLG oligomers. Data show mean of eight leaf discs and error bars represent SEM. The experiment was performed three times with similar results. (B) MAPK activation upon MLG treatment. Leaf discs of second leaves of barley plants were treated for 12 min with water, 10 µg ml^{-1} chitin, 50 nM flg22 or 10 µg ml^{-1} MLG oligomers. Activation of MAPK was analysed via Western Blot using the p44/42-antibody. Lower panel shows Coomassie Brilliant Blue (CBB) staining as loading control. The experiment was repeated two times with similar results.

To determine if the three MLGs from Carbosynth are able to induce immune responses in Arabidopsis, Arabidopsis Col-0 seedlings expressing the Ca^{2+} sensor protein aequorin were used to monitor the calcium response. The tetramer G4G3G4G as well as the two trimers G3G4G and G4G3G induced the influx of Ca^{2+} ions. The Ca^{2+} peak induced by the MLG tetramer was stronger in comparison to the Ca^{2+} influx induced by the two MLG trimers. Also, the Ca^{2+} influx upon MLG treatment was faster than upon flg22 treatment (Figure 14 A). Next, a luminol-based assay was performed to determine whether MLGs induce the generation of ROS. The ROS burst generation was clearly observed upon treatment with chitin and flg22, however, could not be observed upon treatment with MLG oligomers in Col-0 (Figure 14 B). ROS generation was also not observed in Ws-0 and Ws-4 upon MLG elicitation (Figure S17 A and B). Western blot analysis using the p44/42-antibody revealed that MAPK6 and MAPK3 were phosphorylated upon treatment with the MLG tetramer G4G3G4G and very slightly upon treatment with the MLG trimers G3G4G and G4G3G in Col-0, Ws-0 and Ws-4 (Figure 14 C, Figure S17 C).

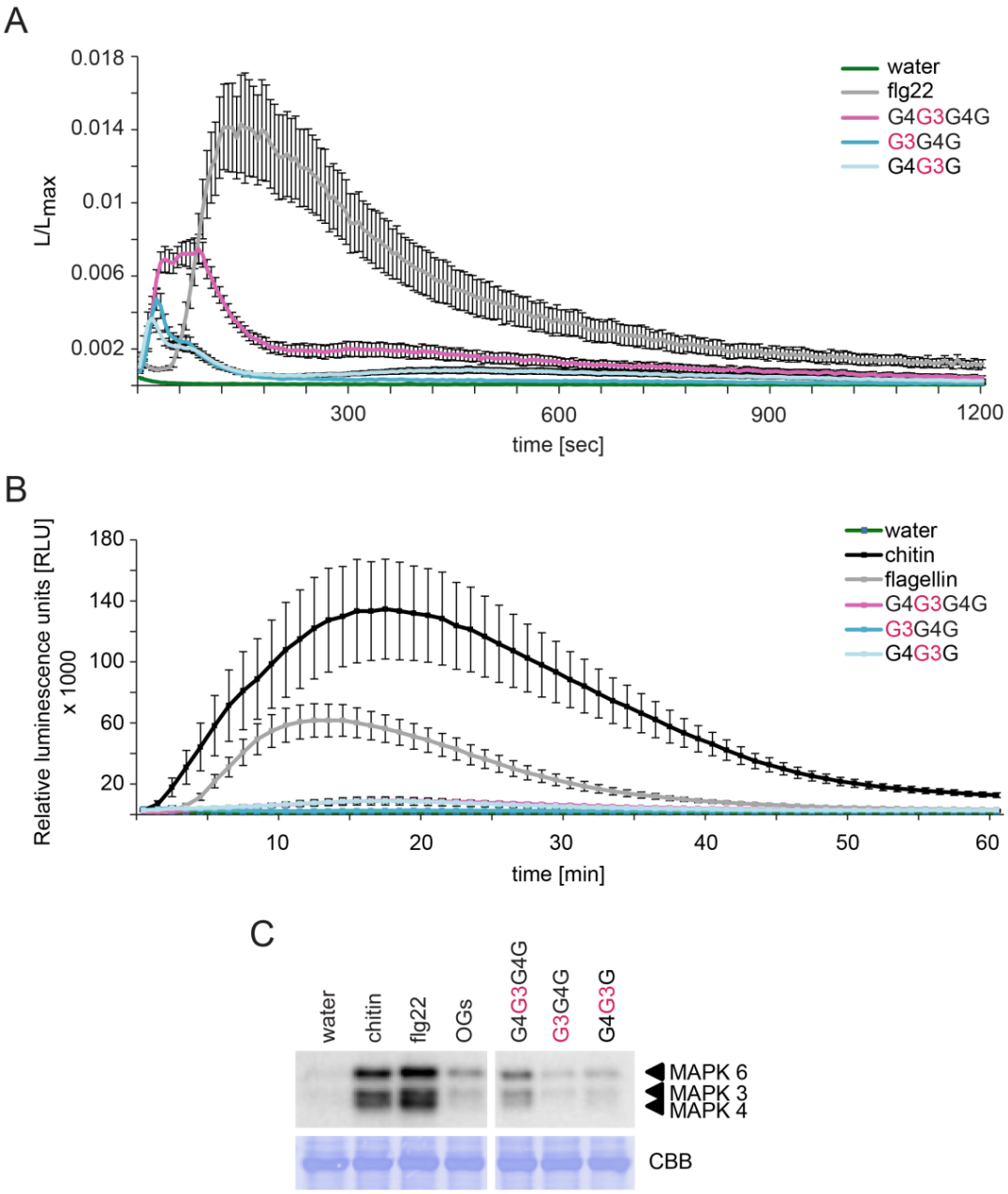

Figure 14. Activation of immune responses in Arabidopsis Col-0 upon treatment with MLG oligomers from Carbosynth. (A) Influx of Ca^{2+} upon MLG oligomer treatment. 8-10-day old Arabidopsis Col-0 seedlings expressing the Ca^{2+} sensor protein aequorin were treated with water, 100 µg ml^{-1} chitin, 100 nM flg22 or 100 µg ml^{-1} MLG oligomers. Elevation in Ca^{2+} was measured in 6 sec intervals for 1200 sec. Upon treatment, the total remaining luminescence (L_{max}) was obtained by adding $CaCl_2$ to the wells and luminescence was recorded for 3 min in 6 sec intervals. For normalization, luminescence upon elicitor treatment per 6 sec (L) was divided by L_{max}. Data shown represent mean of 12 seedlings with SEM. The experiment was repeated three times with similar results. (B) ROS burst generation upon MLG treatment. Leaf discs of 5-7 week old Arabidopsis Col-0 plants were treated with water, 100 µg ml^{-1} chitin, 100 nM flg22 or 100 µg ml^{-1} MLG oligomers and relative light units (RLU) were recorded every minute for 60 min. The shown data represent mean of 8 leaf discs with SEM. The experiment was repeated two times with similar results. (C) Activation of MAPK upon MLG treatment. *In-vitro* grown 14-day old Col-0 seedlings were treated with water, 10 µg ml^{-1} chitin, 50 nM flg22 or 10 µg ml^{-1} MLG oligomers for 12 min. Activation of MAPK6, MAPK3 and MAPK4 was analysed via Western Blot using the p-44/42 antibody. The lower panel shows Coomassie Brilliant Blue (CBB) staining as loading control. The experiment was repeated three times with similar results.

Additionally, it was tested whether the three MLGs from Carbosynth are able to induce defence gene expression. Thus, the expression of *WRKY33* and *WRKY53* upon MLG elicitation was analysed via qRT-PCR. The tetramer G4G3G4G induced the transcriptional upregulation of *WRKY33* and *WRKY53* 10-fold and 12-fold, respectively, compared to water (Figure 15). The trimer G3G4G did significantly induce the transcription of *WRKY53* (Figure 15). As observed before, the induction of defence gene expression was more pronounced upon treatment with the MLG tetramer than with the MLG trimers.

All ordered MLGs from the second company Carbosynth did induce immune responses in barley as well as in Arabidopsis indicating that MLGs display elicitor activities.

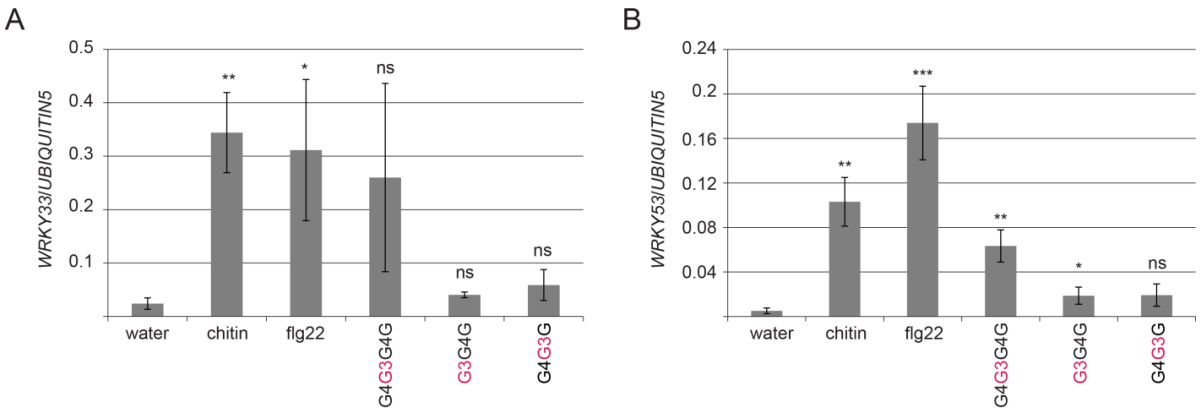

Figure 15. Expression of defence genes upon treatment with MLG oligomers from Carbosynth. *In-vitro* grown 14-day old Arabidopsis Col-0 seedlings were treated with water, 10 µg ml^{-1} chitin, 50 nM flg22 or 10 µg ml^{-1} MLG oligomers for 30 min. Expression of the genes *WRKY33* (A) and *WRKY53* (B) were tested using qRT-PCR. *UBIQUITIN5* served as reference gene. The bars show the mean of three biological replicates consisting of three technical replicates each and error bar represents standard deviation. Statistical significance of the elicitor treatments compared to water treatment is indicated by asterisks with not significant (ns) = $p > 0.5$, * = $p \leq 0.5$, ** = $p \leq 0.001$ and *** = $p \leq 0.001$. The unpaired student's t-teat was used to calculate p-values.

3.2.5 Commercially available MLGs do not contain major quantitative contaminants

To exclude the possibility that a potential contamination in the MLG preparations from Megazyme (Bray, Ireland) and Carbosynth (Compton, UK) induce the immune responses in Arabidopsis and barley, all MLG tetramers and trimers were tested for purity via HPAEC-PAD and matrix-assisted laser desorption ionization with time-of-flight detection (MALDI-TOF).

First, the commercially available MLG tetramers and trimers were analysed via HPAEC-PAD for potential carbohydrate contaminations. No major contaminations could be found in the HPAEC-PAD analysis of the MLG tetramer G4G4G3G from Megazyme, the MLG tetramer mixture G4G3G4G + G3G4G4G from Megazyme and both MLG trimers, G3G4G and G4G3G, from Megazyme and Carbosynth. Furthermore, the respective MLG tetramer and trimers from Megazyme and Carbosynth show the same retention times indicating that they have the same MLG structure (Figure 16 A, C and D). Unexpectedly, the MLG tetramer G4G3G4G from Carbosynth did show two peaks in the

HPAEC-PAD analysis indicating that two carbohydrates are present in this preparation (Figure 16 B). The HPAEC-PAD profile of G4G3G4G from Carbosynth is similar to the HPAEC-PAD profile obtained for the MLG tetramer mixture G4G3G4G + G3G4G4G from Megazyme suggesting that the MLG tetramer G4G3G4G from Carbosynth is not a single MLG tetramer but is also a mixture of G4G3G4G + G3G4G4G (Figure 16 B). Furthermore, minor peaks were observed in the HPAEC-PAD chromatograms of all MLG preparations (Figure 16). Since the MLG tetramers and trimers were generated by hydrolyzing the barley β-1,3;1-4-glucan polymer, these peaks likely correspond to carbohydrates containing less than four glucose monomers e.g. cellotriose, cellobiose or laminaribiose. However, the low intensity of these peaks suggests that their abundance in the preparation is very low and consequently, is negligible.

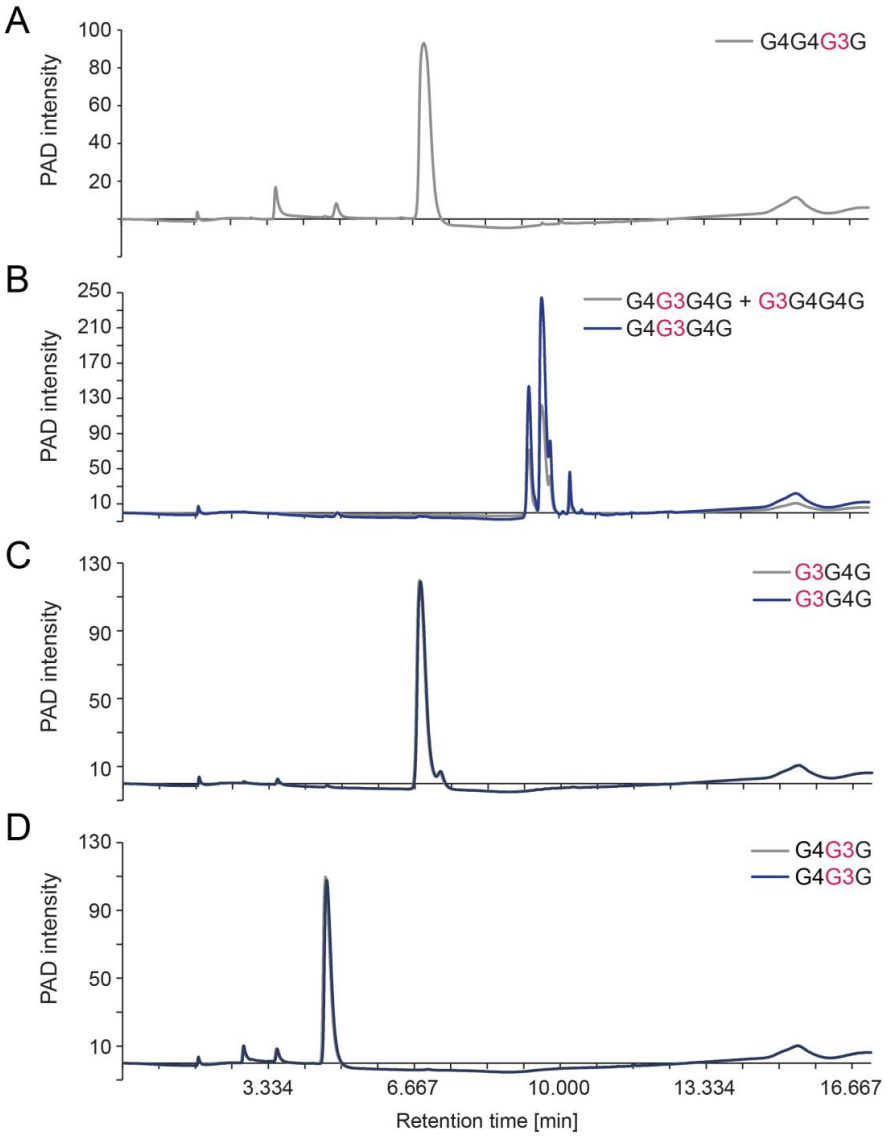

Figure 16. HPAEC-PAD chromatographs of MLG oligomers. (A) to (D) HPAEC-PAD profiles of MLG oligomers from Megazyme (grey) and (B) to (D) HPEAC-PAD chromatograms of MLG oligomers from Carbosynth (blue). 56 µM of the respective MLG tetramers and 45 µM of the respective MLG trimers were analysed via HPAEC-PAD and checked for carbohydrate contamination.

MALDI-TOF can be used to determine the molecular weight of a compound. Therefore, the sample for analysis is mixed with a matrix on a MALDI plate. The matrix as well as the sample are allowed to dry and crystallize. Upon drying, a laser beam is applied to the matrix-sample mixture and the matrix-sample mixture is ionized. The generated ions from the sample are accelerated at a fixed potential and separated according to their mass-to-charge ratio (m/z) (Hosseini and Martinez-Chapa, 2017). To verify the masses of all MLG tetramers and MLG trimers and to exclude possible contaminations, a MALDI-TOF analysis for all MLG tetramers and trimers was performed. For the MLG tetramers a signal 666.6 m/z and for the MLG trimers a signal at 504.4 m/z was expected. During the MALDI-TOF analysis of the MLG tetramers, both Na^+ adducts (666.6 + 22.9 m/z) and K^+ adducts (666.6 + 39 m/z) were observed (Figure 17 A-C). Also, in the MALDI-TOF analysis of the MLG trimers Na^+ (504.4 + 22.9 m/z) as well as K^+ adducts (504.4 + 39 m/z) were found (Figure 17 D-H). These results together with the HPAEC-PAD analysis indicate pure MLG preparations and support the companies' claim of high purity.

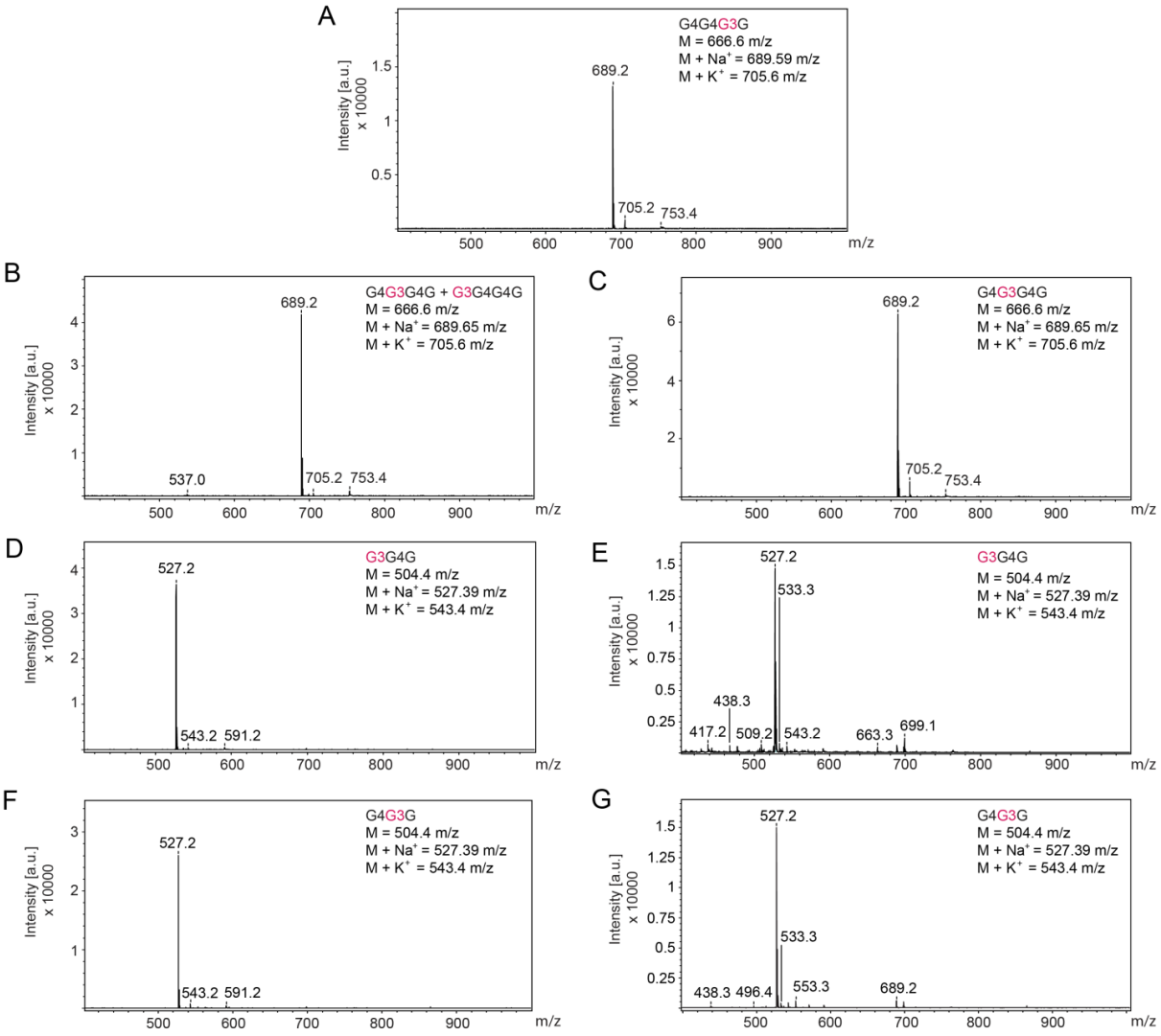

Figure 17. Verification of masses of MLG oligomers. 10 µg ml^{-1} of the respective MLG oligomers from Megazyme (A, B, D, F) or Carbosynth (C, E, G) were mixed with a 2,5-Dihydrobenzoic acid MALDI MATRIX**.** The masses of the oligomers was analysed using MALDI-TOF. Expected masses of the pure MLG tetramers and trimers as well as the Na^+ and K^+ adducts are indicated.

3.2.6 Hydrolysis products of the barley β-1,3;1,4-glucan polymer induce defence responses in Arabidopsis

The commercially available MLG tetramers and MLG trimers are derived from β-1,3;1,4-glucan polymers that were hydrolysed with enzymes that cleave β-1,3;1,4-glucan polymers (Megazyme). Enzymes that act on β-1,3;1,4-glucan polymers exhibit different specificities regarding the position of the cleaved linkage. An endo-β-1,4-glucanase from *Aspergillus japonicus* hydrolyses β-1,4-linkages preceding a β-1,3-linkage resulting in MLG oligosaccharides with the structure G3G4$_n$G with n describing the number of glucose units (Grishutin *et al*., 2006). However, the commercially available *Bacillus subtilis* endo-1,3:1,4-β-D-glucanase (lichenase) cleaves β-1,4-linkages adjacent to β-1,3-linkages and consequently, generates MLG oligosaccharides with the general structure

$G4_nG3G$ (Figure 18) (Planas, 2000). Full lichenase hydrolysis of β-1,3;1,4-polymers of grasses and cereals with the *B. subtilis* lichenase result mainly in the generation of the MLG tetramer G4G4G3G and the trimer G4G3G. However, intermediate products can be achieved upon a partial digest. These intermediate products can e.g. be a hexasaccharide with the structure G4G3G4G4G3G that eventually would by cleaved into two trimers (Figure 18) (Fry *et al.*, 2008). Thus, the *B. subtilis* lichenase can be used to generate MLG oligosaccharides of varying length but the general structure $G4_nG3G$.

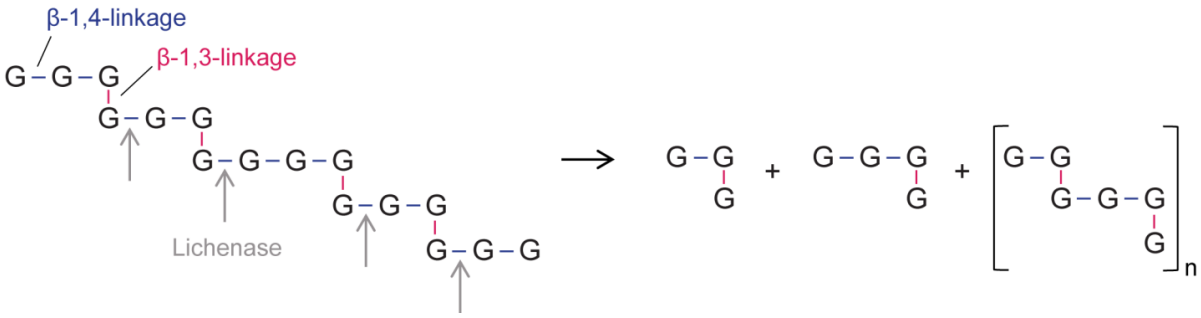

Figure 18. Schematic representation of a β-1,3;1,4-glucan polymer and the obtained oligosaccharides upon treatment with *B. subtilis* lichenase. Abbreviations: G – glucose, n –number of residues linked together.

To further verify the ability of MLG oligosaccharides to elicit immune responses, MLG oligosaccharides of varying length were generated using the barley β-1,3;1,4-glucan polymer and the *B. subtilis* lichenase. In a next step, the obtained MLG oligosaccharides were analysed regarding their capacity to induce PTI responses including the calcium response, activation of MAPK and induction of defence gene expression.

First, optimal conditions for barley β-1,3;1,4-glucan polymer hydrolysis were identified by using different buffers with varying pHs and different enzyme concentrations. Samples were taken upon different incubation times and consequently, the lichenase was inactivated by incubating the hydrolysate for 15 min in boiling water. The hydrolysis was checked via Thin Layer Chromatography (TLC). The goal was to obtain hydrolysates in which the MLG oligosaccharide concentration increases over time. Optimal conditions were achieved by hydrolyzing the barley β-1,3;1,4-glucan polymer in 100 mM Sodium phosphate buffer (pH = 6.5) at 40°C with either 0.025 U ml^{-1} or 0.05 U ml^{-1} lichenase and taking samples upon incubation for 0, 5, 15, 30, 45, 60, 120 and 240 min (Figure S18). No MLG oligosaccharides can be found in the sample taken upon 0 min incubation time while the amount of MLG oligosaccharides increases over time. The MLG oligosaccharides obtained upon 45 min or longer incubation times co-migrated with the standards for G4G4G3G and G4G3G indicating that the tetramer as well as the trimer are abundant in the respective hydrolysates. Additionally, MLG oligosaccharides were obtained that migrated more slowly than the MLG tetramer and the MLG trimer suggesting that these oligosaccharides are longer than the trimer and tetramer. However, the exact length cannot be determined from the TLC since MLG standards with a length of

six or more glucose monomers are not commercially available. The β-1,3;1,4-glucan polymer can still be found in the hydrolysates, however, the hydrolysates were not further processed to obtain a polysaccharide-free MLG oligosaccharide mixture (Figure S18).

Again, to determine whether the enzymatically generated MLG oligosaccharides have the ability to induce the influx of Ca^{2+} ions, the calcium responses was monitored in Arabidopsis Col-0 seedlings expressing the Ca^{2+} sensor protein aequorin. Upon treatment with MLG oligosaccharides that were obtained upon incubation of the β-1,3;1,4-glucan polymer with either 0.05 U ml^{-1} or 0.025 U ml^{-1} active lichenase for 30, 60 or 240 min, a rapid increase in Ca^{2+} was observed. Comparing the intensities of the induced Ca^{2+} influx upon treatment with MLG oligosaccharides upon the three different incubation times, the MLG oligosaccharides obtained upon 60 min incubation induced the lowest Ca^{2+} influx while the strongest Ca^{2+} peak was observed with MLG oligosaccharides obtained upon incubation for 240 min. This suggests a positive correlation between the MLG oligosaccharide concentration and intensity of Ca^{2+} influx (Figure 19 A and B). In comparison to the Ca^{2+} peak upon chitin treatment, the Ca^{2+} spikes resulting from MLG oligosaccharide treatment occurred faster. No Ca^{2+} influx was induced upon control treatments with either Sodium phosphate buffer, the untreated β-1,3;1,4-glucan polymer or the β-1,3;1,4-glucan polymer incubated with heat-inactivated lichenase (0.05 U ml^{-1} or 0.025 U ml^{-1}) indicating that only MLG oligosaccharides that were enzymatically produced from a MLG polymer can induce a Ca^{2+} influx (Figure 19 A and B).

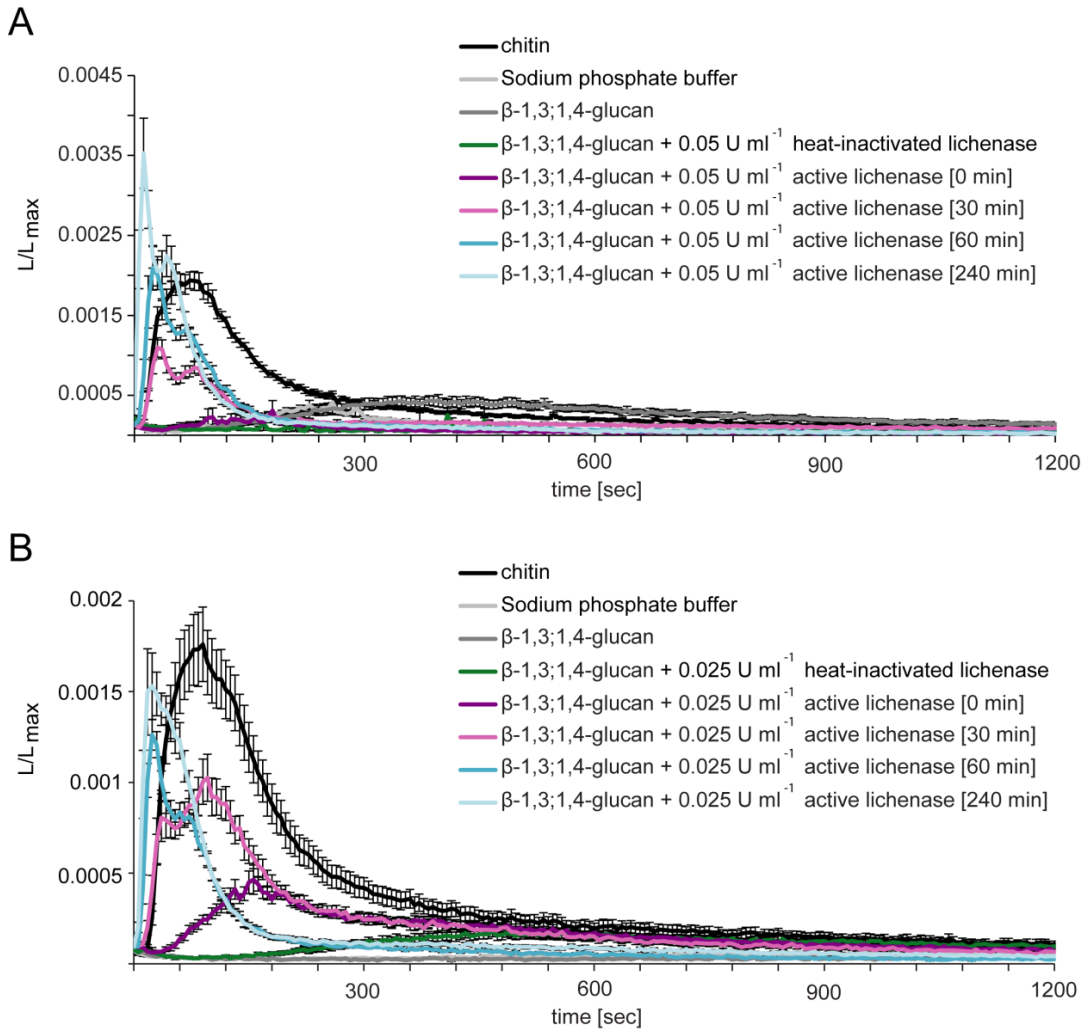

Figure 19. Calcium influx in Arabidopsis Col-0 upon treatment with MLG oligosaccharides. To obtain MLG oligosaccharides of varying length, 10 mg ml^{-1} barley β-1,3;1,4-glucan polymer dissolved in 100 mM Sodium Phosphate buffer (pH = 6.5) was hydrolysed with 0.05 (A) or 0.025 (B) U ml^{-1} lichenase and the reaction was stopped upon 0, 5, 15, 30, 45, 60, 120 or 240 min incubation. 8-10 day old Arabidopsis Col-0 seedlings expressing the Ca^{2+} sensor protein aequorin were treated with 10 µg ml^{-1} chitin, 10 mM Sodium Phosphate buffer, 1 mg ml^{-1} β-1,3;1,4-glucan, 0.05 or 0.025 U ml^{-1} heat inactivated lichenase, 1 mg ml^{-1} β-1,3;1,4-glucan plus either 0.05 or 0.025 U ml^{-1} heat-treated lichenase or a 1:10 dilution of MLG oligosaccharides (β-1,3;1,4-glucan + 0.05 or 0.025 U ml^{-1} active lichenase incubated for 0, 30, 60 or 240 min). The Ca^{2+} elevation upon treatment (L) was recorded in 6 sec intervals for 1200 sec. To obtain the total remaining luminescence (L_{max}), $CaCl_2$ was added to the wells and luminescence was recorded for 3 min in 6 sec intervals. For normalization, luminescence counts per 6 sec upon treatment (L) were divided by L_{max}. Data shown represent mean of 12 seedlings with SEM. The experiment was performed twice with similar results.

Furthermore, the MAPK activation upon MLG oligosaccharide elicitation was tested via immunoblot analysis using the p44/42-antibody. Treatment with active lichenase did not induce MAPK activation in Arabidopsis Col-0 suggesting that Col-0 does not contain MLGs itself which could be cleaved upon pathogen attack and consequently, lead to the activation of immune responses. The activity of the lichenase was verified by testing the hydrolysis of barley β-1,3;1,4-glucan polymer in ½ MS plus sucrose medium and the hydrolysis was analysed via TLC (Figure S19). Additionally, the control treatments as well as the β-1,3;1,4-glucan polymer incubated with either 0.05 U ml^{-1} or 0.025 U ml^{-1}

lichenase for 0 min did not induce MAPK activation. MAPK6 and MAPK3 phosphorylation was only induced upon treatment with MLG oligosaccharides obtained from β-1,3;1,4-glucan polymer incubated with either 0.05 U ml^{-1} or 0.025 U ml^{-1} lichenase for at least 15 min (Figure 20). The intensity of the MAPK activation increased over time, thus correlating with increasing amounts of MLG oligosaccharides. This result demonstrates that oligomeric MLGs act as elicitor of immune responses (Figure 20).

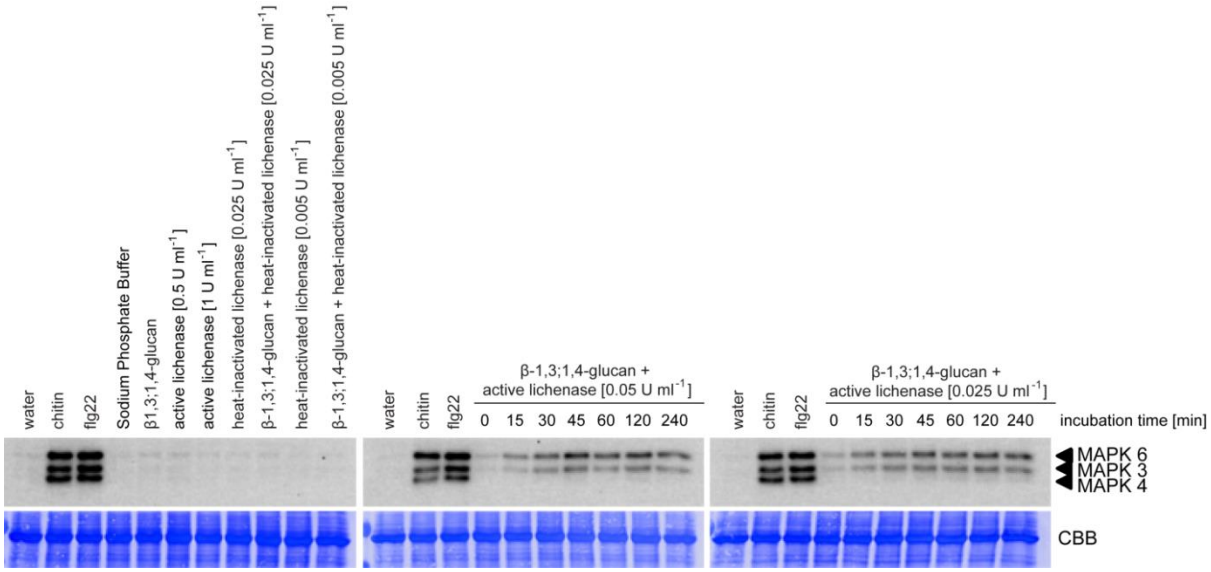

Figure 20. Activation of MAPK in Arabidopsis Col-0 upon treatment with MLG oligosaccharides. To obtain MLG oligosaccharides of varying length, 10 mg ml^{-1} barley β-1,3;1,4-glucan polymer dissolved in 100 mM Sodium Phosphate buffer was hydrolysed with 0.05 or 0.025 U ml^{-1} lichenase and the reaction was stopped upon 0, 5, 15, 30, 45, 60, 120 or 240 min incubation. *In-vitro* grown 14-day old Arabidopsis Col-0 seedlings were treated for 12 min with 10 µg mL^{-1} chitin, 50 nM flg22, 10 mM Sodium Phosphate buffer, 1 mg ml^{-1} β-1,3;1,4-glucan, 0.005 or 0.0025 U ml^{-1} heat inactivated lichenase, 1 mg ml^{-1} β-1,3;1,4-glucan with 0.0025 or 0.005 U ml^{-1} heat-treated lichenase or a 1:10 dilution of MLG oligosaccharides (β-1,3;1,4-glucan + active lichenase upon different incubation times). Activation of MAPK6, MAPK3 and MAPK4 was analysed via Western Blot with the p44/42-antibody. Lower panel shows Coomassie Brilliant Blue (CBB) staining as loading control. The experiment was performed two times with similar results.

To further investigate whether the enzymatically generated MLG oligosaccharides trigger immune responses in Arabidopsis, the expression of the defence genes *WRKY33* and *WRKY53* was tested via qRT-PCR. The expression of the defence gene *WRKY33* is significantly induced upon treatment with MLG oligosaccharides upon hydrolysis of β-1,3;1,4-glucan polymer for all different incubation times (Figure 21 A and C). Similarly, *WRKY53* expression was induced significantly upon treatment with MLG oligosaccharides obtained from β-1,3;1,4-glucan polymer incubated with 0.05 U ml^{-1} lichenase for 15, 30, 120 and 240 min or MLG oligosaccharides obtained from β-1,3;1,4-glucan polymer incubated with 0.025 U ml^{-1} lichenase for 15, 30, 45, 60 and 240 min (Figure 21 B and D). As the expression of the two tested defence genes was only significantly induced upon treatment with MLG oligosaccharides but not upon control treatments including Sodium phosphate buffer, this result

confirms that oligomeric MLGs are perceived by Arabidopsis which subsequently leads to the initiation of defence responses.

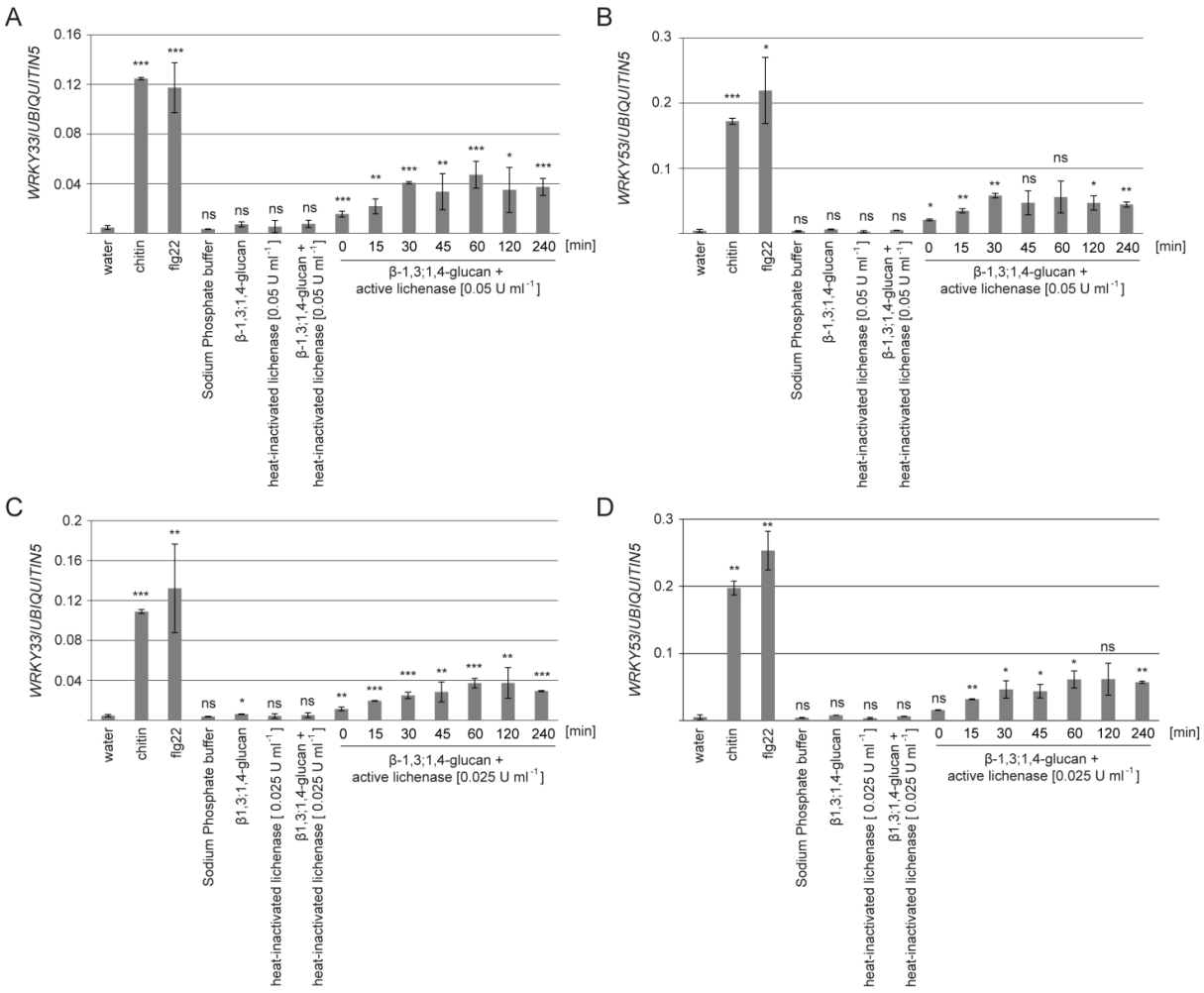

Figure 21. Defence gene expression in Arabidopsis Col-0 upon treatment with MLG oligosaccharides. To obtain MLG oligosaccharides of varying length, 10 mg ml^{-1} barley β-1,3;1,4-glucan polymer dissolved in 100 mM Sodium Phosphate buffer was hydrolysed with 0.05 U ml^{-1} lichenase (A and B) or 0.025 U ml^{-1} lichenase (C and D) and the reaction was stopped upon 0, 15, 30, 45, 60, 120 or 240 min incubation. 14-day old *in-vitro* grown Arabidopsis Col-0 seedlings were treated for 30 min with 10 µg mL^{-1} chitin, 50 nM flg22, 10 mM Sodium phosphate buffer, 1 mg ml^{-1} β-1,3;1,4-glucan, 0.005 U ml^{-1} or 0.025 U ml^{-1} heat inactivated lichenase, 1 mg ml^{-1} β-1,3;1,4-glucan with 0.005 U ml^{-1} or 0.025 U ml^{-1} heat-treated lichenase or a 1:10 dilution of MLG oligosaccharides (β-1,3;1,4-glucan + active lichenase upon different incubation times). The expression of the defence genes *WRKY33* (A and C) and *WRKY53* (B and D) was analysed via qRT PCR. *UBIQUITIN5* served as reference gene. The bars represent means of two biological replicates with each three technical replicates. Error bars represent STDEV. Statistical significance is indicated with asterisks with not significant (ns) = $p > 0.5$, * = $p \leq 0.5$, ** = $p \leq 0.001$ and *** = $p \leq 0.001$. The unpaired student's t-teat was used to calculate p-values.

3.2.7 Hydrolysis products of the barley β-1,3;1,4-glucan polymer do not inhibit seedling growth

Typically, seedlings show an inhibition of growth when they are exposed to high concentrations of elicitors e.g. flg22 or elf18 (Gómez-Gómez and Boller, 2000; Zipfel *et al.*, 2006). The receptor for elf18 was identified in a reverse genetic screen in which several T-DNA insertion lines were tested for their sensitivity towards elf18 in seedling growth experiments (Zipfel *et al.*, 2006). Similarly, if MLGs negatively influence seedling growth, receptors or co-receptors required for MLG perception could be identified with a forward genetic screen using the seedling growth assay.

To test whether MLG oligosaccharides can inhibit seedling growth, 5-day old *in-vitro* grown Col-0 seedlings were transferred to ½ MS medium plus sucrose containing either no elicitor, Sodium phosphate buffer, flg22 or MLG oligosaccharides that were generated upon β-1,3;1,4-glucan hydrolysis (Figure S20). The seedlings were grown for eight further days and then, the size of the seedlings as well as the dry weight of the 13-day old seedlings was analysed. A dramatic reduction in growth was only directly observed for seedlings that were grown in the presence of the bacterial MAMP flg22 but not for seedlings grown in medium containing MLG oligosaccharides or Sodium phosphate buffer (Figure 22 A). Furthermore, the dry weight of seedlings growing in medium containing MLG oligosaccharides was not significantly reduced in comparison to seedlings growing in ½ MS plus sucrose medium without elicitor indicating that MLG oligosaccharides do not influence seedling growth (Figure 22 B). Consequently, testing the sensitivity of several mutants or ecotypes to MLGs in a seedling growth assay cannot be used to identify molecular components required for MLG perception.

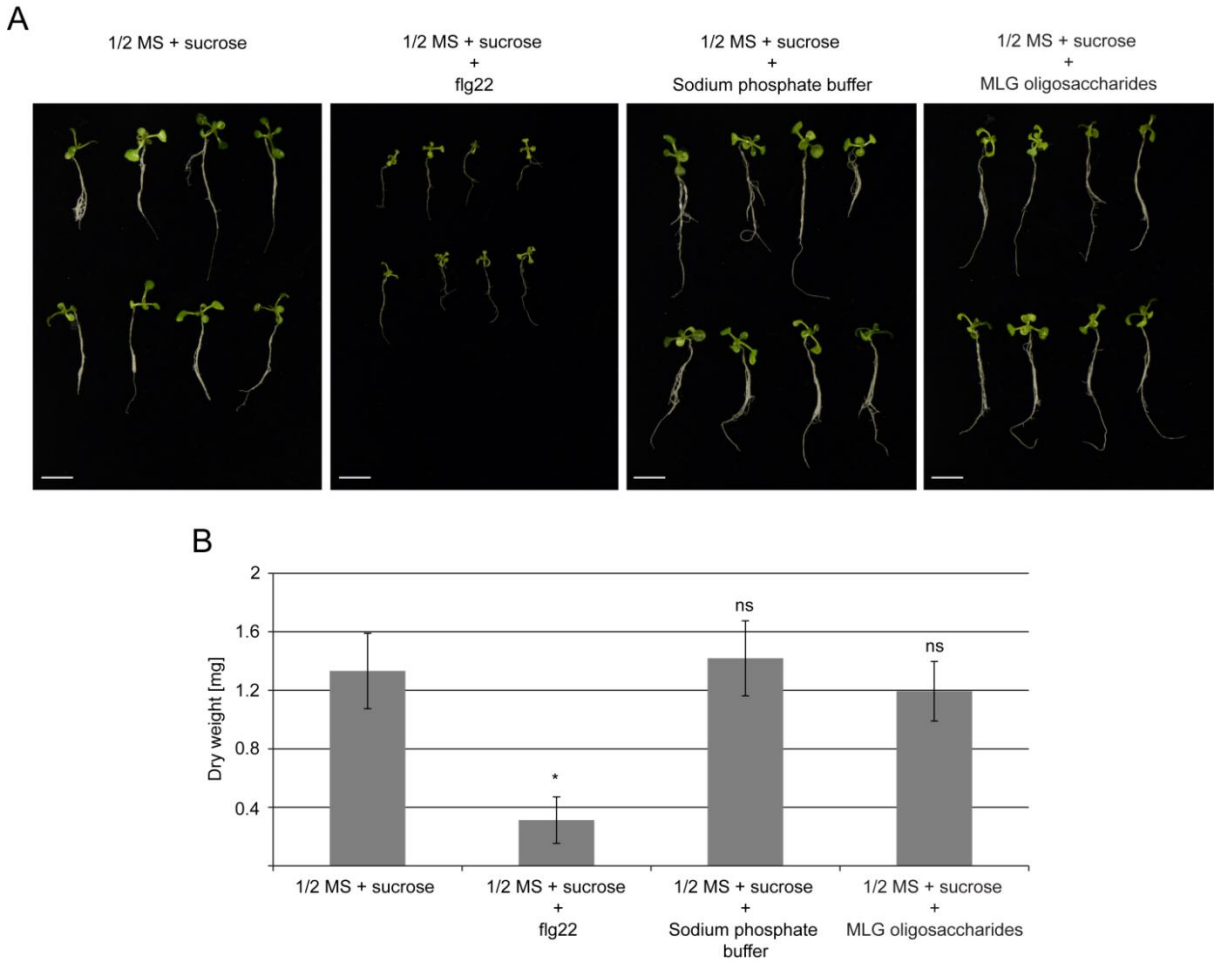

Figure 22. Effect of MLG oligosaccharides on seedling growth. To obtain MLG oligosaccharides of varying length, 10 mg ml^{-1} barley β-1,3;1,4-polymer dissolved in 100 mM Sodium phosphate buffer was hydrolysed with 1 U ml^{-1} lichenase and the reaction was stopped upon 1h. 5-day old *in-vitro* grown Arabidopsis Col-0 seedlings were transferred to liquid ½ MS plus sucrose medium containing no elicitor, 10 mM Sodium Phosphate buffer (pH = 6.5), 1 µM flg22 or a 1:10 dilution of MLG oligosaccharides and grown for 8 further days. (A) Pictures were taken of 13-day old seedlings. Scale bar represents 1 cm. (B) 13-day old seedlings were dried and the weight of 7 to 8 seedlings per treatment was measured. The weight of one seedling was calculated by dividing the weight of all seedlings of one treatment by the total number of seedlings. Bars represent the average weight of one seedling of two biological replicated consisting of 7 to 8 seedlings each. Error bars represent STDEV. Statistical significance is indicated by asterisk with not significant (ns) = $p > 0.5$, * = $p \leq 0.5$, ** = $p \leq 0.01$ and *** = $p \leq 0.001$. To calculate p values, the unpaired student's t-teat was used.

3.3 Molecular components involved in MLG perception could not be identified with reverse and forward genetic screens

3.3.1 MLG perception does not involve LysM domain containing RLK and RLPs

So far, known PRRs are either RLKs or RLPs. RLKs that contain LysM domains were shown to be involved in the perception of oligosaccharide MAMPs, e.g. chitin and peptidoglycan (Macho and Zipfel, 2014). In Arabidopsis five genes encode for LysM domain containing RLKs (LYKs): LYK1/CERK1 and LYK2 to LYK5 (Zhang *et al.*, 2007). The LysM RLKs CERK1, LYK4 and LYK5 are involved in perception of the fungal MAMP chitin whereas LYK2 does not seem to play a role in chitin perception (Miya *et al.*, 2007; Petutschnig *et al.*, 2010; Wan *et al.*, 2012; Cao *et al.*, 2014). Furthermore, CERK1 was shown to play a role in the perception of β-1,3-glucan oligomers as well as in bacterial peptidoglycan perception together with LYM1 and LYM3 (Willmann *et al.*, 2011; Mélida *et al.*, 2018).

To test the involvement of CERK1, LYK2, LYK4 and LYK5 in MLG perception, MAPK activation upon treatment with MLG oligosaccharides was monitored in the chitin receptor mutant *cerk1*-2 (GABI_096F09), the T-DNA insertion line *lyk2*-1 (SALK_152226) and the double mutant *lyk5*-2 *lyk4*-2 (SALK_131911C x GABI_897A10) via immunoblot analysis using the p44/42-antibody. MLG oligosaccharides were obtained from hydrolyzing barley β-1,3;1,4-polymer with 1 U ml^{-1} lichenase. The hydrolysis was checked via TLC (Figure S20). Upon treatment with MLG oligosaccharides, MAPKs were phosphorylated in *cerk1*-2, *lyk2*-1 and the *lyk5*-2 *lyk4*-1 double mutant to the same level as in Col-0 suggesting that neither CERK1, LYK2, LYK4 nor LYK5 are involved in MAPK activation upon MLG perception (Figure 23 A and B).

LYM2 mediates the decrease in molecular flux between cells through plasmodesmata in response to chitin (Faulkner *et al.*, 2013). LYT1 is an extracellular LysM domain containing protein that was found to be co-regulated with CERK1 and might be involved in elicitor perception with CERK1 (Dr. Elena Petutschnig, personal communication). To address whether LYM2 or LYT1 are involved in the perception of MLGs, MAPK activation upon MLG oligosaccharide treatment in *lym2*-1 (SAIL_343_B03), *lym2*-4 (GABI-Kat 165 H02) and *lyt1*-1 (SALK_144729) was analysed with Western Blot using the p44/42-antibody. MAPK6 and MAPK3 phosphorylation was not compromised in *lym2*-1, *lym2*-4 or *lyt1*-1 indicating that LYM2 and LYT1 are not involved in MLG perception (Figure 23 B).

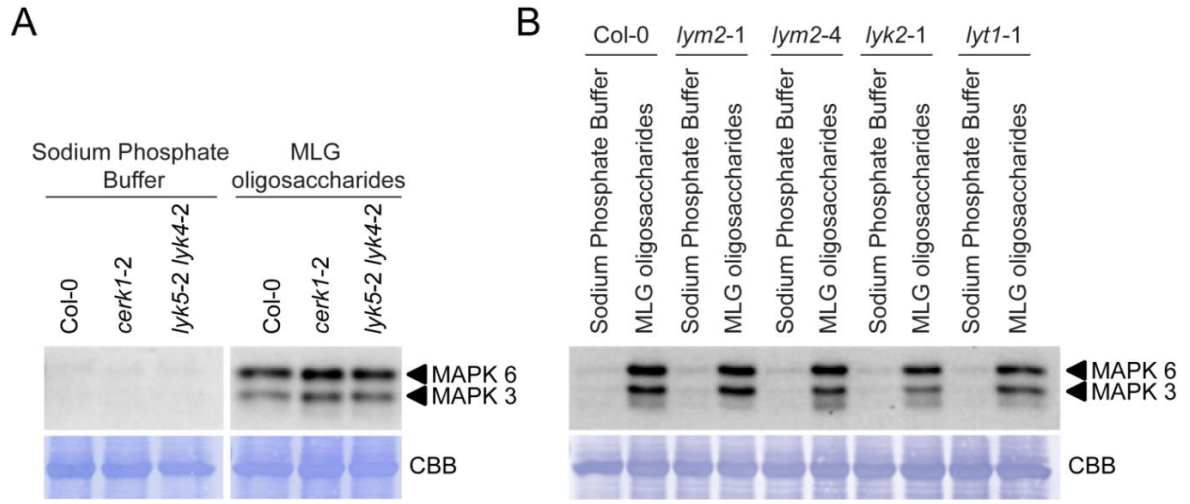

Figure 23. Activation of MAPK6 and MAPK3 in different LysM-RLKs and LysM-RLPs mutants upon MLG oligosaccharide treatment. To obtain MLG oligosaccharides of varying length, 10 mg ml^{-1} barley β-1,3;1,4-glucan polymer dissolved in 100 mM Sodium phosphate buffer (pH = 6.5) was hydrolysed with 1 U ml^{-1} lichenase and the reaction was stopped upon 1h. 14-day old *in-vitro* grown Arabidopsis seedlings of Col-0, *cerk1*-2 and *lyk5*-2 *lyk4*-1 (A) or Col-0, *lym2*-1, *lym2*-4, *lyk2*-1 or *lyt1*-1 (B) were treated for 12 min with 10 mM Sodium phosphate buffer or a 1:10 dilution of MLG oligosaccharides. Activation of MAPK was analysed via Western Blot using p44/42 antibody. Lower panel shows Coomassie Brilliant Blue (CBB) staining as loading control. The experiment was performed once.

3.3.2 LRR-RLKs are not involved in MLG perception

The bacterial MAMPs flg and EF-TU induce a set of immune responses in *A. thaliana* and are perceived by the receptor kinases FLS2 and EFR, respectively (Chinchilla *et al.*, 2006; Zipfel *et al.*, 2006).

To test whether FLS2 and EFR are required in MLG perception, the activation of MAPK upon treatment with enzymatically generated MLG oligosaccharides (Figure S20) was tested in *fls2c* (SAIL_691_C4) and *efr*-1 (SALK_044334) via immunoblot analysis using the p44/42-antibody. Loss of FLS2 in the *fls2c* mutant did not abolish MAPK activation upon MLG oligosaccharide treatment (Figure 24). Similarly, loss of EFR in the *efr-1* mutant did not affect MAPK activation upon treatment with MLG oligosaccharides (Figure 24). These results indicate that neither FLS2 nor EFR are involved in MAPK activation upon MLG perception.

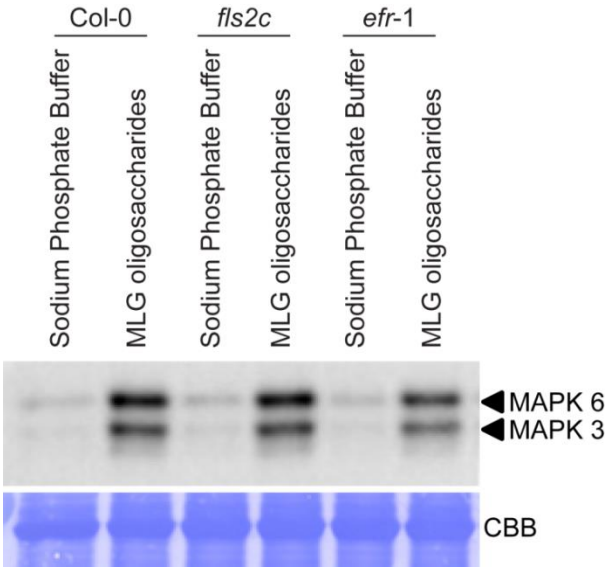

Figure 24. Activation of MAPK6 and MAPK3 in *fls2c* and *efr-1* upon MLG oligosaccharide treatment. To obtain MLG oligosaccharides of varying length, 10 mg ml^{-1} barley β-1,3;1,4-polymer dissolved in 100 mM Sodium phosphate buffer (pH = 6.5) was hydrolysed with 1 U ml^{-1} lichenase and the reaction was stopped upon 1h. 14-day old *in vitro* grown Arabidopsis seedlings of Col-0, *fls2c* and *efr*-1 were treated for 12 min with 10 mM Sodium phosphate buffer or a 1:10 dilution of MLG oligosaccharides. Activation of MAPK was analysed via Western Blot using p44/42-antibody. Lower panel shows Coomassie Brilliant Blue (CBB) staining as loading control. The experiment was performed once.

The LRR-RLK BAK1 is involved in brassinosteroid signaling and also plays a role as positive regulator in plant immunity (Li *et al.*, 2002; Nam and Li, 2002; Heese *et al.*, 2007; Chinchilla *et al.*, 2007). BAK1 is required for early immune responses induced by flg22 and elf18 and was shown to form a complex with the respective receptors FLS2 and EFR (Heese *et al.*, 2007; Chinchilla *et al.*, 2007; Roux *et al.*, 2011). Furthermore, BAK1 is involved in PEPR1/2-dependent responses that are the corresponding receptors for the Pep DAMP molecules. These results demonstrate that BAK1 is involved in multiple PRR-signalling pathways (Roux *et al.*, 2011).

To test a potential involvement of BAK1 as co-receptor in the perception of MLGs, the activation of MAPK was monitored over time in *bak1*-4 and *bak1*-5 upon MLG oligosaccharide treatment. *Bak1*-4 (SALK_116202) is a knock-out mutant, while *bak1*-5 harbours a single amino acid exchange in the 10^{th} exon and is specifically impaired in PTI responses (Schwessinger *et al.*, 2011). Activation of MAPKs was neither reduced nor delayed in *bak1*-4 and *bak1*-5 in comparison to Col-0 upon treatment with MLG oligosaccharides of varying length (Figure 25 A) that were enzymatically generated using the commercially available *B. subtilis* lichenase (Figure S20). This suggests that the co-receptor BAK1 is not involved in MLG perception.

The LRR-RLK SOBIR1 plays a role in activating defence responses by certain immune receptors. The RLP RLP30 is involved in perception of the peptide effector SCFE1 and requires SOBIR1 (Zhang *et al.*, 2013). Furthermore, SOBIR1 is indispensable for RBPG1-mediated responses towards fungal polygalacturonases (Zhang *et al.*, 2014).

To test the involvement of SOBIR1 in MLG perception, MAPK activation upon MLG oligosaccharide treatment was analysed in the two knock-out mutants *sobir1*-12 (SALK_050715) and *sobir1*-14 (GABI-Kat_643F07). The activation of MAPK in the two different mutants *sobir1*-12 and *sobir1*-14 was not impaired after MLG elicitation indicating that SOBIR1 is not involved in perception of MLGs (Figure 25 B).

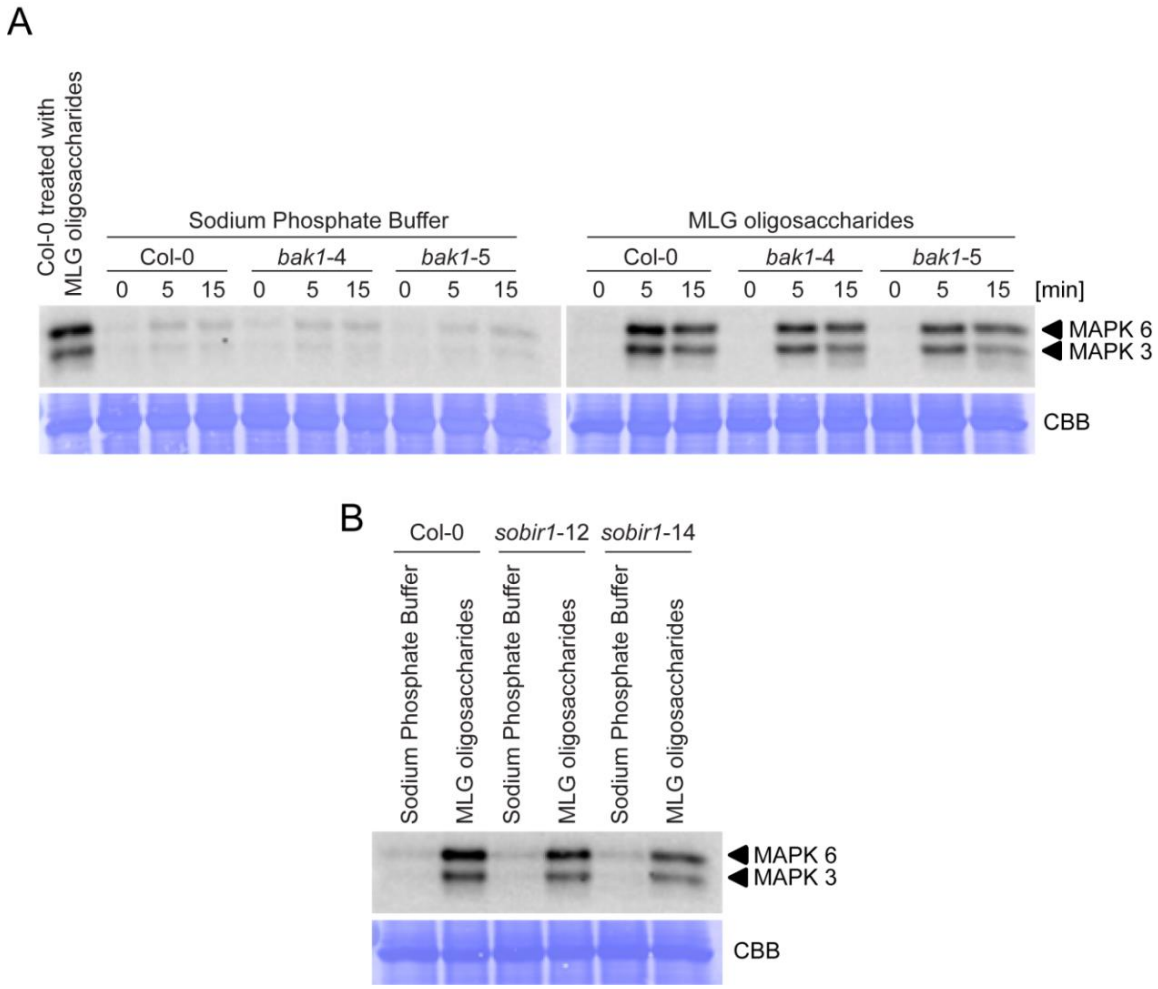

Figure 25. Activation of MAPK6 and MAPK3 in different co-receptor mutants upon MLG oligosaccharide treatment. To obtain β-glucan oligosaccharides of varying length, 10 mg ml^{-1} barley β-1,3;1,4-polymer dissolved in 100 mM Sodium phosphate buffer was hydrolysed with 1 U ml^{-1} lichenase and the reaction was stopped upon 1h. (A) MAPK activation in *bak1*-4 and *bak1*-5. 14-day old *in-vitro* grown seedlings of Col-0, *bak1*- 4 and *bak1*-5 were treated with 10 mM Sodium Phosphate buffer or a 1:10 dilution of MLG oligosaccharides for 0, 5 or 15 min. MAPK activation was analysed via Western Blot using p44/42 antibody. Lower panels show Coomassie Brilliant Blue (CBB) staining as loading control. The experiment was performed once. (B) MAPK activation in *sobir1*-12 and *sobir1*-14. 14-day old *in-vitro* grown seedlings of Col-0, *sobir1*-12 and *sobir1*-14 were treated with 10 mM Sodium phosphate buffer or a 1:10 dilution of MLG oligosaccharide for 12 min. MAPK activation was analysed via Western Blot using p44/42 antibody. Lower panels show Coomassie Brilliant Blue (CBB) staining as loading control. The experiment was performed once.

3.3.3 127 tested Arabidopsis ecotypes are MLG-sensitive

The plant species *A. thaliana* exhibits a high variability regarding their sensitivity towards different MAMPs due to distinct ecotype-specific receptor repertoires (Gómez-Gómez and Boller, 2000; Zhang *et al.*, 2013; Albert *et al.*, 2015). This has been exploited in the past to identify MAMP-receptors e.g. the SCFE1 receptor RLP30 was identified with the help of the insensitive accessions Lov-1, Mt-0 and Sq-1 (Zhang *et al.*, 2013).

In order to identify molecular components required for MLG perception, MLG-insensitive and MLG-sensitive ecotypes should be identified and subsequently, be used to identify the corresponding receptor using map-based cloning strategies. A set of 527 Multiparent Advanced Generation Inter-Cross (MAGIC) lines, derived from crossing 19 parental ecotypes, is available that can be used to identify e.g. novel PRRs via map-based cloning. If MAMP-sensitive and MAMP-insensitive parental lines can be identified, the respective MAGIC lines can be used to identify the corresponding receptor (Kover *et al.*, 2009). To identify MLG-sensitive and MLG-insensitive Arabidopsis accessions and potentially the MLG receptor or co-receptors, all parental ecotypes of the MAGIC lines, except for Ler-0, were analysed regarding the phosphorylation of MAPK upon MLG elicitation. The *B. subtilis* lichenase was used to enzymatically produce oligomeric MLGs (Figure S20). The immunoblot analysis revealed that all tested parental lines showed MAPK activation upon MLG oligosaccharide treatment (Figure 26). Although the MAPK activation for the ecotype Zu-0 was less pronounced in comparison to the other ecotypes, this result indicates that all of these ecotypes harbour the molecular components involved in MLG perception (Figure 26).

Since the parental lines of the MAGIC lines did not reveal an ecotype that could not respond to MLGs, 110 further ecotypes were tested for MAPK activation upon MLG oligosaccharide elicitation. However, MAPK activation was not impaired in one of the 110 tested ecotypes in response to MLG oligosaccharides indicating that the tested ecotypes are sensitive towards MLGs and contain the molecular components required for MLG perception (Figure S21, Figure S22, Figure S23). In conclusion, none of the 127 tested ecotypes can be used to identify components of the MLG perception system.

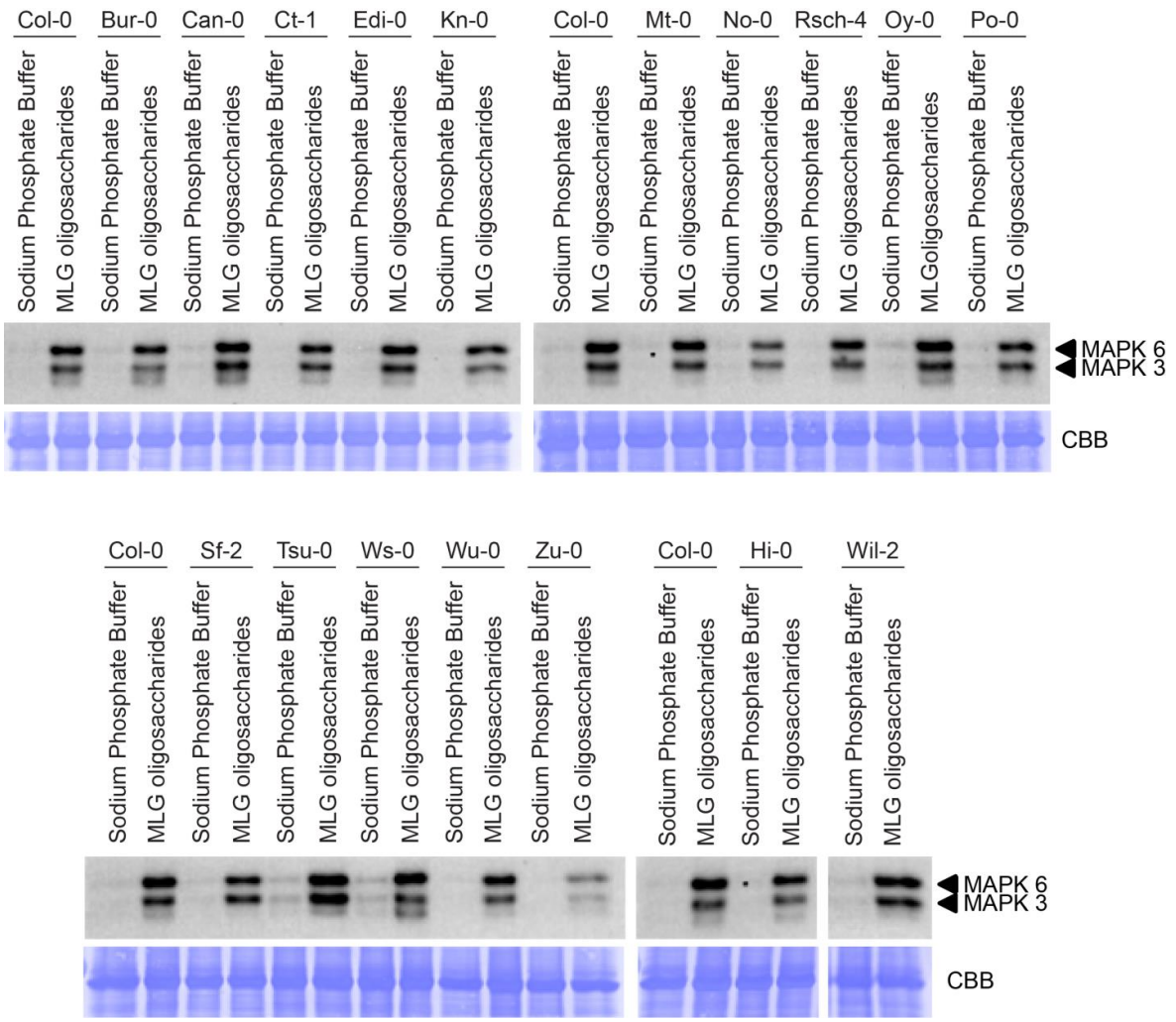

Figure 26. MAPK activation in the parental ecotypes of the MAGIC lines. To obtain MLG oligosaccharides of varying length, 10 mg ml^{-1} barley β-1,3;1,4-polymer dissolved in 100 mM Sodium Phosphate buffer was hydrolysed with 1 U ml^{-1} lichenase and the reaction was stopped upon 1h. 14-day old *in-vitro* grown seedlings of the respective ecotypes were treated with either 1 mM Sodium Phosphate buffer or a 1:10 dilution of MLG oligosaccharides for 12 min. Activation of MAPK was analysed via Western Blot using the p44/42-antibody. Lower panel shows Coomassie Brilliant Blue (CBB) staining as loading control. The experiment was performed once.

4 Discussion

The first physical barrier that pathogens encounter is the plant cell wall. In order to successfully infect a plant, pathogens need to overcome this physical barrier and evolved several mechanisms to do so. Fungal penetration structures called appressoria are used to penetrate the cell wall with pressure (Chisholm *et al.*, 2006). Furthermore, secreted CWDEs have been shown to be involved in cell wall degradation and pathogenicity of necrotrophic and hemibiotrophic pathogens. For example, simultaneous knockdown of ten genes encoding for xylanases of the hemibiotrophic fungus *Magnaporthe oryzae* resulted in a reduced penetration rate and a reduction in lesion size on barley and wheat (Nguyen *et al.*, 2011). So far, however, the involvement of CWDEs in the pathogenicity of biotrophic pathogens has not been elucidated. The first part of this study focuses on the functional characterization of *Bgh* enzymes that might be involved in pathogenicity.

4.1 Identification and functional characterization of fungal CWDEs

4.1.1 Genomic and transcriptomic data reveal GH family 17 as potentially involved in pathogenicity

A genome analysis conducted by our collaborators at the IPK Gatersleben (research group of the late Dr. Patrick Schweizer) identified a total of 75 CWDEs in the genome of *Bgh*. The majority of these proteins (62) were designated to 18 different GH families and one Auxiliary Activity family that was formerly described as GH family 61 (unpublished data, Dr. Patrick Schweizer, personal communication). The result of this analysis is contradictory to a genome analysis conducted in 2010 in which only seven CWDEs were identified and designated to two different GH families and one Auxiliary Activity family (Spanu *et al.*, 2010). However, analysis of the protein sequences of the 62 GHs for carbohydrate active enzyme domain signatures verified 60 of the proteins indicating that the genome of *Bgh* contains more CWDEs as previously thought (Table S1). The presence of 60 GHs and in total 72 CWDEs in *Bgh* nevertheless supports the finding of a study observing a reduced number of CWDEs in biotrophic pathogens compared to necrotrophic or hemibiotrophic pathogens (Zhao *et al.*, 2014). For example, the biotrophic plant pathogen *Ustilago maydis* contains 238 CWDE-encoding genes in its genome, while the hemibiotrophic rice blast fungus *M. oryzae* contains 522 genes encoding for CWDEs and the necrotrophic pathogen *Verticillium dahliae* genome harbours 545 genes for CWDEs (Zhao *et al.*, 2014).

In order to identify GH families that are involved in pathogenicity, the expression of the 60 identified GHs were analysed using publicly available transcriptomic data (Hacquard *et al.*, 2013). This analysis revealed that members of five different GH families including GH5, GH16, GH17, GH47 and GH76 were highly up-regulated during the first 24 h of the infection indicating their potential importance in the infection process (Table S2). Upon fungal attack, the plant cell wall is reinforced. For example, papillae are formed in immediate proximity to fungal penetration sites as observed in barley upon *Bgh* attack (Underwood, 2012). Papillae are mainly composed of callose, a polymer of β-1,3-linked

glucose monomers. As *Bgh* has to overcome the plant cell wall and defence-associated papillae for a successful infection, β-1,3-glucan degrading enzymes might be involved in pathogenicity. Of the five different GH families, the family GH17 was chosen for further functional characterization due to its designated substrate specificities towards β-1,3-glucans (Hrmova and Fincher, 1993; Carbohydrate Active Enzymes database, http://www.cazy.org/, Lombard *et al.*, 2014). Additionally, analysis of the protein sequences of all seven members of the GH family 17 revealed that all proteins contain either a canonical N-terminal signal peptide or an unconventional secretion signal indicating that all proteins are secreted into the plant apoplast and potentially act on the plant cell wall. As two of the seven GH17 members showed an enhanced penetration rate in HIGS analysis indicating that they negatively affect pathogenicity, these two members were excluded from further analysis and only five *Bgh* GH17 members will be functionally analysed.

4.1.2 Only BGH06777 could be expressed and purified using the *P. pastoris* expression system

For functional characterization of the five selected *Bgh* GH17 members, all five genes should be expressed and consequently, purified using the *P. pastoris* expression system. No distinct signals at the expected sizes could be detected for BGH00219, BGH00220, BGH00734 or BGH00736 in the supernatant of the cultures of different clones grown under four different conditions (Figure S1 A, B, C, D). There are several reasons why these proteins might not be expressed. One explanation could be that the GH17 proteins are susceptible to extracellular neutral pH proteases and are proteolytically degraded. This was also observed for gelatins produced in *P. pastoris*. The degradation of gelatins could be minimized by performing the expression at pH 3 (Werten *et al.*, 1999). To test whether BGH00219, BGH00220, BGH00734 or BGH00736 are degraded by extracellular proteases, the expression of the four GH17 members could also be performed at pH 3. To induce the expression of genes in *P. pastoris*, methanol is added to the culture. However, methanol does not only induce expression of the desired gene but was also shown to activate the generation of proteases in *P. pastoris* and cell lysis in high density cultures. Consequently, proteases that are found intracellular are present in the medium upon cell lysis and can degrade the secreted protein (Sinha *et al.*, 2005). It might be possible that during the expression of *Bgh00219*, *Bgh00220*, *Bgh00734* and *Bgh00736*, several proteases were generated and released into the medium due to cell lysis in a high density culture. To prevent proteolytic degradation, the optimal induction times as well as methanol feeding strategies have to be determined (Sinha *et al.*, 2005). Alternatively, protease inhibitors could be added to the medium. Another explanation for the absence of the four proteins in the supernatant could be that the genes of interest might not be transcribed due to the presence of multiple AT rich regions (Gurkan and Ellar, 2003). To test whether the respective genes are expressed in *P. pastoris*, mRNA could be extracted and semi-quantitative PCR or qRT-PCR could be performed.
A distinct signal, however, could be obtained for BGH06777 at the expected size in all tested clones (Figure S1 E). The clone that showed the strongest signal for BGH06777 was chosen to express and

purify the protein in high amounts. The recombinant purified protein was then subject for further biochemical characterization.

4.1.3 BGH06777 was glycosylated by *P. pastoris*

Of the five selected GH17 proteins, only BGH06777 could be expressed and purified in high amounts from *P. pastoris*. In SDS gel electrophoresis experiments the recombinant protein migrated at a size of approximately 35 kDa (Figure S2), which fits well to the predicted molecular weight of 32.9 kDa. Additional mass spectrometry analysis detected masses of the purified protein in the range between 35 kDa and 36.9 kDa (Figure 4 A). *P. pastoris* is known to N-glycosylate proteins at an asparagine residue in the sequence asparagine-x-threonine/serine where x can be any amino acid (Bretthauer and Castellino, 1999). An online tool for the prediction of N-glycosylation sites (http://www.cbs.dtu.dk/services/NetNGlyc/) revealed one glycosylation site for BGH06777 at the asparagine at position 191 (Table 18) suggesting that the difference in size as well as the occurrence of different masses may be due to glycosylation. *P. pastoris* was shown to have N-glycosylation of a high-mannose type with mainly 8-14 mannose residues per chain but also longer chains of up to 30 mannose residues have been found. Furthermore, the N-linked oligosaccharides can also be phosphorylated (Bretthauer and Castellino, 1999). Thus, the masses identified in mass spectrometry likely correspond to BGH06777 with either N-linked oligosaccharides with 11-20 mannose residues or N-linked phosphorylated oligosaccharides containing 13-18 mannose residues. PNGase F is an amidase that cleaves N-linked oligosaccharides from glycoproteins (Plummer *et al.*, 1984). Treatment of BGH06777 with PNGase F resulted in the migration of BGH06777 at approximately 33 kDa (Figure S2) and the identification of a mass at 32.97 kDa in mass spectrometry (Figure 4 B) which supports the hypothesis that BGH06777 was glycosylated. N-glycosylation is a co- and post-translational modification that occurs in all eukaryotes (Strasser, 2016) and thus, it is likely that BGH06777 is also glycosylated in *Bgh*. N-glycosylation fulfills a variety of different functions including induction of proper folding and biological activity as well as preventing proteolytic degradation of the respective protein (Rayon *et al.*, 1998). Recently, the role of N-linked glycans on the enzymatic activity of a xylanase designated as GH10 from *A. fumigatus* has been studied (Chang *et al.*, 2017). The deglycosylated protein exhibited the same pH optimum as the glycosylated protein, however, the pH range in which it showed activity was narrower. Furthermore, the thermal stability as well as the biological activity was lower for the deglycosylated protein in comparison to the glycosylated protein. These results further supported the positive effect of N-glycosylation on enzyme stability (Chang *et al.*, 2017). To study the effect of glycosylation on BGH06777, the deglycosylated protein could also be functionally characterized in future experiments. The glycosylated form of BGH06777 was used in the following detailed biochemical characterization. To our knowledge, this is the first GH17 protein from the powdery mildew *Bgh* studied so far.

4.1.4 BGH06777 is a typical GH17 β-1,3-glucanase

Substrate analysis revealed that BGH06777 hydrolysed β-1,3-glucan oligosaccharides with a minimum length of four glucose monomers (Figure 5) demonstrating that BGH06777 is an active β-1,3-glucanase and that binding of at least four monomers is required for efficient hydrolysis. The hydrolysis products generated by BGH06777 were oligosaccharides with a length of two to four glucose monomers. This finding is in agreement with previous studies about substrate specificities of other enzymes designated as GH17. Three β-1,3-glucan endohydrolases from barley were shown to hydrolyse the β-1,3-glucan polymer laminarin and the main hydrolysis products for two of the isoenzymes were laminaribiose and laminaritriose (Hrmova and Fincher, 1993). A GH17 enzyme from banana fruit was also shown to be active on laminarin (Peumans *et al.*, 2000). Additionally, the GH17 β-1,3-glucanosyltransferase Bgt2p of *A. fumigatus* was shown to cleave laminaribiose from a β-1,3-glucan chain (Gastebois *et al.*, 2010).

The hydrolytic activity of BGH06777 on β-1,3-glucan oligosaccharides can further be described kinetically. The substrate concentration at which the half-maximal reaction rate is achieved is described by the Michaelis constant K_M (Michaelis and Menten, 1913). K_M is influenced by the binding affinity of a substrate to the enzyme as well as the rate of product formation. Thus, K_M is only an approximate measure of binding affinity and can only be used as measure for binding affinity if binding of the substrate to the enzyme is slower than formation of the enzyme-substrate complex and the product (Kessel and Ben-Tal, 2018). The K_M value of BGH06777 for laminarihexaose was slightly higher than the K_M value for laminaripentaose (Table 19). Under the assumption that product formation occurs faster than binding of the substrate to the enzyme, the obtained K_M values indicates that BGH06777 has a lower affinity for laminarihexaose than for laminaripentaose. However, during hydrolysis of the β-1,3-glucan hexamer laminaribiose and laminaritetraose are generated. The generated product laminaritetraose might act as additional substrate during β-1,3-glucan hexamer degradation and might therefore influence the K_M value obtained for laminarihexaose. On the contrary, products generated during laminaripentaose hydrolysis do not represent potential substrates for BGH06777 and thus, might not influence the K_M value. Nevertheless, the obtained K_M values are similar to reported K_M values for the three barley β-1,3-glucan endohydrolases (Hrmova and Fincher, 1993). The turnover number k_{cat} describes the number of substrate molecules that are converted into products per active site per time unit (Michaelis and Menten, 1913). K_{cat} obtained for laminarihexaose degradation was about 5-fold higher compared to laminaripentaose degradation suggesting that BGH06777 favors longer oligosaccharide chains (Table 19). This is also supported by the observation that the catalytic efficiency was higher for laminarihexaose degradation than for laminaripentaose degradation (Table 19). This further suggests that the active site of the enzyme contains a minimum of six subsites. The active site of a GH can be labelled with negative subsites (-n) away from the cleavage site to the non-reducing end and with positive subsites (+n) away from the cleavage site towards the reducing end of a sugar. The glycosidic linkage of the oligosaccharide bound to the enzyme is hydrolysed between the subsites -1 and +1 (Davies *et al.*, 1997). ^{18}O labelling of the product and subsequent mass spectrometry revealed that BGH06777 contains in total six subsites

with four negative and two positive subsites (Figure 9, Table 20). The length of the active site of BGH06777 is comparable to active sites of other GH17 enzymes. The three barley β-1,3-glucan endohydrolases were shown to contain eight subsites ranging from -3 to +5 (Hrmova *et al.*, 1995) while the crystal structure of a tomato β-1,3-glucan endohydrolases revealed a total of 6 subsites with two negative and four positive subsites (Wojtkowiak *et al.*, 2013). The crystal structure of a β-1,3-glucanosyltransferase from the fungus *Rhizomucor miehei* designated as a GH17 revealed a total of 5 subsites ranging from -3 to +2 (Qin *et al.*, 2015). The number of negative and positive subsites determines the catalytic mode of an enzyme, thus, BGH06777 has a -4/+2 catalytic mode. This catalytic activity indicates that the product laminaribiose is released from the reducing end of the respective substrate.

The catalytic activity of BGH06777 was shown to be optimal at a pH of 5.5 and in a temperature range from 25°C to 51°C (Figure 6). The obtained pH optimum is similar to reported pH optima of other GH17 enzymes. While the three barley β-1,3-glucan endohydrolases have an optimal pH at 4.8 (Hrmova and Fincher, 1993), a β-1,3-glucanase from olive exhibits its highest activity in a pH range from 4.5 to 6 (Huecas *et al.*, 2001). Taken together, these data suggest that BGH06777 is a typical β-1,3-glucanase.

4.1.5 BGH06777 might be involved in papillae degradation

In this study, the biological function of BGH06777 could not be elucidated. However, the pH optimum of BGH06777 in addition to the presence of the signal peptide supports the idea that BGH06777 is active in the apoplastic space. The pH of the plant apoplast was shown to be between 5 and 6.5 (Grignon and Sentenac, 1991; Felle, 2006) and therefore corresponds to the pH optimum of BGH06777. Furthermore, plants generate callose-rich papillae upon fungal penetration that are thought to hinder further penetration (Underwood, 2012). Callose is a β-1,3-linked homopolymer of glucose monomers and thus represents a potential substrate for BGH06777. It might be possible that BGH06777 is involved in degrading papillae. A comparison of papillae that were either effective or ineffective in preventing *Bgh* penetration showed that ineffective papillae contain less callose, cellulose and arabinoxylan and lack an outer layer consisting of cellulose and arabinoxylan (Chowdhury *et al.*, 2014). Consequently, it is conceivable to postulate that ineffective papillae might be overcome by *Bgh* employing a combination of pressure and enzymatic degradation of callose by BGH06777 and other GH17 enzymes. In contrast, the outer layer of cellulose and arabinoxylan present in effective papillae might provide the structural strength to prevent *Bgh* penetration, and may be due to lack of CWDEs with efficient cellulose and arabinoxylan hydrolytic activity.

4.1.6 Conclusion

In the first part of this study, CWDEs involved in pathogenicity of *Bgh* were identified and functionally characterized. Analysis of genomic and transcriptomic data indicated that the family GH17 of *Bgh* might be involved in pathogenicity. The *Bgh* GH17 member BGH06777 was expressed and purified from *P. pastoris* and functionally characterized. To our knowledge, this is the first CWDE of *Bgh* that was characterized. BGH06777 hydrolyses β-1,3-glucans with a minimum length of four glucose monomers and the respective products are released from the reducing end of the sugar. The enzyme is most active in a temperature range from 25°C to 51°C and at a pH of 5.5 which corresponds to the pH in the plant apoplast.

4.1.7 Outlook

The glycosylated protein BGH06777 was heterologously expressed in *P. pastoris* and functionally characterized. To test the effect of glycosylation on the biological activity of BGH06777, the recombinant protein could be deglycosylated enzymatically and functionally characterized regarding pH and temperature optimum. Furthermore, the kinetic parameters K_M and k_{cat} as well as the catalytic efficiency could be determined. A narrower pH and temperature range as well as a lower catalytic efficiency would indicate a positive impact of N-glycosylation on the biological activity of BGH06777. Furthermore, it would suggest that BGH06777 is present in the glycosylated form in *Bgh*.

The biological role of BGH06777 could not be identified during the course of this project. To substantiate the preliminary HIGS experiments conducted in the lab of our collaboration partner, the late Dr. Schweizer (IPK Gatersleben), which had suggested a potential involvement in pathogenicity, these should be repeated with a significant number of replicates. A reduced penetration rate compared to the wild-type empty HIGS vector control experiments would suggest an involvement of BGH06777 on pathogenicity while no change in the penetration rate would indicate that BGH06777 does not play a role. Previously it was shown that silencing of a single CWDE has no effect on the severity of the infection while simultaneous HIGS of several genes of one CWDE family resulted in reduced pathogenicity (Gómez-Gómez *et al.*, 2002; Wu *et al.*, 2006; Nguyen *et al.*, 2011). This effect might be explained with a redundant function of CWDEs of the same family (Nguyen *et al.*, 2011). Analogous experiments could be used in the future to address the question whether or not GH17 members of *Bgh* act redundantly and thus jointly contribute to pathogenicity.

Of course, it would also be interesting to functionally characterize the other members of the GH17 family, namely BGH00219, BGH00220, BGH00734 and BGH00736. Therefore, further *P. pastoris* clones should be generated and tested for the integration of the respective gene in the genome. Next, the expression of the respective gene should be tested. To circumvent possible proteolytic degradation, the expression could be performed at a pH of 3 and/or the medium could further be supplemented with a protease inhibitor mix. If a protein can be successfully purified, it can be

functionally characterized concerning substrate specificity, pH optimum, temperature optimum and Michaelis-Menten kinetics.
Overall, the proposed experiments would shed light into the substrate specificities of GH17 enzymes of *Bgh* and their potential biological role.

4.2 Identification of new cell-wall derived DAMP molecules

Plants evolved several mechanisms to induce immune signaling upon pathogen attack. The perception of non-self MAMP molecules by PRRs leads to the activation of defence responses. Similarly, perception of DAMPs, self-molecules that are only abundant upon e.g. wounding or cell damage, triggers the induction of immune responses (Jones and Dangl, 2006; Boller and Felix, 2009). The action of CWDEs on the plant cell wall might release cell-wall oligosaccharides (Bacete *et al.*, 2018). It is likely that plants are able to perceive the released cell wall oligosaccharide as DAMPs which leads to the initiation of defence responses. The second part of this study focuses on the identification of new cell-wall derived DAMP molecules in Arabidopsis and barley and the corresponding signaling components.

4.2.1 Cellohexaose, xylohexaose and linear β-1,3-glucan oligosaccharides could slightly induce immune responses in Arabidopsis

In this study, a screen to identify new cell-wall derived DAMP molecules was conducted with a collection of 41 poly- and oligosaccharides. The majority of poly- and oligosaccharides did not activate immune responses (Figure S3, Figure S4, Figure S5, Figure S6, Figure S7, Figure S8, Figure S9), whereas eight of the ordered substances did trigger the influx of Ca^{2+} and/or activation of MAPK in Arabidopsis (Figure 10, Figure 11, Figure 12, Figure S10, Figure S11, Figure S12, Figure S13, Figure S14, Figure S15). These data suggested that plants evolved the ability to perceive some, but not all cell wall derived oligosaccharides that might be generated during pathogen attack.

4.2.1.1 Arabidopsis can perceive cellulose-derived oligomers

The cellulose derivative cellohexaose did not induce the generation of ROS but induced a slight influx of Ca^{2+} as well as the activation of MAPK in Arabidopsis (Figure S10, Figure S11) indicating that cellohexaose can be perceived by Arabidopsis which subsequently leads to the activation of immune responses. The observation that cellohexaose did not trigger the generation of ROS is in agreement with a previous study revealing that cellohexaose treatment did also not result in the generation of ROS in *V. vinifera* (Aziz *et al.*, 2003). Cellulose is a major component of the cell wall of dicot plants and cellohexaose might be generated upon degradation of cellulose by microbial cellulose degrading

enzymes. The degradation of cellulose by ascomycete and basidiomycete fungi involves at least three different enzyme classes, namely endo-β-1,4-glucanases, exo-β-1,4-glucanases or cellobiohydrolases and β-glucosidases (Baldrian and Valášková, 2008; Van Den Brink and De Vries, 2011; Glass *et al.*, 2013). These three enzyme classes can be categorized in a minimum of 12 different GH families including GH3, GH5, GH6 as well as GH7 and are commonly found in hemibiotrophic and necrotrophic pathogens (King *et al.*, 2011; Kubicek *et al.*, 2014; Carbohydrate Active Enzymes database, http://www.cazy.org/, Lombard *et al.*, 2014). Endo-β-1,4-glucanases cleave internal β-1,4-linkages within the cellulose chain leading to the release of β-1,4-glucan oligosaccharides of variable length, whereas exo-β-1,4-glucanases cleave the cellulose chain at the end of the chain thereby releasing cellobiose (Baldrian and Valášková, 2008; Van Den Brink and De Vries, 2011; Glass *et al.*, 2013). The oligosaccharides as well as cellobiose are degraded into glucose monomers through the action of β-glucosidases (Baldrian and Valášková, 2008; Van Den Brink and De Vries, 2011). The products generated by endo-1,4-β-glucanases might include oligosaccharides with six glucose monomers further suggesting that cellohexaose acts as a DAMP in Arabidopsis. The finding that cellohexaose activates plant immune responses confirms observations from a study that was published during the course of this project. This study showed that cellobiose acts as an elicitor of defence responses and that cellotriose as well as cellotetraose induce the expression of the defence gene *WRKY30* (de Azevedo Souza *et al.*, 2017) but exclude further analysis of molecular components involved in cellulose-derived oligomer perception. The data generated in this study and from the publication by Shauna Somerville's research group suggest that cellulose degradation products can be perceived by plants and induce the activation of immune responses.

4.2.1.2 Xylohexaose elicitation induces the activation of MAPK

Treatment of Arabidopsis with the hemicellulose derivative xylohexaose resulted in the activation of MAPKs (Figure S13 B). As the induction of MAPK was only slight and treatment with xylohexaose did not result in a calcium response and a detectable generation of ROS (Figure S12, Figure S13), this carbohydrate was excluded from further analysis. A reason for the non-conclusive results could be the used carbohydrate concentration. To test the elicitor activity of xylohexaose, 10 or 100 µg ml^{-1} were used in the conducted assays. However, to detect the induction of defence responses upon β-1,3-glucan oligosaccharide treatment, 250 µg ml^{-1} were used (Mélida *et al.*, 2018). Furthermore, a strong induction of MAPK activation in *V. vinifera* and Arabidopsis is observed upon treatment with 0.5 and 1 mg ml^{-1} xyloglucan oligosaccharides (Claverie *et al.*, 2018). This indicates that a high DAMP concentration is needed to obtain detectable readouts suggesting that the respective receptors have a low affinity towards the respective ligands (de Azevedo Souza *et al.*, 2017). However, it is not known whether these high concentrations are of physiological relevance and can be achieved during pathogen invasion. It might also be possible that treating plants with a high concentration may induce indirect effects such as osmotic stress leading to the initiation of responses that are similar to defence responses. It has been shown that hyperosmotic stress leads to a fast calcium response in

Arabidopsis (Stephan *et al.*, 2016). Furthermore, MAPK6 and MAPK3 are activated in response to hyperosmotic stress while MAPK6, MAPK3 and MAPK4 are phosphorylated upon hypoosmotic stress (Droillard *et al.*, 2002; Droillard *et al.*, 2004; Colcombet and Hirt, 2008). A comparison of genes regulated upon *B. cinerea* infection and several abiotic stresses revealed that about 40-50% of the genes that were differentially regulated upon infection with *B. cinerea* were also subject to transcriptional reprogramming upon osmotic stress (Sham *et al.*, 2015). To test whether xylohexaose triggers immune responses, the induction of defence responses upon xylohexaose treatment could be repeated with a higher carbohydrate concentration that is still in a physiological relevant range. As xylohexaose induced the activation of MAPK slightly, it seems likely that this carbohydrate also activated further immune responses upon treatment with a higher concentration. Xylohexaose is comprised of a chain of six β-1,4-linked unsubstituted xylose monomers and might be generated upon degradation of the hemicellulose class of xylans. The degradation of xylan involves mainly two enzyme classes: endo-β-1,4-xylanases and β-xylosidases (Polizeli *et al.*, 2005). Endo-β-1,4-xylanases hydrolyse β-1,4-glycosidic linkages in the xylan chain, however the position of the bonds selected for hydrolysis depends on the chain length, presence of side chains and degree of branching (Polizeli *et al.*, 2005; Kubicek *et al.*, 2014). During the hydrolysis, xylooligosaccharides of varying length including xylohexaose are generated but also smaller products e.g. xylobiose are produced (Polizeli *et al.*, 2005; Gonçalves *et al.*, 2012; da Silva *et al.*, 2015). The majority of fungal xylanases have been categorized to GH10 and GH11 (Kubicek *et al.*, 2014) and can be found in plant pathogenic fungi including *M. oryzae*, *V. dahliae* and *Fusarium oxysporum* (Zhao *et al.*, 2014). Furthermore, xylanases were shown to play a role in virulence. Simultaneous knockdown of ten xylanase encoding genes of *M. oryzae* resulted in a reduced penetration rate and a reduction in lesion size on barley (Nguyen *et al.*, 2011). This supports the idea that plant arabinoxylan is degraded during the infection process by certain fungi leading to the release of xylooligosaccharides. Subsequently, xylohexaose or other xylooligosaccharides might be perceived by the plant as DAMP.

4.2.1.3 Treatment with linear β-1,3-glucan oligosaccharides triggers MAPK phosphorylation

Previously, unsubstituted linear β-1,3-glucans were shown to induce immune responses in tobacco (Klarzynski *et al.*, 2000). In marked contrast, experiments conducted in this study in *A. thaliana* revealed that β-1,3-glucans of a length of five or six oligosaccharides were only able to slightly activate MAPK but not the influx of Ca^{2+} ions and the generation of ROS (Figure S14, Figure S15). As the induction of MAPK was only slight and the other tested responses were not induced, β-1,3-glucans were excluded from further analysis. However, a study from 2018 claimed that β-1,3,glucan hexamers and pentamers induce an influx in Ca^{2+} ions, activation of MAPK and induction of defence gene expression in a CERK1-dependent manner in Arabidopsis (Mélida *et al.*, 2018). The discrepancies in the obtained results might be explained with the concentration that was used in the assays. Whilst 10 to 100 µg ml^{-1} of the β-1,3-glucan oligosaccharides were used in this study,

250 µg ml^{-1} of the respective substrates were used in the publication of Antonio Molina's research group (Mélida *et al.*, 2018). β-1,3-glucans are the most abundant β-glucan in the fungal cell wall (Fesel and Zuccaro, 2016). Upon pathogen attack, chitinases as well as β-1,3-glucanase are secreted by the plant to hydrolyse fungal cell wall components and release elicitor-active oligosaccharides (Keen and Yoshikawa, 1983; Chisholm *et al.*, 2006; Balasubramanian *et al.*, 2012). Previous studies have shown that β-1,3-glucanases from soybean decompose fungal cell walls which result in the release of elicitor active β-1,3-oligosaccharides (Keen and Yoshikawa, 1983; Ham, 1991). Furthermore, a number of β-1,3-glucanases of Arabidopsis were shown to be transcriptionally up-regulated upon pathogen attack and proposed to function in pathogen defence (Dong *et al.*, 1991; Uknes *et al.*, 1992; Doxey *et al.*, 2007). Similarly to soybean β-1,3-glucanases, β-1,3-glucanases from Arabidopsis could be involved in the degradation of β-1,3-glucan in the fungal cell wall and thereby generating β-1,3-glucan oligosaccharides. However, β-1,3-glucans are also present in plants and can be found in callose-rich papillae that are generated in close proximity to fungal penetration sites or are deposited at plasmodesmata for conductivity control and in the cell plate during cytokinesis (Chen and Kim, 2009; Underwood, 2012). Previously, it has also been suggested that β-1,3-glucan oligosaccharides might originate from plant papillae (Klarzynski *et al.*, 2000). Thus, β-1,3-glucan oligosaccharides might represent a MAMP and/or DAMP.

4.2.2 MLGs act as DAMP and/or MAMP in barley

MLG is an unbranched homopolymer consisting of glucose that are interconnected via both β-1,3- and β-1,4-glycosidic linkages (Pauly *et al.*, 2013). The experimental data generated in this study demonstrated that MLG oligosaccharides consisting of three or four glucose monomers from Megazyme elicit the generation of ROS and the activation of MAPK in barley (Figure 10). This indicates that these MLG derivatives can be perceived by barley and trigger the induction of immune responses and that there is no required minimal length for the eliciting activity. Additionally, MLG tri- and tetrasaccharides from a second carbohydrate supplier resulted in the generation of ROS and activation of MAPK (Figure 13) which verified the previous results. HPAEC-PAD and MALDI-TOF analysis of the MLG oligosaccharides revealed no major carbohydrate contamination (Figure 16, Figure 17) supporting the manufacturer's claim of high purity of a minimum of 95% and virtually excluding that possible contaminations in the preparation might be the causal elicitor. To elicit immune responses, MLGs were used at a concentration of 10 µg ml^{-1} (for MAPK assays) or at 100 µg ml^{-1} (for ROS burst assays). The used concentrations are in accordance or lower compared to concentrations used to trigger chitin-induced immune responses in barley (Scheler *et al.*, 2016).

MLGs are found in the cell walls of most members of the Poales including the crop plants barley and oat (Burton and Fincher, 2009). In young barley plants, MLGs can be found e.g. in the epidermal and mesophyll cells in first leaves (Trethewey and Harris, 2002). Barley MLGs consist predominantly of β-1,4-linked cellotriosyl or cellotetrasyl units connected via β-1,3-linkages that are randomly distributed along the chain. The MLG oligosaccharides obtained from Megazyme were generated via

enzymatic hydrolysis of the barley MLG polymer (Megazyme, Compton, Ireland). Thus, the MLG oligosaccharides exhibit the same structure as the MLG oligosaccharides found in barley. This together with the fact that the MLG oligosaccharides are derived from barley support the idea that MLG oligosaccharides act as DAMP in this crop plant. MLG oligosaccharides might be generated from the MLG polymer present in the cell wall of monocots during the infection process by microbial β-1,3;1,4-glucanases. The first fungal β-1,3;1,4-glucanases have been identified and characterized in the anaerobic fungal strain *Orpinomyces* sp. PC-2 (Chen *et al.*, 1997) and the aerobic fungus *Talaromyces emersonii* (Murray *et al.*, 2001). Additionally, three extracellular β-1,3;1,4-glucanases were identified in the plant pathogenic fungus *Cochliobolus carbonum* and shown to act on the MLG polymer of barley (Görlach *et al.*, 1998). Enzymes that catalyze the hydrolysis of β-1,3;1,4-glucans can be found in the GH families 5, 6, 7, 8, 9, 11, 12, 16, 17, 26 and 51 (Carbohydrate Active Enzymes database, http://www.cazy.org/, Lombard *et al*., 2014). Plant pathogenic fungi that infect monocot species e.g. *U. maydis*, *Fusarium graminerarum* and *M. oryzae* were shown to harbour genes encoding for CWDEs that can be categorized in GH5, GH7, GH8, GH12 or GH16 (Zhao *et al.*, 2014). Some of these enzymes may be secreted during the infection and exhibit β-1,3;1,4-glucanase activity to degrade the β-1,3;1,4-polymer present in the monocot cell wall. The activity of these enzymes might lead to the release of MLG oligosaccharides.

Interestingly, in the past years, MLGs have also been found in lichen as well as in fungal and bacterial species suggesting that they are more widespread than previously thought. For example, MLGs are present in thalli of the two lichens *Cetaria islandica* and *Evernia prunastri* (Honegger and Haisch, 2001). Also, MLGs are abundant cell wall components in the hyphal cell wall of the ascomycete *A. fumigatus,* a human pathogen that causes Aspergillus infections in immunocompromised patients (Samar *et al.*, 2015). Notably, the inner walls of hyphae from the plant pathogen *R. commune* were also shown to contain MLGs. Structural analysis revealed that the *R. commune* MLG polymer consisted of the MLG tetrasaccharide G4G4G3G, the trisaccharide G4G3G and the dimer laminaribiose (Pettolino *et al.*, 2009). The structure of the MLG oligosaccharides found in *R. commune* resembles the structures of the MLG oligosaccharides used in this study suggesting that MLGs oligosaccharides might be released from the fungal cell wall through the activity of extracellular β-1,3;1,4-glucanases. The perception of the released MLG oligosaccharides leads subsequently to the activation of defence responses. So far, two genes encoding for β-1,3;1,4-glucanases have been identified in barley and the corresponding proteins, *Hv*GlbI and *Hv*GlbII, have been characterized. Both enzymes were active on the barley β-1,3;1,4-polymer resulting in the release of tri-, tetra- and penta-saccharides (Woodward and Fincher, 1982). Transcripts of *HvGlbI* can be detected in young leaves correlating with β-1,3;1,4-glucanase activity found in the leaf extracts (Slakeski and Fincher, 1992). Similarly, β-1,3;1,4-glucanases of the monocot crop plant wheat are present in young developing leaves (Roulin and Feller, 2001). Although the function and the exact localization of these proteins are not known, it was proposed that the identified β-1,3;1,4-glucanases rather play a role in development than in immunity (Slakeski and Fincher, 1992; Roulin and Feller, 2001). This suggests that the characterized β-1,3;1,4-glucanases are not implicated in the generation of MLG oligosaccharides from the fungal cell wall. However, further genes encoding for β-1,3;1,4-polymer

degrading enzymes could be present in the barley or wheat genome that play a role in fungal cell wall degradation.

Taken together, the data suggest that barley evolved the ability to perceive MLG oligosaccharides which results in the activation of immune responses. MLGs could originate either from barley or from a pathogen and therefore, might act as DAMP or MAMP or both.

4.2.3 MLGs act as a MAMP in Arabidopsis

It was demonstrated here that MLG oligosaccharides from two different carbohydrate suppliers were able to induce the influx of Ca^{2+} ions, the activation of MAPK and expression of the defence genes *WRKY33* and *WRKY53* in Arabidopsis (Figure 11, Figure 12, Figure 14, Figure 15). In contrast to barley, the generation of ROS could not be elicited robustly by the different MLG oligosaccharides in Arabidopsis (Figure 11 B, Figure 14 B). The luminol-based ROS burst assay is a comparatively variable and insensitive method and to obtain a reliable read-out, a high elicitor concentration has to be used. The concentration used to elicit a ROS burst might not be sufficient to induce the generation of ROS in Arabidopsis in a detectable amount while it might be sufficient to induce the ROS in barley. Nevertheless, the data generated in this study clearly demonstrate that Arabidopsis can perceive MLGs and that MLG recognition results in the activation of defence responses. No major carbohydrate contaminations could be identified during the analysis of the MLG oligosaccharides via HPAEC-PAD and MALDI-TOF which further support the conclusion that MLGs act as elicitors (Figure 16, Figure 17). The immune responses were elicited with MLG concentrations of 10 µg ml^{-1} or 100 µg ml^{-1} which is in accordance or even lower to the amounts used to trigger chitin, peptidoglycan or β-1,3-glucan induced immune responses (Miya *et al.*, 2007; Gust *et al.*, 2007; Mélida *et al.*, 2018). To further verify the eliciting activity of MLG oligosaccharides in Arabidopsis, MLG oligosaccharides of varying lengths were generated by hydrolyzing the barley β-1,3;1,4-polymer with the *B. subtilis* lichenase. The hydrolysis products induced a fast calcium response, phosphorylation of MAPK6 and MAPK3 and expression of the defence genes *WRKY33* and *WRKY53* (Figure 19, Figure 20, Figure 21), providing further support that MLGs act as elicitors of immune responses in Arabidopsis.

MLGs are present in the cell walls of monocots and evolutionarily older plant lineages such as brown algae (Salmeán *et al.*, 2017), liverworts (Popper and Fry, 2003) and *Equisetum* spp. (Fry *et al.*, 2008; Sørensen *et al.*, 2008), but are absent from Arabidopsis leaves (Zablackis *et al.*, 1995). Thus, MLGs cannot act as DAMP in Arabidopsis. In the fungal kingdom, MLGs have been identified in the human pathogen *A. fumigatus* as well as in the plant pathogenic fungus *R. commune* (Pettolino *et al.*, 2009; Samar *et al.*, 2015). Furthermore, MLGs have been identified as exopolysaccharide of the bacterial species *S. meliloti,* which is an endosymbiont of *Medicago sativa*. The exopolysaccharide was shown to be important for root attachment but not nodulation (Pérez-Mendoza *et al.*, 2015). The structure of the β-1,3;1,4-polymer differs between the fungal and bacterial species. While the fungal MLG polymer consists of cellotriose units connected via β-1,3-linkages with only small amounts of cellotetraose units, the bacterial MLG consists of repeating units of β-1,3 and β-1,4 linkages (Pettolino *et al.*, 2009;

Pérez-Mendoza *et al.*, 2015). Only the structure of the MLG trisaccharide used in this study resembles the structure of the bacterial MLG, while the structure of the MLG trisaccharide, MLG tetrasaccharide and longer MLG oligosaccharides generated during hydrolysis of the barley β-1,3;1,4-polymer is identical to the MLG structure found in *R. commune*. This suggests that MLG oligosaccharides might act as fungal MAMP in Arabidopsis. As only MLG oligosaccharides but not the β-1,3;1,4-polymer induced immune responses (Figure 19, Figure 20, Figure 21), MLG oligosaccharides of variable length have to be released from the polymer likely through the action of β-1,3;1,4-glucanases. During plant-pathogen interactions, genes encoding for chitinases as well as their activity increase. Chitinases hydrolyse chitin present in the fungal cell wall, which results in the generation of chitin oligomers that can be perceived by the plant (Pusztahelyi, 2018). Thus, it is conceivable to postulate that plants may also secrete β-1,3;1,4-glucanases which act on fungal MLG polymers. Glucanases that hydrolyse MLGs are found in GH family 5, 6, 7, 8, 9, 11, 12, 16, 17, 26 and 51. The Arabidopsis genome harbours 13, 26, 33, 51 and 2 gene sequences encoding for enzymes in GH5, GH9, GH16, GH17 and GH51, respectively (Carbohydrate Active Enzymes database, http://www.cazy.org/, Lombard *et al*., 2014). Of these 125 proteins only two GH5 proteins, three GH9 proteins, twelve GH16 proteins, three enzymes categorized as GH17 and one protein designated as GH51 have been characterized (Carbohydrate Active Enzymes database, http://www.cazy.org/, Lombard *et al*., 2014). None of these proteins exhibit β-1,3;1,4-glucanase activity, however, it might still be possible that not yet characterized enzymes belonging to these Arabidopsis GH families are able to hydrolyse fungal MLG polymers and thus are involved in the generation of MLG oligosaccharide MAMPs.

4.2.4 The MLG tetrasaccharide elicits stronger responses than the MLG trisaccharide in Arabidopsis

In this study, MLGs oligosaccharides were shown to robustly induce immune responses in Arabidopsis similar to those of well-characterized MAMPs e.g. fungal chitin and bacterial flg22 (Figure 11, Figure 12, Figure 14, Figure 15, Figure 19, Figure 20, Figure 21). The MLG tetramer as well as the MLG trimer were able to induce immune responses indicating that there is not a minimum length of MLGs required for activity. However, comparing the intensities of the Ca^{2+} influx, activation of MAPK6 and MAPK3 as well as defence gene expression induced by either the MLG tetrasaccharide or the MLG trisaccharide in Arabidopsis, it became evident that the tetramer triggered stronger responses than the trimer (Figure 11 A and C, Figure 12, Figure 14 A and C, Figure 15). The observation that longer oligosaccharides may have a higher MAMP activity is in line with previous studies for the carbohydrate MAMP chitin and the cell-wall derived DAMP OGs. In addition to polymeric chitin, chitin oligomers were shown to function as MAMPs. However, chitin tri- and tetramers were less effective in triggering immune responses than the chitin pentamer or longer chitin oligosaccharides (Petutschnig *et al.*, 2010). Furthermore, treatment of Arabidopsis with trimeric OGs lead to activation of MAPK as well as expression of defence genes, but these responses were less

pronounced than the responses induced by a mixture of long OGs (Davidsson *et al.*, 2017). One explanation for the weaker responses upon trimer treatment could be that the putative MLG receptor has a higher binding affinity for the MLG tetrasaccharide than for the trimer. It was previously shown that phosphorylation of CERK1 is required for the induction of immune responses. Chitin oligomers that were able to trigger CERK1 phosphorylation comparable to the phosphorylation induced by polymeric chitin were also able to activate the generation of ROS and activation of MAPK, while chitin oligomers that induced less phosphorylation did not trigger immune responses (Petutschnig *et al.*, 2010). A similar scenario might be possible for MLG perception. It might be possible that upon MLG perception, the respective receptor or the co-receptor are phosphorylated. The phosphorylation upon binding of the MLG trimer or the MLG tetramer might lead to an effective phosphorylation, albeit it might be less pronounced upon MLG trimer perception and thus resulting in a weaker response compared to the MLG tetramer. Furthermore, it could also be possible that due to a lower binding affinity of the receptor to the MLG trimer less receptor molecules are phosphorylated resulting in a weaker response. Previously, a dimerization model or “sandwich-like” dimerization for CERK1 and *Os*CEBiP was proposed in which one chitin oligosaccharide is bound to two CERK1 or two *Os*CEBiP molecules leading to the crosslinking of the two receptor molecules (Liu *et al.*, 2012b; Hayafune *et al.*, 2014). However, the formation of a stable complex required ligands of a minimum length of seven residues, while shorter chains lead to the formation of less-stable complexes (Liu *et al.*, 2012b; Hayafune *et al.*, 2014). Similarly, the putative MLG receptor may form a dimer upon cross-ligand binding. The complex may be formed upon MLG tetramer and MLG trimer perception but may be less stable upon treatment with the MLG trimer resulting in a reduced response in comparison to the MLG tetramer. To summarize, the data for chitin perception and signaling suggest that dimerization and phosphorylation are important for the induction and strength of the triggered immune responses and depend on the length of the elicitor. Similarly, these factors might also be important determinants for the amplitude and timing of MLG-induced responses. However, it remains to be shown whether these factors are determinants of the induction and amplitude of MLG triggered responses.

4.2.5 The amplitude and timing of MLG-triggered responses in Arabidopsis differs from chitin- and flg22-induced responses

4.2.5.1 The calcium peak upon MLG elicitation occurs faster compared to chitin- and flg22-triggered calcium responses

MLG treatment resulted in a rapid and transient calcium response. The shape of the MLG-induced Ca^{2+} signature was similar to the calcium response upon flg22 or chitin treatment but the peak occurred faster. Additionally, the calcium response induced by the MLG tri- and tetrasaccharide was less pronounced in comparison to flg22 and chitin, while the calcium spike in response to longer MLG oligosaccharides was higher than the chitin-induced calcium influx (Figure 11 A, Figure 14 A, Figure 19). This observation may indicate that either the concentration of MLG tri- or tetrasaccharides was not sufficient to induce the maximum calcium response or that longer MLG oligosaccharides are more

efficient elicitors than shorter MLG oligosaccharides. This together with the finding that the timing of the MLG-induced calcium response is different from the chitin- and flg22-induced calcium spike supports the idea that the nature and efficiency of a stimulus perceived by the cell determines the calcium response including e.g. the amplitude, duration and frequency (Aldon *et al.*, 2018). Although different MAMPs induce similar responses, these responses differ qualitatively and quantitatively. It has been proposed that the amplitude as well as the timing of the calcium response determine the outcome of MAMP treatment, although the exact mechanism is currently still unknown (Seybold *et al.*, 2014). It is therefore possible that the amplitude and kinetic differences of calcium signatures might result in qualitative and quantitative differences between distinct immune responses such as ROS generation or transcriptional reprogramming triggered by MLGs and the MAMPs chitin and flg22.

4.2.5.2 MLG perception leads to activation of MAPK6 and MAPK3

Notably, treatment of Arabidopsis with MLG oligosaccharides resulted in the activation of MAPK6 and MAPK3 but not in the phosphorylation of MAPK4 (Figure 11 C, Figure 14 C, Figure 20). This is in contrast to results obtained for the MAMPs flg22 and chitin which trigger the activation of MAPK6, MAPK3 and MAPK4 (Figure 11 C, Figure 14 C, Figure 20). Plant MAPK cascades contribute to plant immune signaling and consist of three layers including a MAP kinase kinase kinase (MAP3K, MAPKKK or MEKK), a MAPK kinase kinase (MAP2K or MKK) and a MAP kinase (MAPK) (Rasmussen *et al.*, 2012). Two cascades involved in plant immunity have been identified and well-characterized in Arabidopsis: 1) MAPKKK3/5-MKK4/5-MAPK3/6 and 2) MEKK1-MKK1/2-MPK4 (Devendrakumar *et al.*, 2018). MAPK3, MAPK6 and MAPK4 exhibit different roles in plant defence responses. MAPK3 and MAPK6 are implicated in stomatal immunity and the biosynthesis of the secondary metabolites indole glucosinolates which upon enzymatic degradation releases biologically active compounds (Piasecka *et al.*, 2015; Devendrakumar *et al.*, 2018). Furthermore, biosynthesis of the phytohormone ethylene as well as of the antimicrobial compound camalexin is activated by MAPK3 and MAPK6 through the transcription factor WRKY33 (Rasmussen *et al.*, 2012; Devendrakumar *et al.*, 2018). MAPK4 is implicated in positive as well as negative regulation of flg22-responsive genes (Frei dit Frey *et al.*, 2014; Li *et al.*, 2015). Additionally, MAPK4 is also involved in jasmonic acid-mediated resistance as MAPK4 has a negative impact on salicylic acid accumulation (Petersen *et al.*, 2000; Brodersen *et al.*, 2006; Berriri *et al.*, 2012). The observation that MAPK4 is not phosphorylated upon MLG perception might indicate that genes regulated by MAPK4 are not affected and therefore not involved in response to MLGs. To test whether the transcriptional reprogramming differs following MLG, flg22 or chitin perception, RNAseq analysis or microarray experiments could be performed on Arabidopsis seedlings treated with MLG oligosaccharides, chitin or flg22.

4.2.5.3 Activation of MAPKs and upregulation of *WRKY33* and *WRKY53* was less induced upon MLG treatment than upon chitin or flg22 elicitation

This study showed that in comparison to MAPK activation and transcriptional upregulation in response to the MAMPs chitin and flg22, the activation of MAPK as well as the up-regulation of the transcription of the two defence genes *WRKY33* and *WRKY53* was less induced upon MLG perception (Figure 11 A, Figure 12, Figure 14 C, Figure 15, Figure 20, Figure 21). One explanation could be that the MLG oligosaccharide concentration was not sufficient to induce the maximum induction of gene transcription and MAPK phosphorylation. Alternatively, MLGs might be less efficient MAMPs compared to chitin and flg22. Previous studies have shown that a high number of genes are commonly upregulated upon MAMP treatment by flg22, elf18 or fungal chitin, however, the timing as well as the amplitude of the upregulation was different depending on the MAMP (Zipfel *et al.*, 2006; Gust *et al.*, 2007; Wan *et al.*, 2008a; Li *et al.*, 2016). The transcription of defence genes is controlled by MAPK activation and Ca^{2+}-binding transcription factors that perceive changes in the intracellular Ca^{2+} concentration (Seybold *et al.*, 2014). Thus, the lower transcriptional upregulation of *WRKY33* and *WRKY53* upon MLG treatment could be the result of the different timing and amplitude of the calcium response and MAPK activation, reinforcing the scenario already described above. More specifically, the activity as well as the transcription of WRKY33 is regulated through MAPK3 and MAPK6. The transcription factor WRKY33 is phosphorylated and thereby activated by MAPK3 and MAPK6. Phosphorylated WRKY33 can induce the expression of camalexin biosynthesis genes but also of itself by binding to its own promoter (Mao *et al.*, 2011). The reduced phosphorylation status of MAPK6 and MAPK3 upon MLG perception might in turn result in a reduced number of phosphorylated WRKY33 and therefore in a lower transcript abundance of *WRKY33* upon MLG treatment in comparison to transcript levels upon chitin or flg22 treatment. Furthermore, WRKY33 is found in a complex with MAPK4 and the MAPK4 substrate 1 (MKS1). Upon MAPK4 phosphorylation, WRKY33 is released and can be phosphorylated by MAPK3 and MAPK6 (Andreasson *et al.*, 2005; Qiu *et al.*, 2008). MLG oligosaccharide perception did not result in a detectable phosphorylation of MAPK4 while chitin and flg22 treatment induced activation of MAPK4 (Figure 11 C, Figure 14 C, Figure 20). Thus, no or only a low number of WRKY33 molecules might be released from the complex resulting in a lower induction of *WRKY33* upon recognition of MLGs in comparison to chitin or flg22.

In conclusion, the data from the literature indicate that the calcium signature as well as the activation of specific MAPKs and the respective downstream components are important determinants of the transcriptional reprogramming. A valuable approach to test whether the transcriptional reprogramming differs after MLG oligosaccharide, chitin or flg22 treatment, RNAseq analysis of seedlings upon elicitor treatment could be performed.

4.2.5.4 MLG oligosaccharides treatment does not influence seedling growth

The seedling growth inhibition represents a defence response that occurs within days and was previously observed for seedlings growing in the presence of flg22 or elf18 (Gómez-Gómez and Boller, 2000; Zipfel *et al.*, 2006; Boller and Felix, 2009). To test whether MLG oligosaccharide treatment inhibits seedling growth, 5 day old seedlings were grown for 8 days in medium containing MLG oligosaccharides. However, the growth of Arabidopsis seedlings in presence of MLG oligosaccharides was not affected (Figure 22). This finding is in contrast to previous studies. The proteinaceous MAMPs flg22 and elf18 as well as the carbohydrate DAMP OGs were shown to inhibit seedling growth (Gómez-Gómez and Boller, 2000; Zipfel *et al.*, 2006; Davidsson *et al.*, 2017). On the opposite chitin dimers, trimers and tetramers as well as cellobiose were shown to promote seedling growth (Winkler *et al.*, 2017; de Azevedo Souza *et al.*, 2017). Possible explanations for this outcome could be that either the used MLG concentration was not sufficient to affect seedling growth positively or negatively and/or that the MLG oligosaccharides are not as efficient MAMPs. This result indicates that MLG oligosaccharides have no impact on seedling growth.

4.2.6 Reverse genetics analyses reveal that so far unknown molecular components govern MLG perception in Arabidopsis

The fast initiation of defence responses to MLG oligosaccharides suggests that MLG oligosaccharides are perceived at the cell surface as observed for chitin, flg22 and elf18. To identify molecular components involved in MLG perception, a reverse genetic screen was conducted in this study. Therefore, the MAPK activation upon MLG perception was analysed in multiple potentially involved MAMP/DAMP receptor and signaling mutants. The absence or reduction of MAPK phosphorylation in a mutant would indicate the involvement of the respective component in MLG perception. LysM-domain containing RLKs and RLPs are involved in the recognition of oligosaccharide MAMPs including β-1,3-glucan (Miya *et al.*, 2007; Petutschnig *et al.*, 2010; Willmann *et al.*, 2011; Mélida *et al.*, 2018) and represent potential components of the MLG perception system. However, MLG induced MAPK activation in *cerk1*-2, *lyk5*-2 *lyk4*-1, *lym2*-1, *lym2*-4, *lyk2*-1 and *lyt1*-1 was as strong as in Col-0 indicating that these LysM-RLKs and LysM-RLPs are not required for MLG signaling (Figure 23). Furthermore, the LRR-RLKs FLS2 and EFR as well as the two co-receptor LRR-RLKs BAK1 and SOBIR1 were tested for their involvement in MLG perception. The MAPK activation upon MLG treatment in the respective mutants was neither compromised nor delayed compared to Col-0 suggesting that the tested LRR-RLKs are dispensable for MLG perception (Figure 24, Figure 25). Taken together, these data show that receptors and co-receptors that were already described to be involved in PTI signaling are not required for MLG perception. This suggests that MLG perception involves yet to be identified components. The Arabidopsis genome encodes for over 600 RLKs and RLPs that might function as PRR or co-receptor in plant immunity, however, the ligands for only a few of these potential PRRs have been identified (Shiu and Bleecker, 2003; Macho and Zipfel, 2014).

Thus, it is very likely that yet uncharacterized RLKs and RLPs mediate MLG perception and subsequent signaling.
Additionally, a forward genetic screen was performed to identify MAMP-sensitive and MAMP-insensitive *A. thaliana* ecotypes which could be used to identify molecular components involved in MLG perception and subsequent signal transduction. MAPK phosphorylation was observed in all 127 tested accessions suggesting that these ecotypes harbour the signaling machinery required to perceive MLGs and induction of immune responses (Figure 26, Figure S21, Figure S22, Figure S23). It also indicates that the required molecular components are evolutionary conserved among the tested accessions.

4.2.7 Conclusion

In the second part of this study, novel cell-wall derived DAMPs were identified by testing the ability of multiple poly- and oligosaccharides to induce immune responses. In agreement with studies published during the course of this project, cellohexaose as well as β-1,3-glucan oligosaccharides were shown to act as elicitors of immune responses. Interestingly, MLG oligosaccharide treatment induced immune responses in the dicot model plant Arabidopsis and the monocot barley similar to defence responses triggered by other MAMPs or DAMPs. MLGs are not abundant cell wall components in Arabidopsis but are present in monocot grasses, including barley, as well as the fungal plant pathogen *R. commune*, suggesting that MLGs function in a plant species-specific manner as DAMP or MAMP (or both). So far, neither a reverse genetic screen nor a forward genetic screen revealed molecular components required for MLG perception and signal transduction. This suggests that novel components that have not been identified yet are required for MLG perception and signaling. The involvement of new components might explain the differences in the amplitude and timing of MLG-induced and chitin- or flg22-induced responses.

4.2.8 Outlook

It was demonstrated in this study that over 100 different Arabidopsis accessions and barley perceive MLGs leading to the subsequent activation of immune responses. In future studies, more monocot species such as *Brachypodium distachyon* or *O. sativa* and dicot species such as *Medicago truncatula* or poplar could be tested for their ability to perceive MLG oligosaccharides or the β-1,3;1,4-polymer. Furthermore, it could be tested whether immune responses are induced in evolutionary older plant lineages such as mosses e.g. *Marchantia polymorpha* or *Physcomitrella patens*, horsetails e.g. *Equisetum* spp. or ferns e.g. *Ceratopteris richardii* upon MLG elicitation. This could answer the question whether the MLG perception system is evolutionary conserved or whether it evolved independently in several plant species.

The identification and characterization of RLKs and RLPs involved in MLG signaling in Arabidopsis represents another very interesting subject for further analysis. The RLCK BIK1 is implicated in immune signaling as BIK1 interacts with FLS2, EFR, CERK1 and PEPRs (Tang *et al.*, 2017). Thus, it might be possible that BIK1 does play a role in MLG signaling. To address the involvement of BIK1 in MLG signalling, MLG-triggered MAPK activation could be analysed in BIK1 mutants. Alternatively, a second forward genetic screen could be conducted. Therefore, wild-type Col-0 or Col-0 aequorin seeds could be mutagenized and screened for mutant plants that are impaired in MLG-induced MAPK activation or Ca^{2+} response, respectively. Mutant plants that are insensitive to MLGs can be screened for mutations in potential components required for MLG perception. This strategy has already been successfully exploited in the past to identify the *FLS2* gene (Gómez-Gómez and Boller, 2000).

Analysis of the cell walls of the two ascomycete fungi *A. fumigatus* and *R. commune* revealed the presence of MLGs. Furthermore, mycelial morphology of three plant pathogenic fungi was deconstructed upon treatment with a bacterial β-1,3;1,4-glucanase suggesting that they may contain MLGs (Xu *et al*., 2016). These data indicate that MLGs might be present in the cell wall of further fungi which would support the hypothesis that MLGs act as MAMPs. To address whether MLGs are abundant cell wall components of other fungi, the cell wall composition of further plant-pathogenic fungi could be analysed by immunohistological and enzymatic analysis. A β-1,3;1,4-glucan specific antibody could be used to label β-1,3;1,4-glucans that might be present in the tested fungal cell walls. Furthermore, cell wall preparations could be prepared from the respective fungi and be subjected to enzymatic hydrolysis with a lichenase. The resulting hydrolysates could be tested via TLC and/or HPAEC-PAD for the presence of MLG oligosaccharides.

So far, it has not been elucidated how elicitor active MLG oligosaccharides might be generated from the fungal cell wall. In soybean, the release of β-1,3-glucan oligosaccharides has been shown to be facilitated by the action of β-1,3-glucanases present in the secretome of soybean (Keen and Yoshikawa, 1983). Similarly, the secretome of Arabidopsis and barley could be analysed for the presence of β-1,3;1,4-glucanases. The abundance of β-1,3;1,4-glucanases in the secretome represents a first hint that MLG oligosaccharides might be generated upon hydrolysis of the fungal cell wall by plant of β-1,3;1,4-glucanases. Additionally, the potentially identified β-1,3;1,4-glucanases could be functionally characterized to verify their mode of action.

Overall, the proposed future analysis would provide novel insights into generation and perception of MLG oligosaccharides and might reveal yet unidentified molecular components involved in plant immunity. Furthermore, such analyses may reveal that MLGs are abundant cell wall components in more fungal species than previously thought.

5 References

Albert, I., Böhm, H., Albert, M., Feiler, C.E., Imkampe, J., Wallmeroth, N., Brancato, C., Raaymakers, T.M., Oome, S., Zhang, H., Krol, E., Grefen, C., Gust, A.A., Chai, J., Hedrich, R., Van den Ackerveken, G. and Nürnberger, T. (2015) An RLP23-SOBIR-BAK1 complex mediates NLP-triggered immunity. *Nature Plants*, **1**, 15140.

Aldon, D., Mbengue, M., Mazars, C. and Galaud, J.P. (2018) Calcium signalling in plant biotic interactions. *Int. J. Mol. Sci.*, **19**, 1–19.

Andreasson, E., Jenkins, T., Brodersen, P., Thorgrimsen, S., Petersen, N.H.T., Zhu, S., Qiu, J.-L., Micheelsen, P., Rocher, A., Petersen, M., Newman, M.-A., Nielsen, H.B., Hirt, H., Somssich, I., Mattson, O. and Mundy, J. (2005) The MAP kinase substrate MKS1 is a regulator of plant defense responses. *EMBO J.*, **24**, 2579–2589.

Antolín-Llovera, M., Petutsching, E.K., Ried, M.K., Lipka, V., Nürnberger, T., Robatzek, S. and Parniske, M. (2014) Knowing your friends and foes - plant receptor-like kinases as initiators of symbiosis or defence. *New Phytol.*, **204**, 791–802.

Ao, Y., Li, Z., Feng, D., Xiong, J.L., Liu, J., Li, J.-F., Wang, M., Wang, J., Liu, B. and Wang, H..B. (2014) OsCERK1 and OsRLCK176 play important roles in peptidoglycan and chitin signaling in rice innate immunity. *Plant J.*, **80**, 1072–1084.

Ardèvol, A. and Rovira, C. (2015) Reaction Mechanisms in Carbohydrate-Active Enzymes: Glycoside Hydrolases and Glycosyltransferases. Insights from ab Initio Quantum Mechanics/Molecular Mechanics Dynamic Simulations. *J. Am. Chem. Soc.*, **137**, 7528–7547.

Aspeborg, H., Coutinho, P.M., Wang, Y., Brumer, H. and Henrissat, B. (2012) Evolution, substrate specificity and subfamily classification of glycoside hydrolase family 5 (GH5). *BMC Evol. Biol.*, **12**, 186. Available at: BMC Evolutionary Biology.

Atmodjo, M.A., Hao, Z. and Mohnen, D. (2013) Evolving Views of Pectin Biosynthesis. *Annu. Rev. Plant Biol.*, **64**, 747–779.

Azevedo Souza, C. de, Li, S., Lin, A.Z., Boutrot, F., Grossmann, G., Zipfel, C. and Somerville, S.C. (2017) Cellulose-derived oligomers act as damage-associated molecular patterns and trigger defense-like responses. *Plant Physiol.*, **173**, 2383–2398.

Aziz, A., Poinssot, B., Daire, X., Adrian, M., Bézier, A., Lambert, B., Joubert, J.M. and Pugin, A. (2003) Laminarin Elicits Defense Responses in Grapevine and Induces Protection Against Botrytis cinerea and Plasmopara viticola. *Mol. Plant-Microbe Interact.*, **16**, 1118–1128.

Bacete, L., Mélida, H., Miedes, E. and Molina, A. (2018) Plant cell wall-mediated immunity: cell wall changes trigger disease resistance responses. *Plant J.*, **93**, 614–636.

Balasubramanian, V., Vashisht, D., Cletus, J. and Sakthivel, N. (2012) Plant β-1,3-glucanases: Their biological functions and transgenic expression against phytopathogenic fungi. *Biotechnol. Lett.*, **34**, 1983–1990.

Baldrian, P. and Valášková, V. (2008) Degradation of cellulose by basidiomycetous fungi. *FEMS Microbiol. Rev.*, **32**, 501–521.

Bartels, S. and Boller, T. (2015) Quo vadis, Pep? Plant elicitor peptides at the crossroads of immunity, stress, and development. *J. Exp. Bot.*, **66**, 5183–5193.

Bartels, S., Lori, M., Mbengue, M., Verk, M. Van, Klauser, D., Hander, T., Böni, R., Robatzek, S. and Boller, T. (2013) The family of peps and their precursors in Arabidopsis: Differential expression and localization but similar induction of pattern-Triggered immune responses. *J. Exp.*

Bot., **64**, 5309–5321.

Bellincampi, D., Cervone, F. and Lionetti, V. (2014) Plant cell wall dynamics and wall-related susceptibility in plant-pathogen interactions. *Front. Plant Sci.*, **5**, 1–8. Available at: http://journal.frontiersin.org/article/10.3389/fpls.2014.00228/abstract.

Berriri, S., Garcia, A.V., dit Frey, N.F., Rozhon, W., Pateyron, S., Leonhardt, N., Montillet, J.-L., Leung, J., Hirt, H. and Colcombet, J. (2012) Constitutively active mitogen-activated protein kinase versions reveal functions of Arabidopsis MPK4 in pathogen defense signaling. *Plant Cell*, **24**, 4281–4293.

Bi, G., Liebrand, T.W.H., Cordewener, J.H.G., America, A.H.P., Xu, X. and Joosten, M.H.A.J. (2014) Arabidopsis thaliana receptor-like protein At RLP23 associates with the receptor-like kinase At SOBIR1. Plant Signaling and Behavior, 9:e27937.

Bigeard, J., Colcombet, J. and Hirt, H. (2015) Signaling mechanisms in pattern-triggered immunity (PTI). *Mol. Plant*, **8**, 521–539. Available at: http://dx.doi.org/10.1016/j.molp.2014.12.022.

Block, A., Guangyong, L., Fu, Z.Q., and Alfano, J.R. (2008) Phytopathogen type III effector weaponry and their plant targets. *Curr Opin Plant Biol*., **11**(4), 369-403.

Boller, T. and Felix, G. (2009) A Renaissance of Elicitors: Perception of Microbe-Associated Molecular Patterns and Danger Signals by Pattern-Recognition Receptors. *Annu. Rev. Plant Biol.*, **60**, 379–406.

Bradford, M.M., (1976) A rapid and sensitive method for the quantification of microgram quantities of protein utilizing the principle of protein-dye binding. *Analytical Biochemistry*, **72**, 248-254.

Bretthauer, R.K. and Castellino, F.J. (1999) Glycosylation of Pichia pastoris-derived proteins. *Biotechnol. Appl. Biochem.*, **30**, 193–200.

Brink, J. Van Den and Vries, R.P. De (2011) Fungal enzyme sets for plant polysaccharide degradation. *Appl. Microbiol. Biotechnol.*, **91**, 1477–1492.

Brodersen, P., Petersen, M., Nielsen, H.B., Zhu, S., Newman, M.A., Shokat, K.M., Rietz, S., Parker, J. and Mundy, J. (2006) Arabidopsis MAP kinase 4 regulates salicylic acid- and jasmonic acid/ethylene-dependent responses via EDS1 and PAD4. *Plant J.*, **47**, 532–546.

Brutus, A., Sicilia, F., Macone, A., Cervone, F. and Lorenzo, G. De (2010) A domain swap approach reveals a role of the plant wall-associated kinase 1 (WAK1) as a receptor of oligogalacturonides. *Proc. Natl. Acad. Sci. U. S. A.*, **107**, 9452–9457.

Burton, R.A., Wilson, S.M., Hrmova, M., Harvey, A.J., Shirley, N.J., Medhurst, A., Stone, B.A., Newbigin, E.J., Bacic, A. and Fincher, G.B. (2006) Cellulose Synthase – Like CslF Genes Mediate Synthesis of Cell Wall (13;1,4)-β-D-glucans. *Science,* **311**(5769), 1940–1942.

Burton, R.A. and Fincher, G.B. (2009) (1,3;1,4)-β-D-glucans in cell walls of the poaceae, lower plants, and fungi: A tale of two linkages. *Mol. Plant*, **2**, 873–882. Available at: http://dx.doi.org/10.1093/mp/ssp063.

Burton, R.A. and Fincher, G.B. (2014) Evolution and development of cell walls in cereal grains. *Front. Plant Sci.*, **5**, 1–15.

Burton, R.A., Gidley, M.J. and Fincher, G.B. (2010) Heterogeneity in the chemistry, structure and function of plant cell walls. *Nat. Chem. Biol.*, **6**, 724–732. Available at: http://dx.doi.org/10.1038/nchembio.439.

Cabrera, J.C., Boland, A., Messiaen, J., Cambier, P. and Cutsem, P. Van (2008) Egg box conformation of oligogalacturonides: The time-dependent stabilization of the elicitor-active

conformation increases its biological activity. *Glycobiology*, **18**, 473–482.

Caffall, K.H. and Mohnen, D. (2009) The structure, function, and biosynthesis of plant cell wall pectic polysaccharides. *Carbohydr. Res.*, **344**, 1879–1900. Available at: http://dx.doi.org/10.1016/j.carres.2009.05.021.

Cao, Y., Liang, Y., Tanaka, K., Nguyen, C.T., Jedrzejczak, R.P., Joachimiak, A. and Stacey, G. (2014) The kinase LYK5 is a major chitin receptor in Arabidopsis and forms a chitin-induced complex with related kinase CERK1. *Elife*, **3:e03766**.

Chang, X., Xu, B., Bai, Y., Luo, H., Ma, R., Shi, P. and Yao, B. (2017) Role of N-linked glycosylation in the enzymatic properties of a thermophilic GH 10 xylanase from Aspergillus fumigatus expressed in Pichia pastoris. *PLoS One*, **12**, 1–13.

Chatterjee, S., Chaudhury, S., McShan, A.C., Kaur, K., and De Guzman, R.N. (2013) Structure and Biophysics of Type III Secretion in Bacteria. *Biochemistry*, **52**(15), 2508-2517.

Chen, H., Li, X.L. and Ljungdahl, L.G. (1997) Sequencing of a 1,3-1,4-β-D-glucanase (lichenase) from the anaerobic fungus Orpinomyces strain PC-2: Properties of the enzyme expressed in Escherichia coli and evidence that the gene has a bacterial origin. *J. Bacteriol.*, **179**, 6028–6034.

Chen, X.Y. and Kim, J.Y. (2009) Callose synthesis in higher plants. *Plant Signal. Behav.*, **4**, 489–492.

Chinchilla, D., Bauer, Z., Regenass, M., Boller, T. and Felix, G. (2006) The Arabidopsis receptor kinase FLS2 binds flg22 and determines the specificity of flagellin perception. *Plant Cell*, **18**, 465–476.

Chinchilla, D., Zipfel, C., Robatzek, S., Kemmerling, B., Nürnberger, T., Jones, J.D.G., Felix, G. and Boller, T. (2007) A flagellin-induced complex of the receptor FLS2 and BAK1 initiates plant defence. *Nature*, **448**, 497–500.

Chisholm, S.T., Coaker, G., Day, B. and Staskawicz, B.J. (2006) Host-microbe interactions: Shaping the evolution of the plant immune response. *Cell*, **124**, 803–814.

Chomczynski, P. (1993) A reagent for the single-step simultaneous isolation of RNA, DNA and proteins from cell and tissue samples. *Biotechniques*, **15**, 532–537.

Chowdhury, J., Henderson, M., Schweizer, P., Burton, R.A., Fincher, G.B. and Little, A. (2014) Differential accumulation of callose, arabinoxylan and cellulose in nonpenetrated versus penetrated papillae on leaves of barley infected with Blumeria graminis f. sp. hordei. *New Phytol.*, **204**, 650–660.

Christov, L.P. and Prior, B.A. (1993) Esterases of xylan-degrading microorganisms: Production, properties, and significance. *Enzyme Microb. Technol.*, **15**, 460–475.

Claverie, J., Balacey, S., Lemaître-Guillier, C., Brulé, D., Chiltz, A., Granet, L., Noirot, E., Daire, X., Darblade, B., Héloir, M.-C. and Poinssot, B. (2018) The cell wall-derived xyloglucan is a new DAMP triggering plant immunity in vitis vinifera and arabidopsis thaliana. *Front. Plant Sci.*, **871**, 1–14.

Colcombet, J. and Hirt, H. (2008) Arabidopsis MAPKs: A complex signalling network involved in multiple biological processes. *Biochem. J.*, **413**, 217–226.

Corradini, C., Cavazza, A. and Bignardi, C. (2012) High-Performance Anion-Exchange Chromatography Coupled with Pulsed Electrochemical Detection as a Powerful Tool to Evaluate Carbohydrates of Food Interest: Principles and Applications. *Int. J. Carbohydr. Chem.*, **2012**, 1–13.

Cuskin, F., Lowe, E.C., Temple, M.J., Zhu, Y., Cameron, E.A., Pudlo, N.A., Porter, N.T., Urs, K., Thompson, A.J., Cartmell, A., Rogowski, A., Hamilton, B.S., Chen, R., Tolbert, T.J., Piens, K., Bracke, D., Vervecken, W., Hakki, Z., Speciale, G., Munoz-Munoz, J.L., Day, A., Pena, M.J., McLean, R., Suits, M.D., Boraston, A.B., Atherly, T., Ziemer, C.J., Williams, S.J., Davies, G.J., Abbott, D.W., Martens, E.C. and Gilbert, H.J. (2015) Human gut Bacteroidetes can utilize yeast mannan through a selfish mechanism. *Nature*, **517**, 165–169.

Daly, R. and Hearn, M.T.W. (2005) Expression of heterologous proteins in Pichia pastoris: A useful experimental tool in protein engineenring and production. *J. Mol. Recognit.*, **18**, 119–138.

Dangl, J.L., Horvath, D.M. and Staskawicz, B.J. (2013) Pivoting the Plant Immune System. *Science.*, **341**, 745–751.

Davidsson, P., Broberg, M., Kariola, T., Sipari, N., Pirhonen, M. and Palva, E.T. (2017) Short oligogalacturonides induce pathogen resistance-associated gene expression in Arabidopsis thaliana. *BMC Plant Biol.*, **17**, 1–17. Available at: http://dx.doi.org/10.1186/s12870-016-0959-1.

Davies, G. and Henrissat, B. (1995) Structures and mechanisms of glycosyl hydrolases. *Structure*, **3**, 853–859.

Davies, G.J., Wilson, K.S. and Henrissat, B. (1997) Nomenclature for sugar-binding subsites in glycosyl hydrolases [1]. *Biochem. J.*, **321**, 557–559.

Decreux, A. and Messiaen, J. (2005) Wall-associated kinase WAK1 interacts with cell wall pectins in a calcium-induced conformation. *Plant Cell Physiol.*, **46**, 268–278.

Denoux, C., Galletti, R., Mammarella, N., Gopalan, S., Werck, D., Lorenzo, G. De, Ferrari, S., Ausubel, F.M. and Dewdney, J. (2008) Activation of defense response pathways by OGs and Flg22 elicitors in Arabidopsis seedlings. *Mol. Plant*, **1**, 423–445.

Devendrakumar, K.T., Li, X. and Zhang, Y. (2018) MAP kinase signalling: interplays between plant PAMP- and effector-triggered immunity. *Cell. Mol. Life Sci.*, **75**, 1–9. Available at: http://link.springer.com/10.1007/s00018-018-2839-3.

Doblin, M.S., Pettolino, F.A., Wilson, S.M., Campbell, R., Burton, R.A., Fincher, G.B., Newbigin, E. and Bacic, A. (2009) A barley cellulose synthase-like CSLH gene mediates (1,3;1,4)-β-D-glucan synthesis in transgenic Arabidopsis. *Proc. Natl. Acad. Sci. U. S. A.*, **106**, 5996–6001.

Dodds, P.N. and Rathjen, J.P. (2010) Plant immunity: towards an integrated view of plant–pathogen interactions. *Nat. Rev. Genet.*, **11**, 539–548. Available at: http://www.nature.com/doifinder/10.1038/nrg2812.

Dong, X., Mindrinos, M., Davis, K.R. and Ausubel, F.M. (1991) Induction of Arabidopsis defense genes by virulent and avirulent Pseudomonas syringae strains and by a cloned avirulence gene. *Plant Cell*, **3**, 61–72.

Doxey, A.C., Yaish, M.W.F., Moffatt, B.A., Griffith, M. and McConkey, B.J. (2007) Functional divergence in the Arabidopsis β-1,3-glucanase gene family inferred by phylogenetic reconstruction of expression states. *Mol. Biol. Evol.*, **24**, 1045–1055.

Droillard, M.J., Boudsocq, M., Barbier-Brygoo, H. and Laurière, C. (2002) Different protein kinase families are activated by osmotic stresses in Arabidopsis thaliana cell suspensions: Involvement of the MAP kinases AtMPK3 and AtMPK6. *FEBS Lett.*, **527**, 43–50.

Droillard, M.J., Boudsocq, M., Barbier-Brygoo, H. and Laurière, C. (2004) Involvement of MPK4 in osmotic stress response pathways in cell suspensions and plantlets of Arabidopsis thaliana: Activation by hypoosmolarity and negative role in hyperosmolarity tolerance. *FEBS Lett.*, **574**, 42–48.

Eisenthal, R., Danson, M.J. and Hough, D.W. (2007) Catalytic efficiency and kcat/KM: a useful comparator? *Trends Biotechnol.*, **25**, 247–249.

Faulkner, C., Petutschnig, E., Benitez-Alfonso, Y., Beck, M., Robatzek, S., Lipka, V. and Maule, A.J. (2013) LYM2-dependent chitin perception limits molecular flux via plasmodesmata. *Proc. Natl. Acad. Sci. U. S. A.*, **110**, 9166–9170.

Felle, H.H. (2006) Apoplastic pH during low-oxygen stress in barley. *Ann. Bot.*, **98**, 1085–1093.

Ferrari, S., Galletti, R., Denoux, C., Lorenzo, G. De, Ausubel, F.M. and Dewdney, J. (2007) Resistance to Botrytis cinerea induced in Arabidopsis by elicitors is independent of salicylic acid, ethylene, or jasmonate signaling but requires PHYTOALEXIN DEFICIENT3. *Plant Physiol.*, **144**, 367–379.

Ferrari, S., Savatin, D. V., Sicilia, F., Gramegna, G., Cervone, F. and Lorenzo, G. De (2013) Oligogalacturonides: Plant damage-associated molecular patterns and regulators of growth and development. *Front. Plant Sci.*, **4**, 1–9.

Fesel, P.H. and Zuccaro, A. (2016) β-glucan: Crucial component of the fungal cell wall and elusive MAMP in plants. *Fungal Genet. Biol.*, **90**, 53–60. Available at: http://dx.doi.org/10.1016/j.fgb.2015.12.004.

Frei dit Frey, N., Garcia, A.V., Bigeard, J., et al. (2014) Functional analysis of Arabidopsis immune-related MAPKs uncovers a role for MPK3 as negative regulator of inducible defences. *Genome Biol.*, **15**, 1–22.

Fry, S.C., Nesselrode, B.H.W.A., Miller, J.G. and Mewburn, B.R. (2008) Mixed-linkage (1→3,1→4)-β-D-glucan is a major hemicellulose of Equisetum (horsetail) cell walls. *New Phytol.*, **179**, 104–115.

Galletti, R., Denoux, C., Gambetta, S., Dewdney, J., Ausubel, F.M., Lorenzo, G. De and Ferrari, S. (2008) The AtrbohD-mediated oxidative burst elicited by oligogalacturonides in Arabidopsis is dispensable for the activation of defense responses effective against Botrytis cinerea. *Plant Physiol.*, **148**, 1695–1706.

Galletti, R., Ferrari, S. and Lorenzo, G. de (2011) Arabidopsis MPK3 and MPK6 play different roles in basal and oligogalacturonide- or flagellin-induced resistance against Botrytis cinerea. *Plant Physiol.*, **157**, 804–814.

Garron, M.L. and Cygler, M. (2014) Uronic polysaccharide degrading enzymes. *Curr. Opin. Struct. Biol.*, **28**, 87–95. Available at: http://dx.doi.org/10.1016/j.sbi.2014.07.012.

Gastebois, A., Mouyna, I., Simenel, C., Clavaud, C., Coddeville, B., Delepierre, M., Latgé, J.P. and Fontaine, T. (2010) Characterization of a new β(1-3)-glucan branching activity of Aspergillus fumigatus. *J. Biol. Chem.*, **285**, 2386–2396.

Gibson, D.G., Young, L., Chuang, R.Y., Venter, J.C., Hutchison, C.A. and Smith, H.O. (2009) Enzymatic assembly of DNA molecules up to several hundred kilobases. *Nat. Methods*, **6**, 343–345.

Gimenez-Ibanez, S., Ntoukakis, V. and Rathjen, J.P. (2009) The LysM receptor kinase CERK1 mediates bacterial perception in Arabidopsis. *Plant Signal. Behav.*, **4**, 539–541.

Glass, N.L., Schmoll, M., Cate, J.H.D. and Coradetti, S. (2013) Plant Cell Wall Deconstruction by Ascomycete Fungi. *Annu. Rev. Microbiol.*, **67**, 477–498.

Gomes, A.R., Byregowda, S.M., Veeregowda, B.M. and Balamurugan, V. (2016) An Overview of Heterologous Expression Host Systems for the Production of Recombinant Proteins. *Adv. Anim. Vet. Sci.*, **4**, 346–356.

Gómez-Gómez, E., Ruíz-Roldán, M.C., Pietro, A. Di, Roncero, M.I.G. and Hera, C. (2002) Role in pathogenesis of two endo-β-1,4-xylanase genes from the vascular wilt fungus Fusarium oxysporum. *Fungal Genet. Biol.*, **35**, 213–222.

Gómez-Gómez, L. and Boller, T. (2000) FLS2: An LRR receptor-like kinase involved in the perception of the bacterial elicitor flagellin in Arabidopsis. *Mol. Cell*, **5**, 1003–1011.

Gómez-Gómez, L., Felix, G. and Boller, T. (1999) A single locus determines sensitivity to bacterial flagellin in Arabidopsis thaliana. *Plant J.*, **18**, 277–284.

Gonçalves, T.A., Damásio, A.R.L., Segato, F., Alvarez, T.M., Bragatto, J., Brenelli, L.B., Citadini, A.P.S., Murakami, M.T., Roller, R., Paes Leme, A.F., Prade, R.A. and Squina, F.M. (2012) Functional characterization and synergic action of fungal xylanase and arabinofuranosidase for production of xylooligosaccharides. *Bioresour. Technol.*, **119**, 293–299.

Görlach, J.M., Knaap, E. Van Der and Walton, J.D. (1998) Cloning and targeted disruption of MLG1, a gene encoding two of three extracellular mixed-linked glucanases of Cochliobolus carbonum. *Appl. Environ. Microbiol.*, **64**, 385–391.

Grignon, C. and Sentenac, H. (1991) pH and ionic conditions in the apoplast. *Annu. Rev. Plant Physiol. Plant Mol. Biol*, **42**, 103-128.

Grishutin, S., Gusakov, A.V., Dzedzyulya, E.I. and Sinitsyn, A.P. (2006) A lichenase-like family 12 endo-(1→4)-β-glucanase from Aspergillus japonicus: study of the substrate specificity and mode of action on β-glucans in comparison with other glycoside hydrolases. *Carbohydrate Research*, **341**, 218-229.

Gurkan, C. and Ellar, D.J. (2003) Expression in Pichia pastoris and purification of a membrane-acting immunotoxin based on a synthetic gene coding for the Bacillus thuringiensis Cyt2Aa1 toxin. *Protein Expr Purif*, **29**, 103-116.

Gust, A.A. (2015) Peptidoglycan Perception in Plants. *PLoS Pathog.*, **11**, 1–7.

Gust, A.A., Biswas, R., Lenz, H.D., Rauhut, T., Ranf, S., Kemmerling, B., Götz, F., Glawischnig, E., Lee, J., Felix, G. and Nürnberger, T. (2007) Bacteria-derived peptidoglycans constitute pathogen-associated molecular patterns triggering innate immunity in Arabidopsis. *J. Biol. Chem.*, **282**, 32338–32348.

Gust, A.A. and Felix, G. (2014) Receptor like proteins associate with SOBIR1-type of adaptors to form bimolecular receptor kinases. *Curr. Opin. Plant Biol.*, **21**, 104–111. Available at: http://dx.doi.org/10.1016/j.pbi.2014.07.007.

Hacquard, S., Kracher, B., Maekawa, T., Vernaldi, S., Schulze-Lefert, P. and Themaat, E.V.L. Van (2013) Mosaic genome structure of the barley powdery mildew pathogen and conservation of transcriptional programs in divergent hosts. *Proc. Natl. Acad. Sci. U. S. A.*, **110**, 2219–2228.

Ham, K.-S., Kauffmann, S., Albersheim, P. and Darvill, A.G. (1991) Host-Pathogen Interactions XXXIX. A Soybean Pathogenesis-Related Protein with β -1,3-Glucanase Activity Releases Phytoalexin Elicitor-Active Heat-Stable Fragments from Fungal Walls. *Mol. Plant-Microbe Interact.*, **4**, 545.

Hann, D.R. and Rathjen, J.P. (2007) Early events in the pathogenicity of Pseudomonas syringae on Nicotiana benthamiana. *Plant J.*, **49**, 607–618.

Hayafune, M., Berisio, R., Marchetti, R., Silipo, A., Kayama, M., Desaki, Y., Arima, S., Sqegila, F., Ruggiero, A., Tokuyasu, K., Molinaro, A., Kaku, H. and Shibuya, N. (2014) Chitin-induced activation of immune signaling by the rice receptor CEBiP relies on a unique sandwich-type dimerization. *Proc. Natl. Acad. Sci. U. S. A.*, **111**.

Heese, A., Hann, D.R., Gimenez-Ibanez, S., Jones, A.M.E., He, K., Li, J., Schroeder, J.I., Peck, S.C. and Rathjen, J.P. (2007) The receptor-like kinase SERK3/BAK1 is a central regulator of innate immunity in plants. *Proc. Natl. Acad. Sci. U. S. A.*, **104**, 12217–12222.

Henrissat, B. (1991) A classification of glycosyl hydrolases based on amino acid sequence similarities. *Biochem. J.*, **280**, 309–316.

Herscovics, A. (2001) Structure and function of Class I α1,2-mannosidases involved in glycoprotein synthesis and endoplasmic reticulum quality control. *Biochimie*, **83**, 757–762.

Honegger, R. and Haisch, A. (2001) Immunocytochemical localtion of the (1→3) (1→4)-β-glucan lichenin in the lichen-forming ascomycete *Cetraria islandica* (Icelandic moss). *New Phytologist*, **150**, 739-746.

Hosseini, S. and Martinez-Chapa, S.O. (2017) *Fundamentals of MALDI-ToF-MS Analysis*,.

Houston, K., Tucker, M.R., Chowdhury, J., Shirley, N. and Little, A. (2016) The plant cell wall: A complex and dynamic structure as revealed by the responses of genes under stress conditions. *Front. Plant Sci.*, **7**, 1–18.

Hrmova, M. and Fincher, G.B. (1993) Purification and properties of three (1→3)-β-D-glucanase isoenzymes from young leaves of barley (Hordeum vulgare). *Biochem. J.*, **289**, 453–461.

Hrmova, M., Garrett, T.P.J. and Fincher, G.B. (1995) Subsite affinities and disposition of catalytic amino acids in the substrate-binding region of barley 1,3-β-glucanases. Implications in plant-pathogen interactions. *J. Biol. Chem.*, **270**, 14556–14563.

Huecas, S., Villalba, M. and Rodríguez, R. (2001) Ole e 9, a major olive pollen allergen is a 1,3-β-glucanase: Isolation, characterization, amino acid sequence, and tissue specificity. *J. Biol. Chem.*, **276**, 27959–27966.

Huffaker, A., Pearce, G. and Ryan, C.A. (2006) An endogenous peptide signal in Arabidopsis activates components of the innate immune response. *Proc. Natl. Acad. Sci. U. S. A.*, **103**, 10098–10103.

Jacobs, A.K., Lipka, V., Burton, R.A., Panstruga, R., Strizhov, N., Schulze-lefert, P. and Fincher, G.F. (2003) An Arabidopsis Callose Synthase, GSL5, Is Required for Wound and Papillary Callose Formation, *The Plant* Cell., **15**, 2503–2513.

Jehle, A.K., Fürst, U., Lipschis, M., Albert, M. and Felix, G. (2013a) Perception of the novel MAMP eMax from different Xanthomonas species requires the Arabidopsis receptor-like protein ReMAX and the receptor kinase SOBIR. *Plant Signal. Behav.*, **8**, 11–13.

Jehle, A.K., Lipschis, M., Albert, M., Fallahzadeh-Mamaghani, V., Fürst, U., Mueller, K. and Felix, G. (2013b) The receptor-like protein ReMAX of Arabidopsis detects the microbe-associated molecular pattern eMax from Xanthomonas. *Plant Cell*, **25**, 2330–2340.

Jones, J.D.G. and Dangl, J.L. (2006) The plant immune system. *Nature*, 444, 323–329.

Kaku, H., Nishizawa, Y., Ishii-Minami, N., Akimoto-Tomiyama, C., Dohmae, N., Takio, K., Minami, E. and Shibuya, N. (2006) Plant cells recognize chitin fragments for defense signaling through a plasma membrane receptor. *Proc. Natl. Acad. Sci. U. S. A.*, **103**, 11086–11091.

Kamoun, S. (2006) A Catalogue of the Effector Secretome of Plant Pathogenic Oomycetes. *Annu. Rev. Phytopathol.*, **44**, 41–60.

Keegstra, K. (2010) Plant Cell Walls. *Plant Physiol.*, **154**, 483–486.

Keen, N.T. and Yoshikawa, M. (1983) β-1,3-Endoglucanase from Soybean Releases Elicitor-Active Carbohydrates from Fungus Cell Walls. *Plant Physiol.*, **71**, 460–465.

Kessel, A. and Ben-Tal, N. (2018). Enzyme Kinetics in Kessel, A. and Ben-Tal, N., eds**.** Introduction to Proteins: Structure, Function and Motion. Second Edition. Chapman and Hall/CRC.

King, B.C., Waxman, K.D., Nenni, N. V., Walker, L.P., Bergstrom, G.C. and Gibson, D.M. (2011) Arsenal of plant cell wall degrading enzymes reflects host preference among plant pathogenic fungi. *Biotechnol. Biofuels*, **4**, 1–14.

Kishimoto, K., Kouzai, Y., Kaku, H., Shibuya, N., Minami, E. and Nishizawa, Y. (2010) Perception of the chitin oligosaccharides contributes to disease resistance to blast fungus Magnaporthe oryzae in rice. *Plant J.*, **64**, 343–354.

Klarzynski, O., Plesse, B., Joubert, J.M., Yvin, J.C., Kopp, M., Kloareg, B. and Fritig, B. (2000) Linear β-1,3 glucans are elicitors of defense responses in tobacco. *Plant Physiol.*, **124**, 1027–1037.

Koshland, D.E. (1953) Stereochemistry and the Mechanism of Enzymatic Reactions. *Biological Reviews*, **28**, 416-436.

Kouzai, Y., Mochizuki, S., Nakajima, K., Desaki, Y., Hayafune, M., Miyazaki, H., Yokotani, N., Ozawa, K., Minami, E., Kaku, H., Shibuya, N. and Nishizawa, Y. (2014) Targeted gene disruption of OsCERK1 reveals its indispensable role in chitin perception and involvement in the peptidoglycan response and immunity in rice. *Mol. Plant-Microbe Interact.*, **27**, 975–982.

Kouzai, Y., Nakajima, K., Hayafune, M., Ozawa, K., Kaku, H., Shibuya, N., Minami, E. and Nishizawa, Y. (2014) CEBiP is the major chitin oligomer-binding protein in rice and plays a main role in the perception of chitin oligomers. *Plant Mol. Biol.*, **84**, 519–528.

Kover, P.X., Valdar, W., Trakalo, J., Scarcelli, N., Ehrenreich, I.M., Purugganan, M.D., Durrant, C. and Mott, R. (2009) A multiparent advanced generation inter-cross to fine-map quantitative traits in Arabidopsis thaliana. *PLoS Genet.*, **5**:e1000551.

Kubicek, C.P., Starr, T.L. and Glass, N.L. (2014) Plant Cell Wall–Degrading Enzymes and Their Secretion in Plant-Pathogenic Fungi. *Annu. Rev. Phytopathol.*, **52**, 427–451.

Kunze, G., Zipfel, C., Robatzek, S., Niehaus, K., Boller, T. and Felix, G. (2004) The N terminus of bacterial elongation factor Tu elicits innate immunity in Arabidopsis plants. *Plant Cell*, **16**, 3496–3507.

Lagaert, S., Beliën, T. and Volckaert, G. (2009) Plant cell walls: Protecting the barrier from degradation by microbial enzymes. *Semin. Cell Dev. Biol.*, **20**, 1064–1073.

Li, B., Jiang, S., Yu, X., Cheng, C., Chen, S., Cheng, A., Yuan, J.S., Jiang, D., He, P. and Shan, L. (2015) Phosphorylation of trihelix transcriptional repressor ASR3 by MAP KINASE4 negatively regulates Arabidopsis immunity. *Plant Cell*, **27**, 839–856.

Li, B., Meng, X., Shan, L. and He, P. (2016) Transcriptional Regulation of Pattern-Triggered Immunity in Plants. *Cell Host Microbe*, **19**, 641–650.

Li, J., Wen, J., Lease, K.A., Doke, J.T., Tax, F.E. and Walker, J.C. (2002) BAK1, an Arabidopsis LRR receptor-like protein kinase, interacts with BRI1 and modulates brassinosteroid signaling. *Cell*, **110**, 213–222.

Liang, X. and Zhou, J.-M. (2018) Receptor-Like Cytoplasmic Kinases: Central Players in Plant Receptor Kinase–Mediated Signaling. *Annu. Rev. Plant Biol.*, **69**, 267–299.

Liebrand, T.W.H., Berg, G.C.M. Van Den, Zhang, Z., Smit, P., Cordewener, J.H.G., America, A.H.P., Sklenar, J., Jones, A.M.E., Tameling, W.I.L., Robatzek, S., Thomma, B.H.J. and Joosten, M.H.A.J. (2013) Receptor-like kinase SOBIR1/EVR interacts with receptor-like proteins in plant immunity against fungal infection. *Proc. Natl. Acad. Sci. U. S. A.*, **110**, 10010–10015.

Liebrand, T.W.H., Burg, H.A. van den and Joosten, M.H.A.J. (2014) Two for all: Receptor-associated kinases SOBIR1 and BAK1. *Trends Plant Sci.*, **19**, 123–132. Available at: http://dx.doi.org/10.1016/j.tplants.2013.10.003.

Liu, B., Li, J.F., Ao, Y., Qu, J., Li, Z., Su, J., Zhang, Y., Liu, J., Feng, D., Qi, K., He, Y., Wang, J. and Wang, H.-B. (2012a) Lysin motif-containing proteins LYP4 and LYP6 play dual roles in peptidoglycan and chitin perception in rice innate immunity. *Plant Cell*, **24**, 3406–3419.

Liu, T., Liu, Z., Song, C., Hu, Y., Han, Z., She, J., Fan, F., Wang, J., Jin, C., Chang, J., Zhou, J.-M. and Chai, J. (2012b) Chitin-induced dimerization activates a plant immune receptor. *Science.* **336**, 1160–1164.

Liu, Z., Wu, Y., Yang, F., Zhang, Y., Chen, S., Xie, Q., Tian, X. and Zhou, J.M. (2013) BIK1 interacts with PEPRs to mediate ethylene-induced immunity. *Proc. Natl. Acad. Sci. U. S. A.*, **110**, 6205–6210.

Lombard, V., Golaconda Ramulu, H., Drula, E., Coutinho, P.M. and Henrissat, B. (2014) The carbohydrate-active enzymes database (CAZy) in 2013. *Nucleic Acids Res.*, **42**, 490–495.

Lorenzo, G. De and Ferrari, S. (2002) Polygalacturonase-inhibiting proteins in defense against phytopathogenic fungi. *Curr. Opin. Plant Biol.*, **5**, 295–299.

Lovering, A.L., Safadi, S.S. and Strynadka, N.C.J. (2012) Structural Perspective of Peptidoglycan Biosynthesis and Assembly. *Annu. Rev. Biochem.*, **81**, 451–478.

Lu, D., Wu, S., Gao, X., Zhang, Y., Shan, L. and He, P. (2010) A receptor-like cytoplasmic kinase, BIK1, associates with a flagellin receptor complex to initiate plant innate immunity. *Proc. Natl. Acad. Sci. U. S. A.*, **107**, 496–501.

Macho, A.P. and Zipfel, C. (2014a) Plant PRRs and the activation of innate immune signaling. *Mol. Cell*, **54**, 263–272. Available at: http://dx.doi.org/10.1016/j.molcel.2014.03.028.

Macho, A.P. and Zipfel, C. (2015) Targeting of plant pattern recognition receptor-triggered immunity by bacterial type-III secretion system effectors. *Curr. Opin. Microbiol.*, **23**, 14–22. Available at: http://dx.doi.org/10.1016/j.mib.2014.10.009.

Malinovsky, F.G., Fangel, J.U. and Willats, W.G.T. (2014) The role of the cell wall in plant immunity. *Front. Plant Sci.*, **5**, 1–12.

Mao, G., Meng, X., Liu, Y., Zheng, Z., Chen, Z. and Zhang, S. (2011) Phosphorylation of a WRKY transcription factor by two pathogen-responsive MAPKs drives phytoalexin biosynthesis in Arabidopsis. *Plant Cell*, **23**, 1639–1653.

McFarlane, H.E., Döring, A. and Persson, S. (2014) The Cell Biology of Cellulose Synthesis. *Annu. Rev. Plant Biol.*, **65**, 69–94.

McGregor, N., Morar, M., Fenger, T.H., Stogios, P., Lenfant, N., Yin, V., Xu, X., Evdokimova, E., Cui, H., Henrissat, B., Savchenko, A. and Brumer, H. (2016) Structure-function analysis of a mixed-linkage β-glucanase/xyloglucanase from the key ruminal bacteroidetes prevotella bryantii B14. *J. Biol. Chem.*, **291**, 1175–1197.

Mélida, H., Sopeña-Torres, S., Bacete, L., Garrido-Arandia, M., Jordá, L., López, G., Muñoz-Barrios, A., Pacios, L.F. and Molina, A. (2018a) Non-branched β-1,3-glucan oligosaccharides trigger immune responses in Arabidopsis. *Plant J.*, **93**, 34–49.

Michaelis, L. and Menten, M.L. (1913) Die Kinetik der Invertinwirkung. *Biochem. Z.* **49**, 333-369

Michaud, P., Costa, A. Da, Courtois, B. and Courtois, J. (2003) Polysaccharide lyases: Recent developments as biotechnological tools. *Crit. Rev. Biotechnol.*, **23**, 233–266.

Miya, A., Albert, P., Shinya, T., et al. (2007) CERK1, a LysM receptor kinase, is essential for chitin elicitor signaling in Arabidopsis. *Proc. Natl. Acad. Sci. U. S. A.*, **104**, 19613–19618.

Monaghan, J. and Zipfel, C. (2012) Plant pattern recognition receptor complexes at the plasma membrane. *Curr. Opin. Plant Biol.*, **15**, 349–357. Available at: http://dx.doi.org/10.1016/j.pbi.2012.05.006.

Murray, P.G., Grassick, A., Laffey, C.D., Cuffe, M.M., Higgins, T., Savage, A. V., Planas, A. and Tuohy, M.G. (2001) Isolation and characterization of a thermostable endo-β-glucanase active on 1,3-1,4-β-D-glucans from the aerobic fungus Talaromyces emersonii CBS 814.70. *Enzyme Microb. Technol.*, **29**, 90–98.

Muzzarelli RAA (1977) *Chitin*, 1st ed. edn. Oxford ; New York: Pergamon Press.

Nakamura, A.M., Nascimento, A.S. and Polikarpov, I. (2017) Structural diversity of carbohydrate esterases. *Biotechnol. Res. Innov.*, **1**, 35–51. Available at: http://dx.doi.org/10.1016/j.biori.2017.02.001.

Nam, K.H. and Li, J. (2002) BRI1/BAK1, a receptor kinase pair mediating brassinosteroid signaling. *Cell*, **110**, 203–212.

Nguyen, Q.B., Itoh, K., Vu, B. Van, Tosa, Y. and Nakayashiki, H. (2011) Simultaneous silencing of endo-β-1,4 xylanase genes reveals their roles in the virulence of Magnaporthe oryzae. *Mol. Microbiol.*, **81**, 1008–1019.

Nowara, D., Schweizer, P., Gay, A., Lacomme, C., Shaw, J., Ridout, C., Douchkov, D., Hensel, G. and Kumlehn, J. (2010) HIGS: Host-induced gene silencing in the obligate biotrophic fungal pathogen Blumeria graminis. *Plant Cell*, **22**, 3130–3141.

Park, Y.B. and Cosgrove, D.J. (2015) Xyloglucan and its interactions with other components of the growing cell wall. *Plant Cell Physiol.*, **56**, 180–194.

Patova, O.A., Golovchenko, V. V. and Ovodov, Y.S. (2014) Pectic polysaccharides: Structure and properties. *Russ. Chem. Bull.*, **63**, 1901–1924.

Pauly, M., Gille, S., Liu, L., Mansoori, N., Souza, A. de, Schultink, A. and Xiong, G. (2013) Hemicellulose biosynthesis. *Planta*, **238**, 627–642.

Pérez-Mendoza, D., Rodríguez-Carvajal, M.Á., Romero-Jiménez, L., Araujo Farias, G. De, Lloret, J., Gallegos, M.T. and Sanjuán, J. (2015) Novel mixed-linkage β-glucan activated by c-di-GMP in Sinorhizobium meliloti. *Proc. Natl. Acad. Sci. U. S. A.*, **112**, E757–E765.

Petersen, M., Brodersen, P., Naested, H., Andreasson, E., Lindhart, U., Johansen, B., Nielsen, H.B., Lacy, M., Austin, M.J., Parker, J.E., Sharma, S.B., Klessig, D.F., Martienssen, R., Mattson, O., Jensen, B. and Mundy, J. (2000) Arabidopsis MAP kinase 4 negatively regulates systemic acquired resistance. *Cell*, **103**, 1111–1120.

Pettolino, F., Sasaki, I., Turbic, A., Wilson, S.M., Bacic, A., Hrmova, M. and Fincher, G.B. (2009) Hyphal cell walls from the plant pathogen Rhynchosporium secalis contain (1,3/1,6)-β-D-glucans, galacto- and rhamnomannans, (1,3;1,4)-β-D- glucans and chitin. *FEBS J.*, **276**, 4122–4133.

Petutschnig, E.K., Jones, A.M.E., Serazetdinova, L., Lipka, U. and Lipka, V. (2010) The Lysin Motif Receptor-like Kinase (LysM-RLK) CERK1 is a major chitin-binding protein in Arabidopsis

thaliana and subject to chitin-induced phosphorylation. *J. Biol. Chem.*, **285**, 28902–28911.

Peumans, W.J., Barre, A., Derycke, V., Rougé, P., Zhang, W., May, G.D., Delcour, J.A., Leuven, F. Van and Damme, E.J.M. Van (2000) Purification, characterization and structural analysis of an abundant β-1,3-glucanase from banana fruit. *Eur. J. Biochem.*, **267**, 1188–1195.

Piasecka, A., Jedrzejczak-Rey, N. and Bednarek, P. (2015) Secondary metabolites in plant innate immunity: Conserved function of divergent chemicals. *New Phytol.*, **206**, 948–964.

Planas, A. (2000) Bacterial 1,3-1,4-β-glucanases: Structure, function and protein engineering. *Biochim. Biophys. Acta - Protein Struct. Mol. Enzymol.*, **1543**, 361–382.

Plummer, T.H., Elder, J.H., Alexander, S., Phelan, A.W. and Tarentino, A.L. (1984) Demonstration of peptide:N-glycosidase F activity in endo-β-N-acetylglucosaminidase F preparations. *J. Biol. Chem.*, **259**, 10700–10704.

Polizeli, M.L.T.M., Rizzatti, A.C.S., Monti, R., Terenzi, H.F., Jorge, J.A. and Amorim, D.S. (2005) Xylanases from fungi: Properties and industrial applications. *Appl. Microbiol. Biotechnol.*, **67**, 577–591.

Popper, Z.A. and Fry, S.C. (2003) Primary cell wall composition of bryophytes and charophytes. *Ann. Bot.*, **91**, 1–12.

Postel, S. and Kemmerling, B. (2009) Plant systems for recognition of pathogen-associated molecular patterns. *Semin. Cell Dev. Biol.*, **20**, 1025–1031.

Pusztahelyi, T. (2018) Chitin and chitin-related compounds in plant–fungal interactions. *Mycology*, **9**, 189–201. Available at: https://doi.org/10.1080/21501203.2018.1473299.

Qin, Z., Yan, Q., Lei, J., Yang, S., Jiang, Z. and Wu, S. (2015) The first crystal structure of a glycoside hydrolase family 17 β-1,3-glucanosyltransferase displays a unique catalytic cleft. *Acta Crystallogr. Sect. D Biol. Crystallogr.*, **71**, 1714–1724.

Qiu, J.L., Fiil, B.K., Petersen, K., Nielsen, H.B., Botanga, C.J., Thorgrimsen, S., Palma, K., Suarez-Rodriguez, M.C., Lichota, J., Brodersen, P., Grasser, K.D., Mattson, O., Glazebrook, J., Mundy, J. and Petersen, M. (2008) Arabidopsis MAP kinase 4 regulates gene expression through transcription factor release in the nucleus. *EMBO J.*, **27**, 2214–2221.

Ranf, S. Grimmer, J., Pöschl, Y., Pecher, P., Chinchilla, D., Scheel, D. and Lee, J. (2012) Defense-Related Calcium Signaling Mutants Uncovered via a Quantitative High-Throughput Screen in Arabidopsis thaliana. *Molecular Plant*, **5**, 115-130.

Rasmussen, M.W., Roux, M., Petersen, M. and Mundy, J. (2012) MAP kinase cascades in Arabidopsis innate immunity. *Front. Plant Sci.*, **3**, 1–6.

Rayon, C., Lerouge, P. and Faye, L. (1998) The protein N-glycosylation in plants. *J. Exp. Bot.*, **49**, 1463–1472.

Rentel, M.C. and Knight, M.R. (2004) Oxidative stress-induced calcium signaling in Arabidopsis. *Plant Physiol*., **53**, 287-299.

Robatzek, S., Bittel, P., Chinchilla, D., Köchner, P., Felix, G., Shiu, S.H. and Boller, T. (2007) Molecular identification and characterization of the tomato flagellin receptor LeFLS2, an orthologue of Arabidopsis FLS2 exhibiting characteristically different perception specificities. *Plant Mol. Biol.*, **64**, 539–547.

Robinson, P.K. (2015) Enzymes: principles and biotechnological applications. *Essays Biochem.*, **59**, 1–41.

Roulin, S. and Feller, U. (2001) Reversible accumulation of (1→3,1→4)-β-glucan endohydrolase in wheat leaves under sugar depletion. *J. Exp. Bot.*, **52**, 2323–2332.

Roux, M., Schwessinger, B., Albrecht, C., Chinchilla, D., Jones, A., Holton, N., Malinovsky, F.G., Tör, M., de Vries, S. and Zipfel, C. (2011) The Arabidopsis leucine-rich repeat receptor-like kinases BAK1/SERK3 and BKK1/SERK4 are required for innate immunity to hemibiotrophic and biotrophic pathogens. *Plant Cell*, **23**, 2440–2455.

Salmeán, A.A., Duffieux, D., Harholt, J., Qin, F., Michel, G., Czjzek, M., Willats, W.G.T. and Hervé, C. (2017) Insoluble (1 → 3), (1 → 4)-β-Dglucan is a component of cell walls in brown algae (Phaeophyceae) and is masked by alginates in tissues. *Sci. Rep.*, **7**, 1–11.

Samar, D., Kieler, J.B. and Klutts, J.S. (2015) Identification and deletion of Tft1, α predicted glycosyltransferase necessary for cell wall β-1,3;1,4-glucan synthesis in Aspergillus fumigatus. *PLoS One*, **10**, 1–14.

Schagerlöf, H., Nilsson, C., Gorton, L., Tjerneld, F., Stålbrand, H. and Cohen, A. (2009) Use of ^{18}O water and ESI-MS detection in subsite characterisation and investigation of the hydrolytic action of an endoglucanase. *Anal. Bioanal. Chem.*, **394**, 1977–1984.

Scheler, B., Schnepf, V., Galgenmüller, C., Ranf, S. and Hückelhoven, R. (2016) Barley disease susceptibility factor RACB acts in epidermal cell polarity and positioning of the nucleus. *J. Exp. Bot.*, **67**, 3263–3275.

Scheller, H.V. and Ulvskov, P. (2010) Hemicelluloses. *Annu. Rev. Plant Biol.*, **61**, 263–289.

Schultink, A., Liu, L., Zhu, L. and Pauly, M. (2014) Structural diversity and function of xyloglucan sidechain substituents. *Plants*, **3**, 526–542.

Schulze, B., Mentzel, T., Jehle, A.K., Mueller, K., Beeler, S., Boller, T., Felix, G. and Chinchilla, D. (2010) Rapid heteromerization and phosphorylation of ligand-activated plant transmembrane receptors and their associated kinase BAK1. *J. Biol. Chem.*, **285**, 9444–9451.

Schwessinger, B., Roux, M., Kadota, Y., Ntoukakis, V., Sklenar, J., Jones, A. and Zipfel, C. (2011) Phosphorylation-dependent differential regulation of plant growth, cell death, and innate immunity by the regulatory receptor-like kinase BAK1. *PLoS Genet.*, **7**.

Selin, C., Kievit, T.R. de, Belmonte, M.F. and Fernando, W.G.D. (2016) Elucidating the role of effectors in plant-fungal interactions: Progress and challenges. *Front. Microbiol.*, **7**, 1–21.

Seybold, H., Trempel, F., Ranf, S., Scheel, D., Romeis, T. and Lee, J. (2014) Ca^{2+} signalling in plant immune response: From pattern recognition receptors to Ca^{2+} decoding mechanisms. *New Phytol.*, **204**, 782–790.

Sham, A., Moustafa, K., Al-Ameri, S., Al-Azzawi, A., Iratni, R. and AbuQamar, S. (2015) Identification of Arabidopsis candidate genes in response to biotic and abiotic stresses using comparative microarrays. *PLoS One*, **10**, 1–21.

Shimizu, T., Nakano, T., Takamizawa, D., et al. (2010) Two LysM receptor molecules, CEBiP and OsCERK1, cooperatively regulate chitin elicitor signaling in rice. *Plant J.*, **64**, 204–214.

Shinya, T., Motoyama, N., Ikeda, A., Wada, M., Kamiya, K., Hayafune, M., Kaku, H. and Shibuya, N. (2012) Functional characterization of CEBiP and CERK1 homologs in arabidopsis and rice reveals the presence of different chitin receptor systems in plants. *Plant Cell Physiol.*, **53**, 1696–1706.

Shinya, T., Nakagawa, T., Kaku, H. and Shibuya, N. (2015) Chitin-mediated plant-fungal interactions: Catching, hiding and handshaking. *Curr. Opin. Plant Biol.*, **26**, 64–71. Available at: http://dx.doi.org/10.1016/j.pbi.2015.05.032.

Shiu, S.H. and Bleecker, A.B. (2003) Expansion of the receptor-like kinase/Pelle gene family and receptor-like proteins in Arabidopsis. *Plant Physiol.*, **132**, 530–543.

Shoseyov, O., Shani, Z. and Levy, I. (2006) Carbohydrate Binding Modules: Biochemical Properties and Novel Applications. *Microbiol. Mol. Biol. Rev.*, **70**, 283–295.

Silva, L.A. de O. da, Terrasan, C.R.F. and Carmona, E.C. (2015) Purification and characterization of xylanases from Trichoderma inhamatum. *Electron. J. Biotechnol.*, **18**, 307–313. Available at: http://dx.doi.org/10.1016/j.ejbt.2015.06.001.

Sinha, J., Plantz, B.A., Inan, M. and Meagher, M.M. (2005) Causes of proteolytic degradation of secreted recombinant proteins produced in methylotrophic yeast Pichia pastoris: Case study with recombinant ovine interferon-τ. *Biotechnol. Bioeng.*, **89**, 102–112.

Slakeski, N. and Fincher, G.B. (1992) Developmental Regulation of (1->3,1->4)-β-D-Glucanase Gene Expression in Barley. *Plant. Physiol*., **99**, 1226–1231.

Sørensen, I., Pettolino, F.A., Wilson, S.M., Doblin, M.S., Johansen, B., Bacic, A. and Willats, W.G.T. (2008) Mixed-linkage (1 → 3),(1 → 4)-β-D-glucan is not unique to the Poales and is an abundant component of Equisetum arvense cell walls. *Plant J.*, **54**, 510–521.

Spanu, P.D., Abbott, J.C., Amselem, J., et al. (2010) Genome expansion and gene loss in powdery mildew fungi reveal tradeoffs in extreme parasitism. *Science.,* **330**, 1543–1546.

Stephan, A.B., Kunz, H.H., Yang, E. and Schroeder, J.I. (2016) Rapid hyperosmotic-induced Ca^{2+} responses in Arabidopsis thaliana exhibit sensory potentiation and involvement of plastidial KEA transporters. *Proc. Natl. Acad. Sci. U. S. A.*, **113**, E5242–E5249.

Strasser, R. (2016) Plant protein glycosylation. *Glycobiology*, **26**, 926–939.

Sundqvist, G., Stenvall, M., Berglund, H., Ottoson, J. and Brumer, H. (2007) A general and robust method for the quality control of intact proteins using LC-ESI-MS. *Journal of Chromatography*, **852**, 188-194.

Takai, R., Isogai, A., Takayama, S. and Che, F.S. (2008) Analysis of flagellin perception mediated by flg22 receptor OsFLS2 in rice. *Mol. Plant-Microbe Interact.*, **21**, 1635–1642.

Tang, D., Wang, G. and Zhou, J.-M. (2017) Receptor Kinases in Plant-Pathogen Interactions: More Than Pattern Recognition. *Plant Cell*, **29**, 618-637.

Tang, J., Han, Z., Sun, Y., Zhang, H., Gong, X. and Chai, J. (2015) Structural basis for recognition of an endogenous peptide by the plant receptor kinase PEPR1. *Cell Res.*, **25**, 110–120. Available at: http://dx.doi.org/10.1038/cr.2014.161.

Trethewey, J.A.K. and Harris, P.J. (2002) Location of (1 → 3)- and (1 → 3),(1 → 4)-β-D-glucans in vegetative cell walls of barley (Hordeum vulgare) using immunogold labelling. *New Phytol.*, **154**, 347–358.

Uknes, S., Mauch-Mani, B., Moyer, M., et al. (1992) Acquired resistance in arabidopsis. *Plant Cell*, **4**, 645–656.

Underwood, W. (2012) The plant cell wall: A dynamic barrier against pathogen invasion. *Front. Plant Sci.*, **3**, 1–6.

Varrot, A., Schuelein, M., Fruchard, S., Driguez, H. and Davies, G.J. (2001) Atomic resolution structure of endoglucanase Cel5A in complex with methyl 4,4II,4III,4IV-tetrathio-α-cellopentoside hihlights the alternative binding modes targeted by substrate mimics. *Acta Crystallogr Sect D Biol Crystallogr*, **57**(11), 1739-1742.

Viborg, A.H., Terrapon, N., Lombard, V., Michel, G., Czjzek, M., Henrissat, B. and Brumer, H. (2019) A subfamily roadmap for functional glycogenomics of the evolutionarily diverse Glycoside Hydrolase Family 16 (GH16). *J. Biol. Chem.*, **16**, jbc.RA119.010619.

Voigt, C.A. (2014) Callose-mediated resistance to pathogenic intruders in plant defense-related papillae. *Front. Plant Sci.*, **5**, 1–6.

Vuong, T. V. and Wilson, D.B. (2010) Glycoside hydrolases: Catalytic base/nucleophile diversity. *Biotechnol. Bioeng.*, **107**, 195–205.

Wan, J., Tanaka, K., Zhang, X.C., Son, G.H., Brechenmacher, L., Nguyen, T.H.N. and Stacey, G. (2012) LYK4, a lysin motif receptor-like kinase, is important for chitin signaling and plant innate immunity in Arabidopsis. *Plant Physiol.*, **160**, 396–406.

Wan, J., Zhang, X. and Stacey, G. (2008a) Chitin signaling and plant disease resistance. *Mol. Plant Pathol.*, **6**, 831–833.

Wan, J., Zhang, X.C., Neece, D., Ramonell, K.M., Clough, S., Kim, S.Y., Stacey, M.G. and Stacey, G. (2008b) A LysM receptor-like kinase plays a critical role in chitin signaling and fungal resistance in Arabidopsis. *Plant Cell*, **20**, 471–481.

Wang, C., Wang, G., Zhang, C., Zhu, P., Dai, H., Yu, N., He, Z., Xu, L. and Wang, E. (2017) OsCERK1-Mediated Chitin Perception and Immune Signaling Requires Receptor-like Cytoplasmic Kinase 185 to Activate an MAPK Cascade in Rice. *Mol. Plant*, **10**, 619–633. Available at: http://dx.doi.org/10.1016/j.molp.2017.01.006.

Werten, M.W.T., Bosch, T.J. van den, Wind, R.D., Mooibroek, H. and Wolf, F.A. de (1999) High-yield secretion of recombinant gelatins by Pichia pastoris. *Yeast*, **15**, 1087–1096.

Willmann, R., Lajunen, H.M., Erbs, G., Newman, M.-A., Kolb, D., Tsuda, K., Katagiri, F., Fliegmann, J., Bono, J.-J., Cullimore, J.V., Jehle, A.K., Götz, F., Kulik, F., Molinaro, A., Lipka, V., Gust, A.A. and Nürnberger, T. (2011) Arabidopsis lysin-motif proteins LYM1 LYM3 CERK1 mediate bacterial peptidoglycan sensing and immunity to bacterial infection. *Proc. Natl. Acad. Sci. U. S. A.*, **108**, 19824–19829.

Winkler, A.J., Dominguez-Nuñez, J.A., Aranaz, I., Poza-Carrión, C., Ramonell, K., Somerville, S. and Berrocal-Lobo, M. (2017) Short-chain chitin oligomers: Promoters of plant growth. *Mar. Drugs*, **15**, 1–21.

Wojtkowiak, A., Witek, K., Hennig, J. and Jaskolski, M. (2013) Structures of an active-site mutant of a plant 1,3-B-glucanase in complex with oligosaccharide products of hydrolysis. *Acta Crystallogr. Sect. D Biol. Crystallogr.*, **69**, 52–62.

Woodward, J.R. and Fincher, G.B. (1982) Substrate specificities and kinetic properties of two (1→3), (1→4)-β-d-glucan endo-hydrolases from germinating barley (Hordeum vulgare). *Carbohydr. Res.*, **106**, 111–122.

Wu, S., Halley, J.E., Luttig, C., Fernekes, L.M., Darvill, A.G., Albersheim, P. and Barr, H. (2006) Gene Knockout Analysis , Purification , and Heterologous Expression. *Society*, **72**, 986–993.

Xiang, T., Zong, N., Zou, Y., Wu, Y., Zhang, J., Xing, W., Li, Y., Tang, X., Zhu, L., Chai, J. and Zhou, J.-M. (2008) Pseudomonas syringae Effector AvrPto Blocks Innate Immunity by Targeting Receptor Kinases. *Curr. Biol.*, **18**, 74–80.

Xu, T., Zhu, T. and Li, S. (2016) β-1,3-1,4-glucanase gene from *Bacillus vellezensis* ZJ20 exerts antifungal effect on plant pathogenic fungi. *World J Microbiol Biotechnol*, **32**(2):26.

Yamaguchi, K., Yamada, K., Ishikawa, K., Yoshimura, S., Hayashi, N., Uchihashi, K., Ishihama, N., Kishi-Kaboshi, M., Takahasi, A., Tsuge, S., Ochiai, H., Tada, Y., Shimamoto, K., Yoshioka, H. and Kawasaki, T. (2013) A receptor-like cytoplasmic kinase targeted by a plant

pathogen effector is directly phosphorylated by the chitin receptor and mediates rice immunity. *Cell Host Microbe*, **13**, 347–357. Available at: http://dx.doi.org/10.1016/j.chom.2013.02.007.

Yamaguchi, Y., Pearce, G. and Ryan, C.A. (2006) The cell surface leucine-rich repeat receptor for AtPep1, an endogenous peptide elicitor in Arabidopsis, is functional in transgenic tobacco cells. *Proc. Natl. Acad. Sci. U. S. A.*, **103**, 10104–10109.

Yin, Y., Mao, X., Yang, J., Chen, X., Mao, F. and Xu, Y. (2012) DbCAN: A web resource for automated carbohydrate-active enzyme annotation. *Nucleic Acids Res.*, **40**, 445–451.

Yu, X., Feng, B., He, P. and Shan, L. (2017) From Chaos to Harmony: Responses and Signaling upon Microbial Pattern Recognition. *Annu. Rev. Phytopathol.*, **55**, 109–137.

Zablackis, E., Huang, J., Müller, B., Darvill, A.G. and Albersheim, P. (1995) Characterization of the cell-wall polysaccharides of Arabidopsis thaliana leaves. *Plant Physiol.*, **107**, 1129–1138.

Zang, H., Xie, S., Zhu, B., Yang, X., Gu, C., Hu, B., Gao, T., Chen, Y. and Gao, X. (2019) Mannan oligosaccharides trigger multiple defence responses in rice and tobacco as a novel danger-associated molecular pattern. *Mol. Plant Pathol.*, 2**0**, 1067–1079.

Zhang, J., Li, W., Xiang, T., et al. (2010) Receptor-like cytoplasmic kinases integrate signaling from multiple plant immune receptors and are targeted by a Pseudomonas syringae effector. *Cell Host Microbe*, **7**, 290–301. Available at: http://dx.doi.org/10.1016/j.chom.2010.03.007.

Zhang, J., Shao, F., Li, Y., Cui, H., Chen, L., Li, H., Zou, Y., Long, C., Lan, L., Chai, J., Chen, S., Tang, X. and Zhou, J.-M. (2007) A Pseudomonas syringae Effector Inactivates MAPKs to Suppress PAMP-Induced Immunity in Plants. *Cell Host Microbe*, **1**, 175–185.

Zhang, L., Kars, I., Essenstam, B., Liebrand, T.W.H., Wagemakers, L., Elberse, J., Tagkalki, P., Tjoitang, D., van den Acjerceken, G. and van Kan, J.A.L. (2014) Fungal endopolygalacturonases are recognized as microbe-associated molecular patterns by the arabidopsis receptor-like protein RESPONSIVENESS TO BOTRYTIS POLYGALACTURONASES. *Plant Physiol.*, **164**, 352–364.

Zhang, W., Fraiture, M., Kolb, D., Löffelhardt, B., Desaki, Y., Boutrot, F.F.G., Tör, M., Zipfel, C., Gust, A.A. and Brunner, F. (2013) Arabidopsis RECEPTOR-LIKE PROTEIN30 and receptor-like kinase SUPPRESSOR OF BIR1-1/EVERSHED mediate innate immunity to necrotrophic fungi. *Plant Cell*, **25**, 4227–4241.

Zhang, X.C., Wu, X., Findley, S., Wan, J., Libault, M., Nguyen, H.T., Cannon, S.B. and Stacey, G. (2007) Molecular evolution of lysin motif-type receptor-like kinases in plants. *Plant Physiol.*, **144**, 623–636.

Zhao, Z., Liu, H., Wang, C. and Xu, J.R. (2014) Correction to Comparative analysis of fungal genomes reveals different plant cell wall degrading capacity in fungi [BMC Genomics 14(2013) 274]. *BMC Genomics*, **15**.

Zhong, R. and Ye, Z.H. (2015) Secondary cell walls: Biosynthesis, patterned deposition and transcriptional regulation. *Plant Cell Physiol.*, **56**, 195–214.

Zipfel, C., Kunze, G., Chinchilla, D., Caniard, A., Jones, J.D.G., Boller, T. and Felix, G. (2006) Perception of the Bacterial PAMP EF-Tu by the Receptor EFR Restricts Agrobacterium-Mediated Transformation. *Cell*, **125**, 749–760.

Zipfel, C., Robatzek, S., Navarro, L., Oakeley, E.J., Jones, J.D.G., Felix, G. and Boller, T. (2004) Bacterial disease resistance in Arabidopsis through flagellin perception. *Nature*, **428**, 764–767.

6 Supplemental Material

Table S1. Predicted motifs of GHs in *Bgh*.

CWDE family	Predicted Motif	
BluGen Protein Number	**dbCAN**	**Motif Scan**
GH3		
BGH00678	GH3	-
GH5		
BGH06688	GH5_12	Cellulase Motif Glycoside Hydrolase family 5 signature
BGH06810	GH5_9	Bipartite nuclear localization signal profile
BGH00680	GH5_9	Glycoside Hydrolase family 5 signature
BGH00086	GH5_9	-
GH13		
BGH00197	CBM48 GH13_8	Alpha amylase, catalytic domain Alpha amylase, C-terminal all-beta domain
BGH00315	GH13_40	Alpha amylase, catalytic domain
BGH000684000002001	GH13_25	Amylo-alpha-1,6-glucosidase
BGH000061000002001	GH13_40	Alpha amylase, catalytic domain
GH16		
BGH05640	GH16	Glycoside hydrolases family 16 motif
BGH00719	GH16	Glycoside hydrolases family 16 motif Histidine rich profile
BGH00720	GH16	Glycoside hydrolases family 16 motif
BGH00726	GH16	Glycoside hydrolases family 16 motif
BGH00729	GH16	Glycoside hydrolases family 16 motif Prokaryotic membrane lipoprotein lipid attachment site profile
BGH00731	GH16	Glycoside hydrolases family 16 motif
BGH00732	GH16	Glycoside hydrolases family 16 motif Beta-glucan synthesis-associated protein (SKN1)
BGH01441	GH16	Glycoside hydrolases family 16 motif
BGH05042	GH16	Glycoside hydrolases family 16 motif
GH17		
BGH06298	GH17	Glycoside hydrolases family 17 motif

BGH06777	GH17	Glycoside hydrolases family 17 motif
BGH00219	GH17	Glycoside hydrolases family 17 motif
BGH00220	-	Glycoside hydrolases family 17 motif
BGH00734	GH17	Threonine rich region
BGH00736	GH17	-
BGH05070	GH17	-
BGH05207	-	Cytosolic fatty acid binding proteins signature Prokaryotic membrane lipoprotein lipid attachment site profile
GH18		
BGH05372	GH18	Glycoside hydrolases family 18 motif Chitinases family 18 active site
BGH00059	GH18	Glycoside hydrolases family 18 motif Chitin recognition or binding domain signature
BGH00122	GH18	Glycoside hydrolases family 18 motif Chitinases family 18 active site Chitin-binding type-1 domain profile
BGH00634	GH18	Glycoside hydrolases family 18 motif Chitinases family 18 active site
BGH00329	GH18	Glycoside hydrolases family 18 motif Chitinases family 18 active site
BGH00588	GH18	Glycoside hydrolases family 18 motif Chitinases family 18 active site Chitin recognition or binding domain signature and Chitin recognition protein
BGH00738	GH18	Glycoside hydrolases family 18 motif Chitinases family 18 active site
BGH00739	GH18	Glycoside hydrolases family 18 motif Chitinases family 18 active site
BGH02531	-	Serine-rich region profile
GH31		
BGH06910	GH31	Glycosyl hydrolases family 31 active site Glycosyl hydrolases family 31
GH37		
BGH006215000001001	GH37	-
GH38		
BGH00758	GH38	-
GH47		
BGH00762	GH47	Glycoside hydrolases family 47 motif
BGH00763	GH47	Glycoside hydrolases family 47 motif

BGH00764	GH47	Glycoside hydrolases family 47 motif
BGH00768	GH47	Glycoside hydrolases family 47 motif
GH55		
BGH00772	GH55	-
GH61 / AA[4]9		
BGH04794	AA9 AA11	Glycosyl hydrolase family 61 motif
BGH02286	AA11	Proline-rich region profile
GH63		
BGH02562	GH63	
BGH004450000001001	GH63	Endoplasmic reticulum targeting sequence Mannosyl oligosaccharide glucosidase
GH72		
BGH00774	GH72 CBM43	Glycolipid anchored surface protein (GAS1) X8 domain
BGH00775	GH72	Glycolipid anchored surface protein (GAS1) Cellulase (glycosyl hydrolase family 5)
BGH00776	GH72	Glycolipid anchored surface protein (GAS1)
GH76		
BGH00778	GH76	Glycosyl hydrolase family 76 motif
BGH00780	GH76	-
BGH00782	GH76	Glycosyl hydrolase family 76 motif
BGH00783	GH76	Glycosyl hydrolase family 76 motif
BGH05252	GH76	Glycosyl hydrolase family 76 motif
BGH0006450	GH76	Glycosyl hydrolase family 76 motif
BGH00779	GH76	Glycosyl hydrolase family 76 motif Trp-Asp (WD) repeats signature
GH78		
BGH000684000001001	GH78	-
GH81		
BGH004744	GH81	-
GH92		
BGH00795	GH92	Glycosyl hydrolase family 92 motif

[4] AA – Auxiliary Activity

BGH006074000001001	GH92	Glycosyl hydrolase family 92 motif EF-hand calcium-binding domain
GH93		
BGH006353	GH93 GH74	-

Table S2. *In planta* RPM values of *Bgh* GH families 5, 16, 17, 47 and 76 upon 6, 12, 18 and 24 hpi. The Arabidopsis triple mutant *pen2 pad4 sag101* expressing *MLA1* was infected with the *Bgh* isolate A6. Samples were taken upon 6, 12, 18 and 24 hpi, RNA was extracted and RNA sequencing was performed (Hacquard *et al.*, 2013). RPM values were calculated from the raw data available at the National Center for Biotechnology Information Gene Expression Omnibus (GEO) database.

GH family	RPM Values (compatible interaction)			
BluGen Gen Number[5]	**6hpi**	**12 hpi**	**18 hpi**	**24 hpi**
GH5				
Bgh06688	301	69	140	78
Bgh06810	3	8	15	21
Bgh00680	6739	5333	6786	6696
Bgh00086	375	329	1272	1098
GH16				
Bgh05640	67	459	919	611
Bgh00719	918	251	477	639
Bgh00720	6867	15403	6578	4777
Bgh00726	735	196	307	368
Bgh00729	1643	443	1147	1235
Bgh00731	1308	1453	1319	1111
Bgh00732	67	79	102	169
Bgh01441	3357	797	796	495
Bgh05042	31	125	361	2140
GH17				
Bgh06298	351	452	740	454
Bgh06777	16	1301	1053	606
Bgh00219	3	63	115	157
Bgh00220	98	1552	369	145
Bgh00734	906	470	727	595
Bgh00736	43	4409	5580	4357
Bgh05070	642	3873	1464	823
Bgh05207	49	3720	1770	1387
GH47				
Bgh00762	8983	3695	3885	4707
Bgh00763	2338	861	1116	870
Bgh00764	1324	1691	1033	939
Bgh00768	5992	4560	5743	7606
GH76				
Bgh00778	1619	464	757	868
Bgh00780	1060	1270	1881	1634
Bgh00782	450	1185	448	137
Bgh00783	50	37	46	27
Bgh05252	0	0	0	0
Bgh0006450	5650	204	316	340

[5] Gene identification numbers were retrieved from www.blugen.org.

Bgh00779	40346	863	1204	1280

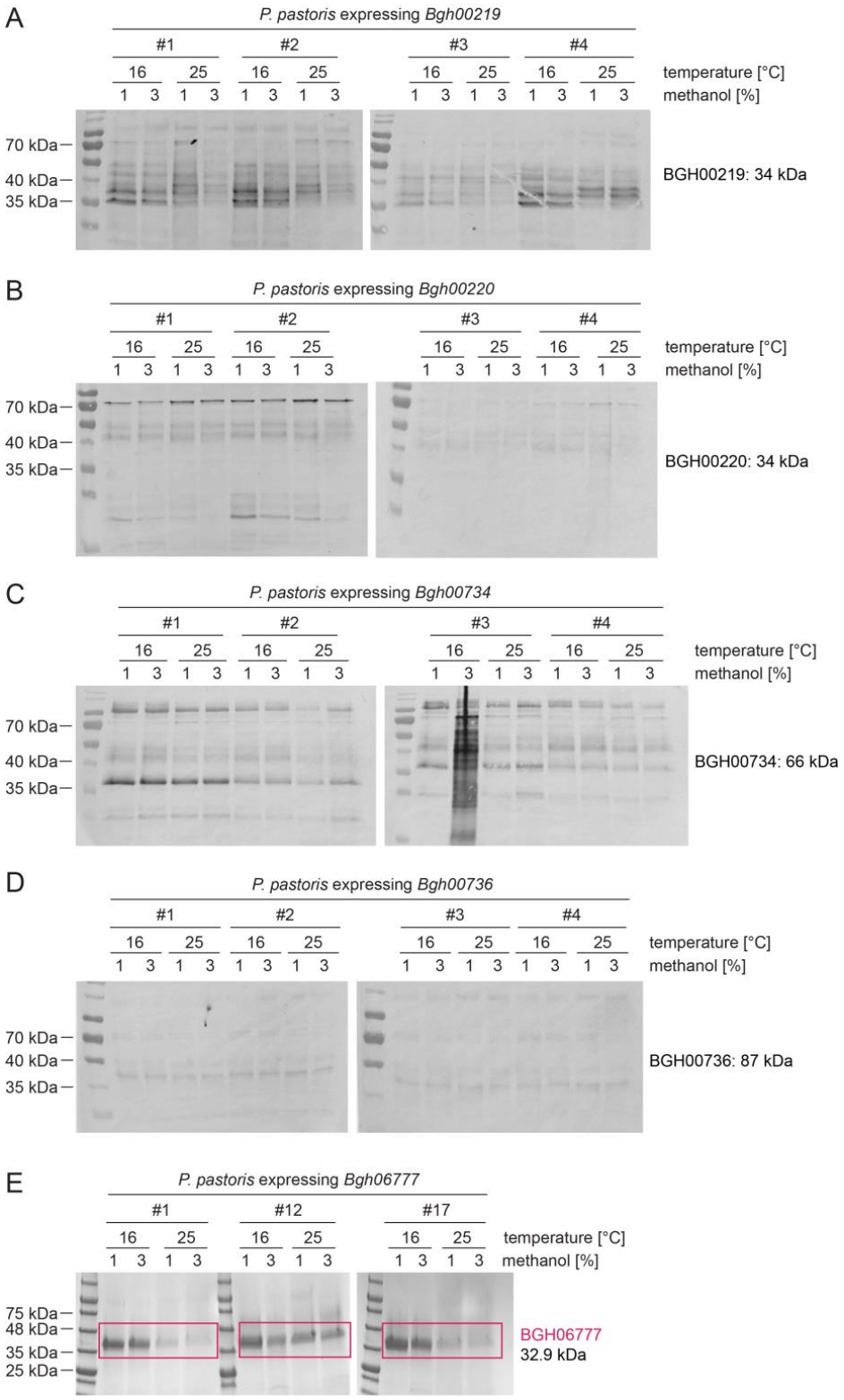

Figure S1. Small scale expression of *Bgh* GH17 genes. Three to four clones were tested for the expression of either *Bgh00219* (A), *Bgh00220* (B), *Bgh00734* (C), *Bgh00736* (D) or *Bgh06777* (E). All clones were grown in YPD at 30°C overnight and then re-inoculated in BMGY and further incubated overnight. The pellet was resuspended in BMMY containing either 1% or 3% methanol to induce the expression and the culture was incubated at either 16°C or 25°C for three to five days. 1% or 3% methanol was added to the cultures every 24h. Upon 3 to 5 days, the supernatant of the cultures was analysed via SDS PAGE and Western Blot. To visualize the presence of the proteins, the membranes or the gel were directly stained with Coomassie Brilliant Blue.

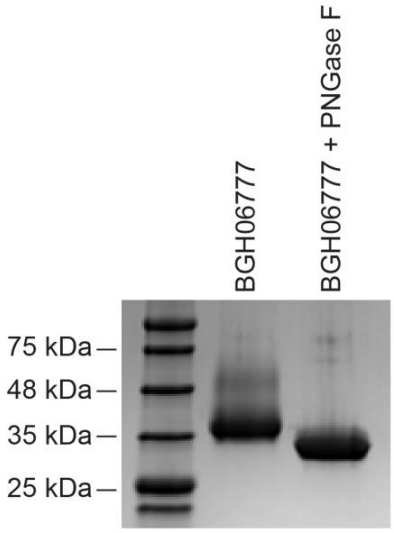

Figure S2. SDS PAGE analysis of recombinant BGH06777. 9 µg recombinant protein before deglycosylation with PNGase F and 9 µg BGH06777 after deglycosylation with PNGase F. To visualize the protein, the SDS gel was stained with Coomassie Brilliant Blue.

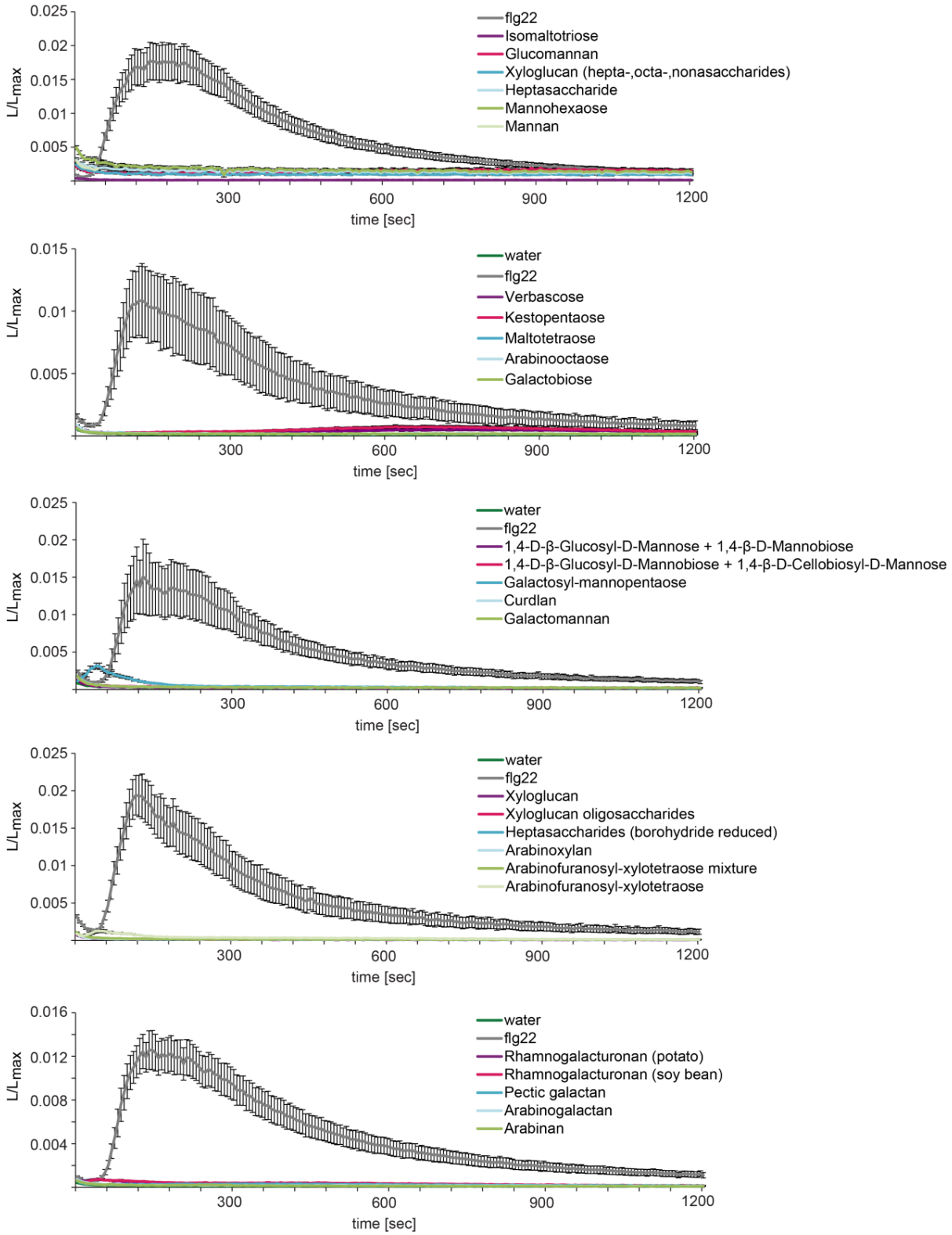

Figure S3. Influx of Ca^{2+} in Col-0 upon oligo- and polysaccharide treatment. 8-10-day old Arabidopsis Col-0 seedlings expressing the calcium sensor protein aequorin were treated with water, 50 nM flg22 and 100 µg ml^{-1} of the respective oligosaccharide or polysaccharide as depicted. The Ca^{2+} elevation was measured every 6 sec for 1200 sec (L). To obtain the total remaining luminescence (L_{max}), the remaining aequorin was discharged by adding $CaCl_2$ to each well and luminescence was recorded for 3 min in 6 sec intervals. For normalization, the elicitor induced luminescence per 6 sec (L) was divided by L_{max}. The data shown represents the mean of 12 seedlings and error bars represent SEM. The experiments were performed once.

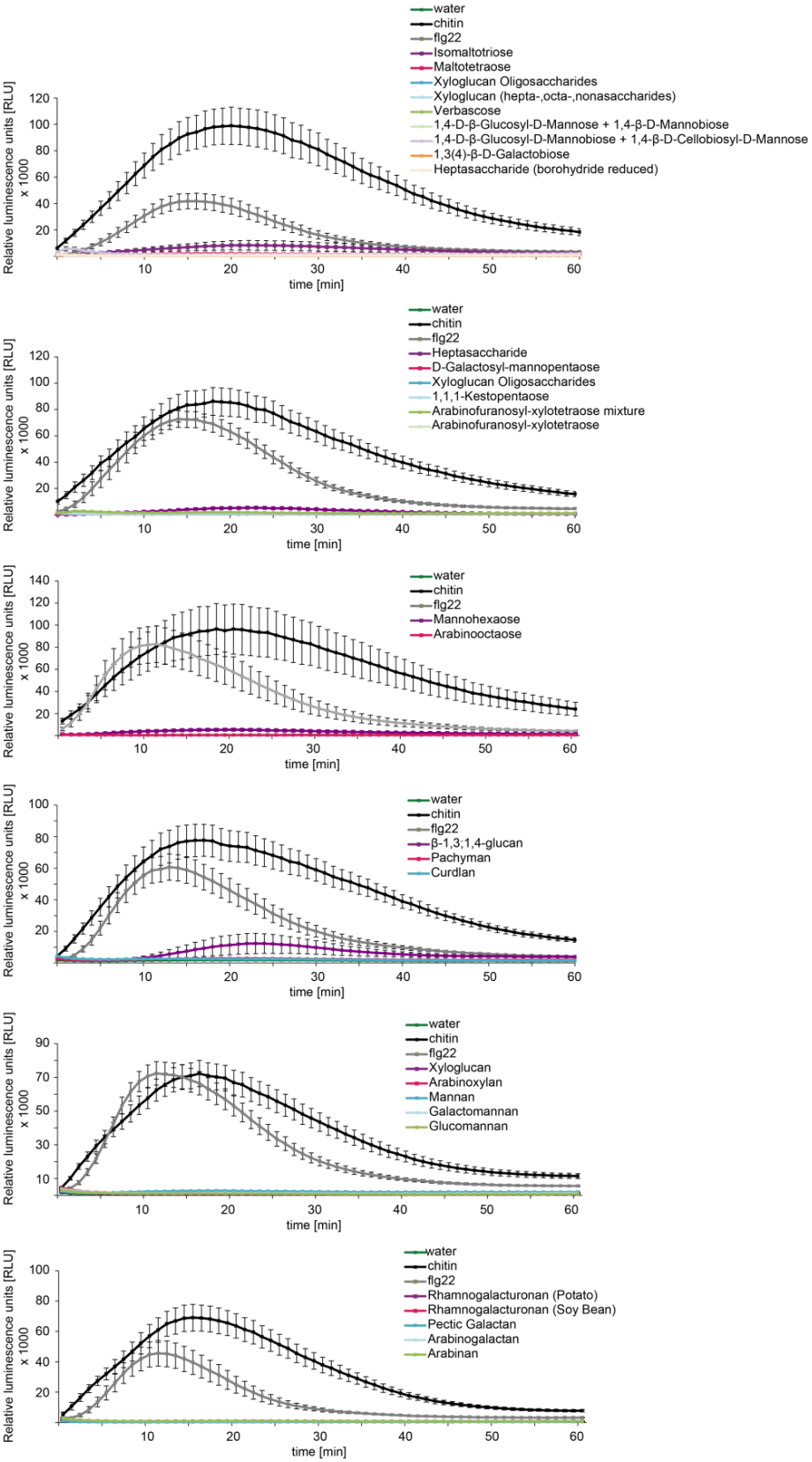

Figure S4. Generation of ROS in Col-0 upon oligo- and polysaccharide treatment. Leaf discs of 5-7 week old Arabidopsis Col-0 plants were treated with water, 100 µg ml^{-1} chitin, 100 nM flg22 or 100 µg ml^{-1} of the respective oligo- or polysaccharide as indicated. Relative luminescence units (RLU) were recorded every minute for 60 min. The shown data represent the mean of eight leaf discs with SEM. The experiment were performed once.

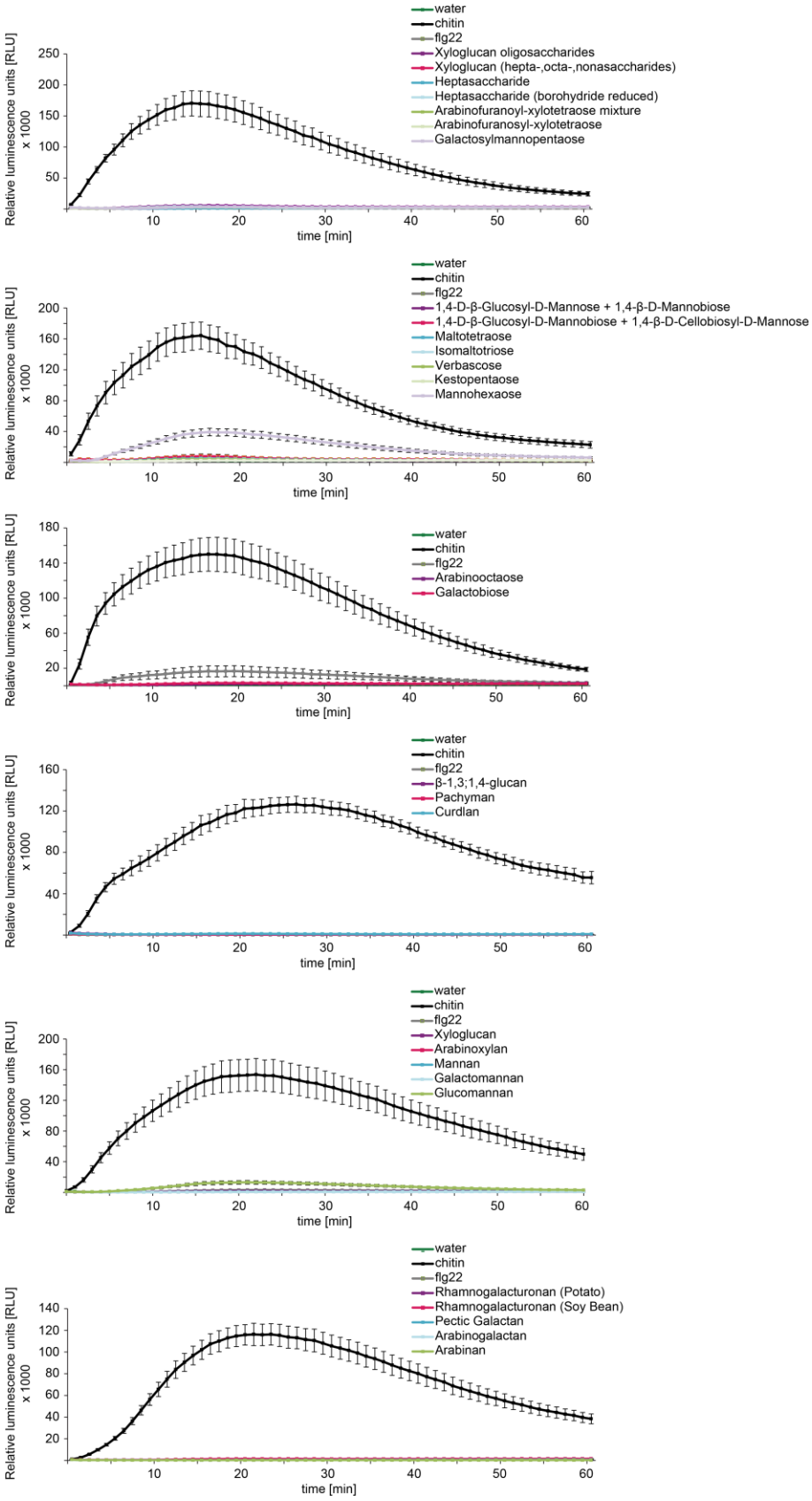

Figure S5. Generation of ROS in Ws-0 upon oligo- and polysaccharide treatment. Leaf discs of 5-7 week old Arabidopsis Ws-0 plants were treated with water, 100 µg ml^{-1} chitin, 100 nM flg22 or 100 µg ml^{-1} of the respective oligo- or polysaccharide as indicated. Relative luminescence units (RLU) recorded every minute for 60 min. The shown data represent the mean of eight leaf discs with SEM. The experiment was performed once.

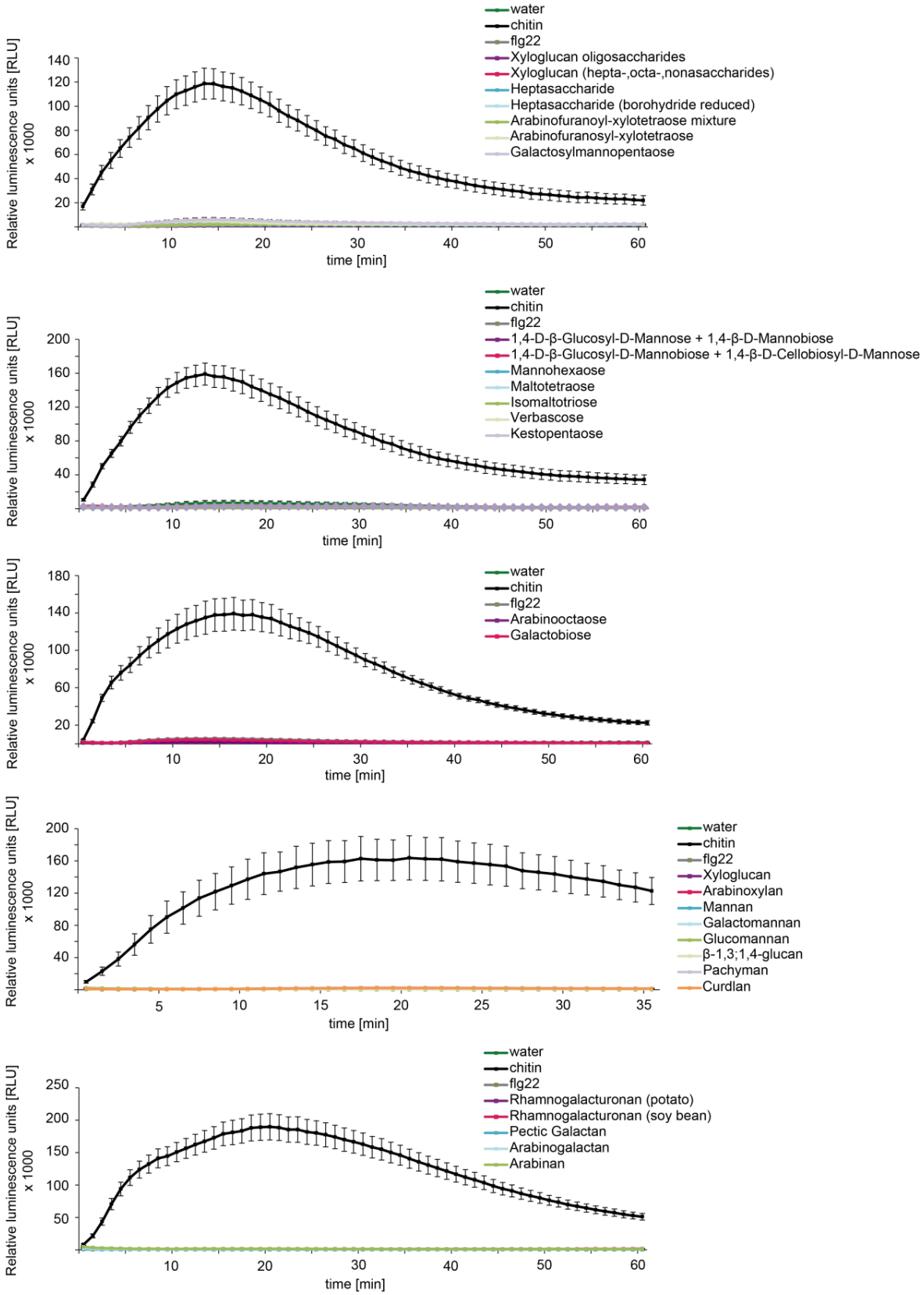

Figure S6. Generation of ROS in Ws-4 upon oligo- and polysaccharide treatment. Leaf discs of 5-7 week old Arabidopsis Ws-4 plants were treated with water, 100 µg ml^{-1} chitin, 100 nM flg22 or 100 µg ml^{-1} of the respective oligo- or polysaccharide as indicated. Relative luminescence units (RLU) were recorded every minute for 60 or 35 min. The shown data represent the mean of eight leaf discs with SEM. The experiment was performed once.

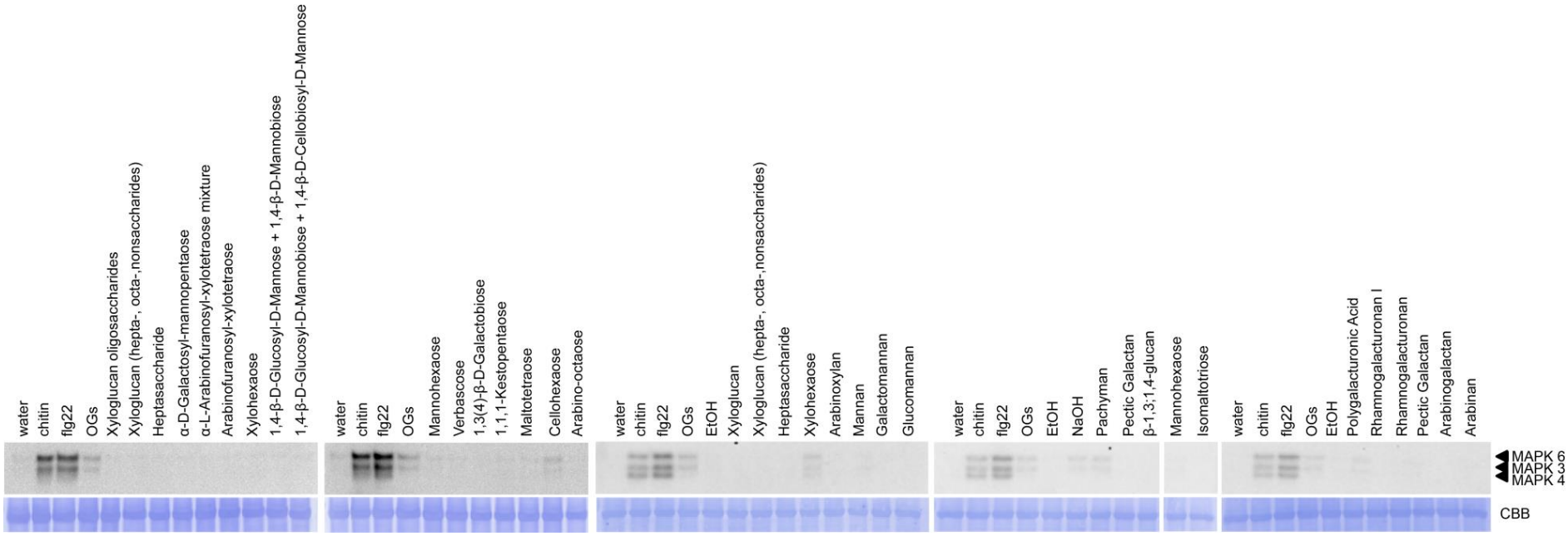

Figure S7. MAPK activation in Col-0 upon treatment with several oligo- and polysaccharides. 14-day old *in-vitro* grown Arabidopsis Col-0 seedlings were treated with water, 10 µg ml^{-1} chitin, 50 nM flg22 or 10 µg ml^{-1} of the respective carbohydrate for 12 min. Activation of MAPK was analysed via immunoblot analyses using the p44/42-antibody. Lower panel shows Coomassie Brilliant Blue (CBB) staining as loading control. The experiment was performed once or twice.

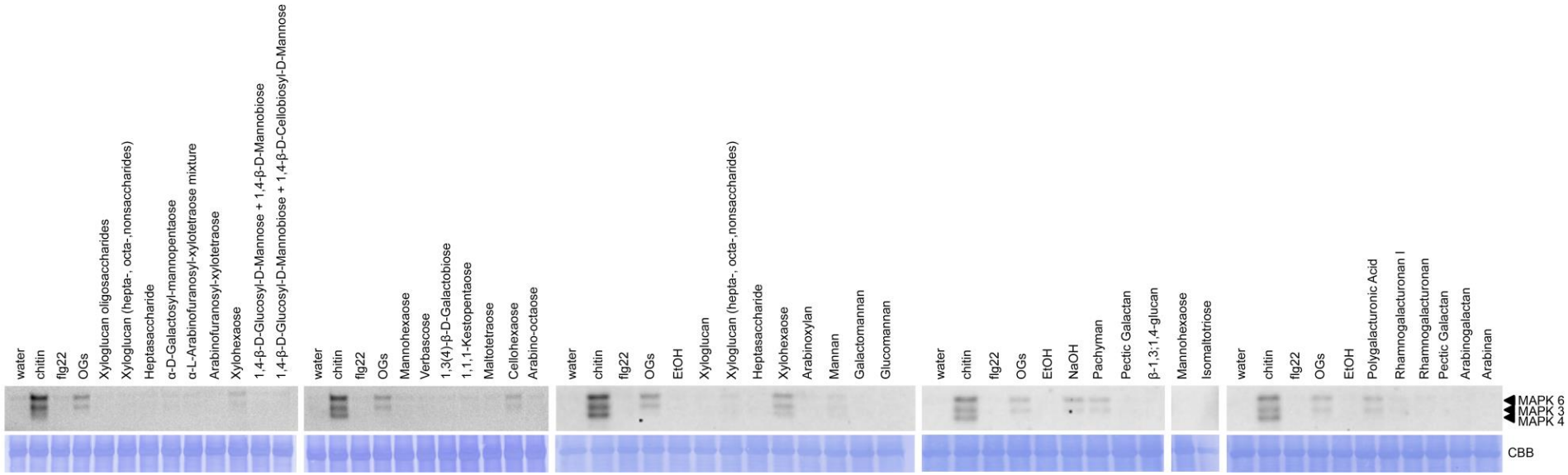

Figure S8. MAPK activation in Ws-0 upon treatment with several oligo- and polysaccharides. 14-day old *in-vitro* grown Arabidopsis Ws-0 seedlings were treated with water, 10 µg ml^{-1} chitin, 50 nM flg22 or 10 µg ml^{-1} of the respective carbohydrate for 12 min. Activation of MAPK was analysed via immunoblot analyses using the p44/42-antibody. Lower panel shows Coomassie Brilliant Blue (CBB) staining as loading control. The experiment was performed once.

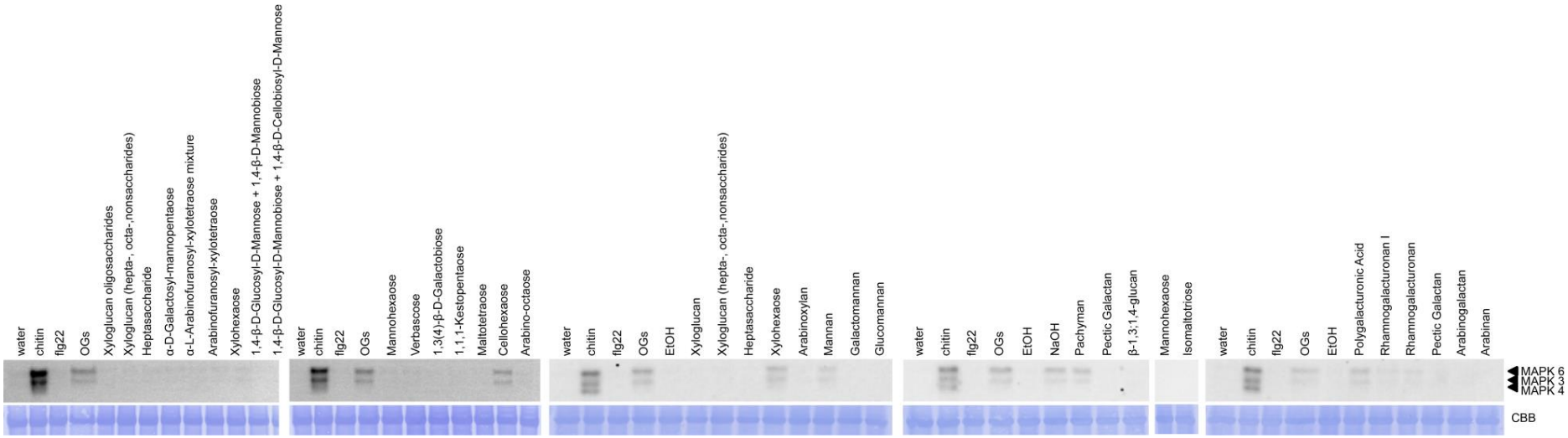

Figure S9. MAPK activation in Ws-4 upon treatment with several oligo- and polysaccharides. 14-day old *in-vitro* grown Arabidopsis Ws-4 seedlings were treated with water, 10 µg ml^{-1} chitin, 50 nM flg22 or 10 µg ml^{-1} of the respective carbohydrate for 12 min. Activation of MAPK was analysed via immunoblot analyses using the p44/42-antibody. Lower panel shows Coomassie Brilliant Blue (CBB) staining as loading control. The experiment was performed once.

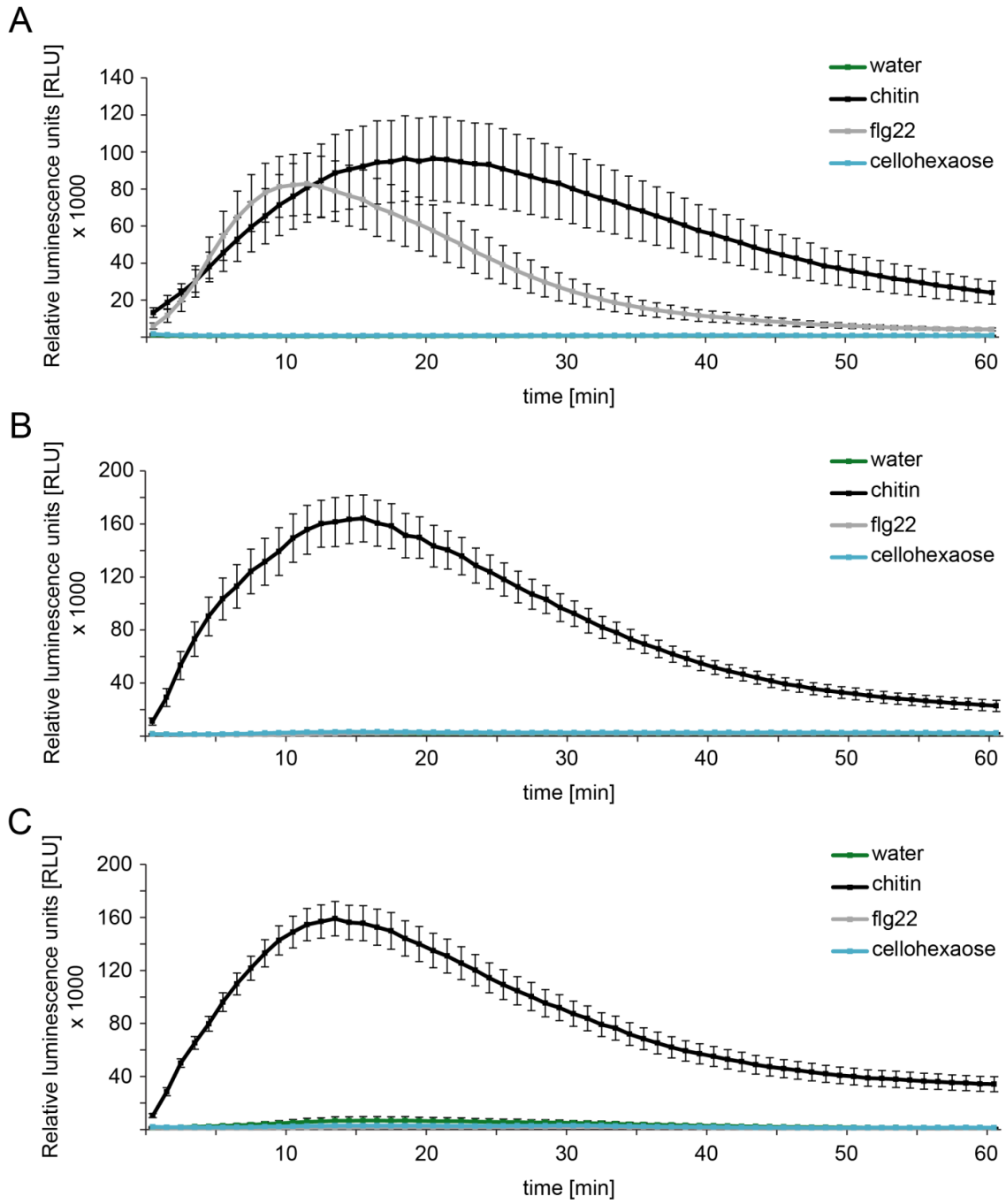

Figure S10. ROS burst generation in three Arabidopsis ecotypes upon cellohexaose treatment. Leaf discs of 5-7 week old Arabidopsis Col-0 (A), Ws-0 (B) or Ws-4 (C) plants were treated with water, 100 µg ml^{-1} chitin, 100 nM flg22 or 100 µg ml^{-1} cellohexaose. Relative luminescence units (RLU) were recorded every minute for 60 min. The shown data represent the mean of eight leaf discs with SEM. The experiment was performed once.

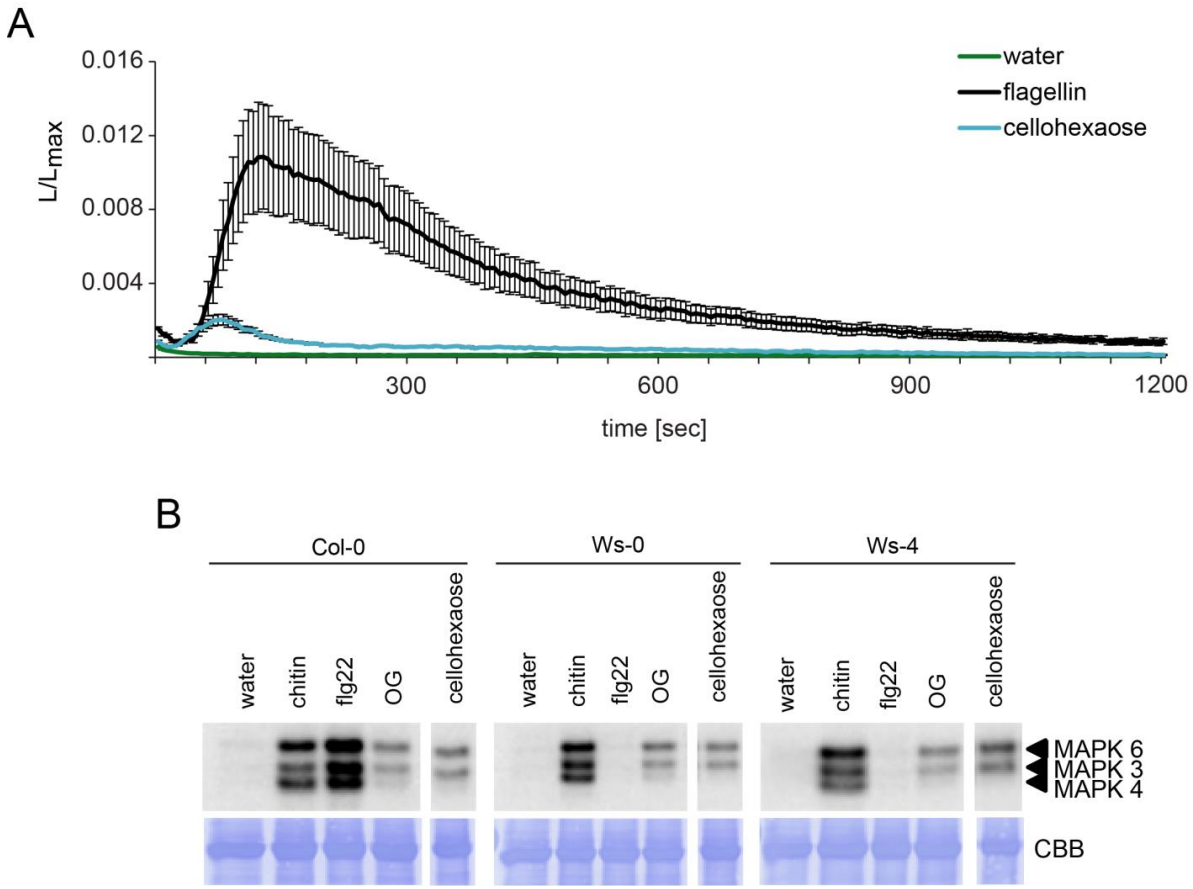

Figure S11. Activation of immune responses upon cellohexaose elicitation. (A) Elevation of intracellular Ca^{2+}. 8-10 day old Arabidopsis seedlings expressing the Ca^{2+} sensor protein aequorin were treated with water, 100 nM flg22 or 100 µg ml^{-1} cellohexaose. Elevation of Ca^{2+} was measured for 1200 sec every 6 sec (L). To obtain the total remaining luminescence (L_{max}), the remaining aequorin was discharged by adding $CaCl_2$ to each well and luminescence was recorded for 3 min in 6 sec intervals. For normalization, the elicitor induced luminescence per 6 sec (L) was divided by L_{max}. The data shown represents the mean of 12 seedlings and error bars represent SEM. The experiment was performed once. (B) MAPK activation upon cellohexaose treatment. 14-day old *in-vitro* grown Arabidopsis Ws-0 and Ws-4 seedlings were treated with water, 10 µg ml^{-1} chitin, 50 nM flg22 or 10 µg ml^{-1} cellohexaose for 12 min. Activation of MAPK was analysed via immunoblot analyses using the p44/42-antibody. Lower panel shows Coomassie Brilliant Blue (CBB) staining as loading control. The experiment was performed twice with similar results.

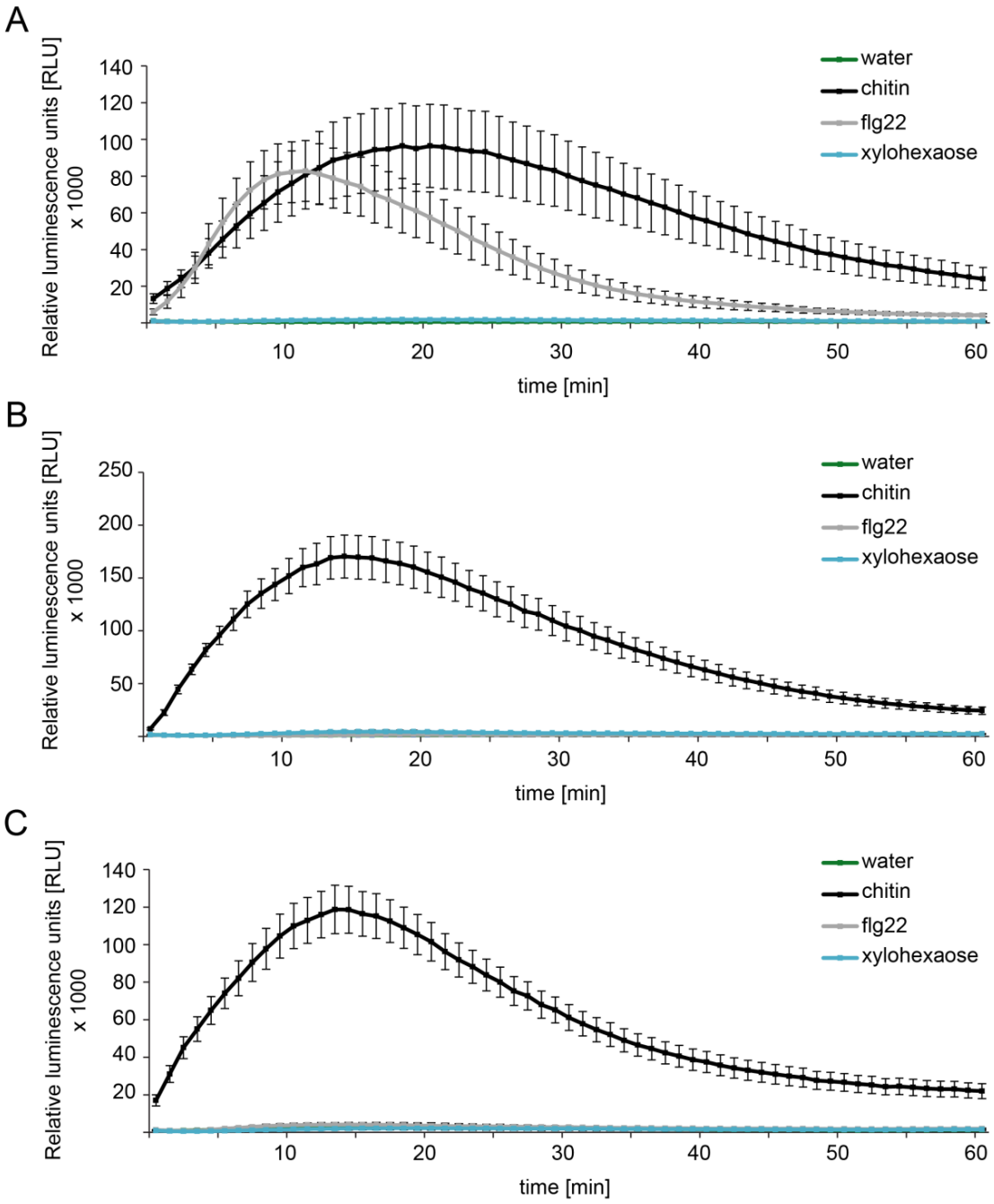

Figure S12. ROS burst generation upon xylohexaose treatment in different Arabidopsis ecotypes. Leaf discs of 5-7 week old Arabidopsis Col-0 (A), Ws-0 (B) or Ws-4 (C) plants were treated with water, 100 µg ml^{-1} chitin, 100 nM flg22 or 100 µg ml^{-1} xylohexaose. Relative light units were recorded every minute for 60 min. The shown data represent the mean of eight leaf discs with SEM. The experiment was performed once.

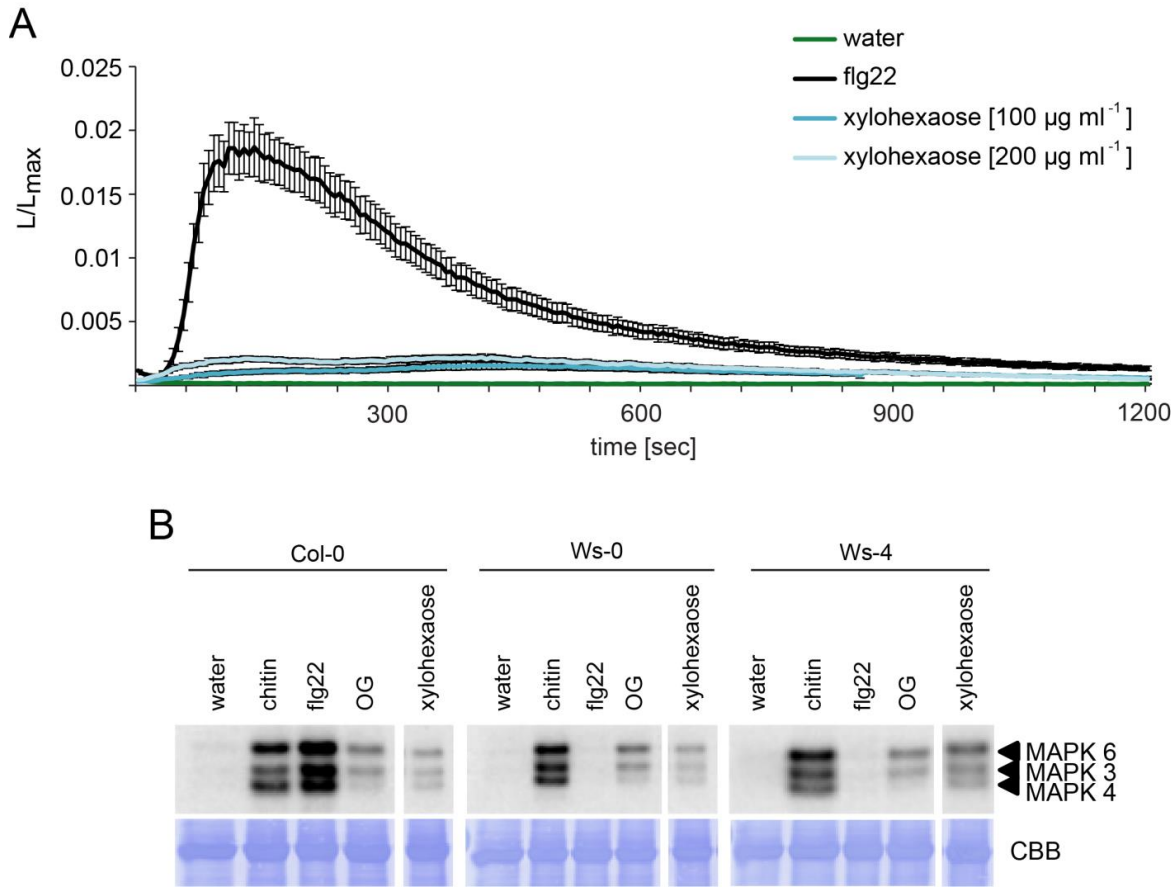

Figure S13. Ca^{2+} influx and MAPK activation upon xylohexaose elicitation. (A) Elevation of intracellular Ca^{2+}. 8-10 day old Arabidopsis seedlings expressing the Ca^{2+} sensor protein aequorin were treated with water, 100 nM flg22, 100 µg ml^{-1} xylohexaose or 200 µg ml^{-1} xylohexaose. Elevation of Ca^{2+} was measured for 1200 sec every 6 sec (L). To obtain the total remaining luminescence (L_{max}), the remaining aequorin was discharged by adding $CaCl_2$ to each well and luminescence was recorded for 3 min in 6 sec intervals. For normalization, the elicitor induced luminescence per 6 sec (L) was divided by L_{max}. The data shown represents the mean of 12 seedlings and error bars represent SEM. The experiment was performed twice with similar results. (B) MAPK activation upon xylohexaose treatment. 14-day old *in-vitro* grown Arabidopsis Ws-0 and Ws-4 seedlings were treated with water, 10 µg ml^{-1} chitin, 50 nM flg22 or 10 µg ml^{-1} xylohexaose for 12 min. Activation of MAPK was analysed via immunoblot analyses using the p44/42-antibody. Lower panel shows Coomassie Brilliant Blue (CBB) staining as loading control. The experiment was performed twice with similar results.

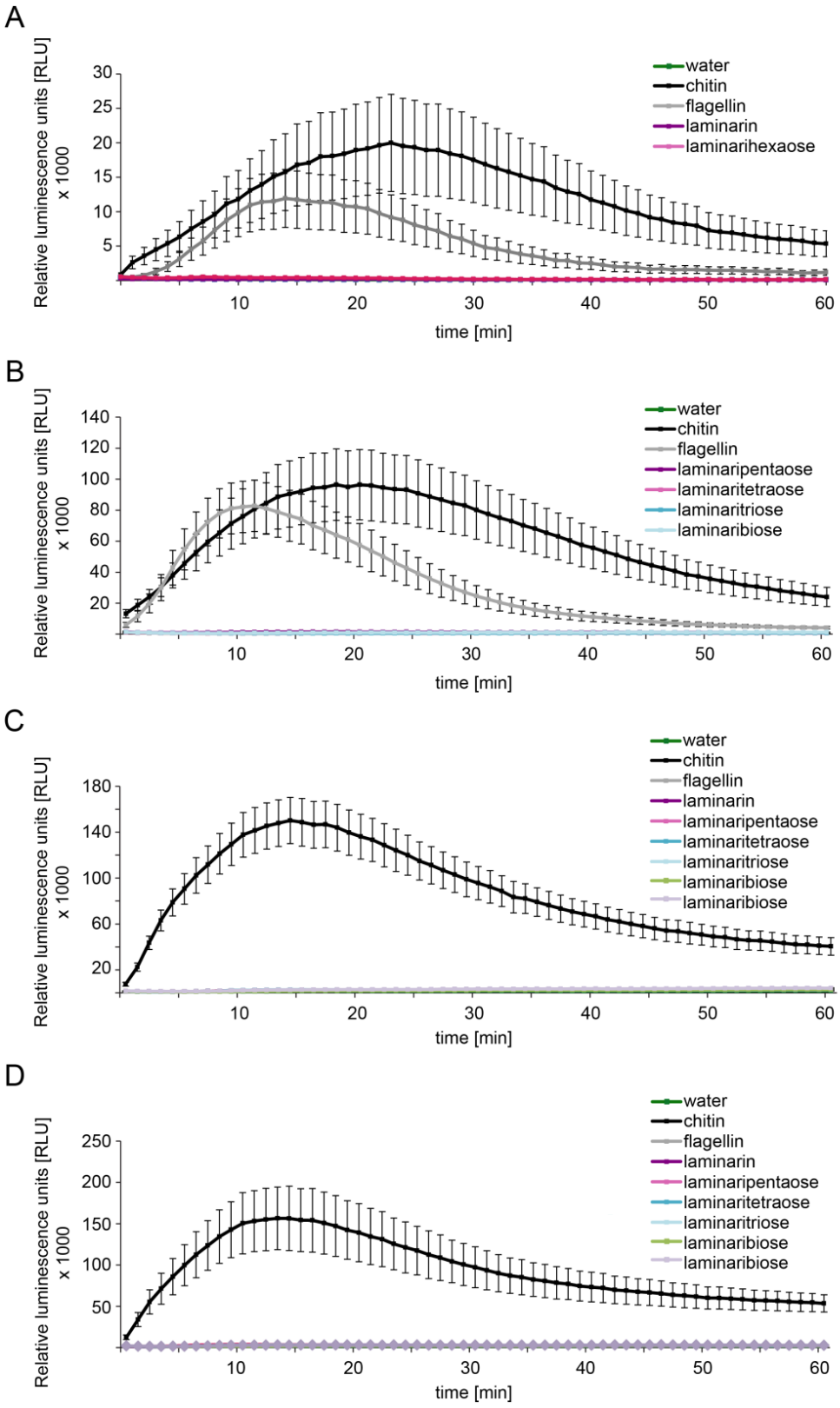

Figure S14. Generation of ROS in Arabidopsis ecotypes upon β-1,3-glucan oligosaccharide treatment. Leaf discs of 5-7 week old Arabidopsis Col-0 (A and B), Ws-0 (C) or Ws-4 (D) plants were treated with water, 100 µg ml^{-1} chitin, 100 nM flg22, 100 µg ml^{-1} laminarin or 100 µg ml^{-1} β-1,3-glucan oligosaccharides of various lengths. Relative luminescence units (RLU) were recorded directly upon treatment every minute for 60 min. The shown data represent the mean of eight leaf discs with SEM. The experiment was performed once.

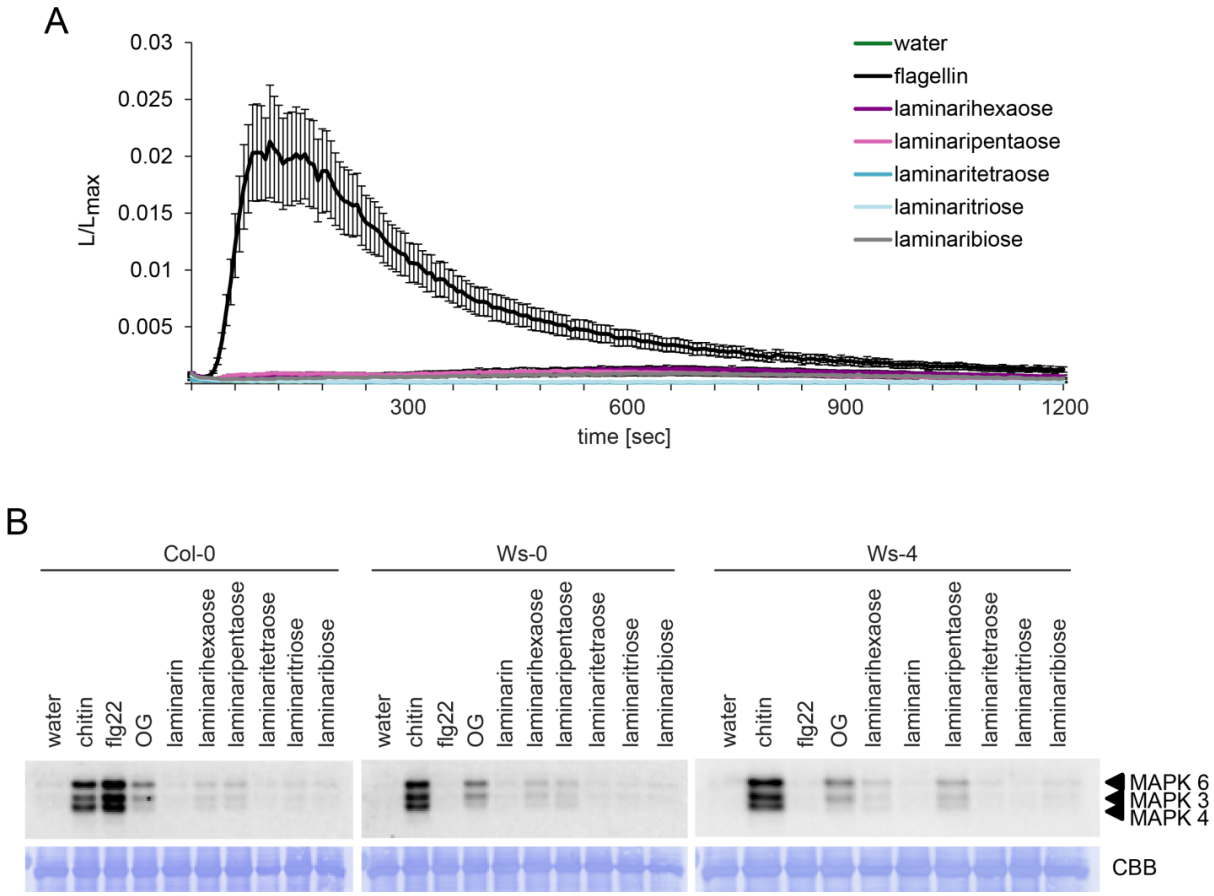

Figure S15. Activation of defence responses in Arabidopsis upon treatment with β-1,3-glucans. (A) Elevation of intracellular Ca^{2+}. 8-10 day old Arabidopsis seedlings expressing the Ca^{2+} sensor protein aequorin were treated with water, 100 nM flg22 or 100 µg ml^{-1} of the respective β-1,3-glucans. Elevation of Ca^{2+} was measured for 1200 sec every 6 sec (L). To obtain the total remaining luminescence (L_{max}), the remaining aequorin was discharged by adding $CaCl_2$ to each well and luminescence was recorded for 3 min in 6 sec intervals. For normalization, the elicitor induced luminescence per 6 sec (L) was divided by L_{max}. The data shown represents the mean of 12 seedlings and error bars represent SEM. The experiment was performed once. (B) MAPK activation upon β-1,3-glucan oligosaccharide treatment. 14-day old *in-vitro* grown Arabidopsis Ws-0 and Ws-4 seedlings were treated with water, 10 µg ml^{-1} chitin, 50 nM flg22 or 10 µg ml^{-1} β-1,3-glucans of varying length for 12 min. Activation of MAPK was analysed via immunoblot analyses using the p44/42-antibody. Lower panel shows Coomassie Brilliant Blue (CBB) staining as loading control. The experiment was performed three times with similar results.

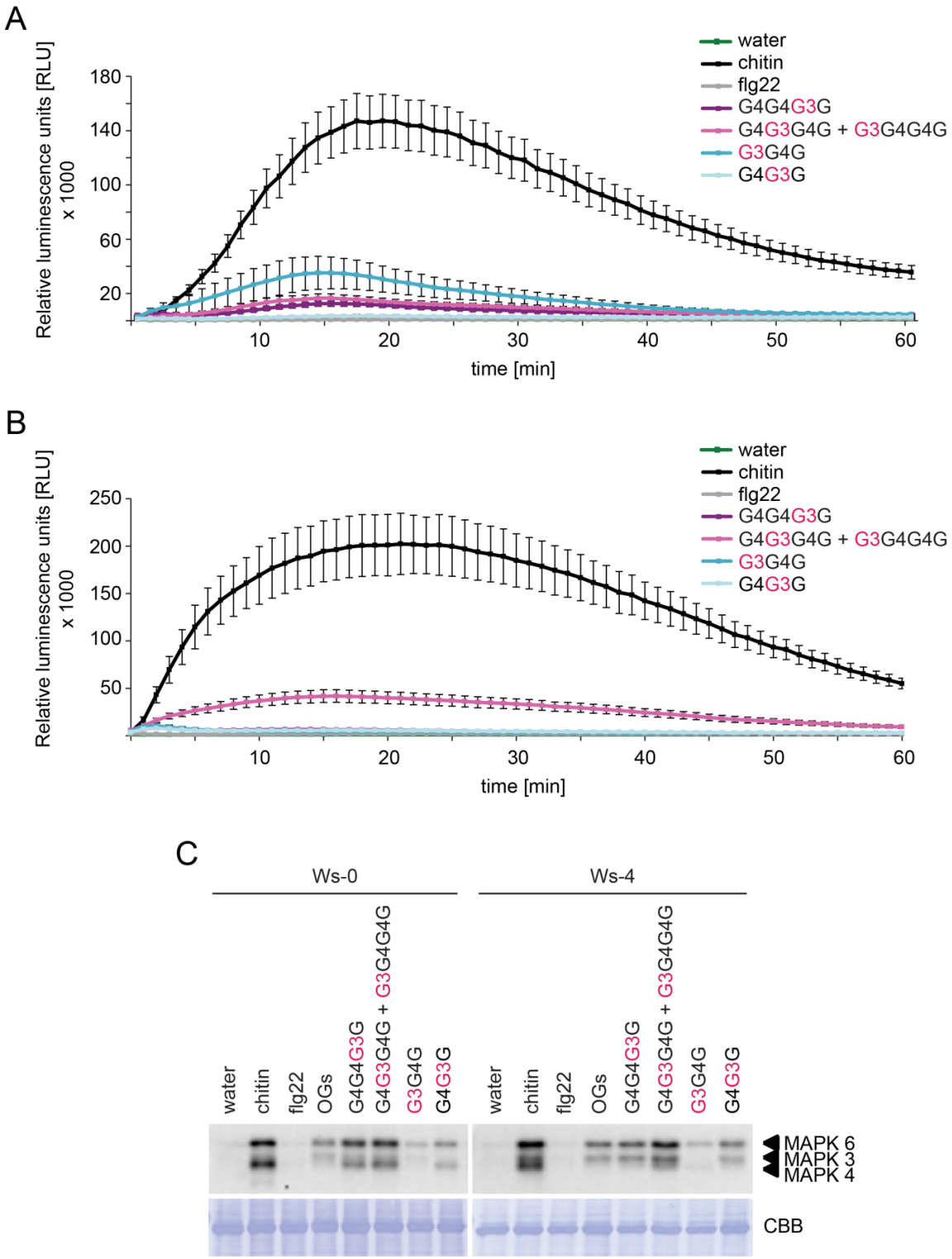

Figure S16. Generation of ROS and activation of MAPK in Ws-0 and Ws-4 upon elicitation with MLGs from Megazyme. (A) and (B). Generation of ROS. Leaf discs of 5-7 week old Arabidopsis Ws-0 (A) or Ws-4 (B) plants were treated with water, 100 µg ml^{-1} chitin, 100 nM flg22 or 100 µg ml^{-1} MLG oligomers. Relative light units (RLU) were recorded every minute for 60 min. The shown data represent the mean of eight leaf discs with SEM. The experiment repeated two times with similar results. (C) MAPK activation upon MLG treatment. 14-day old *in-vitro* grown Arabidopsis Ws-0 and Ws-4 seedlings were treated with water, 10 µg ml^{-1} chitin, 50 nM flg22 or 10 µg ml^{-1} MLG oligomers for 12 min. Activation of MAPK was analysed via immunoblot analyses using the p44/42-antibody. Lower panel shows Coomassie Brilliant Blue (CBB) staining as loading control. The experiment was repeated four times with similar results.

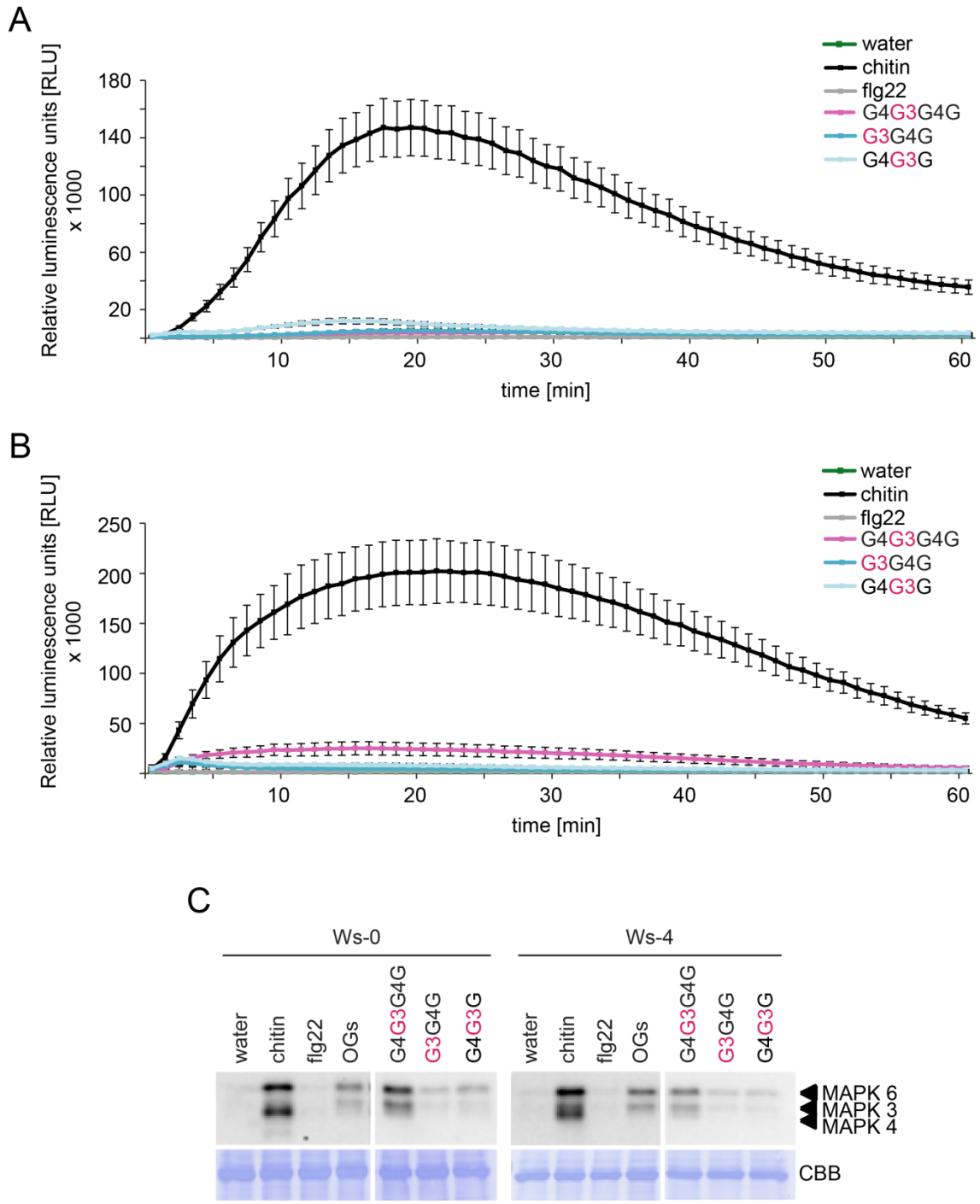

Figure S17. Activation of immune responses in Ws-0 and Ws-4 upon MLG oligomer treatment from Carbosynth. (A) and (B) Generation of ROS. Leaf discs of 5-7 week old Arabidopsis Ws-0 (A) or Ws-4 (B) plants were treated with water, 100 µg ml^{-1} chitin, 100 nM flg22 or 100 µg ml^{-1} MLG oligomers. Relative light units were recorded every minute for 60 min. The shown data represent the mean of eight leaf discs with SEM. The experiment was repeated two times with similar results. (C) MAPK activation upon MLG treatment. 14-day old *in-vitro* grown Arabidopsis Ws-0 and Ws-4 seedlings were treated with water, 10 µg ml^{-1} chitin, 50 nM flg22 or 10 µg ml^{-1} MLG oligomers for 12 min. Activation of MAPK was analysed via immunoblot analyses using the p44/42-antibody. Lower panel shows Coomassie Brilliant Blue (CBB) staining as loading control. The experiment was repeated four times with similar results.

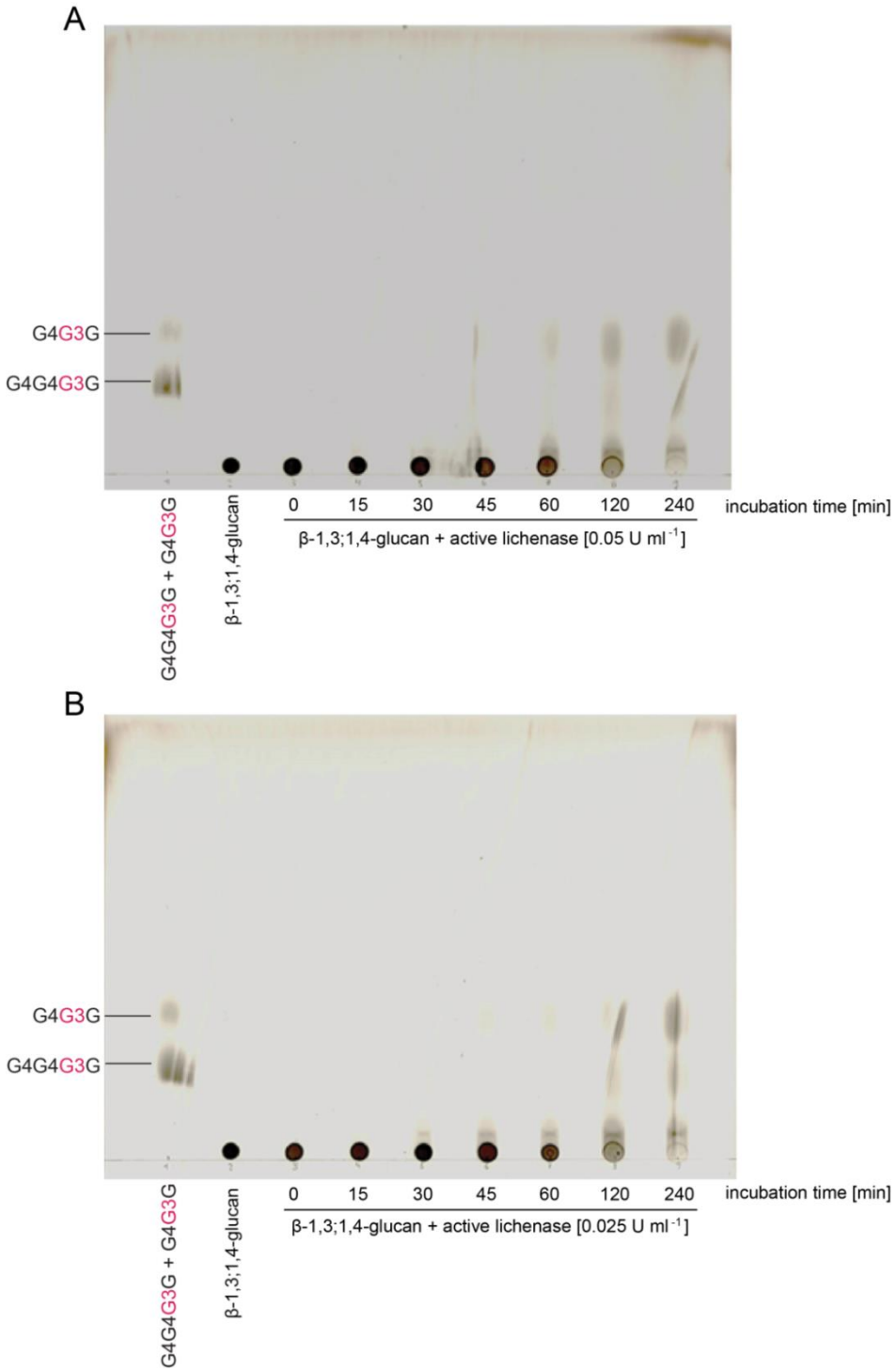

Figure S18. TLC of β-1,3;1,4-glucan polymer hydrolysis. 10 mg/ml barley β-1,3;1,4-glucan polymer was dissolved in 100 mM Sodium Phosphate buffer (pH = 6.5) and incubated with either (A) 0.05 U ml^{-1} lichenase or (B) 0.025 U ml^{-1} lichenase of *B. subtilis*. Upon 0, 15, 30, 45, 60, 120 and 240 min samples were taken and the enzyme was inactivated by incubating the hydrolysate for 15 min in boiling water. 10 µl of the standards G4G4G3G + G4G3G (10 mg ml^{-1}), the β-1,3;1,4-glucan polymer dissolved 100 mM Sodium phosphate buffer (10 mg ml^{-1}) or the respective hydrolysates was dropped onto the plate. Upon drying of the plate, it was put into a TLC running chamber containing TLC running buffer. The plate was developed by wetting it with 10% sulfuric acid in methanol and incubating on a heat plate at 99°C for 30-60 min.

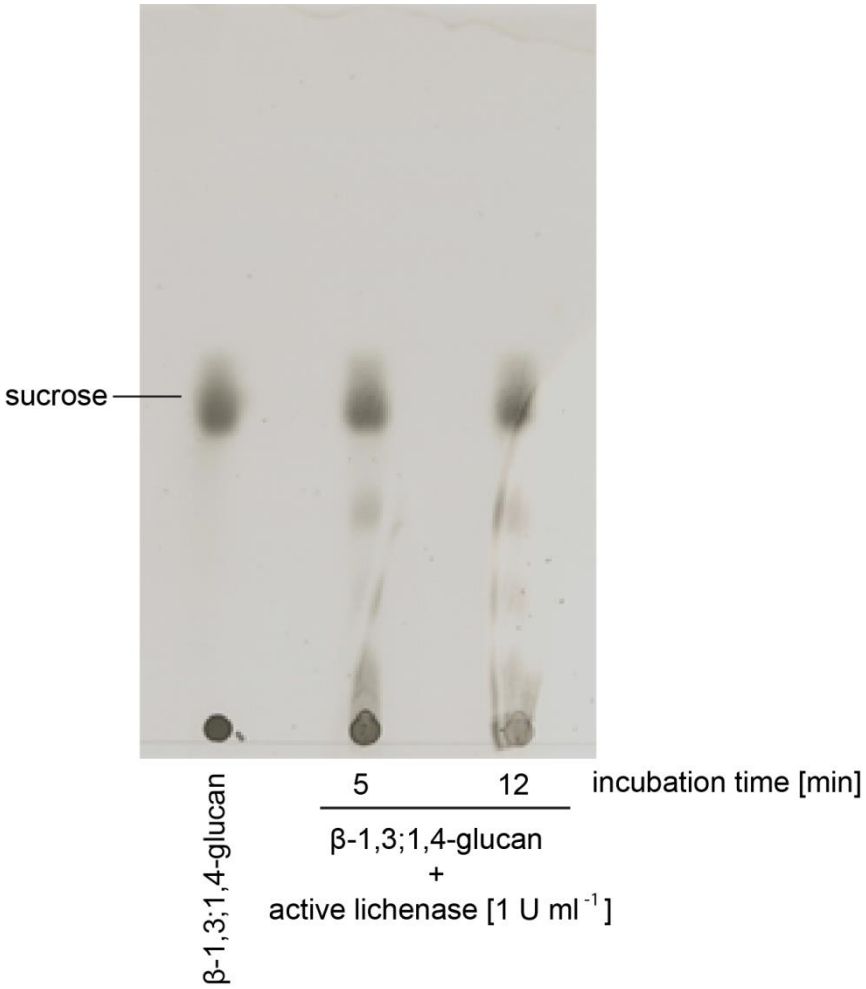

Figure S19. TLC of β-1,3;1,4-glucan polymer hydrolysis in ½ MS + sucrose medium. 10 mg/ml barley β-1,3;1,4-glucan polymer was dissolved in ½ MS + sucrose medium and incubated with 1 U ml^{-1} lichenase of *B. subtilis*. Samples were taken upon 5 or 15 min and the enzyme was inactivated by incubating the hydrolysate for 15 min in boiling water. 10 µl β-1,3;1,4-glucan polymer dissolved ½ MS + sucrose medium (10 mg ml^{-1}) or the respective hydrolysates was dropped onto the plate. Upon drying of the plate, it was put into a TLC running chamber containing TLC running buffer. The plate was developed by wetting it with 10% sulfuric acid in methanol and incubating on a heat plate at 99°C for 30-60 min.

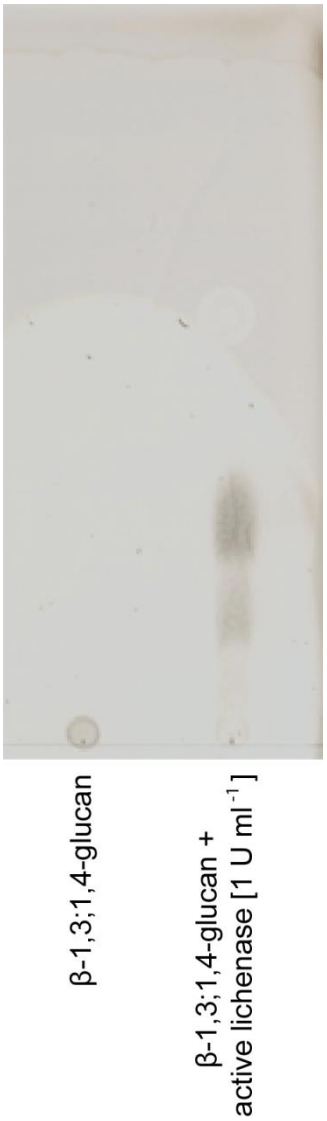

Figure S20. TLC of β-1,3;1,4-glucan polymer hydrolysis for the forward and genetic screen. 10 mg/ml barley β-1,3;1,4-glucan polymer was dissolved in 100 mM Sodium phosphate buffer (pH= 6.5) and incubated with 1 U ml^{-1} lichenase of *B. subtilis*. Upon 1 h incubation time, the enzyme was inactivated by incubating the hydrolysate for 15 min in boiling water. 10 µl β-1,3;1,4-glucan polymer dissolved in 100 mM Sodium phosphate buffer (1 mg ml^{-1}) and the hydrolysate was dropped onto the plate. Upon drying of the plate, the plate was put into a TLC running chamber containing TLC running buffer. The plate was developed by wetting it with 10% sulfuric acid in methanol and incubating on a heat plate at 99°C for 30-60 min.

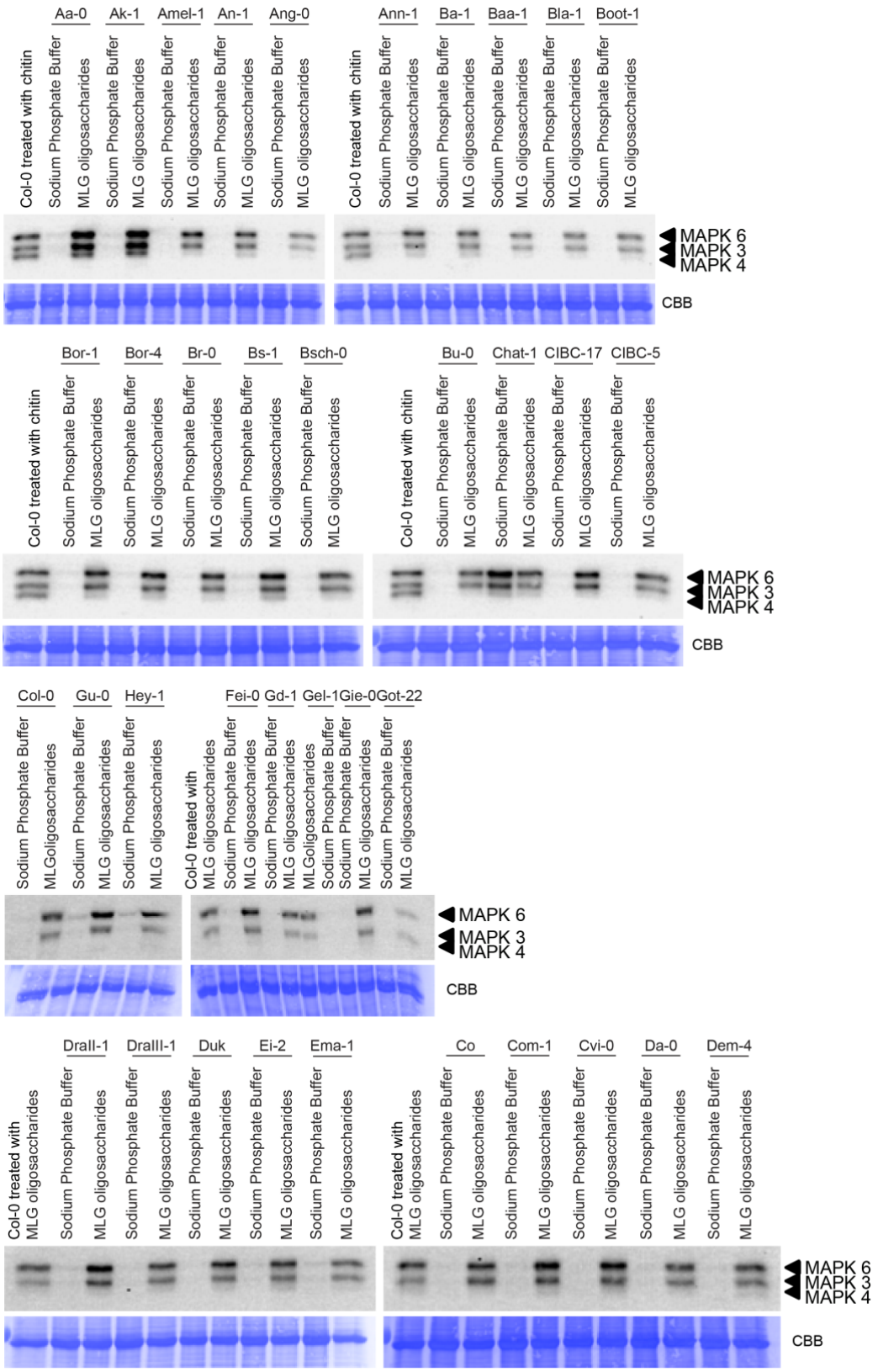

Figure S21. MAPK activation upon MLG treatment in different Arabidopsis ecotypes. 14-day old *in-vitro* grown Arabidopsis seedlings of various accessions were treated with 10 mM Sodium Phosphate buffer or a 1:10 dilution of MLG oligosaccharides for 12 min. Activation of MAPK6, MAPK3 and MAPK4 was analysed via Western Blot with the p44/42-antibody. Lower panel shows Coomassie Brilliant Blue (CBB) staining as loading control. The experiment was performed once.

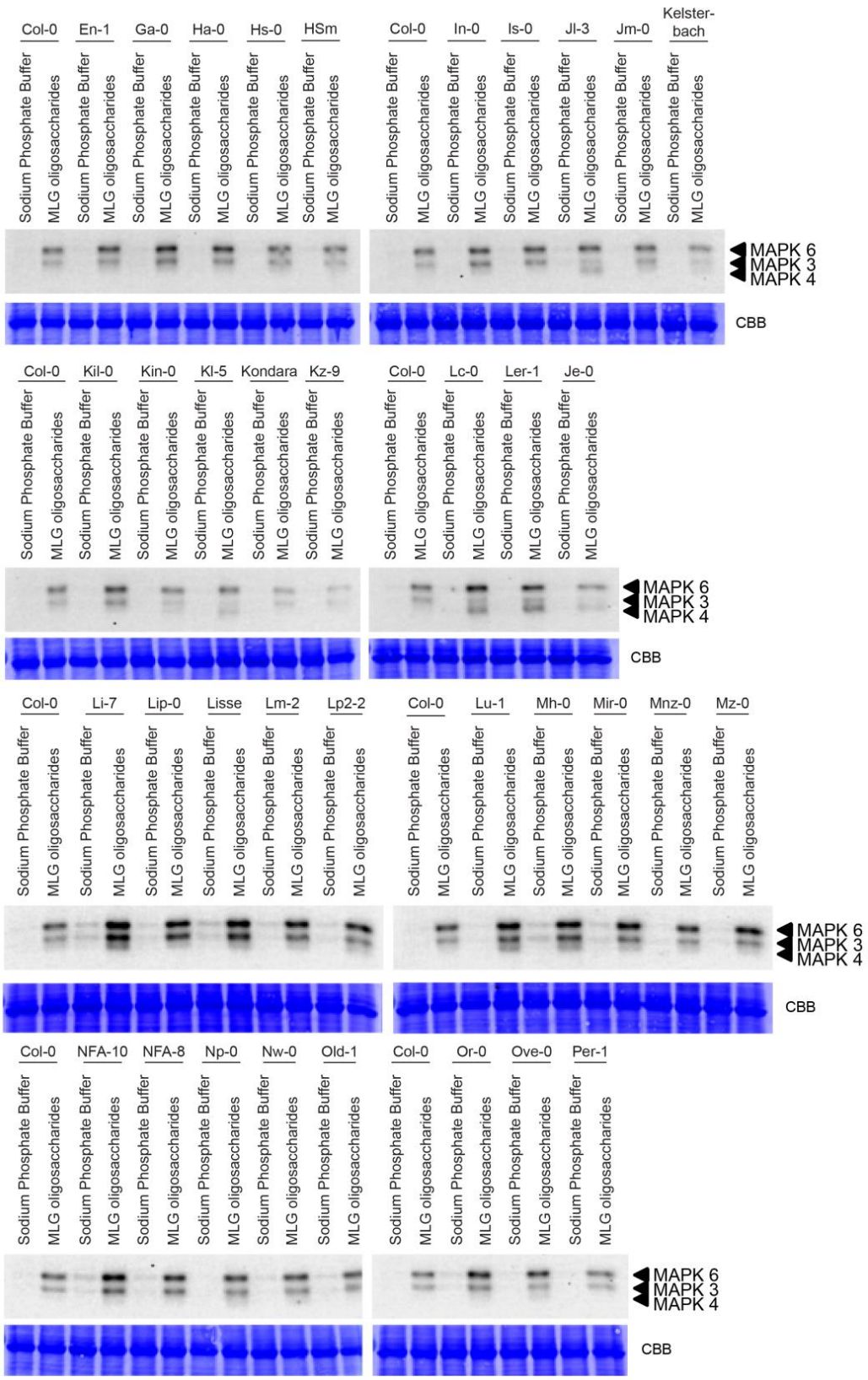

Figure S22. MAPK activation upon MLG treatment in various Arabidopsis accessions. 14-day old *in-vitro* grown Arabidopsis seedlings of various accessions were treated with 10 mM Sodium Phosphate buffer or a 1:10 dilution of MLG oligosaccharides for 12 min. Activation of MAPK6, MAPK3 and MAPK4 was analysed via Western Blot with the p44/42-antibody. Lower panel shows Coomassie Brilliant Blue (CBB) staining as loading control. The experiment was performed once.

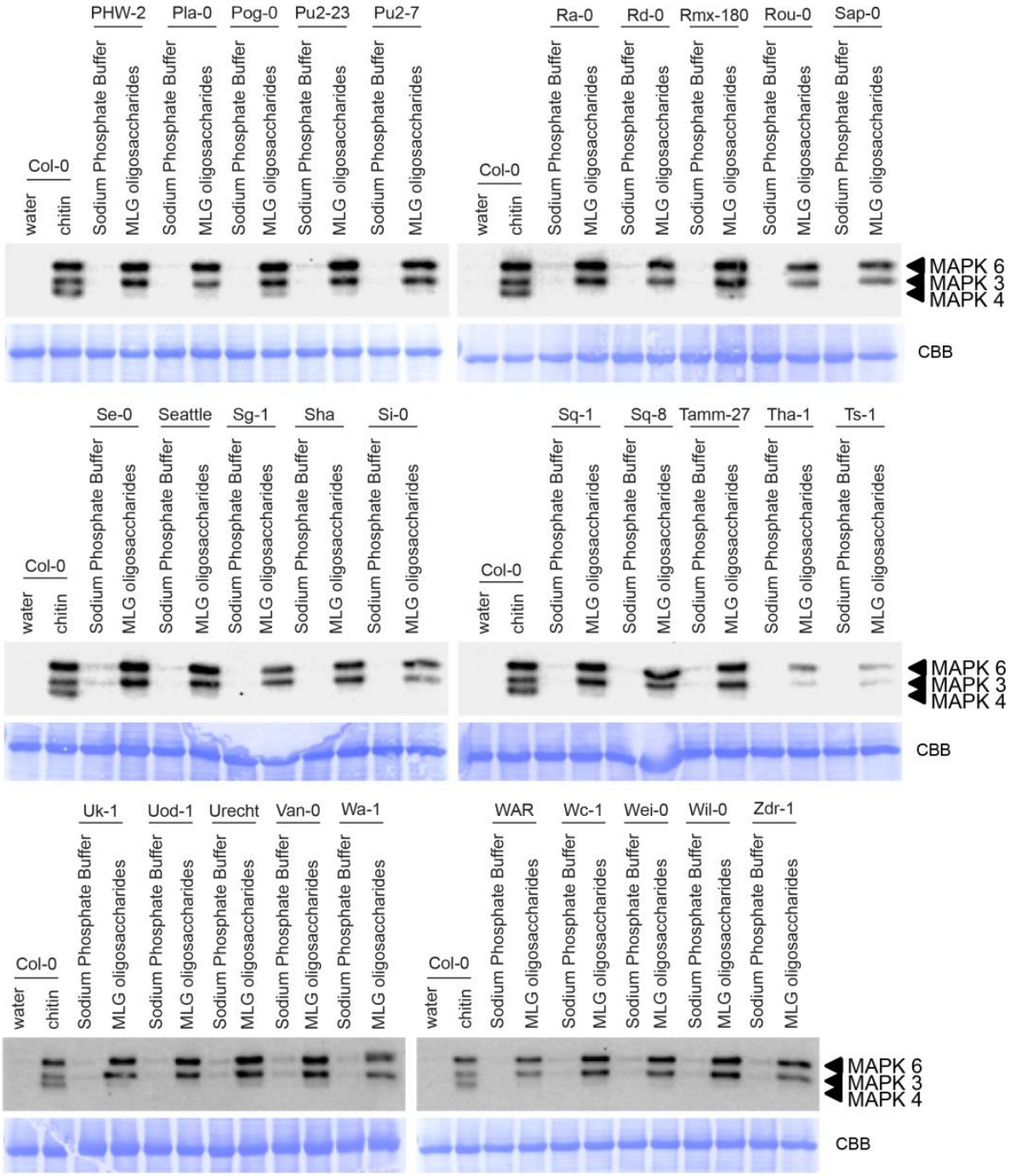

Figure S23. MAPK activation upon MLG treatment in various Arabidopsis ecotypes. 14-day old *in-vitro* grown Arabidopsis seedlings of various accessions were treated with 10 mM Sodium Phosphate buffer or a 1:10 dilution of MLG oligosaccharides for 12 min. Activation of MAPK6, MAPK3 and MAPK4 was analysed via Western Blot with the p44/42-antibody. Lower panel shows Coomassie Brilliant Blue (CBB) staining as loading control. The experiment was performed once.

List of figures

List of tables

List of supplemental tables and figures

Danksagung

An dieser Stelle möchte ich mich bei Allen bedanken, die mich während meiner Promotion unterstützt und begleitet haben – sei es privat oder akademisch.

Zuerst möchte ich mich bei Prof. Dr. Volker Lipka dafür bedanken, dass er mir die Möglichkeit gegeben hat in seiner Abteilung an einem interessanten Projekt zu arbeiten, das molekularbiologische aber auch biochemische Aspekte beinhaltete. Außerdem möchte ich mich für die vielen Diskussionen und die konstruktive Kritik während Meetings oder auch zwischendurch bedanken, die sehr zum Erfolg des Projektes beigetragen haben. Seine Begeisterung während dieser Diskussionen haben mich auch dazu angeregt eigene Ideen zu entwickeln und stets motiviert zu bleiben. Danke außerdem für die wertvolle und uneingeschränkte Unterstützung und das Vertrauen, das ich nicht nur während der Promotion erfahren habe, sondern auch während des gesamten Bachelor- und Masterstudiums. Seine Tür stand jederzeit offen und er hatte immer ein offenes Ohr für kleine und große Probleme oder Anliegen des Alltags oder im Labor. Außerdem war er auch immer für einen Spaß zu haben. Seine Art hat eine familiäre Atmosphäre in der Abteilung geschaffen und die Produktivität gefördert. Weiterhin möchte ich mich herzlich dafür bedanken, dass er mich immer gefördert und gefordert hat. Ich danke ihm außerdem für seine Funktion als Erstprüfer und Doktorvater sowie für die Begutachtung meiner Arbeit.

Ein großes Dankeschön geht auch an PD Dr. Till Ischebeck für die Übernahme des Koreferats. Außerdem möchte ich mich für die Bereitstellung der großen Kollektion an Arabidopsis Ökotypen bedanken ohne die der Screen nicht möglich gewesen wäre.

A great thanks goes also to Prof. Dr. Harry Brumer. He welcomed me warmly in Vancouver and in his lab so that it directly felt like home. His knowledge in enzymology was a great support in the promotion of this project and contributed to the success of this project. During my two stays but also during skype meetings, I benefitted greatly from his experience and learned a lot about carbohydrate enzymology. Thank you also for your patience in proof-reading this work and your constructive comments and suggestions.

Thanks also to both, PD Dr. Till Ischebeck and Prof. Dr. Harry Brumer for being part of my examination board and for your great suggestions and ideas during yearly discussions after the progress reports.

Bei Prof. Dr. Ivo Feußner, Prof. Dr. Gerhard Braus und Dr. Marcel Wiermer möchte ich mich bedanken, dass sie zusammen mit meinem Betreuungsausschuss meine Prüfungskomission bilden.

Vielen Dank auch an Dr. Elena Petutschnig für die Betreuung während der Arbeit. Sie war eine große Hilfe bei der Durchführung vieler Experimente und hat mit vielen Ratschlägen und Vorschlägen das Projekt weiterentwickelt.

Des Weiteren möchte ich mich bei PD Dr. Thomas Teichmann und Dr. Hassan Ghareeb für die Ratschläge und Anregungen während der 2-wöchentlichen „Chitin-Meetings“ bedanken sowie für die Hillfe bei kleinen und großen Problemen.

Ein riesen Dankeschön geht auch an unsere herzensguten technischen Assistenten Gaby, Sabine, Ludmilla und Melanie für die wertvolle Hilfe bei Experimenten, die Bestellung von Labormaterial, das Bereitstellen von Puffern und das Aufräumen von Laborplätzen, aber auch das offene Ohr bei Problemen abseits der Arbeit. Danke auch an unsere fleißigen Gärtnerinnen Feli und Susanne für die Hilfe bei den vielen Siebearbeiten und die vielen Gespräche, die sich nicht nur um die Arbeit drehten. Ohne euch würde der Alltag im Labor nicht so reibungslos ablaufen – danke dafür!

Weiterhin möchte ich mich bei meinen studentischen Hilfskräften Melina Schwier, Esther Schneider und Julia Lechtenberg bedanken, die viele Stunden an der Sterilbank verbracht und mir damit sehr viel Arbeit abgenommen haben.

Ein riesiges Dankeschön geht auch an meine lieben Doktorandenkollegen Leonie, Dimitri, Julia, Mohammed, Chrissi, Lena, Mo, Mascha, Daniel und Denise. Danke für die aufmunternden Worte, wenn es einmal nicht so lief wie geplant, Plaudereien, die sich nicht um Wissenschaft drehten, Albernheiten und die wertvollen Ratschläge für Experimente. Ein besonderer Dank geht dabei an Leonie und Denise. Die Beiden sind während der Promotion gute Freundinnen von mir geworden – vielen Dank, dass ihr mir immer mit Rat und Tat zur Seite standet.

Außerdem möchte ich mich bei der ganzen Abteilung für die familiäre Arbeitsatmosphäre und die vielen Aktivitäten außerhalb des Labors, die mit Freude angegangen wurden, bedanken.

I would also like thank people outside my lab who helped me with this project. Dr. Yann Mathieu and Maria Cleveland taught me how to transform *Pichia pastoris*, screen for transformants and to purify a protein. Nicholas McGregor showed me the biochemical methods to functionally characterize a glycoside hydrolase. A great thanks goes also to Namrata Jain, Gregory Arnal and Kazune Tamura who helped me with the analysis and hydrolysis of carbohydrates. A special thanks to Hila Behar who helped me with general things and became a close friend – I miss you.
Furthermore I would like to take this opportunity and thank the whole Brumer lab for welcoming me so warmly during my two stays. Everyone was so friendly and helpful that Vancouver and the lab felt directly like home – thank you!

Weiterhin möchte ich mich auch bei der unseren Kollaborationspartnern am IPK in Gatersleben für die Bereitstellung der Genomdaten von *Bgh* und den vorläufigen Ergebnissen der HIGS Analysen herzlich bedanken. Die Bereitstellung dieser Daten haben sehr zum Erfolg dieser Arbeit beigetragen.

Ein großes Dankeschön gebührt auch allen Mitgliedern des IRTG PRoTECTs. Danke für die schönen Retreats auf der Burg Ludwigstein mit Lagerfeuer und Musik und in Vancouver. Danke für die vielen Treffen in denen wissenschaftliche, aber auch private Anliegen besprochen wurden. Danke für das gemeinsame Lachen, Aufregen und die Unterstützung. Es wird mir fehlen! Ein besonderer Dank geht dabei an Hila, Kevin, Jessi, Mimi, Daniel, Dimi und Denise – ihr habt die Zeit in Kanada zu etwas noch Besonderem gemacht und unsere vielen Erlebnisse werde ich nicht vergessen. A big thanks also to Jelena and Aswin who had always time for a little talk and were helpful in all regards outside and inside the lab.

Von Herzen möchte ich mich auch bei Ronja bedanken, die seit der Bachelorarbeit nicht nur eine Kommolitonin, sondern auch eine sehr gute Freundin ist (Du, ich und das Agrobakterium!). Danke für deine wunderbare Freunschaft, dein offenes Ohr und die großartige Unterstütztung seit dem Bachelor. Du bist es einfach.

Ein herzliches Dankeschön geht auch an meine Freunde außerhalb des Labors: Melissa, Lisa, Neele und Finn. Danke für die Ablenkung, Aufmunterung und Unterstützung trotz der großen Entfernung in den letzten Jahren!

Nicht zuletzt möchte ich mich herzlich bei meiner Familie für die moralische Unterstützung während der letzten Jahre bedanken. Besonders danke ich meinem Papa, meinem Bruder und meiner Schwägerin, die immer an mich geglaubt haben und ohne die ich es nicht geschafft hätte – danke!